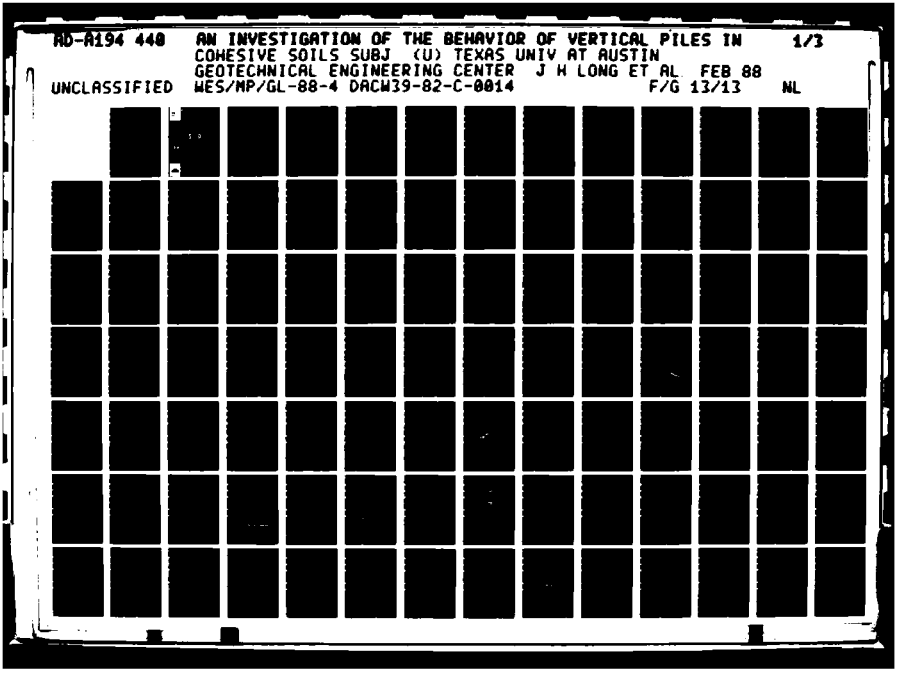
AD-A194 448 AN INVESTIGATION OF THE BEHAVIOR OF VERTICAL PILES IN 1/3
COHESIVE SOILS SUBJ (U) TEXAS UNIV AT AUSTIN
GEOTECHNICAL ENGINEERING CENTER J H LONG ET AL FEB 88
UNCLASSIFIED WES/MP/GL-88-4 DACW39-82-C-0014 F/G 13/13 NL

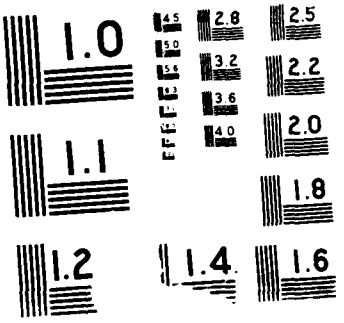
1.0
1.1
1.2
1.4
1.6
1.8
2.0
2.2
2.5
2.8
3.2
3.6
4.0
4.5
5.0

(2)

US Army Corps of Engineers

MISCELLANEOUS PAPER GL-88-4

AN INVESTIGATION OF THE BEHAVIOR OF VERTICAL PILES IN COHESIVE SOILS SUBJECTED TO REPETITIVE LATERAL LOADS

by

James H. Long, Lymon C. Reese

Geotechnical Engineering Center
Bureau of Engineering Research
The University of Texas at Austin
Austin, Texas 78712

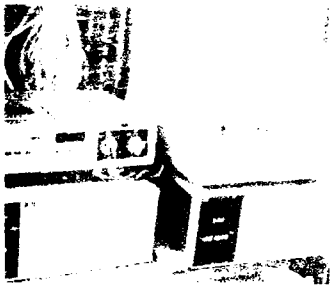

February 1988
Reprint of Geotechnical Engineering Report GR83-7

GEOTECHNICAL LABORATORY

Prepared for US Army Engineer Waterways Experiment Station
PO Box 631, Vicksburg, Mississippi 39180-0631
Under Contract No. DACW39-82-C-0014

Destroy this report when no longer needed. Do not return it to the originator.

The findings in this report are not to be construed as an official Department of the Army position unless so designated by other authorized documents.

The contents of this report are not to be used for advertising, publication, or promotional purposes. Citation of trade names does not constitute an official endorsement or approval of the use of such commercial products.

Unclassified
SECURITY CLASSIFICATION OF THIS PAGE

AD-A194 440

REPORT DOCUMENTATION PAGE

Form Approved
OMB No 0704-0188
Exp Date Jun 30, 1986

1a REPORT SECURITY CLASSIFICATION Unclassified	1b RESTRICTIVE MARKINGS
2a SECURITY CLASSIFICATION AUTHORITY	3 DISTRIBUTION / AVAILABILITY OF REPORT Approved for public release; distribution unlimited.
2b DECLASSIFICATION / DOWNGRADING SCHEDULE	
4 PERFORMING ORGANIZATION REPORT NUMBER(S) Geotechnical Engineering Report GR83-7	5 MONITORING ORGANIZATION REPORT NUMBER(S) Miscellaneous Paper GL-88-4
6a NAME OF PERFORMING ORGANIZATION See reverse 6b OFFICE SYMBOL (If applicable)	7a NAME OF MONITORING ORGANIZATION Geotechnical Laboratory, US Army Engineer Waterways Experiment Station
6c ADDRESS (City, State, and ZIP Code) Austin, TX 78712	7b ADDRESS (City, State, and ZIP Code) PO Box 631 Vicksburg, MS 39180-0631
8a NAME OF FUNDING / SPONSORING ORGANIZATION See reverse 8b OFFICE SYMBOL (If applicable)	9 PROCUREMENT INSTRUMENT IDENTIFICATION NUMBER
8c ADDRESS (City, State, and ZIP Code) Reston, VA 22090	10 SOURCE OF FUNDING NUMBERS PROGRAM ELEMENT NO. / PROJECT NO. / TASK NO / WORK UNIT ACCESSION NO

11 TITLE (Include Security Classification)
An Investigation of the Behavior of Vertical Piles in Cohesive Soils Subjected to Repetitive Lateral Loads

12 PERSONAL AUTHOR(S)
Long, James H.; Reese, Lymon C.

13a TYPE OF REPORT	13b TIME COVERED	14 DATE OF REPORT (Year, Month, Day)	15 PAGE COUNT
Final report	FROM _____ TO _____	February 1988	267

16 SUPPLEMENTARY NOTATION
Available from National Technical Information Service, 5285 Port Royal Road, Springfield, VA 22161.

17 COSATI CODES			18 SUBJECT TERMS (Continue on reverse if necessary and identify by block number)
FIELD	GROUP	SUB-GROUP	Cyclic loads, Lateral loads, Cyclic triaxial, Piles

19 ABSTRACT (Continue on reverse if necessary and identify by block number)

The results of several repetitive lateral load tests on single piles from previous studies were analyzed. Current techniques for predicting the cyclic and static behavior of piles were reviewed, and predictions of both static- and cyclic-lateral-load behavior were compared with measured behavior.

The scour phenomenon that occurs when water above the ground surface flows into and out of any gaps that form between the pile and clay during cyclic loading was examined.

Conclusions are drawn related to the relevance of the studies reported herein to current procedures of estimating the response of piles in clay due to cyclic lateral loading.

20 DISTRIBUTION / AVAILABILITY OF ABSTRACT	21 ABSTRACT SECURITY CLASSIFICATION
☒ UNCLASSIFIED/UNLIMITED ☐ SAME AS RPT ☐ DTIC USERS	Unclassified
22a NAME OF RESPONSIBLE INDIVIDUAL	22b TELEPHONE (Include Area Code) / 22c OFFICE SYMBOL

DD FORM 1473, 84 MAR

83 APR edition may be used until exhausted
All other editions are obsolete

SECURITY CLASSIFICATION OF THIS PAGE
Unclassified

6a. NAME OF PERFORMING ORGANIZATION (Continued).
Geotechnical Engineering Center
Bureau of Engineering Research
The University of Texas at Austin

8a. NAME OF FUNDING/SPONSORING ORGANIZATION (Continued).
Minerals Management Service
US Department of Interior

PREFACE

This study was performed by the Geotechnical Engineering Center, Bureau of Engineering Research, The University of Texas at Austin, under contract to the US Army Engineer Waterways Experiment Station (WES), Vicksburg, Mississippi, for the Minerals Management Service, US Department of Interior. The study was performed under Contract No. DACW 39-82-C-0014.

This report was prepared by Mr. James H. Long and Dr. Lymon C. Reese, University of Texas at Austin, and reviewed by Mr. Gerald B. Mitchell, Chief, Engineering Group, Soil Mechanics Division (SMD), Geotechnical Laboratory (GL), WES. General supervision was provided by Mr. Clifford L. McAnear, Chief, SMD, and Dr. William F. Marcuson III, Chief, GL.

COL Dwayne G. Lee is Commander and Director of WES. Dr. Robert W. Whalin is Technical Director.

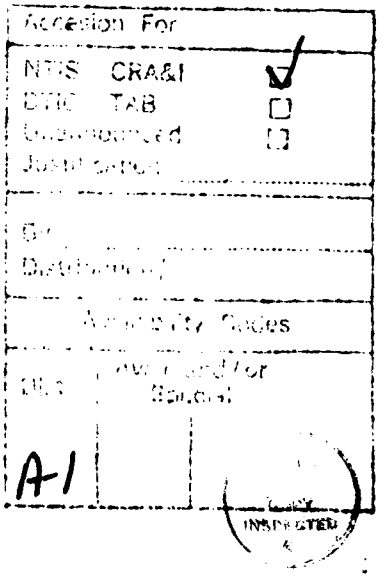

TABLE OF CONTENTS

TABLE OF CONTENTS (Continued)

TABLE OF CONTENTS (Continued)

LIST OF FIGURES

LIST OF FIGURES (continued)

LIST OF FIGURES (continued)

LIST OF FIGURES (continued)

LIST OF FIGURES (continued)

LIST OF FIGURES (continued)

LIST OF FIGURES (continued)

LIST OF FIGURES (continued)

LIST OF FIGURES (continued)

LIST OF FIGURES (continued)

LIST OF TABLES

CHAPTER 1. INTRODUCTION

The behavior of a vertical pile subjected to repetitive horizontal loading is complex. Several factors such as the characteristics of the loading, properties of the pile, properties of the clay, and position of the free-water surface play an important role in determining the behavior of the pile.

Several types of environmental conditions (wind and waves) exist that subject the structure to cyclic or repetitive loads; these loads must be resisted by the foundation. In this study, the effects of inertia are not considered; therefore, repetitive loading or cyclic loading refers to several applications of load at a rate slow enough to be considered static.

The studies reported herein were directed to two factors that affect the behavior of piles due to cyclic loading, namely (1) the changes that occur in properties of clay due to cyclic loading, and (2) the effect of free water above the ground surface. Water above the ground surface flows into and out of any gaps that form between the pile and clay during cyclic loading. This pumping action has the potential to scour soil along the pile-soil gap, thus removing particles of clay that may have otherwise provided lateral support for the pile.

A more detailed presentation of the soil-and-water behavior during cyclic loading of a pile is given in Chapter 2. In addition, in Chapter 2, reasons for conducting specific laboratory tests and for concentrating on certain aspects of the cyclic-lateral-loading problem are discussed. In Chapter 3, the characteristics and results of several lateral load tests are presented in which repetitive loads were applied. Current techniques

for predicting the cyclic and static behavior of piles are reviewed in Chapter 4, and predictions of both static and cyclic-lateral-load behavior are compared with measured behavior in Chapter 5. Soil samples were taken at two sites where lateral-load tests were performed by others on piles that were fully instrumented. The soils at those two sites were predominantly clays. The types of laboratory tests performed on the clays from those sites are discussed in Chapter 6, and the results of the testing program are discussed in Chapter 7. In Chapter 8 studies are presented in which the results of laboratory tests are used to gain insight into the precise reasons for the loss of soil resistance during cyclic loading of piles in clay. In Chapter 9 conclusions are drawn related to the relevance of the studies reported herein to current procedures of estimating the response of piles in clay due to cyclic lateral loading.

CHAPTER 2. FUNDAMENTAL CONSIDERATIONS OF VERTICAL PILES IN COHESIVE SOIL SUBJECTED TO REPETITIVE HORIZONTAL LOADS

Several factors contribute to the response of a vertical pile in cohesive soil subjected to repetitive horizontal loading. Three major factors that are believed to be of primary interest are (1) the nature and characteristics of the load applied to the head of the pile, (2) the mechanical behavior of the soil surrounding the pile, and (3), if the free water surface is above ground level, the susceptibility of the soil to erosion or scour.

In order to attain a basic understanding, a brief review of the behavior of a pile in clay subjected to cyclic loading is presented. This review is followed by a discussion of the effects these three major factors have on pile behavior, and what procedures were used to identify the quantitative effects of these factors.

BEHAVIOR OF PILE AND SOIL DURING CYCLIC LOADING

In order to describe the effects of cyclic loading on the behavior of a pile, a simplified model is used to illustrate how the soil and pile react to a simple loading condition at the head of the pile. In this simplified model, the pile is assumed to be infinitely long and installed vertically. The surface of the water is assumed to be above the ground surface; thus, water is free to enter any gaps that may form between the pile and the cohesive soil. The cyclic loading applied at the head of the pile is assumed to impose equal and opposite horizontal loads to the pile head. Furthermore, the loading is assumed to vary sinusoidally with time

at a frequency in which only the effects of repeated loading are important and the effects of inertia are not important.

The behavior of the pile is described for four phases during one cycle of loading. The effect of each quarter-cycle of load is described and the influence of further cycles are mentioned.

During the first quarter-cycle, the lateral load varies from a magnitude of zero to a maximum horizontal load H_{max}. As the load is applied, the pile head rotates and translates until the lateral force at the top of the pile is carried by the surrounding soil as shown in Fig. 2.1a. If the deflections are large enough, a gap between the cohesive soil and pile-wall will form along the back of the pile and water will flow into the gap. The velocity at which the water flows is dependent on the rate of deformation of the pile, and the geometric characteristics of the gap that is formed.

During the second quarter-cycle, the lateral load decreases from a value of H_{max} to zero; thus, the pile head returns to a point similar to its original position. As the pile moves back toward its original position, the water in the gap between the pile and soil along the back of the pile is forced out of the gap. Along the front of the pile, the pile wall and soil may separate due to irrecoverable permanent deformations induced within the soil mass during loading as shown in Fig. 2.1b. This new gap along the front of the pile allows water to enter into the space. As mentioned before, the velocity at which the water enters the space is dependent on the rate of deformation of the pile and the geometric characteristics of the gap. As the load approaches zero, the pile will return to a configuration similar to its original shape, but displaced in the direction of the lateral load H_{max}.

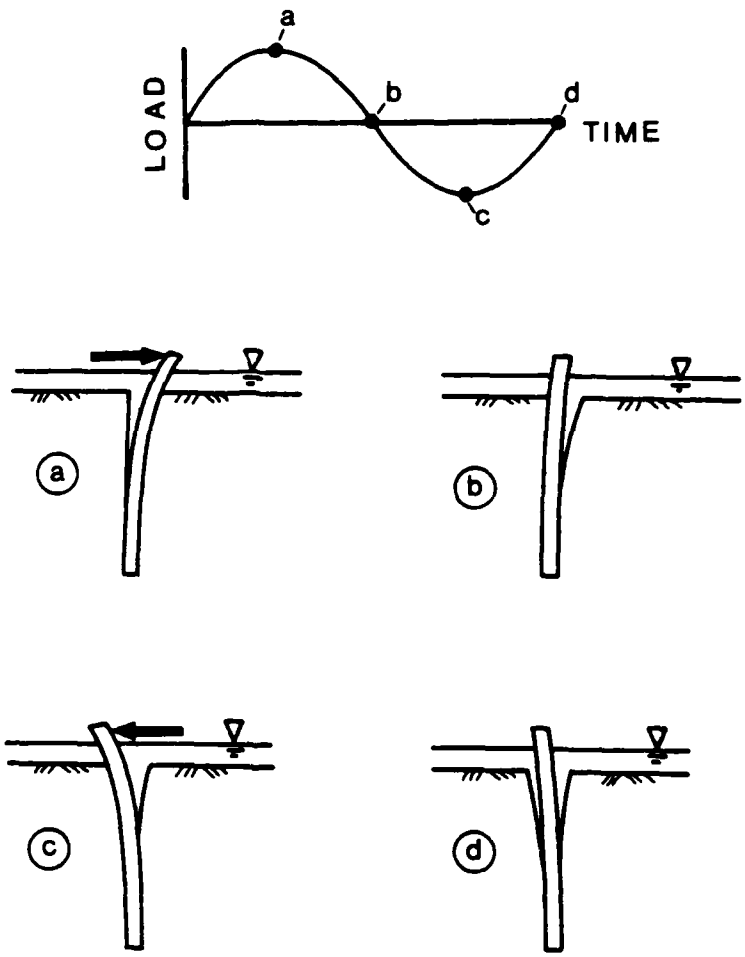

FIG. 2.1. Simplified response of piles in clay due to cyclic loading

During the third quarter-cycle, the direction of the lateral load, H_{max}, and the corresponding deflection of the pile head are reversed. As the load increases from zero to H_{max}, the gap along the loading portion of the pile closes while the gap opens along the unloading portion of the pile as shown in Fig. 2.1c. Along the loading face of the pile, water in the gap between the soil and pile is forced out of the gap until complete contact is made between the soil and pile along the length of the pile. At the unloading face of the pile, water continues to enter the gap as long as the pile continues to displace.

The responses of the pile and soil during the fourth quarter-cycle is similar, but opposite in direction to the response described during the second quarter-cycle. At the end of the fourth quarter-cycle, with no load imposed on the pile head, gaps between the soil and pile occur on both sides of the pile as shown in Fig. 2.1d.

As the cyclic load continues to be applied to the pile head, the general behavior of the pile and soil will be similar to the behavior described above. The possibility of the pile head exhibiting a continued increase in peak deformation will depend on characteristics of the cyclic load applied to the pile head and the characteristics of soil surrounding the pile.

CHARACTERISTICS OF LOADING

For many structures located in the offshore environment, the computation of the maximum lateral loads imposed on the structure during its design life is based on information concerning the heights of ocean waves during a storm. Shown in Fig. 2.2 is a partial record of wave height versus time during a storm in the Gulf of Mexico. Although the relationship

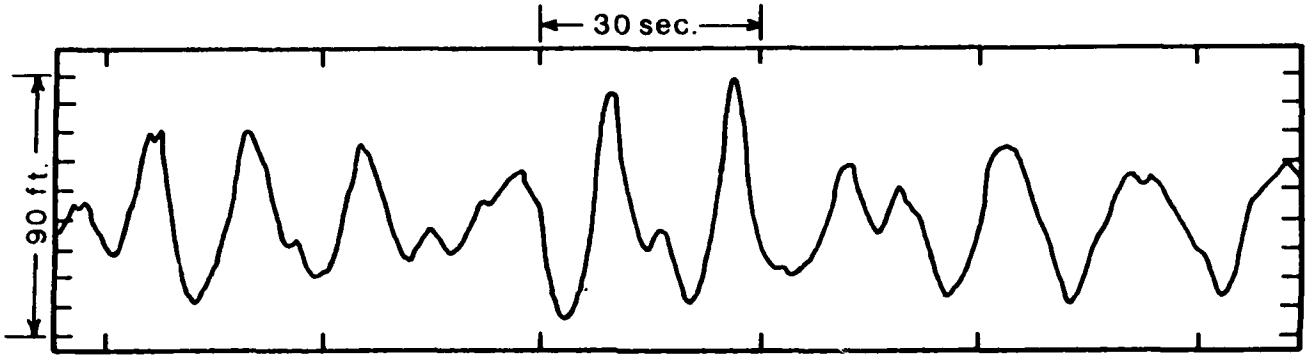

FIG. 2.2. Record of wave height versus time during a storm in the Gulf of Mexico (after Patterson, 1974)

of wave height versus time looks approximately sinusoidal, the magnitude of the wave heights appear to be random in nature. As a wave passes through a structure, it imposes a cyclic load on the structure that must be resisted by the foundation. During a storm, forces from wind and from water currents also act upon the structure. The result of all the forces combined is a static lateral load upon which a cyclic lateral load is superimposed.

CHARACTERISTICS OF COHESIVE SOIL

During the cyclic loading of a pile, the peak deflection increases with continued application of the loads. The increase in the amount of deflection is considered to be due primarily to changes in the characteristics of the soil providing resistance along the side of the pile. These changes can be attributed to two phenomena, namely the reduction of the insitu soil modulus due to cyclic loading, and the erosion of soil along the pile wall due to water entering and exiting the gap. Changes in the mechanical properties of the pile material during cyclic loading could affect the load-deformation behavior of the pile; however, this effect is considered to be minor because typical offshore piles are fabricated of steel, and the stress-strain behavior of steel remains relatively constant as long as no forces causing yield within the pile have been imposed.

The first phemomenon concerns the change in structural behavior of the cohesive soil when subjected to cyclic loading. For specimens of clay subjected to cyclic loading, a decrease in soil modulus has been observed. In addition, if the cyclic loads are not symmetric, that is, if higher levels of loading are applied in one direction, the soil specimen may tend

to these permanent, irrecoverable strains that a gap may form along the interface between the pile and soil. Because of the gap, no soil resistance can be provided along the length of the gap until the pile is loaded and comes into contact with the soil, and because of the cyclic loading, the soil modulus decreases and causes the resistance along the pile wall to decrease with number of cycles.

The behavior of cohesive soil during cyclic loading is dependent on whether the loading is considered to be drained or undrained. The following section addresses the possible dissipation of excess porewater stress in a clay during storm loadings.

Drained or Undrained Behavior of Clay

During the life of an offshore structure, many storms may subject the structure's foundation to cyclic loading. Two situations may arise when considering if an analysis should account for drained or undrained loading. In the first situation, cyclic forces of varying magnitude are imposed on the pile during the life of the storm. As the loads are cycled at the top of the pile, the soil resisting these loads is also loaded cyclically. Due to cyclic loading of the soil, pore pressures (either positive or negative) will be generated and then dissipate with time. The rate at which these pore pressures will dissipate with time is a function of the coefficient of consolidation, the initial excess pore-pressure configuration, and the imposed boundary conditions influencing drainage.

In order to estimate the amount of pore-pressure dissipation that might occur during the loading of a pile, a simplified model suggested by Martin, et al (1980) was studied. In this model, the initial excess pore-pressure distribution is assumed to be axisymmetric with respect to

the pile and to dissipate only in the radial direction. The initial excess pore pressures are further assumed to be defined as follows:

$$P(r) = P_o \, r/r_o \qquad r_o > r > \infty$$

where

$P(r)$ = excess pore pressure at normalized distance, r/r_o, from face of pile,

P_o = initial excess pore pressure adjacent to pile wall,

r = distance from center of pile to point of interest.

r_o = radius of pile.

The solution to the differential equation governing the dissipation of pore pressures with dimensionless time, T_{ps} ($T_{ps} = \frac{c_v t}{r_o^2}$), is shown by the curves in Fig. 2.3. Assuming a pile radius of 55 cm, a range for a cohesive material ($c_v = 5 \times 10^{-4}$ cm²/sec to 5×10^{-2} cm²/sec) and a duration of one day for a storm, the values of T_{ps} are calculated to vary from a low value of 0.014 to a high value of 1.4. As shown in Fig. 2.3, not much pore pressure has been dissipated at these values of T_{ps}, thus it seems a reasonable approach to assume the cyclic loading of the pile may be modelled as undrained, although it is realized that some drainage will occur during the cyclic loading.

A second type of cyclic loading in which drainage plays an important role is the intermittent cyclic loading that occurs during several different storms. As a storm passes, the foundation is subjected to cyclic loading and the excess porewater pressures will dissipate and the soil will consolidate, thus changing the mechanical characterisitics of the soil. This phenomenon is a complex one and is beyond the scope of this investigation.

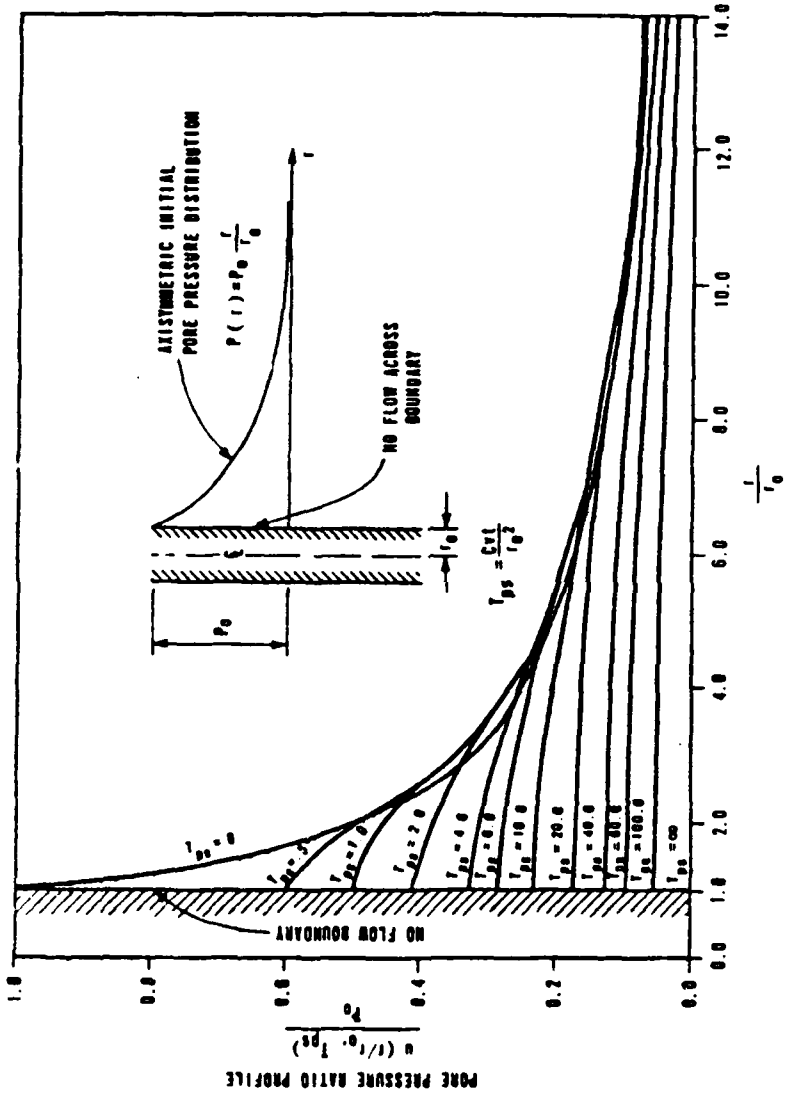

FIG. 2.3. Pore pressure dissipation functions (after Martin, et al, 1980)

The problem of predicting the behavior of a vertical pile due to cyclic lateral loading is complex. In order to provide a basis for analytical techniques, simplified assumptions and relatively simple laboratory techniques must be used. Described below are the types of tests used and the reasons why the particular test was selected.

Laboratory Techniques for Assessing Mechanical Behavior of Soils

In determining the piece of laboratory equipment best suited for testing soil specimens, the decision is often based on which device simulates best the boundary conditions present in the field case, which device yields results that are interpretable and can be applied to analytical methods, and of course, which device is economical and practical to build and operate.

As mentioned previously, the loading due to ocean waves during a storm is complex. In order to deal with a complicated load history, the loading pattern applied to laboratory specimens is often simplified to cyclic loading of a single frequency and of constant amplitude. The results of these tests are then used to define parameters for analytical or empirical models which can be used to predict the soil behavior under a more complex loading history. The effect of cyclic loading on soil behavior and the selection of a procedure for testing soil specimens to model field conditions as well as possible is discussed below.

The behavior of cohesive soils subjected to non-dynamic and cyclic loads is influenced by several factors. Several investigators (Theirs and Seed, 1968, 1969; Anderson, 1976; Sangrey, et al, 1978; Lee and Focht, 1976) have studied these factors. The program of laboratory tests conducted for this investigation was based on conclusions drawn from the referenced investigations. Some of the variables in laboratory procedures

believed to be the most influential in affecting the behavior of cohesive soil under cyclic loading are as follows:

1. type of testing equipment (triaxial or simple shear),
2. type of loading (one-way or two-way cyclic loading),
3. type of cyclic boundary conditions (cyclic stress or cyclic strain), and
4. frequency of loading.

In the following paragraphs, the characteristics of the laboratory testing that was conducted are described. In developing the test program, the above factors were given careful consideration.

Type of Testing Equipment (Cyclic Triaxial or Cyclic Simple Shear). Two popular types of laboratory equipment used for applying cyclic loading to soil specimens are the triaxial and direct-simple-shear devices. Each one of these devices has been used extensively to determine behavior of soil subjected to cyclic loads. However, neither device is able to model exactly the boundary conditions imposed on the soil due to the lateral loading of a pile from environmental effects.

Lee and Focht (1976) present advantages and disadvantages characteristic of both devices and conclude, on the basis of soil behavior, that neither the simple-shear device nor the triaxial device is clearly superior. Consequently, the decision to use the cyclic triaxial test was based on the availability of laboratory equipment.

Type of Loading (One-way or Two-way). Several investigations have been conducted to assess the influence of two-way and one-way cyclic loading. In the following discussion, two-way cyclic loading is considered to define loading in which both a compressive and a tensile load is applied to the cap of the triaxial specimen. The term one-way loading implies a

cyclic loading in one direction only. Shown in Fig. 2.4 are illustrations of what is meant to be one-way and two-way cyclic loading.

Lee and Focht (1976) suggest that laboratory testing of soil specimens should be performed by applying stress-history conditions representative of field conditions. However, considering the stress histories of soil elements surrounding a cyclically and laterally loaded pile, it appears evident that each soil element is experiencing different combinations of stresses depending on its distance from the pile, its depth below the ground surface, and its angular position with respect to the loading direction.

Because the loading conditions imposed on the soil elements are complex, it is necessary to simplify the problem by limiting the discussion to soil elements along the middle of the front face of the pile. Initially, the stresses imposed on the soil element are those corresponding to at-rest conditions and consist of an initial vertical stress, σ_{vo}, and an initial horizontal stress σ_{ho}. As the pile is loaded horizontally, the horizontal stress applied to the soil element increases to a value greater than σ_{ho} and, upon reversing the direction of load applied to the pile, the value of horizontal stress decreases to a value less than σ_{ho}. Limiting values exist for the maximum and minimum horizontal stresses that can be imposed on the soil element; however, the main point is that the horizontal stresses both increase and decrease in magnitude from their original condition. Thus, it seems reasonable that the laboratory test should apply a loading scheme which both increases and decreases the stress within the soil specimen. One such method available in the laboratory is two-way loading to the soil specimen.

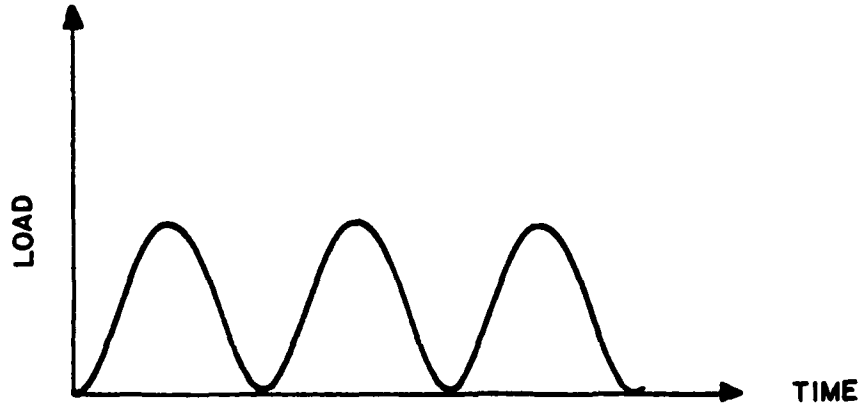

a) One-way Loading

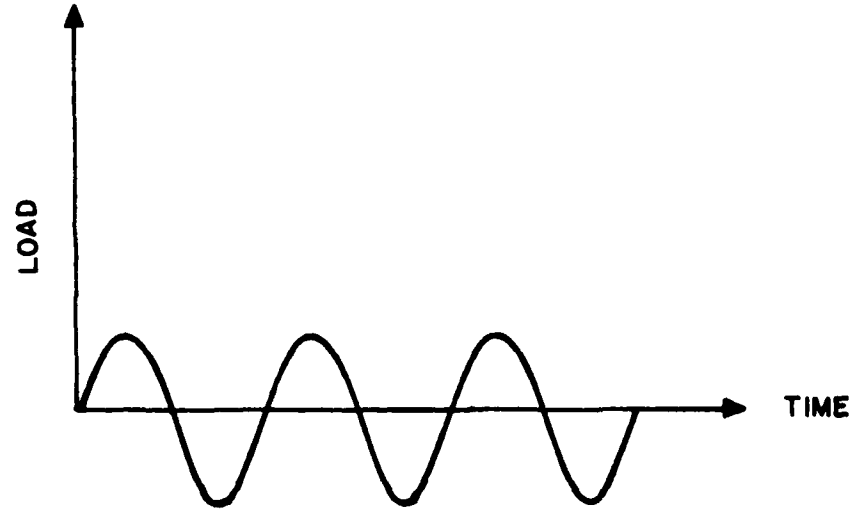

b) Two-way Loading

FIG. 2.4. Illustration of one-way and two-way loading

Type of Cyclic Boundary Conditions (Cyclic Strain or Cyclic Stress). The decision to use controlled-strain tests (instead of controlled-stress tests) in the laboratory was based on the advantage of the controlled-strain test in controlling the behavior of the soil during cyclic loading. Some of the advantages controlled-strain tests possess over controlled-stress tests are shown below:

1. soil specimens experience no drift in strain during cyclic loading, and
2. cyclic resistance versus cyclic strain can be determined for post-failure conditions.

However, neither controlled-strain nor controlled-stress tests are representative of loading conditions imposed in the field during a cyclic lateral-load test. Assuming a pile is loaded cyclically, with a constant maximum value of horizontal load, the surrounding soil is subjected to cyclic loading. If the pile deformed exactly to the same position upon each load cycle, then a controlled-stress test, or even a controlled-strain test, would seem to model field conditions approximately. However, as cycling of the pile continues, the modulus of the surrounding soil decreases, resulting in an increase in the maximum horizontal deflection and, consequently, the distribution of load along the side of the pile is changed. This change in distribution of load alters both the cyclic strains and stresses imposed on the surrounding soil.

Frequency Effects. The effect of frequency on the behavior of cohesive soils subjected to cyclic loading has been investigated. (Motherwell, 1976; Egan, 1977) The effect of an increase in frequency (or strain rate) is a corresponding increase in soil strength and soil modulus. Often, the effects of frequency are considered by performing laboratory

tests at the same frequency as that found in the field condition. Because this study is concerned primarily with offshore piles, frequencies corresponding to those of large ocean waves seem appropriate. Consequently, frequencies on the order of 0.1 Hz to 0.03 Hz were used.

Laboratory Techniques for Assessing Erosional Characteristics of Soils. The mechanism of eroding soil from the pile-soil interface is complex. In order to investigate this phenomenon, two types of tests were conducted. The first test was to model the pumping effect by inserting a rod into a cylindrical block of soil, and then to apply cyclic deformations to the pile head and measure the amount of soil eroded by the pumping action of the water entering and exiting the gap between the soil and pile. The second method employed was to perform pinhole-dispersion tests (Sherard, et al, 1976).

Both methods seem to model field conditions in that the water is flowing across a surface of soil and is free to erode or scour the surface. Both of these tests are discussed in more detail in a previous report (Wang and Reese, 1983), and are discussed in a following chapter.

Conclusions

In consideration of the behavior of a vertical pile subjected to cyclic lateral loads, several factors play a key role in governing the behavior of the pile, and dictating the types of laboratory tests that should be conducted.

The laboratory test best suited for determining the mechanical properties of the cohesive soil in this investigation was selected to be a two-way, controlled-strain, cyclic triaxial test performed under undrained conditions. This test was selected on the basis of the behavior of the soil surrounding the pile during cyclic loading of the pile head.

In addition, a rod test and a pinhole-dispersion test were selected to identify the possibility of erosion of the soil due to water entering and exiting the gap between the soil and pile.

CHAPTER 3. LITERATURE REVIEW

INTRODUCTION

In order to obtain information on the behavior of piles in cohesive soil subjected to repetitive lateral loading, several case histories were reviewed. Both model tests performed in the laboratory and larger scale tests performed in the field were investigated. Background information such as pile, soil, and loading characteristics are given for each case history. The important results and conclusions drawn are then presented.

The principal thrust of the study reported herein was to gain information about the determination of the resistance of cohesive soils around piles subjected to cyclic, later loading where water is above the ground surface. There are only a few experiments reported in the technical literature where water was above the ground surface and those cases are reviewed in this chapter. A number of other cases are discussed where the soils were cohesive and the lateral loading was cyclic but no free water was above the ground surface. These cases are also reviewed in order to gain insight into loss of soil resistance due only to repeated soil deformations.

The rate of loading is also an important variable. If a high rate of loading is employed, the soil resistance can be higher than that for static loading due to both inertial forces and rate-dependent properties of the soil. A comment is made in the presentation of each of the cases if either of these effects appear to have an influence on soil resistance.

Each of the cases reviewed in this chapter is presented without extensive discussion. A section at the end of the chapter will present some conclusions that refer to the aims of this study. Some of the cases

may add a limited amount of information that is pertinent to the study; however, the brief review is of interest of itself in that useful background information is developed of benefit in planning possible future studies.

MODEL TESTS

The results of three model tests are presented below. In each test, the soil was placed in a large container, after which the piles were inserted and tested. Each model test was conducted in a different manner in order to investigate the effects of various phenomena concerning the cyclic lateral behavior of piles.

Gaul (1958)

In a series of model tests performed by Gaul (1958), both static and cyclic lateral loads were applied to a model pile embedded in clay. The model pile used in the study was made of aluminum tubing with an outside diameter of 2.375 in., an inside diameter of 2.067 in., and a length of 96 in. The bending and material properties of the aluminum model piles are given below:

Modulus of Elasticity, $E = 10.3 \times 10^6$ lb/sq in.

Moment of Inertia, $I = 0.666$ in.^{4}

The soil selected for this study was composed of montmorillinite clay. The liquid limit and plastic limit of the clay were determined to be 600 percent and 50 percent, respectively.

The clay was mixed at a water content of 400 percent and placed in a tank. The resulting total unit weight of the soil was reported to be 70 lb/cu ft. In order to keep the exposed surface of clay from drying, a thin layer of water was ponded over the surface of the clay. Later, however, a

piece of oil cloth was used instead of the water. No data were provided regarding the strength properties of the clay.

Loading of the pile was accomplished by connecting one end of a long rod to a loading yoke positioned 0.75 in. below the pile head and the other end of the rod to an eccentric position on a rotating flywheel. The flywheel was rotated at 1.0 Hz and the pile was subjected to equal deflections in both directions. The point of load application was reported to be 1 in. above the ground surface.

One static and four cyclic lateral load tests were conducted. A surface pressure was applied by adding weights to a piece of plywood that sat on the soil. The testing sequence for the model pile is given below:

Test 1. both static and cyclic tests performed on model pile,

Test 2. same as test 1, but with a surface pressure of 25 lb/sq ft,

Test 3. same as test 1, but with a surface pressure of 50 lb/sq ft, and

Test 4. same as test 1, but with no surface pressure.

Shown in Figs. 3.1, 3.2, and 3.3 are the relationships of bending moment versus depth for Tests 1, 2, 3, and 4. Based on these results, it can be seen that the additional overburden decreased the observed maximum moment and lateral load for a specific lateral deflection, and maximum moments due to cyclic loading are only slightly less than those due to static loading as shown in Fig. 3.4.

It should be pointed out, however, that the results of the tests are presented as either cyclic or static. No reference is made to the effect of the number of cycles on the pile behavior nor is any reference given to the number of cycles applied to the pile head when "cyclic" results were presented in Figs. 3.1, 3.2, 3.3, and 3.4.

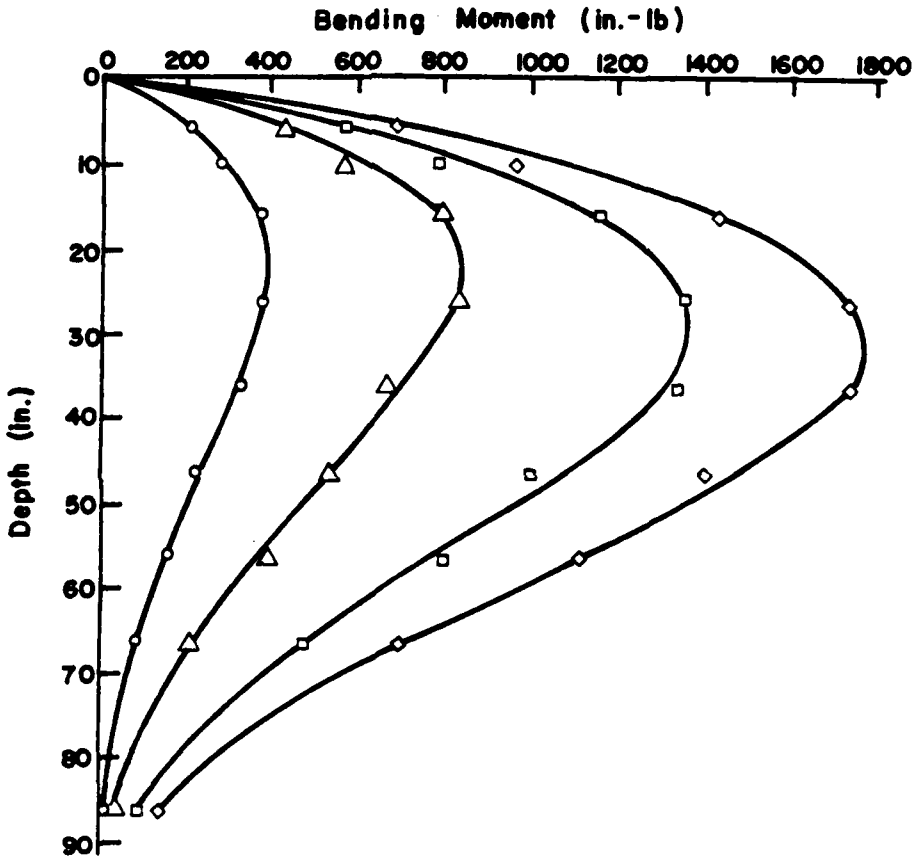

FIG. 3.1. Relationship of bending moment versus depth for static loading, test no. 1 (from Gaul, 1958)

(a)

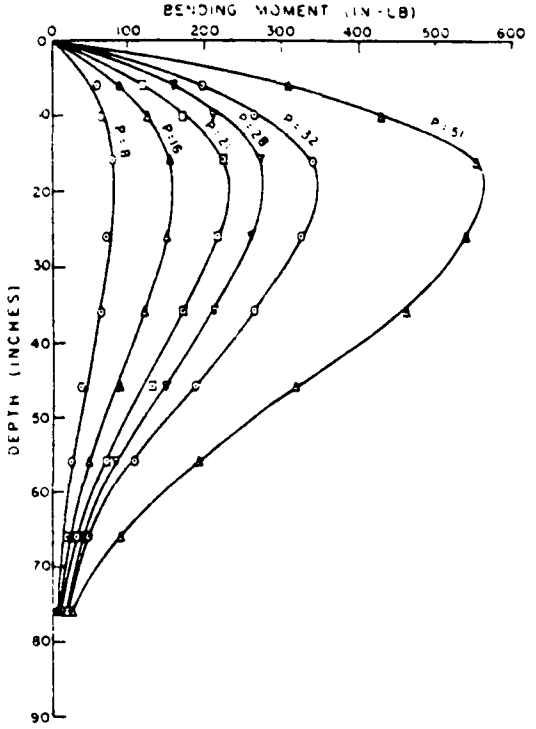

(b)

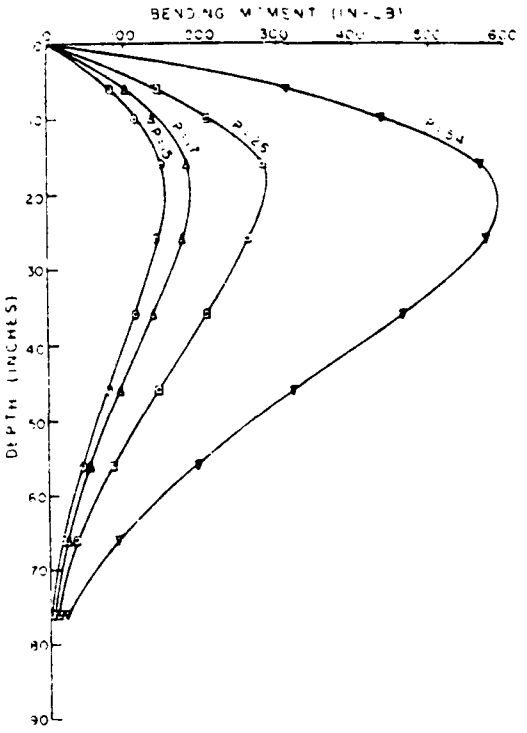

FIG. 3.2. Bending moment versus depth relationship for cyclic loading: a) test no. 1 and b) test no. 2 (from Gaul, 1958)

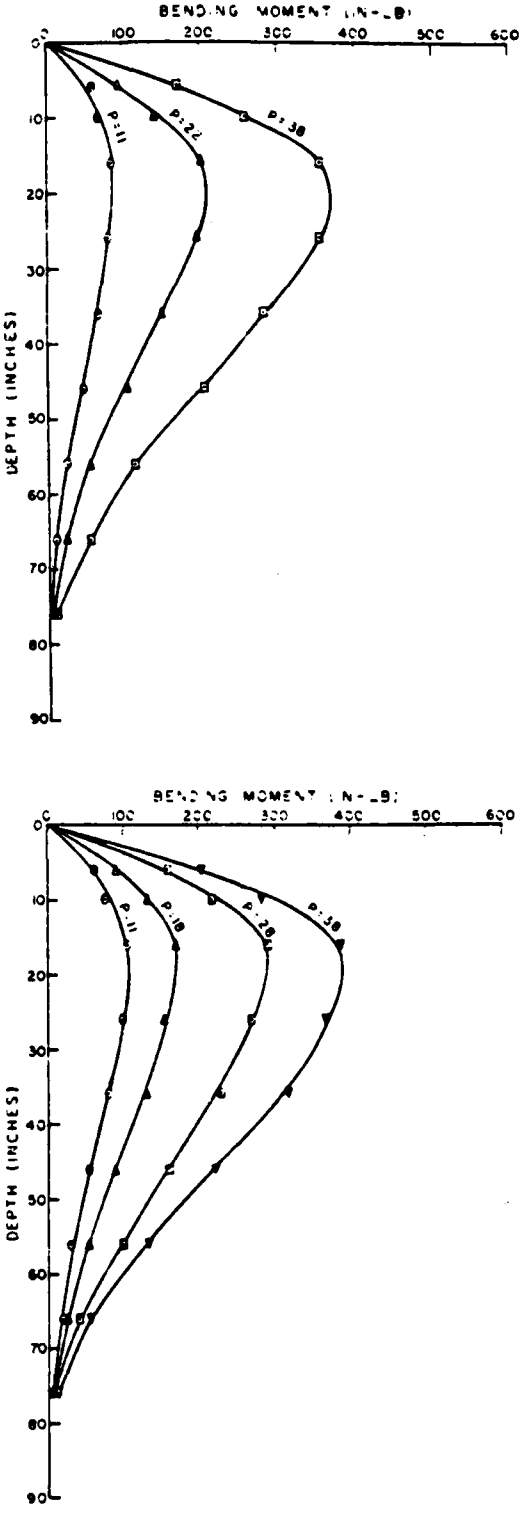

FIG. 3.3. Bending moment versus depth relationship for cyclic loading: a) test no. 3 and b) test no. 4 (from Gaul, 1958)

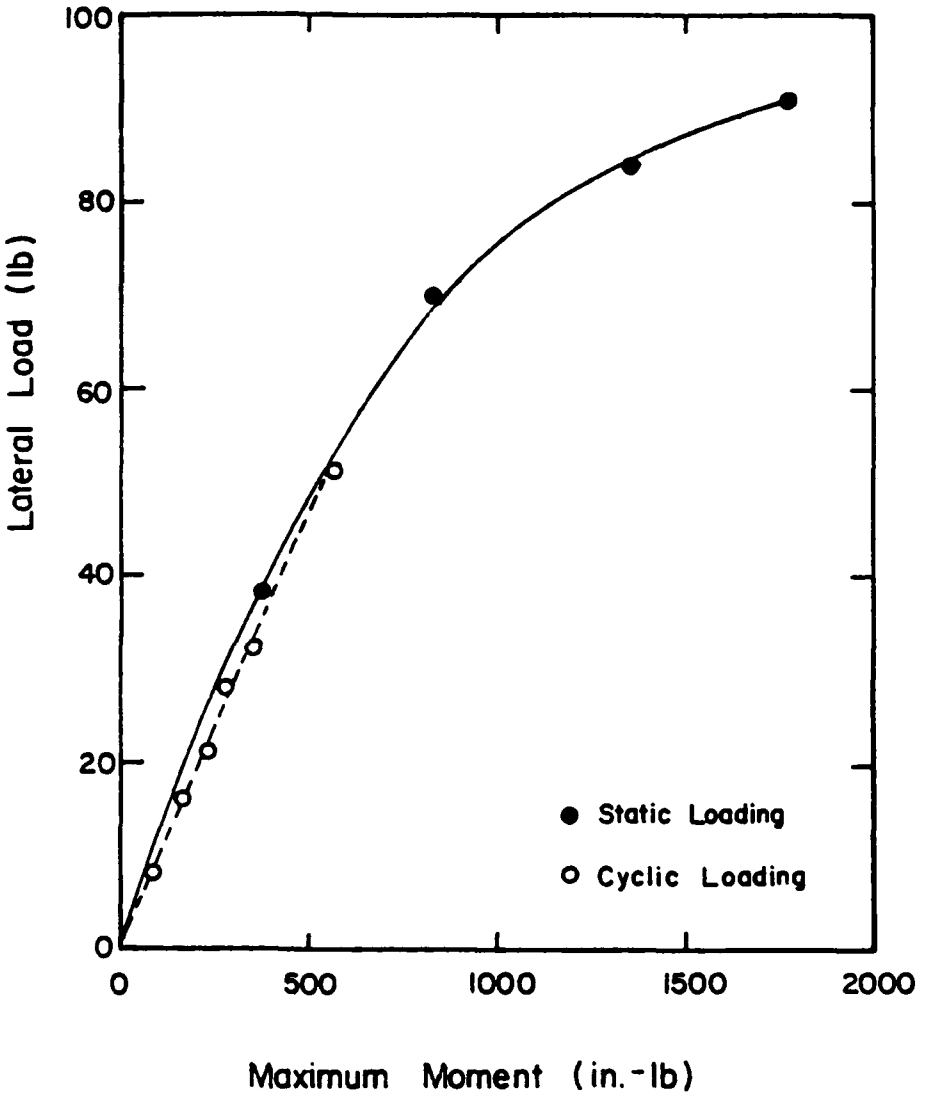

FIG. 3.4. Lateral load versus maximum moment relationship measured from tests performed by Gaul

Valenzuela and Lee (1978)

Valenzuela and Lee (1978) report results of cyclic load tests conducted on aluminum rods measuring 0.127 in. in diameter and 4.5 in. in length and embedded in a clay. These model piles had bending and material properties as presented below:

modulus of elasticity, $E = 10.0 \times 10^6$ lb/sq in.

moment of inertia, $I = 2.043 \times 10^{-4}$ in.^{4} and

bending moment at yield, $M_y = 10.36$ in.-lb.

Model piles were inserted into the soil to an embedment of 3.5 in., and lateral loads were applied to the pile head at a height of 1 in. above the soil surface. The surface of the soil was prevented from drying by covering the top with a thin layer of flexible plastic; therefore, no free water was present around the pile.

The soil, termed EPK clay, used in this study is classified as a kaolinite with 60 percent of the soil particles smaller than two microns. The liquid limit and plastic limit of the clay was determined to be 58 and 21 percent, respectively.

The soil was prepared by adding water to the clay until a soil slurry with a water content of 100 percent was obtained. The soil slurry was then poured into a 10-in. diameter one-dimensional consolidation device, and incremental vertical pressures were applied until a vertical stress of 65 lb/sq in. was achieved.

Strength properties and material characteristics of the soil were determined from the results of several laboratory tests such as triaxial compression and direct simple shear tests. From these tests, a relationship between shear strength and water content of the soil was established. Based on water content measurements, the undrained shear strength of the

clay used during the model tests was determined to be 10.7 lb/sq in., and a typical stress-strain curve for this material is shown in Fig. 3.5.

Shown in Fig. 3.6 is the curve obtained for lateral load versus lateral displacement at the ground surface for static loading. The lateral load resisted by the model pile increases sharply with lateral displacement; however, the slope of the curve decreases with increasing displacement and decreases sharply after a horizontal displacement of the pile head of about 0.1 in. A loading rate of 9.5 lbs/min was employed and according to Valenzuela and Lee (1978), the pile began to yield plastically upon reaching a horizontal deflection of 0.1 in. During loading, a gap between the pile and soil formed along the back (unloading) side of the pile, and upon unloading to a horizontal load of zero, the model pile was displaced slightly in the direction of load and a gap was formed between the front (loading) face of the pile and the soil.

Nineteen cyclic load tests of the model piles were also conducted. The cyclic loading was applied at a frequency of 1 Hz and a two-way loading condition (equal magnitude of load in both directions) to the pile head was attempted. Technical problems with the loading system caused the magnitude of the cyclic load to vary; however, the loads were observed, recorded carefully, and adjusted frequently in an attempt to minimize any large fluctuation of load during the test. After each cyclic test, the pile was removed from its testing position and inserted in another area where the effects of any previous tests were felt to be insignificant.

During the cyclic lateral-load tests, gaps between the pile and soil formed, resulting in load versus deflection curves for the top of the pile as shown in Fig. 3.7. The effect of the gap on the load-deformation relationship is most visible for cycle number 581. As lateral load is

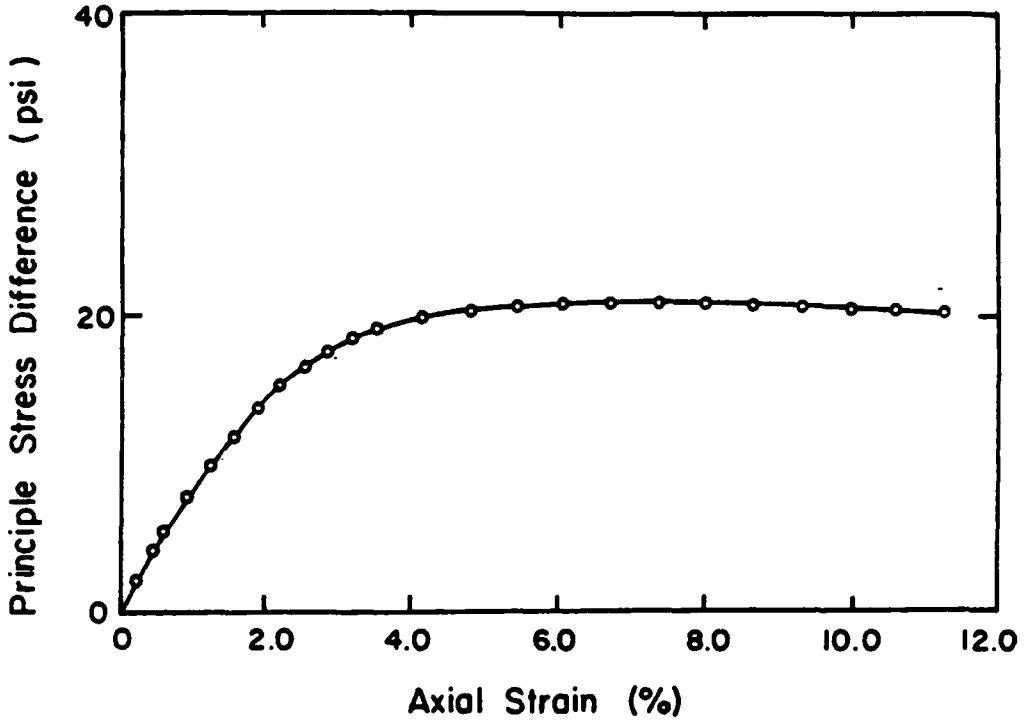

FIG. 3.5. Stress-strain curve for kaolinite soil used in the model pile test series

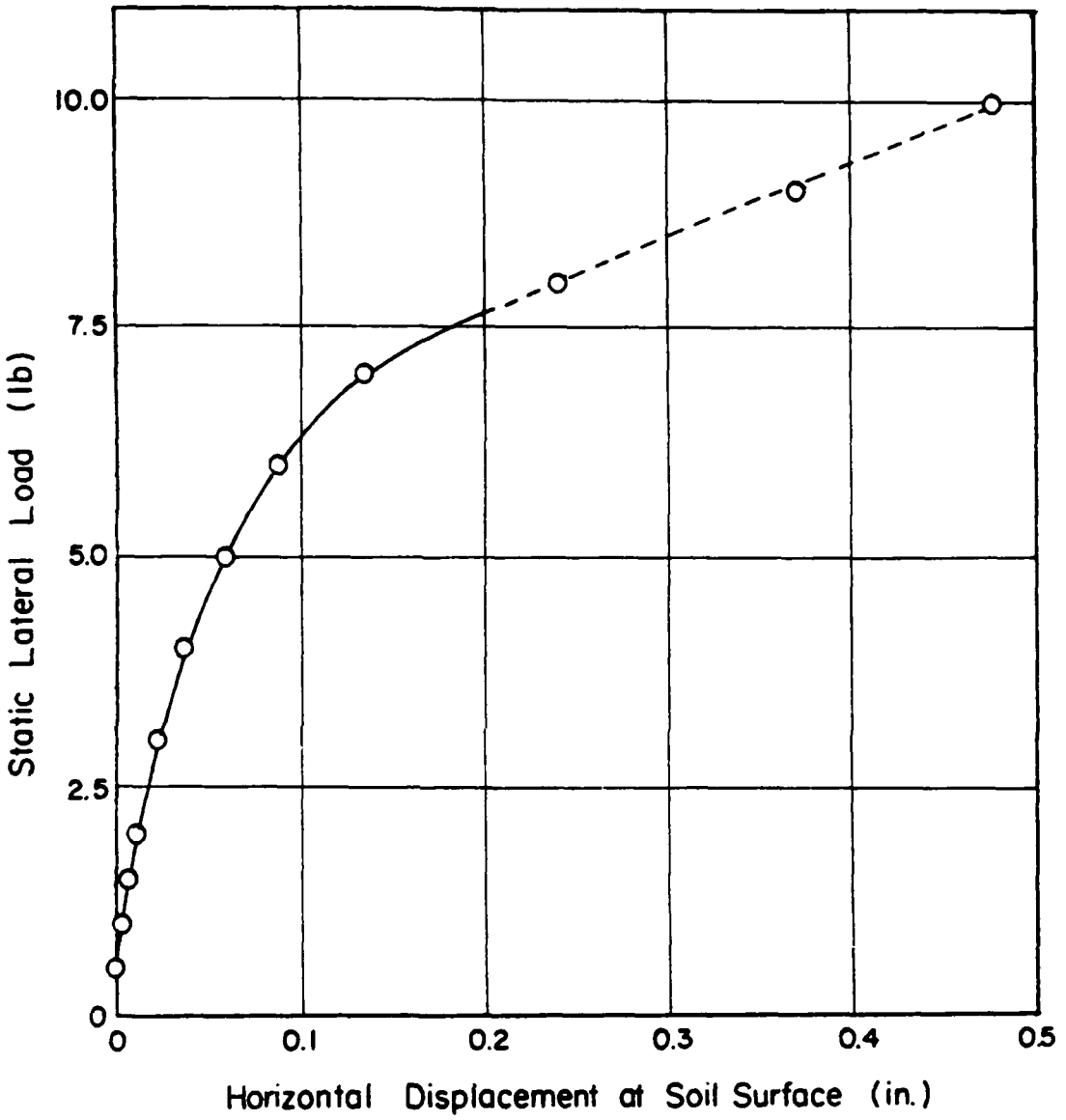

FIG. 3.6. Lateral load versus deflection relationship measured for static loading performed by Valenzuela and Lee (from Valenzuela and Lee, 1978)

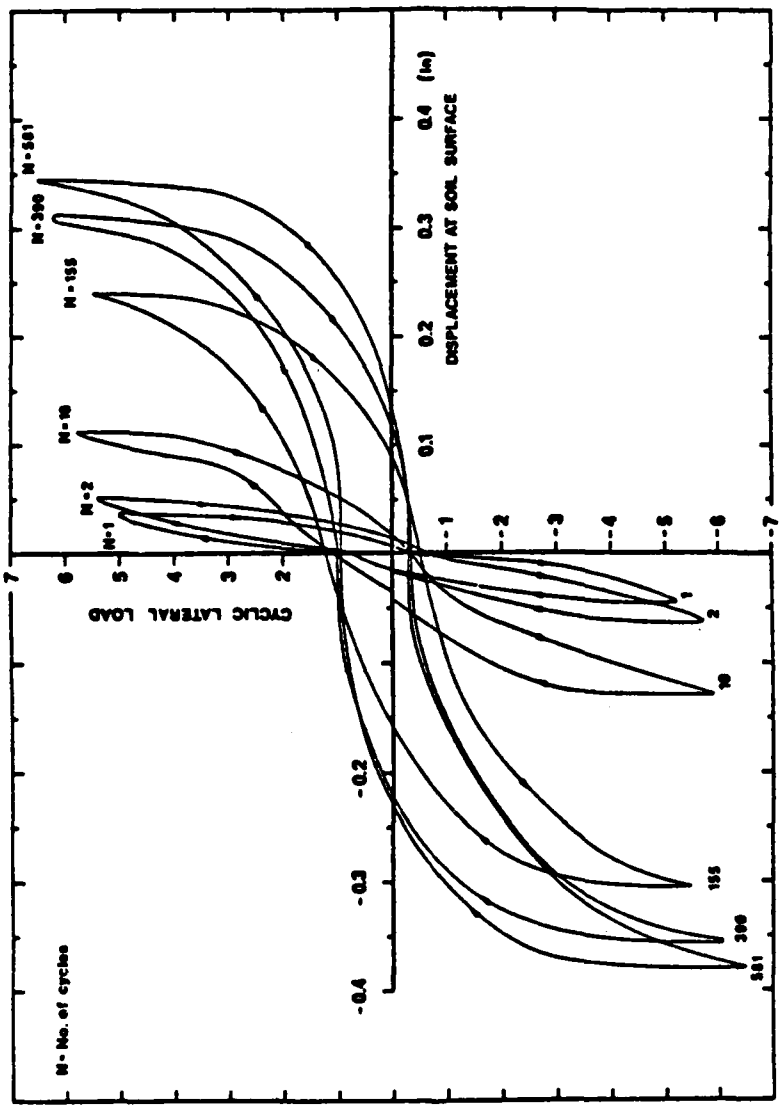

FIG. 3.7. Load versus deflection relationship measured during cyclic loading for tests performed by Valenzuela and Lee (from Valenzuela and Lee, 1978)

applied, the slope of the load-deflection curve is very flat, and remains so until a horizontal deflection of approximately 0.2 in. is reached. At this point, the gap closes and the pile wall and soil begin to come into contact. The soil begins to provide lateral resistance, resulting in a sharp increase in the slope of load-versus-deflection curve as is shown between displacement of 0.2 in. and approximately 0.35 in. Upon unloading, the lateral load drops quickly with deflection and then the slope of the load-deflection curve becomes rather flat until the gap between the soil and pile on the other side come into contact. At this point, the behavior of the pile is very similar (but opposite in direction) to the behavior previously described.

The resulting relationships between peak horizontal deflection, horizontal load, and number of cycles measured during the lateral load testing program are summarized in Figs. 3.8 and 3.9. In Fig. 3.8 is shown the relationship of peak load versus peak deformation for various cycle numbers. As can be seen, the effect of cycling at a constant magnitude of peak load is to increase the peak deflection of the pile head. In addition, it is shown that for 1 and 2 cycles of load, the curve of peak load versus deflection is stiffer than the curve obtained during the static tests. This difference may be due to the different rates of loading employed for the cyclic tests and the static tests.

Shown in Fig. 3.9 are the normalized values of peak displacement versus the number of cycles. Magnitudes of lateral deflection (y) were normalized by dividing the value of y by the diameter (d) of the pile. In general, it can be seen that as the value of y/d increases, the slope of the curve of y/d versus number of cycles has a slight tendency to increase. In addition it can also be seen that for the lower values of

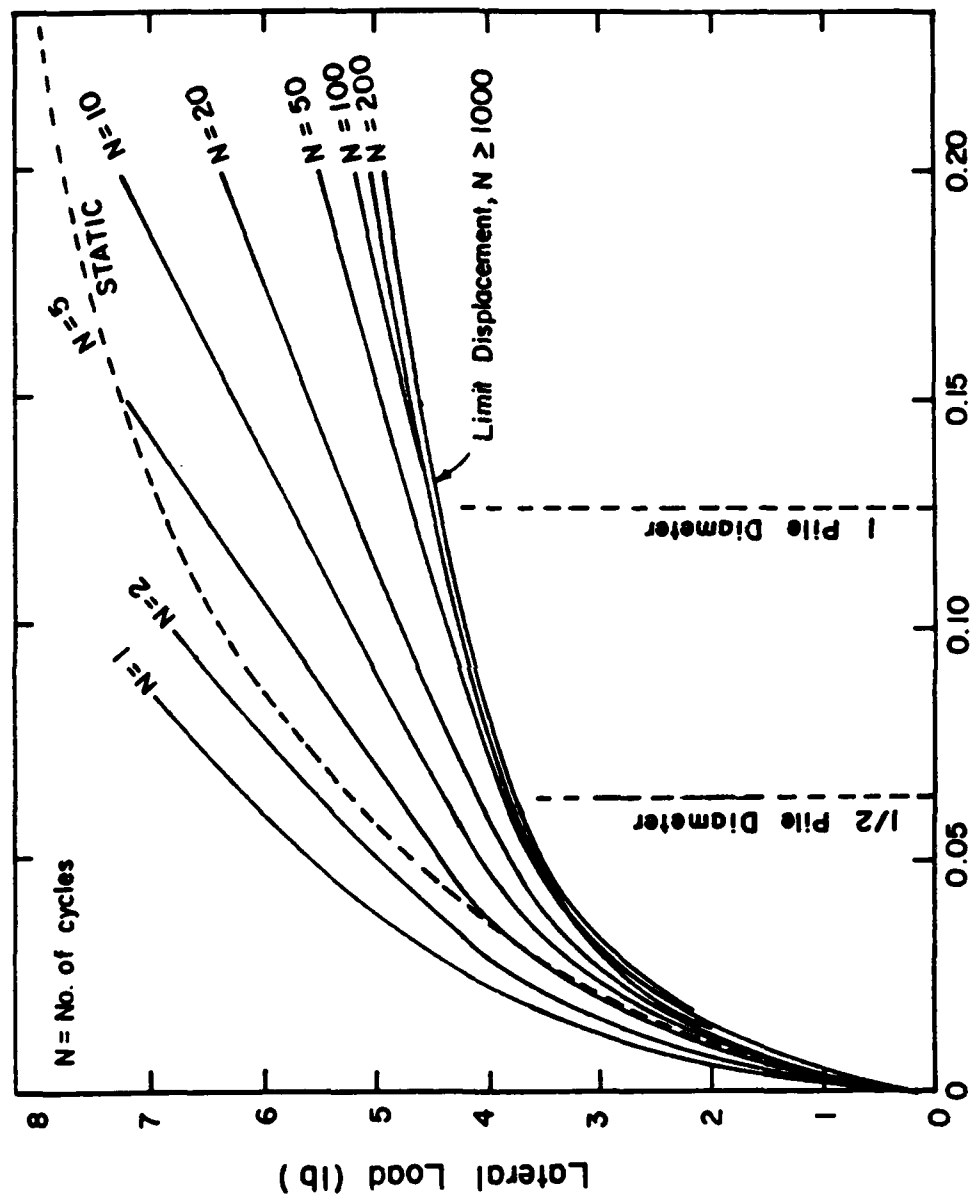

FIG. 3.8. Load versus deflection relationship at pile head for static and cyclic loading measured by Valenzuela and Lee (from Valenzuela and Lee, 1978)

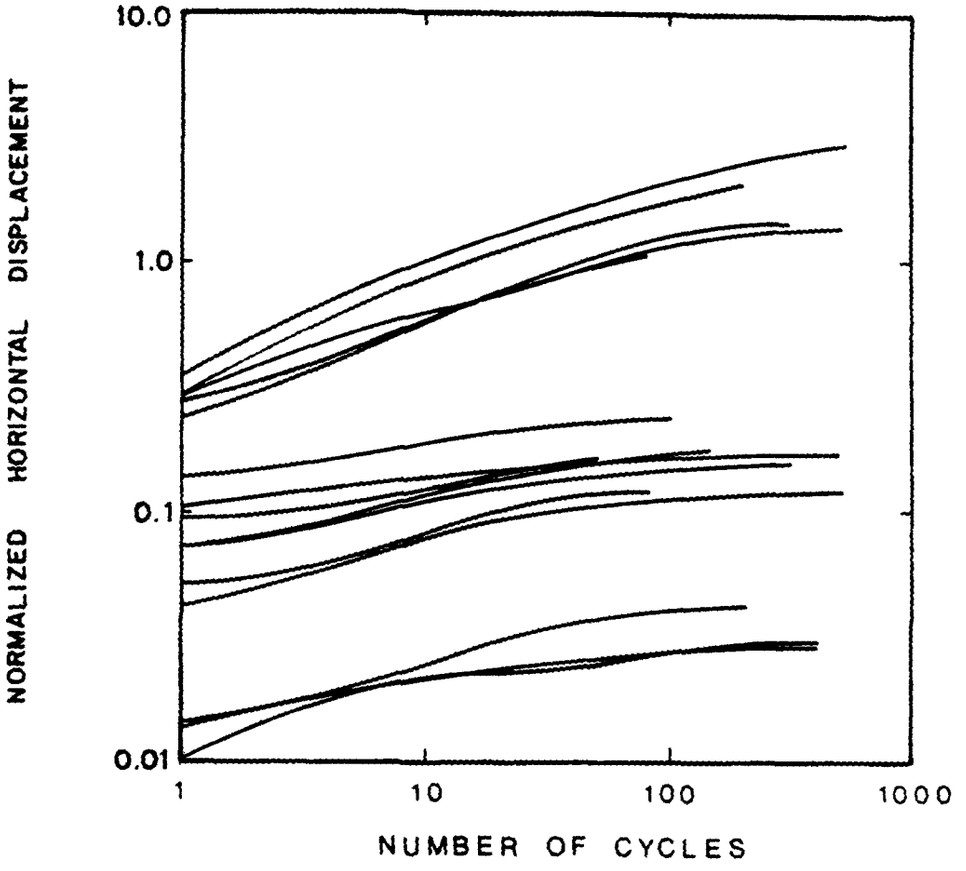

FIG. 3.9. Normalized deflection versus number of cycles relationship measured by Valenzuela and Lee

y/d, there is a tendency of the y/d curve to flatten out and become nearly horizontal.

Scott (1977)

In studies conducted on a model pile in a centrifuge, Scott applied cyclic lateral loads to a model pile embedded in Santa Barbara silt. The tests were performed in a centrifuge and cyclic loading at the top of the pile was applied under two conditions, with the free water surface above the level of silt and with dry soil. Scott reports that the water flowing in and out of the gaps formed at the front and back of the pile tended to mix with the soil and contributed to the softening of soil adjacent to the pile.

Other results found in the study by Scott are not presented, because the study was more oriented toward the behavior of piles in sand. However, the main point presented here is that the water surface was shown to effect the behavior of the pile by entering the gap and mixing with the soil.

FIELD TESTS

Price (1979), Price and Wardle (1980)

The results of several carefully conducted lateral load tests were presented by Price (1979), and Price and Wardle (1980). In these tests, several different lateral loadings were applied to both a single pile and a group of three piles. The magnitude of lateral loading was small in comparison to the ultimate load, because the investigators were interested primarily in the behavior at working loads.

The piles used in this investigation measured 6.6 in. in diameter and 16.7 ft in length; however, no information regarding the bending proper-

ties or thickness of the tubular steel piles was provided. The piles were hydraulically jacked into the ground to an embedment of 15.1 ft; however, a portion of the ground surface around the pile was subsequently removed, resulting in an embedment of 13.6 ft. The point of load application was 3.1 ft above the ground surface.

Several laboratory and in situ investigations were employed to determine the strength characteristics and the stress-strain properties of the weathered, over-consolidated clay. Results of the tests are shown in Fig. 3.10. As can be seen, the strength and modulus of the clay are shown to increase with depth from the ground surface to a depth of 16 ft. The position of the water table was not reported; therefore, it was assumed to be below the ground surface.

Several lateral load tests were conducted on the piles; however, only the results of the controlled-stress cyclic test are discussed herein. In this test, a static lateral load was applied to the pile head, followed by several cycles of lateral load. At the end of the cyclic testing, another static load was applied. The values of deflection at the groundline corresponding to this test are shown below.

Horizontal Deflection (in.)	Test Description
0.0249	static deflection at 450 lb horizontal load (before cyclic testing)
0.0258	deflection at first cycle of ± 450 lb horizontal load
0.0285	deflection on last cycle of ± 450 lb horizontal load (400 cycles)
0.0307	static deflection at 450 lb horizontal load (after cyclic testing)

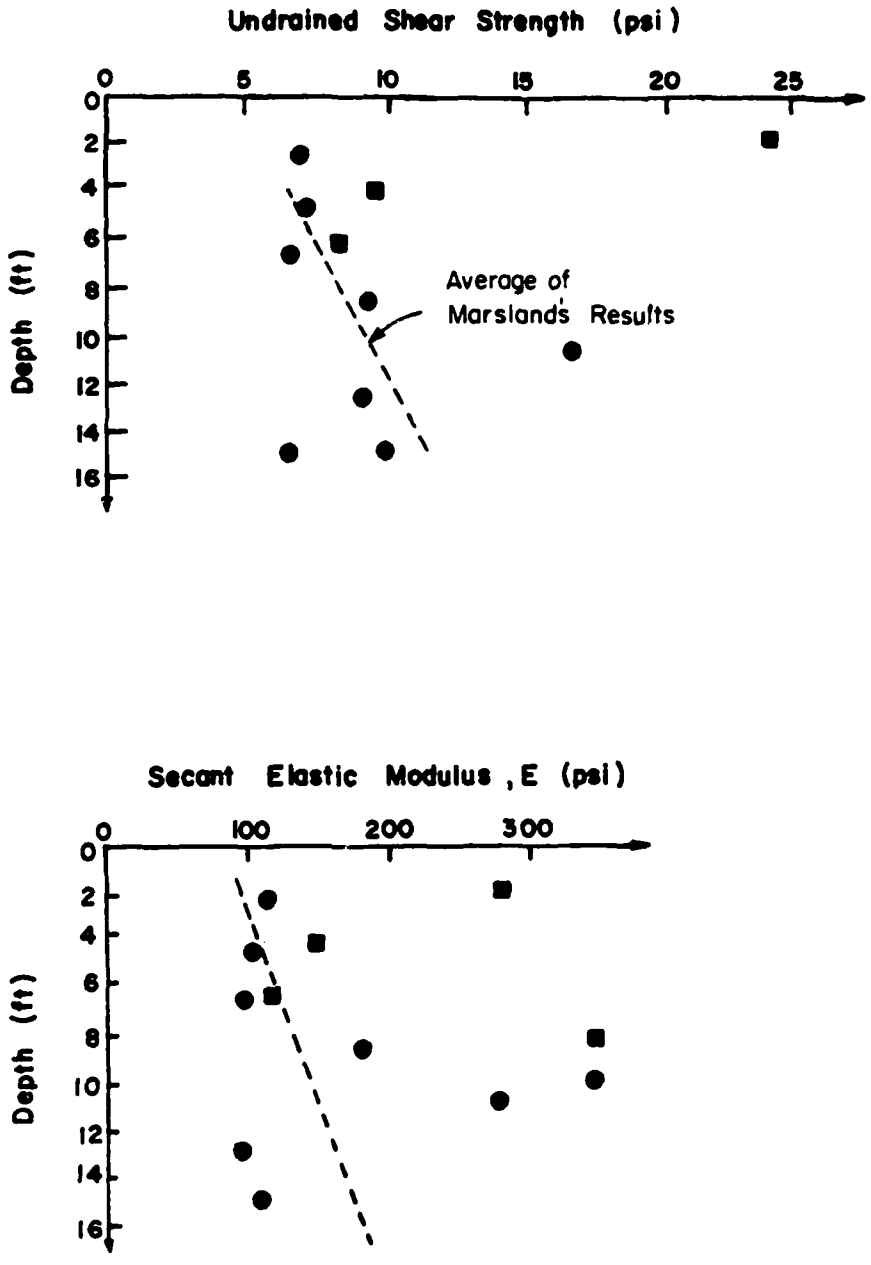

FIG. 3.10. Values of shear strength and soil modulus at test site used by Price and Wardle (from Price and Wardle, 1982)

From the results presented above, it is seen that after 400 cycles of loading, the horizontal deflection increased approximately ten percent of its deflection measured on the first cycle. It is important to emphasize that the effect of cyclic loading was measured even though the relative horizontal displacement (y/d) is regarded to be small (approximately 0.004).

Price and Wardle (1982)

In a series of cyclic lateral load tests conducted by Price and Wardle (1982), two differently shaped piles were tested at low levels (with respect to the ultimate lateral load) of horizontal loads.

The two pile types were specified as tubular and H-shaped. Properties of the two sections are shown in Table 3.1.

TABLE 3.1. PROPERTIES OF TEST PILES, (Price and Wardle, 1982)

Section	Wall Thickness (in.)	Moment of Inertia ($in.^4$)	Buried Length (ft)
Tubular (16.0 in. dia.)	0.394	588	54.1
H (14.7 x 13.9)	0.614	909	68.9

After driving a pile, the top 3.28 ft of soil was removed, and loading was applied to the pile head at a height of 3.28 ft above the newly exposed ground surface. Cyclic, controlled-stress loadings were applied to single piles of both the tubular and H shapes. The resulting deflections measured for the static tests, and at the first and last cycles during the cyclic tests are shown in Table 3.2. For a cyclic lat-

TABLE 3.2. RESULTS OF STATIC AND CYCLIC LATERAL LOAD TESTS ON TUBULAR AND H-SHAPED PILES (from Price and Wardle, 1981)

No.	Test Type	Lateral Load (lb)	Applied No. of Cycles	Pile Head Displacement	
				at start (in.)	at end (in.)
Tubular pile					
1	static	4490	---	0.0886	
2	cyclic	2245	142	0.0394	0.0370
3	cyclic	3370	135	0.0610	0.0626
4	cyclic	4490	216	0.0827	0.0850
5	static	4490	---	0.0898	
6	static	4490	---	0.0827	
7	cyclic	4490	339	0.0772	0.0827
8	static	8980	---	0.2142	
9	cyclic	8980	936	0.2071	0.2472
10	static	13470	---	0.4606	
11	cyclic	13470	337	0.4181	0.4299
12	static	22450	---	1.2874	
13	cyclic	19085	237	0.8992	0.9469
H-Pile Results					
14	static	4490	---	0.1236	
15	cyclic	4490	503	0.1142	0.1205
16	static	8980	---	0.3008	
17	cyclic	8980	282	0.2819	0.3421
18	static	8980	---	0.3543	
24	cyclic	17960	211	0.7244	0.7937
25	static	8980	---	0.4063	

eral load of 8,980 lbs, the values of normalized deflection versus number of cycles is shown in Fig. 3.11.

Several observations can be made from the results presented in Table 3.2. For most of the tests, the horizontal deflection increased as a result of cyclic loading. In addition, for test sequences in which a static load test was followed by a cyclic load test, the magnitude of horizontal deflection for the first and last cycle of load were often less than the magnitude of deflection measured during the static test. This result is due to the different loading rates used for the static and cyclic tests.

The results of the cyclic load tests conducted on the H-shaped and tubular-shaped piles are shown in Fig. 3.11. Values of normalized displacement versus number of cycles are plotted for a cyclic load of 8980 lb. The curves fitted through the data exhibit similar slopes; however, the H-shaped pile showed a higher value of normalized deflection than did the tubular-shaped pile.

U.S. Naval Civil Engineering Lab (1964)

In 1964, the results of a number of cyclic lateral-load tests were reported by the U.S. Naval Civil Engineering Laboratory. It was intended to measure the variation of soil pressures during lateral loading; thus, specially shaped pile cross sections were fabricated and earth pressure cells were installed on the face of the pile.

The piles were 14-in. 16 WF 36 steel sections with the web boxed in by steel plates welded or bolted to the edges of the flanges. Holes were cut along the length of the steel plate, and pressure cells were installed flush with the outside surface of the pile.

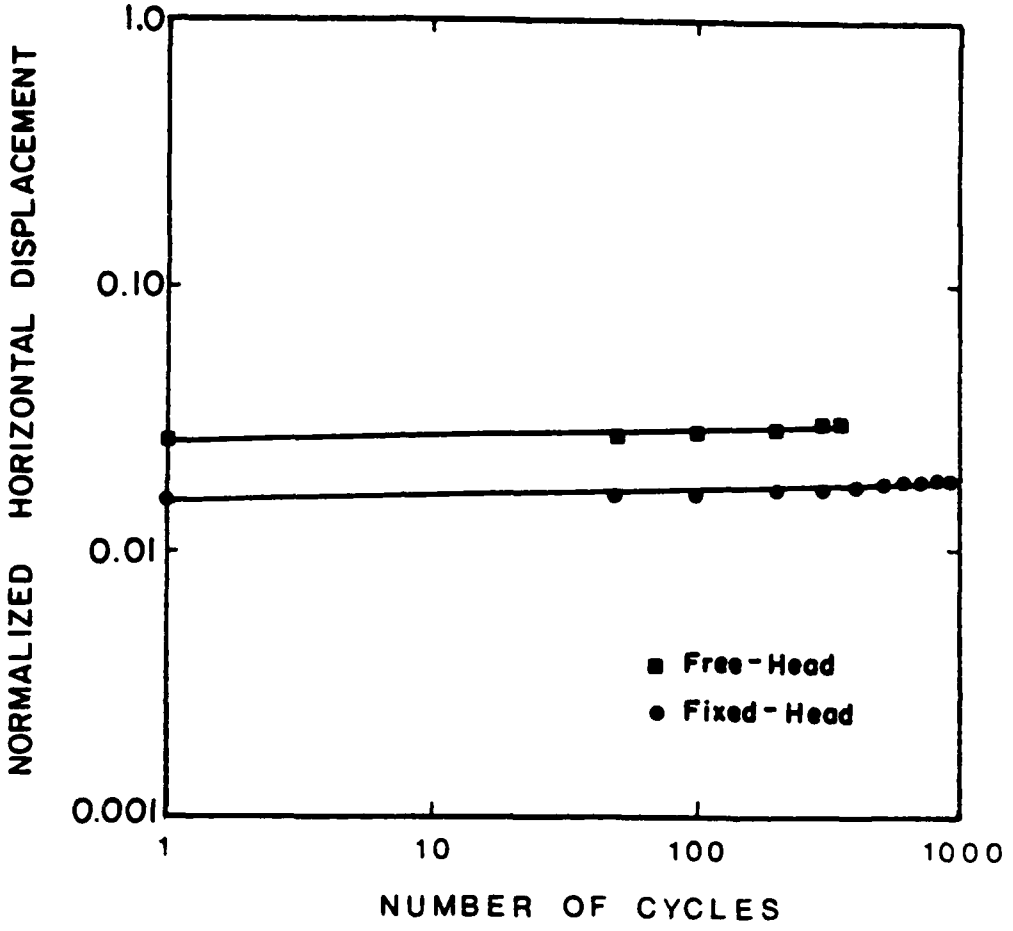

FIG. 3.11. Normalized deflection versus number of cycles relationship for tests conducted by Price and Wardle (1982)

A total of five instrumented piles were used in the testing program. Each of the piles had slightly different structural and geometric properties, and are listed in Table 3.3. Some of the pile tests were conducted with fixed head conditions while other tests simulated fixed head conditions.

The properties of the cohesive soil surrounding the pile varied considerably. Due to seasonal moisture changes in the upper layers of soil, an attempt was made to identify the soil conditions before every test. This usually consisted of obtaining soil specimens from which water contents and undrained strength tests were measured. The testing program was conducted over a period of time exceeding two years; therefore, seasonal variations of water content in the top portion of the soil occurred. Obviously, soil properties changed at shallow depths. Values of moisture content and undrained shear strength versus depth are shown in Fig. 3.12. The data exhibit significant variations in water content, shear strength and blows per foot (N values) in the upper few feet of the clay deposit; however, in an average sense, values of shear strength in the upper layer are approximately 5 to 10 lb/sq in. at the ground surface, decreasing to a value of 2 lb/sq in. at a depth of 10 ft.

Of all the data presented in the USNCEL report, the data investigated and presented here are those obtained from the cyclic pile tests. Several reasons exist why other data was not used; however, the main reason is due to the seasonal variations in soil conditions. Cyclic loadings were typically tested in an elapsed time of one to two days; thus, little change in soil properties due to seasonal variations were expected.

TABLE 3.3. GEOMETRIC AND MATERIAL PROPERTIES OF PILES AT USNCEL SITE

Number	Length ft	EI 10^8 lb-sq in.	Method of Pressure Measurement	Spacing of Pressure Measurement ft	Spacing of Deflection Measurement ft
1	40	23.0 to 29.2	Fluid-filled gauges	5	1 and 5
2	40	11.5	Fluid-filled-gauges	Variable 1 to 5	Variable 1 to 5

TABLE 3.4. LIST OF CYCLIC PILE TESTS PERFORMED AT USNCEL REPORT

Pile	Date	Load	Number of Cycles	Head Condition
1	28 June 1957	3,000	500	Free
2	23 July 1958	5,000	500	Free
2	29 Oct. 1958	10,000	500	Free
2	1 Oct. 1958	5,000	500	Fixed
2	26 Nov. 1958	10,000	500	Fixed

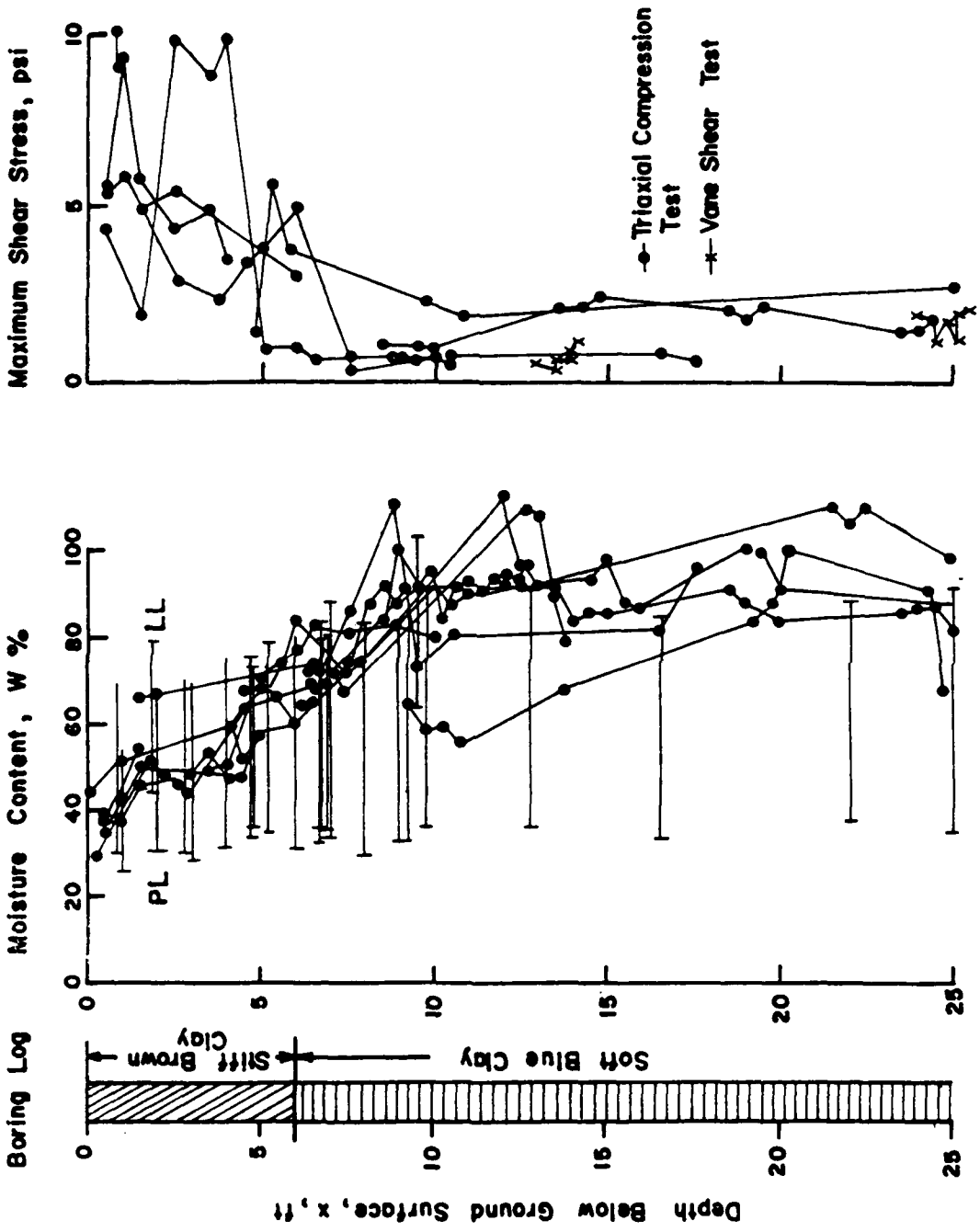

FIG. 3.12. Soil profile and strength characteristics of site tested by U.S. Navy Civil Engineering Laboratory

Shown in Table 3.4 is a list of the cyclic load tests that were carried out, and the results of those load tests, in the form of normalized deflection versus number of cycles, as shown in Fig. 3.13.

Gilbert (1980)

Cyclic lateral load tests were conducted in Louisiana by Gilbert (1980) on two rocket-shaped piles. The large piles were driven into very soft clay and tested both statically and cyclically. Values of moment and slope versus depth were measured as well as groundline deflection. Some pertinent data and the results obtained from the lateral load testing program are presented below.

Two tapered piles were used in this investigation. The first pile, termed pile A , had an octagonally-shaped cross section, and was 44 ft in length. The diameter at the top of the pile was 33 in. and the diameter at the bottom was 22 in. The second pile, pile B, was similar in shape and length to pile A; however, pieces of triangular-shaped plate steel were welded along the upper 20 ft of the pile, as shown in Fig. 3.14. Because the piles were tapered, the values of EI varied with depth. Values of EI determined by Gilbert are shown in Fig. 3.15. The two piles were driven into the ground by a 3000 lb drop hammer.

The soil surrounding the piles was investigated by testing specimens taken from two soil borings. Water content, undrained shear strength and total unit weight versus depth are shown in Fig. 3.16. The site investigation revealed that the upper 15 ft consists primarily of very soft coarse to medium textured fibrous peat. Underlying the peat layer is approximately 40 ft of normally consolidated, very soft to soft clay. The data on water content versus depth reveal water contents in excess of 250 percent in the top 10 ft of the peat deposit. Data on undrained strength

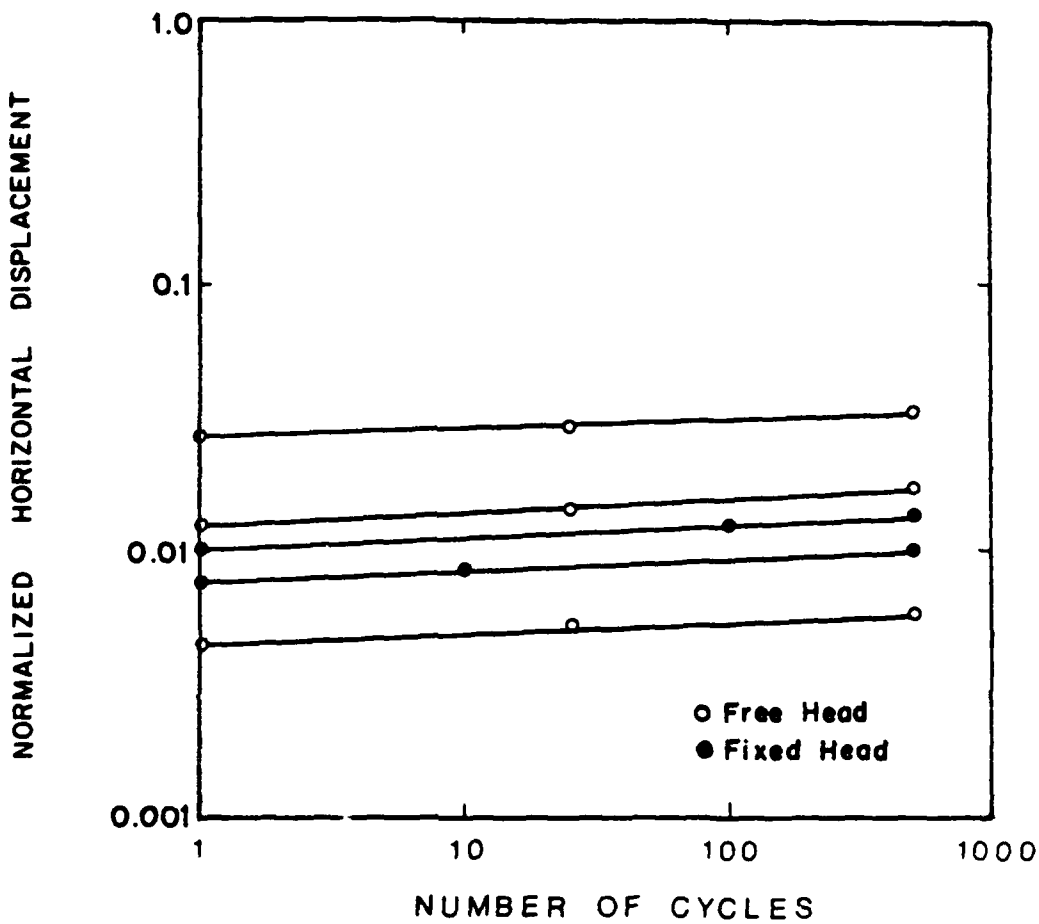

FIG. 3.13. Normalized deflection versus number of cycles for tests performed by U.S. Navy Civil Engineering Laboratory

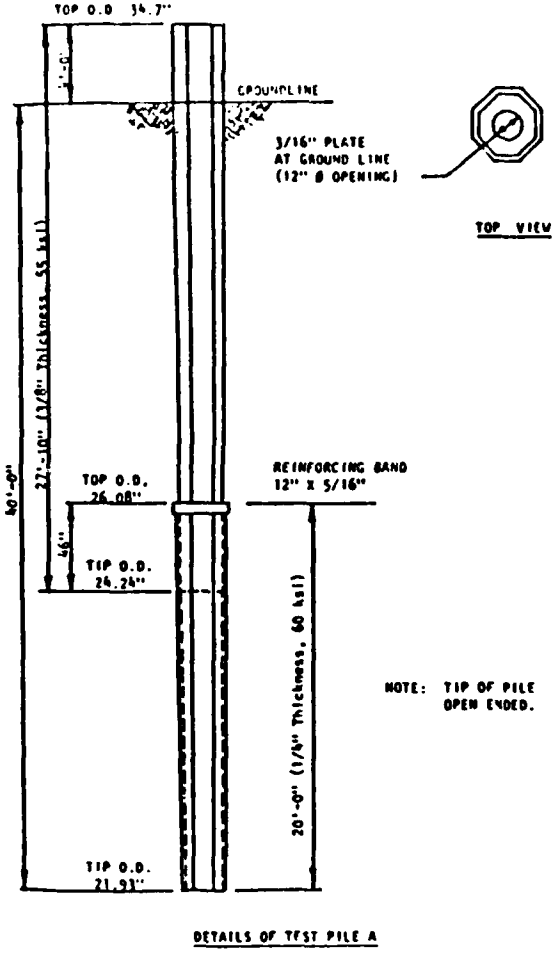

DETAILS OF TEST PILE A

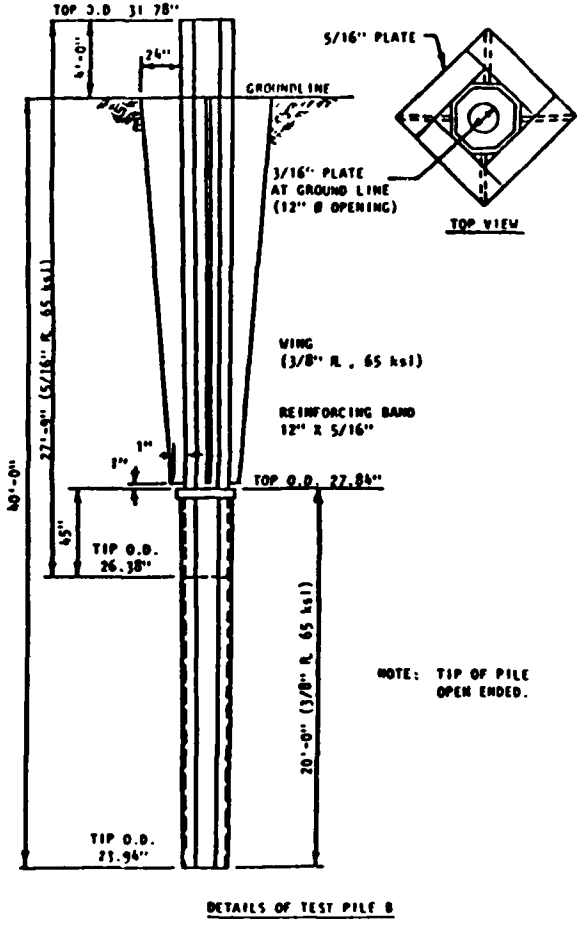

DETAILS OF TEST PILE B

FIG. 3.14. Details of pile A and pile B used at Chalmette, Louisiana (from Gilbert, 1980)

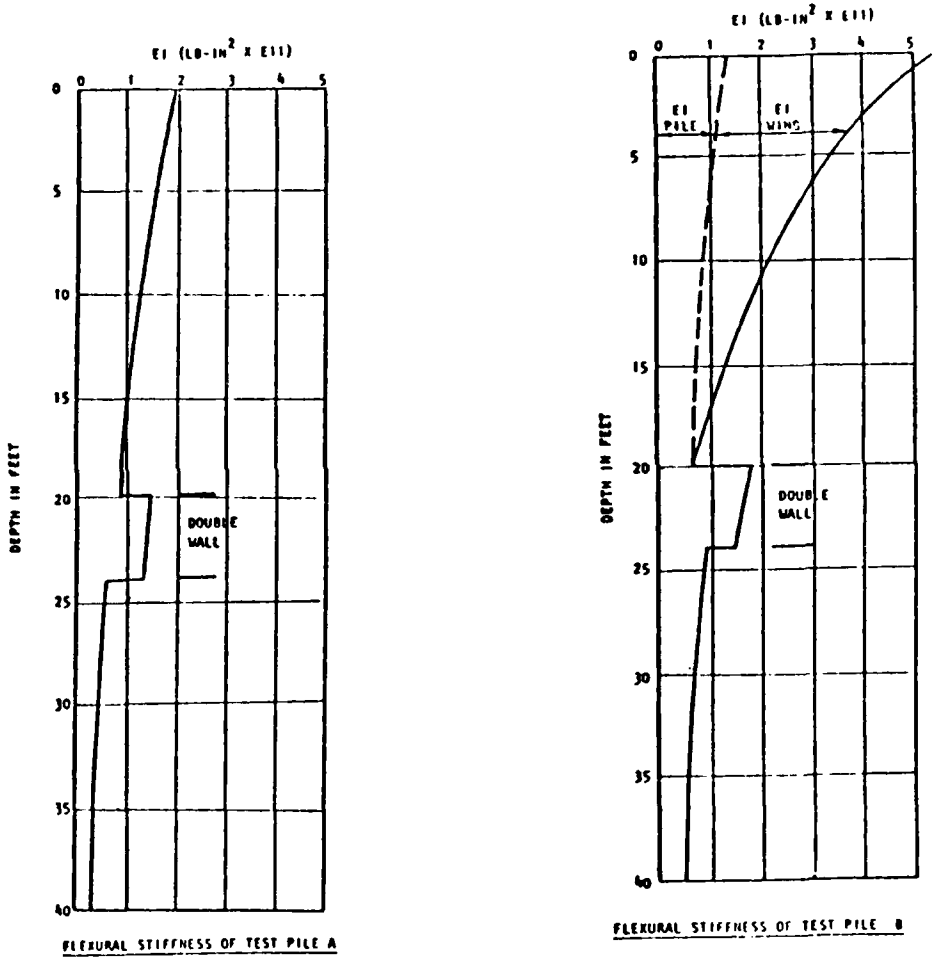

FIG. 3.15. Variation of flexural stiffness of pile A and pile B at Chalmette, Louisiana (from Gilbert, 1980)

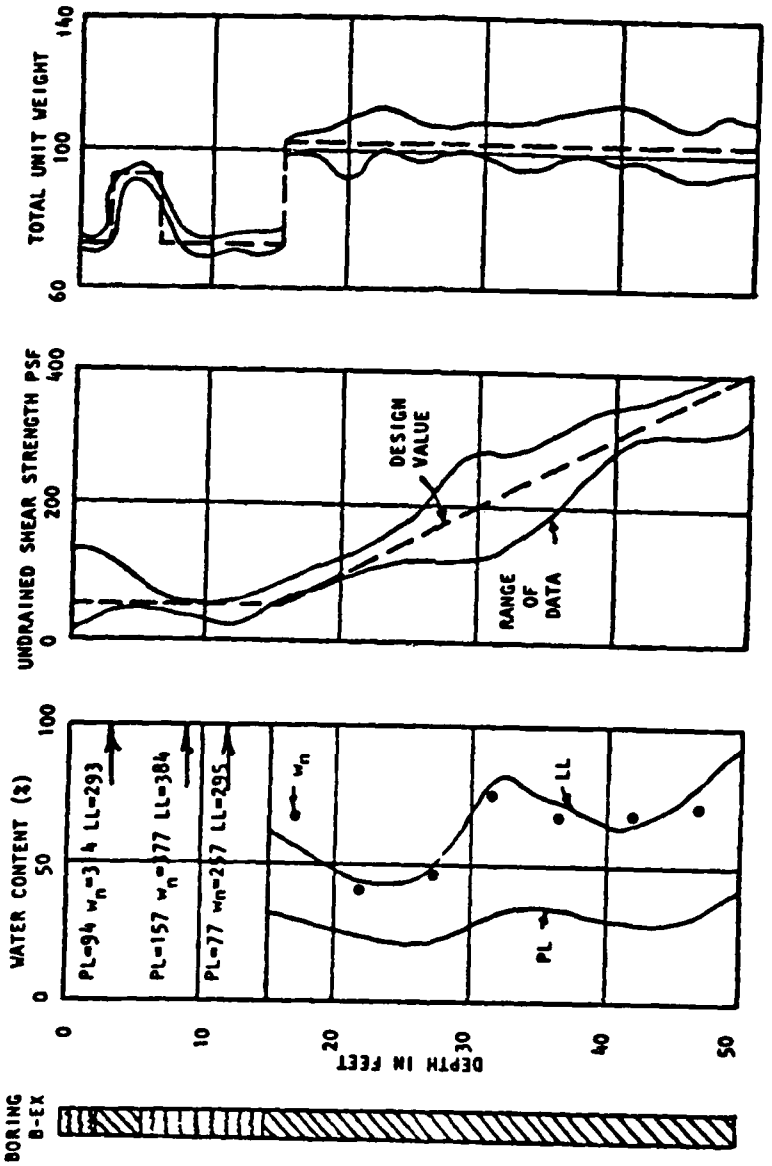

FIG. 3.16. Soil profile and properties at the Chalmette site (from Gilbert, 1980)

suggest values of shear strength in the range of 50 lbs/sq ft within the top 10 ft. Additionally, the water table was reported to be at or above the groundline; however, no mention was made if the water was available to enter and exit a gap between the pile face and the soil.

After the piles were driven, they were allowed to stand for about one week before testing. A pull pole, 59 ft in length, was attached vertically to the top of the pile and a 300-ft cable was attached, to the top of the pull pole and connected to the winch of a crane. A load cell was attached to the cable, and during loadings the crane operator could control the load at the top of the pile by observing the load cell output. Control of the load to +/- 50 lb was reported.

The loading schedule was similar for both piles. First a static load was applied for one hour, or until lateral movement ceased; then cyclic loading began. The cyclic loadings were performed by unloading to one-half the current static load and then reloading to the current value of load again. This cycling was performed 25 times at a frequency of four cycles per minute (or 15 sec per cycle). Shown in Fig. 3.17 are the load-versus-deflection curves for both static and cyclic loading.

In addition to the values of deflection at the start and at the end of each level of cycling, one curve of deflection versus number of cycles was presented. Shown in Fig. 3.18 is the increase in deflection with number of cycles seen for Pile A at a cyclic load varying between 7.5 kips and 15 kips. The slope of the curve is much less than the slopes exhibited in figures presented earlier of normalized deflection versus number of cycles. Thus, it may be interpreted that the effect of cyclic loading experienced here is less than exhibited in the previous case histories.

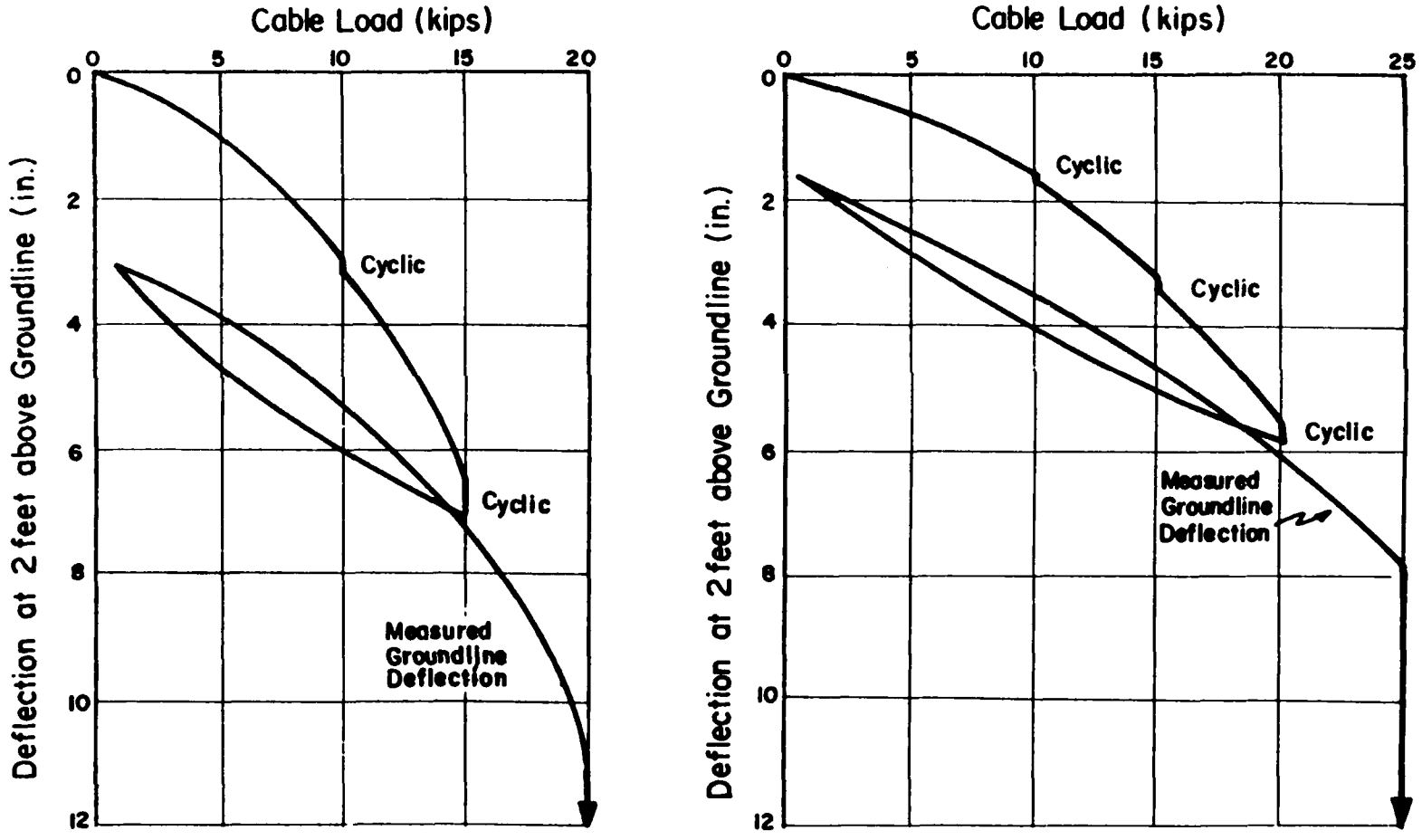

FIG. 3.17. Load versus deflection relationship for the two test piles at Chalmette, Louisiana (from Gilbert, 1980)

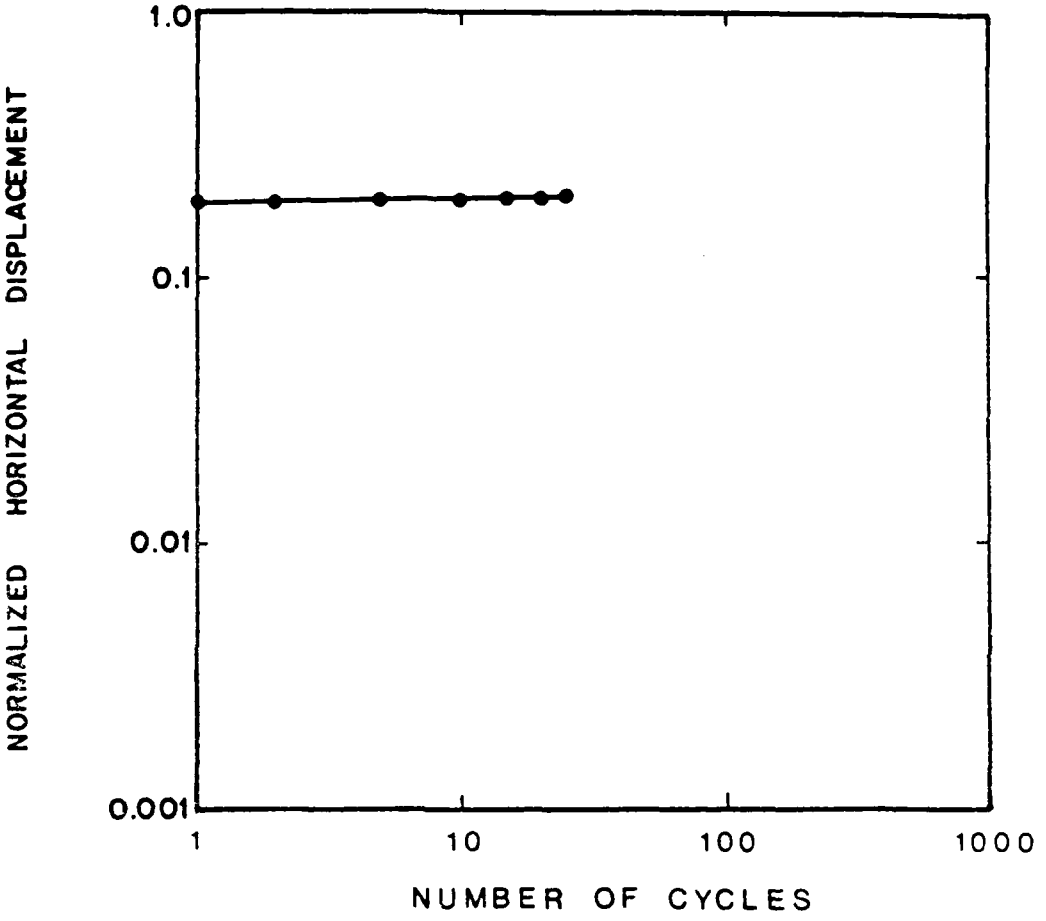

FIG. 3.18. Normalized lateral deflection versus number of cycles at Chalmette, Louisiana

Tassios and Levendis (1974)

The results of several static and cyclic lateral load tests are reported by Tassios and Levendis (1974). These tests were performed on 24 Franki piles located in France.

Although information regarding the characteristics of pile material is not presented, the piles were 20.5 in. in diameter, 32.8 ft in length, and circular in cross section. The piles were tested by jacking apart two adjacent piles. Each cycle of loading took approximately 10 minutes.

The soil was described as a uniform clay, and the soil characteristics were found from laboratory and in situ testing techniques and are presented in Fig. 3.19.

Two types of cyclic-loading tests were conducted. In the first series of tests on two piles, one-way cyclic loading was applied to the head of the pile for maximum values of lateral load of 4.4 kips, 8.8 kips, and 13.2 kips. The results of the tests on two separate piles at a lateral load varying cyclically from zero to 13.2 kips is shown in Fig. 3.20. In addition, two-way cyclic loading was used for a series of piles and the results of these tests are shown in Fig. 3.21 for a lateral load of +/- 13.2 kips. It can readily be seen that the horizontal displacement increases with number of cycles for both cases presented in Figs. 3.20 and 3.21. Additionally, it is important to note the difference between the two curves plotted in each figure. In Fig. 3.20, lateral deflections of Pile D are shown to be 10 to 20 percent greater than measured lateral deflections of Pile G. These differences are attributed to small variations in construction procedure and soil conditions; however, it was attempted to construct the piles in an identical manner and the soil conditions were not expected to vary significantly between piles.

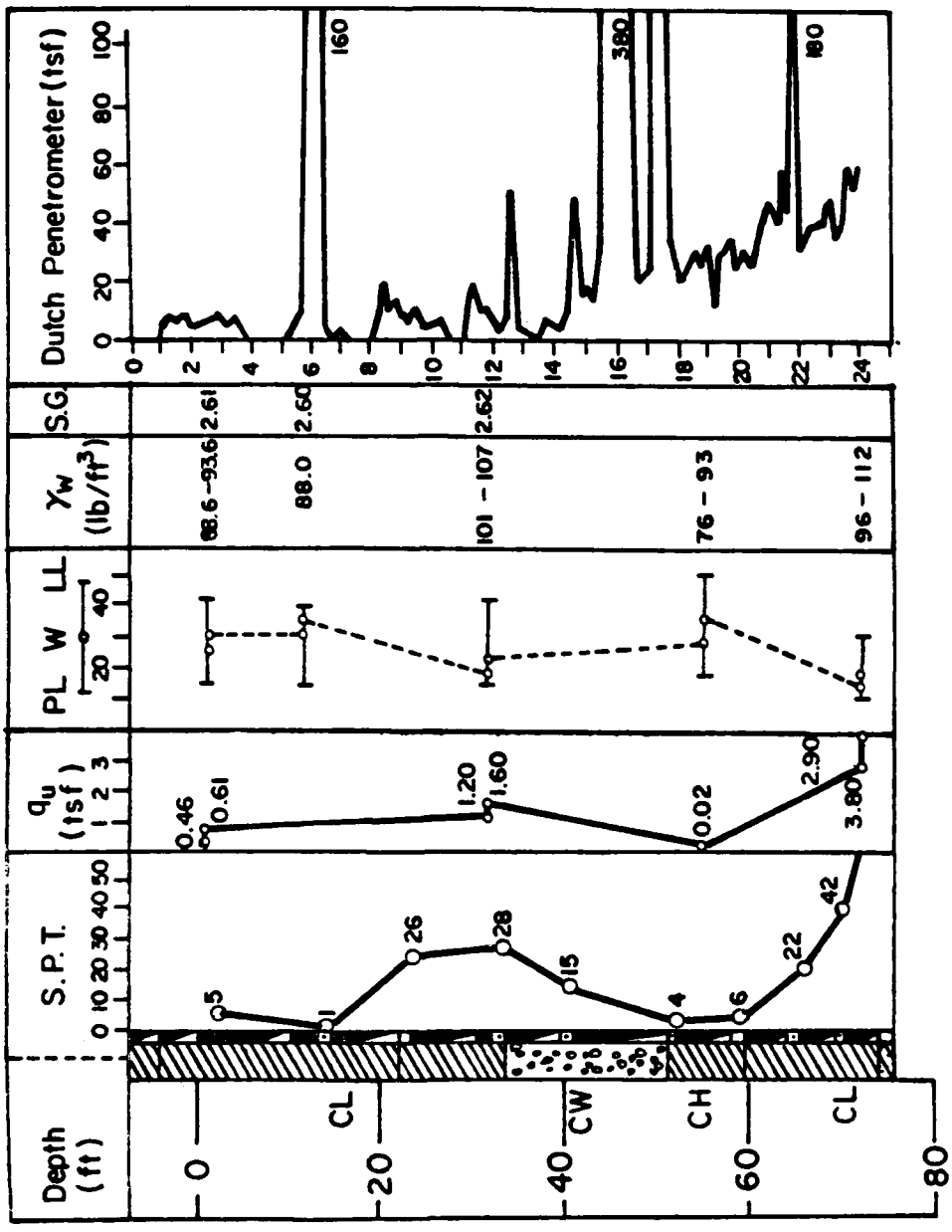

FIG. 3.19. Soil profile at site tested by Tassios and Levendis (1974)

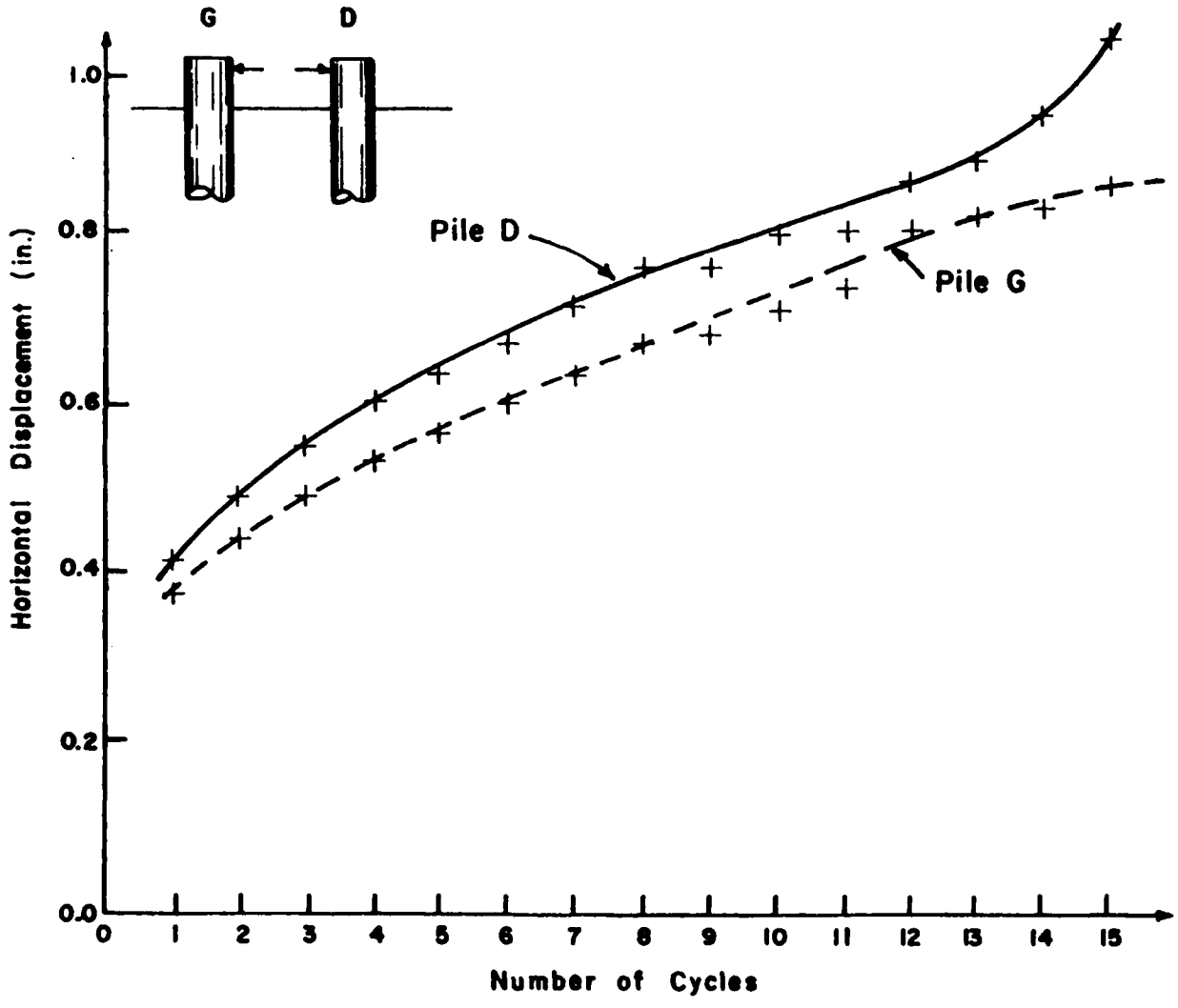

FIG. 3.20. Horizontal displacement versus number of cycles for piles subjected to a 13,200 lb one-way cyclic loading (from Tassios and Levendis, 1974)

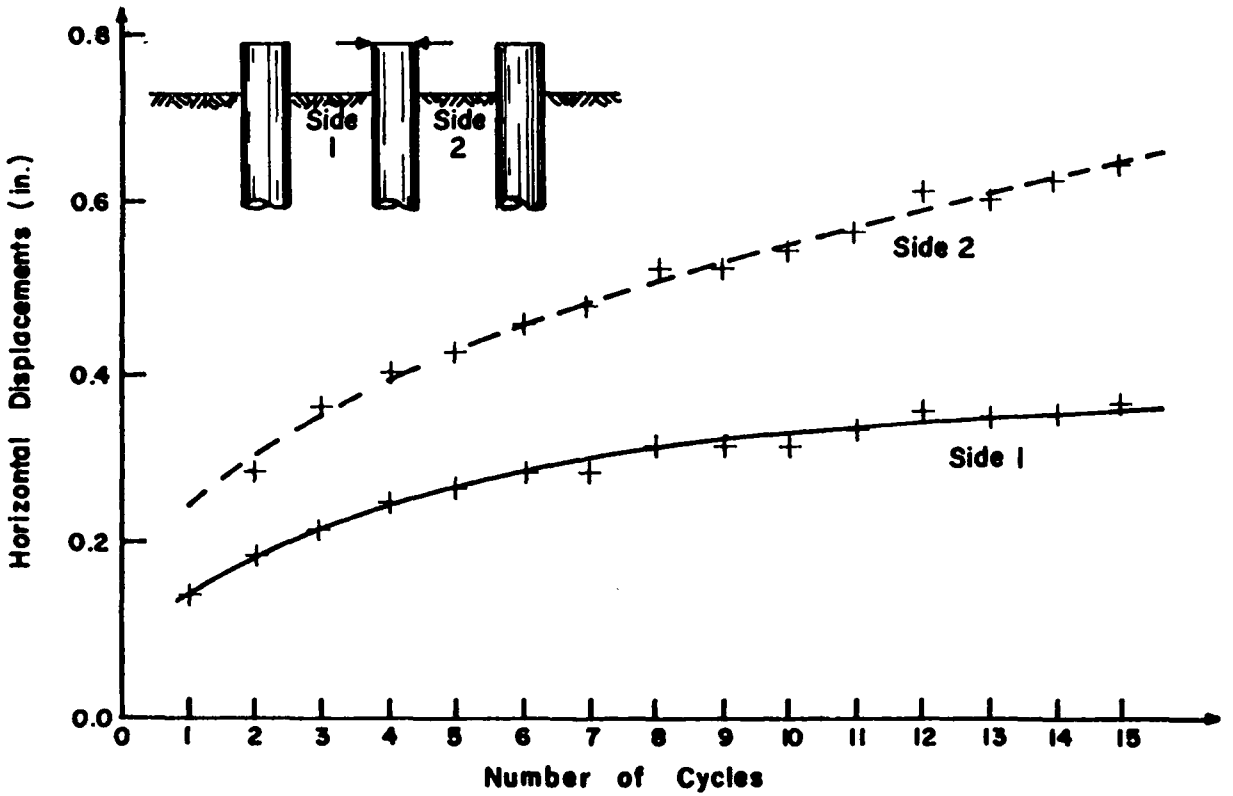

FIG. 3.21. Horizontal displacement versus number of cycles for a pile subjected to a 13,200 lb two-way cyclic loading (from Tassios and Levendis, 1974)

In Fig. 3.21, lateral deflections of the same pile were different depending on the direction of horizontal load. Deflections due to a load from side 1 were 50 to 100 percent greater than deflections due to a load from side 2. This difference cannot be attributed to variations in pile properties because only one pile was tested; therefore, the difference in behavior must be attributed to a variation in the soil properties due to nature, or due to installation of the test pile and the surrounding piles.

Shown in Fig. 3.22 are the curves representing the relationship between normalized horizontal displacement and number of cycles for several of the cyclic lateral load tests conducted on the piles. In this plot, it can be seen that the slope of the curves increases for higher initial values of normalized deflections.

Harvey (1980)

A cyclic, lateral-load test was conducted in Harvey, Louisiana by Matlock, et al (1980). The main scope of the research project was to determine the lateral behavior of pile groups; however, two lateral load tests, one static and one cyclic, were performed on single piles.

The soil at the site consisted of a soft gray clay with occasional thin lenses of peat, silt and sand. Several laboratory and in situ tests were performed to determine soil properties such as undrained shear strength, classification, and Atterberg limits. Shown in Fig. 3.23 is a soil and water content profile at the site. Data on soil strength are shown in Fig. 3.24 .

The piles used in this investigation were 6.625 in. in outside diameter with a wall thickness of 0.280 in. The piles were 45 ft in length with the bottom 15 ft being open-ended, leaving the top 30 ft dry and suitable for instrumentation inside the pile.

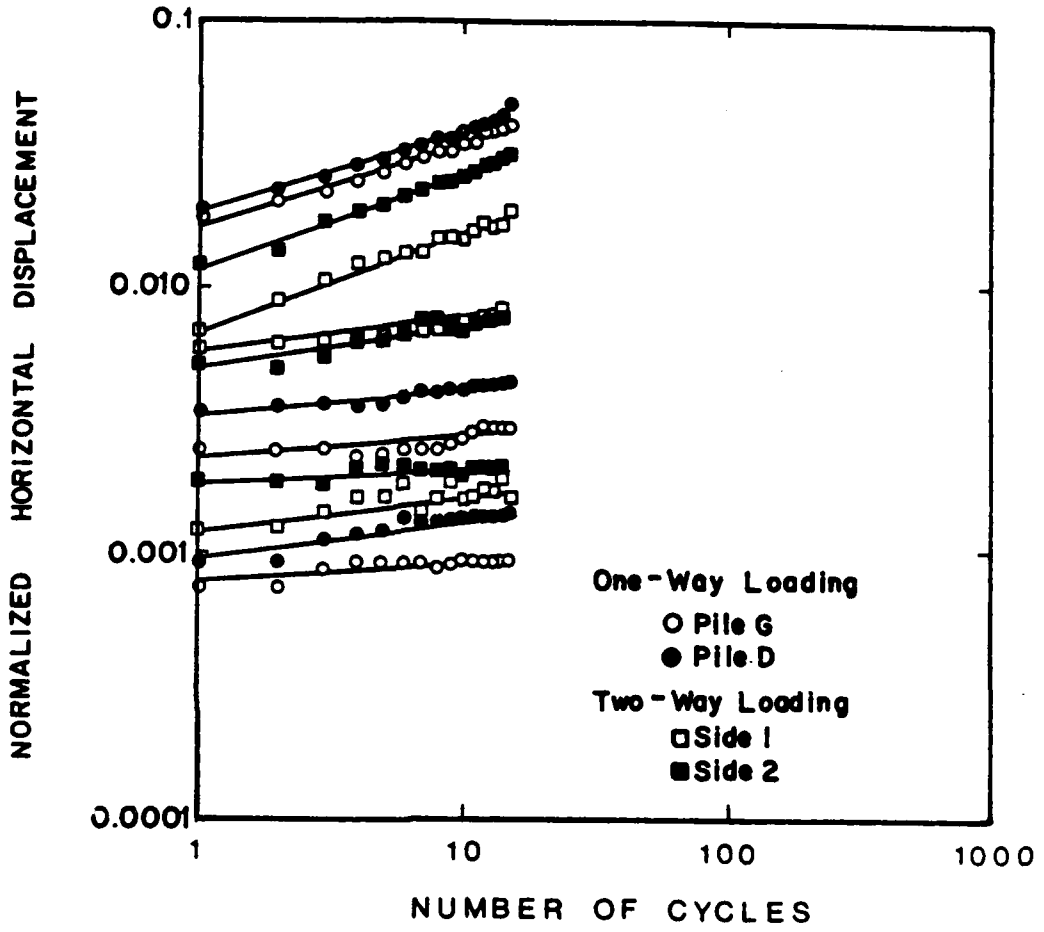

FIG. 3.22. Normalized lateral deflection versus number of cycles for tests performed by Tassios and Levendis (1974)

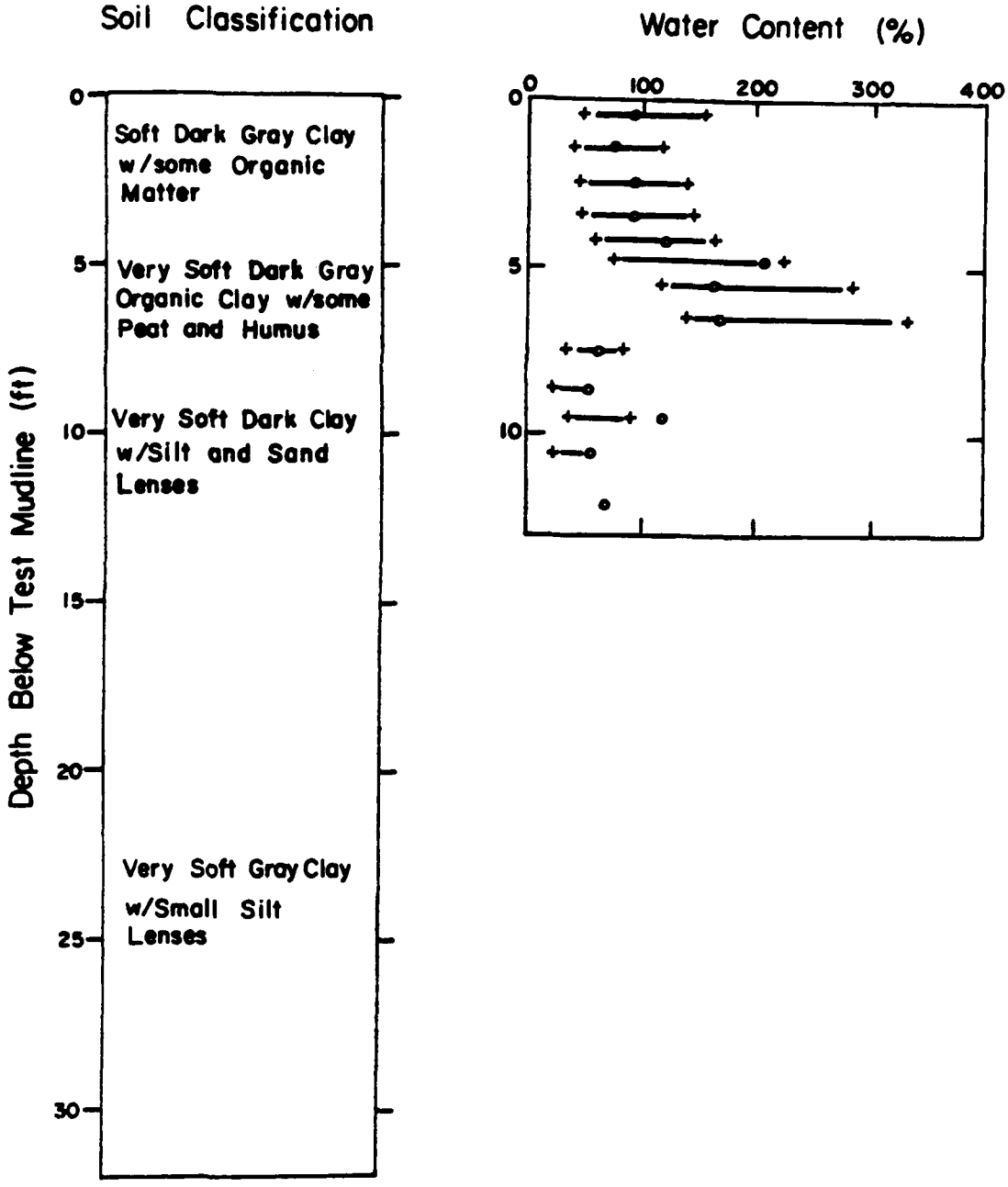

FIG. 3.23. Soil profile at Harvey site (from Matlock, et al, 1980)

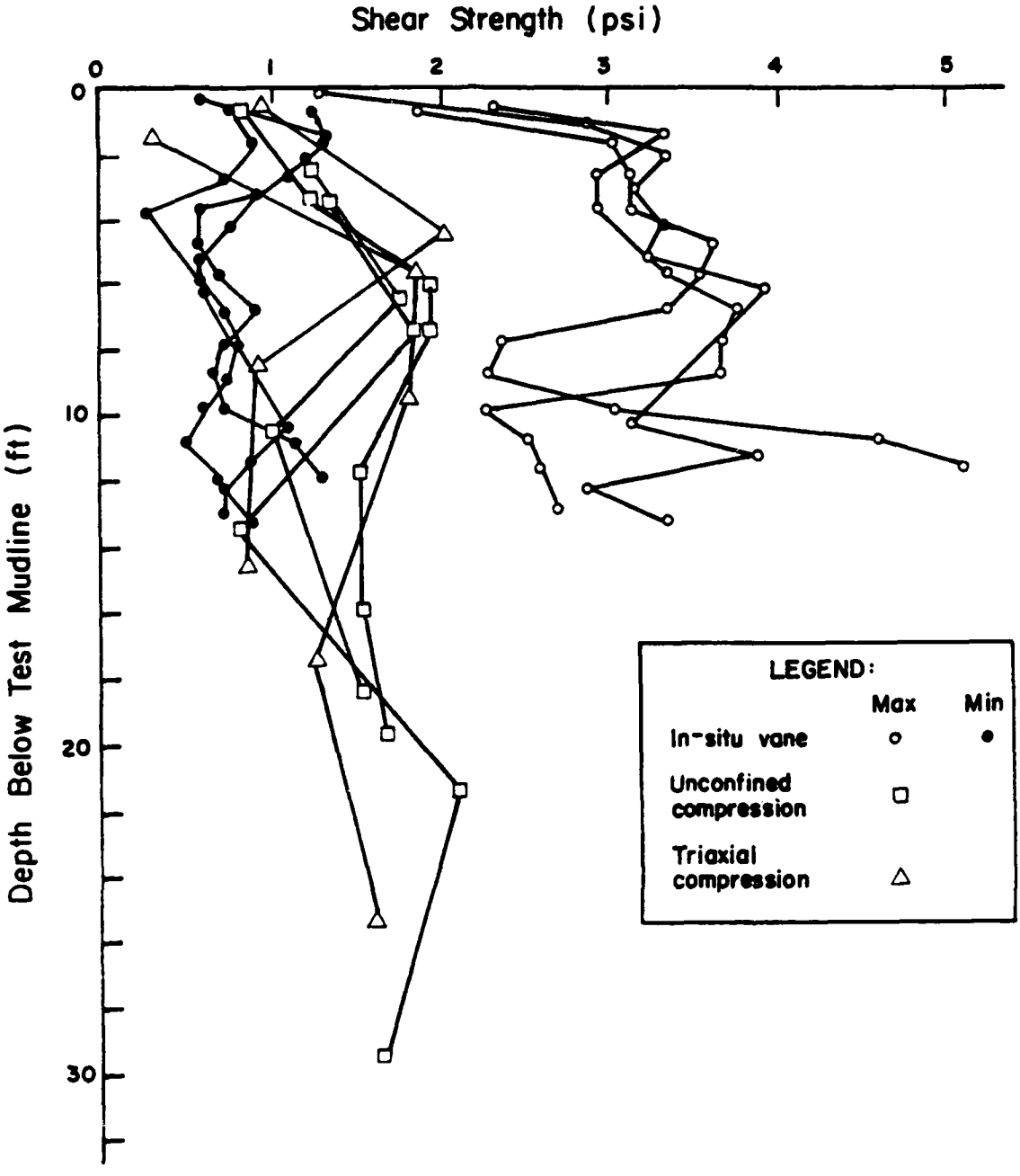

FIG. 3.24. Shear strength profile for soils at Harvey site (from Matlock, et al, 1980)

The piles were driven to an embedded length of 38 ft and loaded with a device that closely simulated a fixed-head condition. The deflection was controlled with deflections in the opposite direction of primary loading maintained at 10 percent of the maximum deflection in the major direction. Cyclic loads were applied at a rate varying from 20 seconds per cycle up to one-and-a-half minutes per cycle. The free water surface was above the ground surface; thus, water was allowed to enter or exit any gaps between the soil and pile.

After the values of moment and load stabilized during cyclic loading, readings were taken. This typically occurred at 20 to 100 cycles. Values of deflection per load cycle are not reported; however, curves for static loading and stabilized cyclic loading were given and are shown in Fig. 3.25.

Lake Austin (1970)

A static and cyclic lateral load test was conducted on a pile in clay near Austin, Texas in 1956. Some results of these tests are presented by Matlock, et al (1970).

The soils in the upper layers at the Lake Austin site are believed to have been deposited within the last century. The soil investigation consisted of in situ vane and three shelby tube samples. Isotropically-consolidated undrained triaxial (CIU) and unconfined compression tests were performed on natural and remolded specimens. In addition, natural water content and Atterberg limits were determined at several depths. The results of these tests are shown in Fig. 3.26.

The steel pile was 12.75 in. in diameter and had a wall thickness of 0.50 in. The length of the pile was 42 ft. The pile was well instrumented with strain gauges.

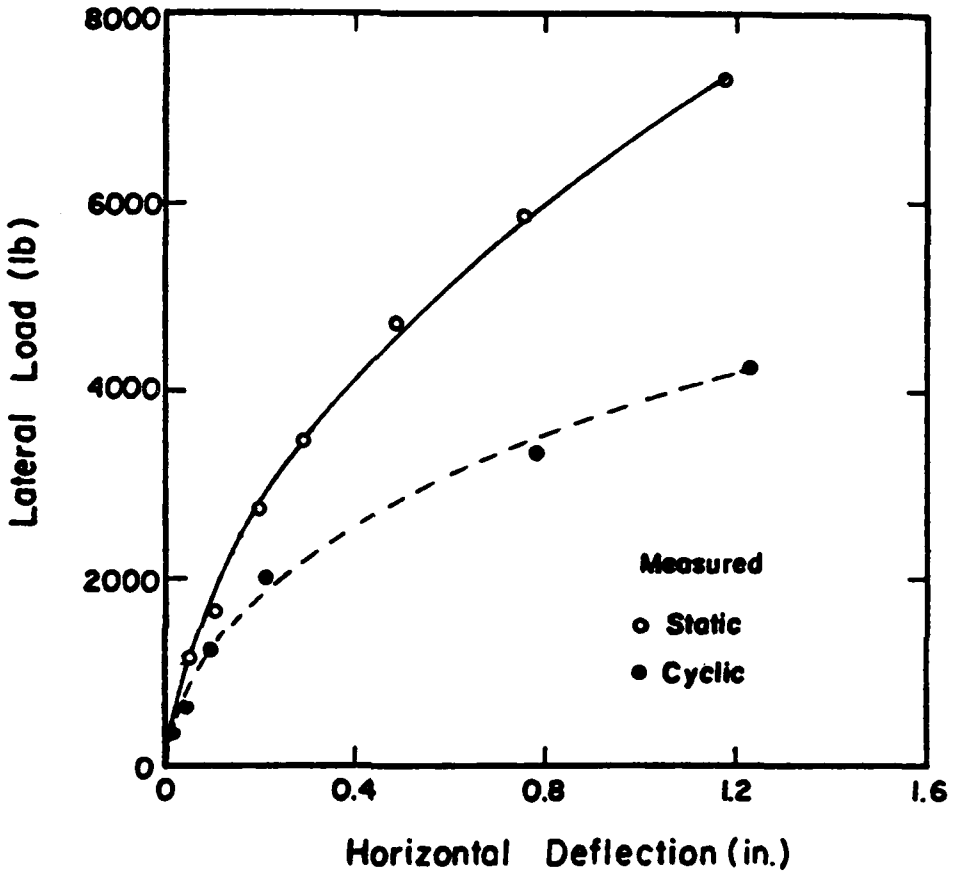

FIG. 3.25. Lateral load versus deflection relationship for Harvey site (from Matlock, et al, 1980)

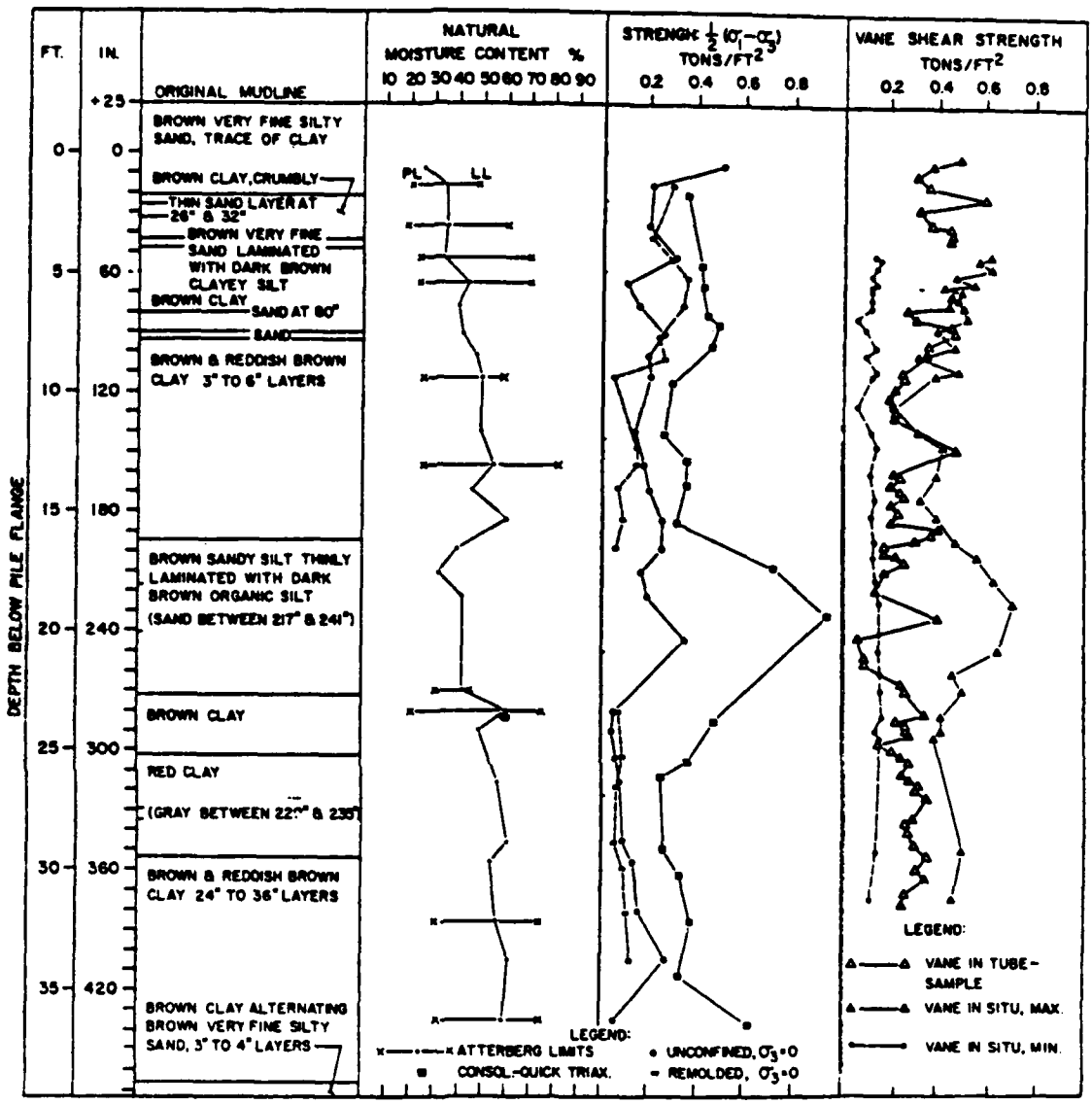

FIG. 3.26. Soil profile for Lake Austin site (from Matlock, et al, 1956)

The pile was driven with a drop hammer and allowed to sit for approximately 15 days before loading. Water was ponded around the pile so that if a gap formed between the pile and soil, fluid would be free to enter and exit the cavity as the pile was cycled. The cyclic loads were applied at a rate of one cycle every 10 to 15 seconds with a load in the minor direction equal to 40 percent of the load in the major direction. However, when readings for bending moment were to be recorded, the load was held constant for strain-gauge readings. Recording data from the strain gauges took a longer amount of time than the rate at which the pile was cycled; therefore, the rate of loading of 10 to 15 seconds per cycle was not preserved for the cycles that were specified, namely cycle numbers 1, 22 and 500.

The results of load versus deflection for the static and cyclic loading are shown in Fig. 3.27. The effect of cyclic loading can be seen clearly as the lateral deflection due to a cyclic load of 15 kips is approximately twice the lateral deflection at a static load of 15 kips.

Plotted in Fig. 3.28 are the measured values of normalized displacement versus number of cycles. Regardless of the level of loading, the slopes of the curves seem to remain constant.

Sabine (1970)

After the tests at Lake Austin, the instrumented pile was pulled and transported to a test site near Sabine, Texas. There a series of static and cyclic tests were performed.

The soil at the site is classified as a soft, slightly over-consolidated marine clay with an estimated undrained shear strength of approximately 300 lb/sq ft. The water contents, Atterberg limits and visual classifications of the soil were determined from tests and speci-

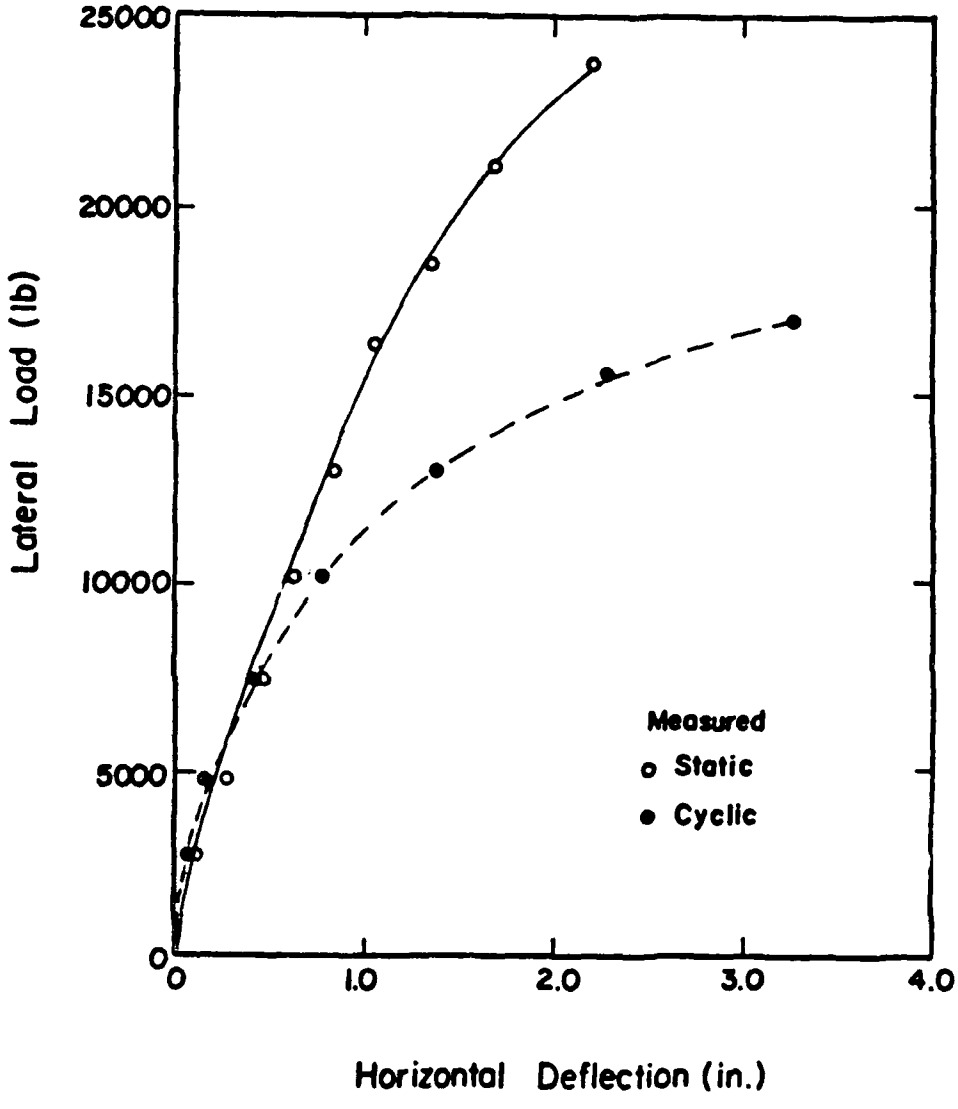

FIG. 3.27. Load versus deflection relationship at groundline for Lake Austin test (from Matlock, et al, 1956)

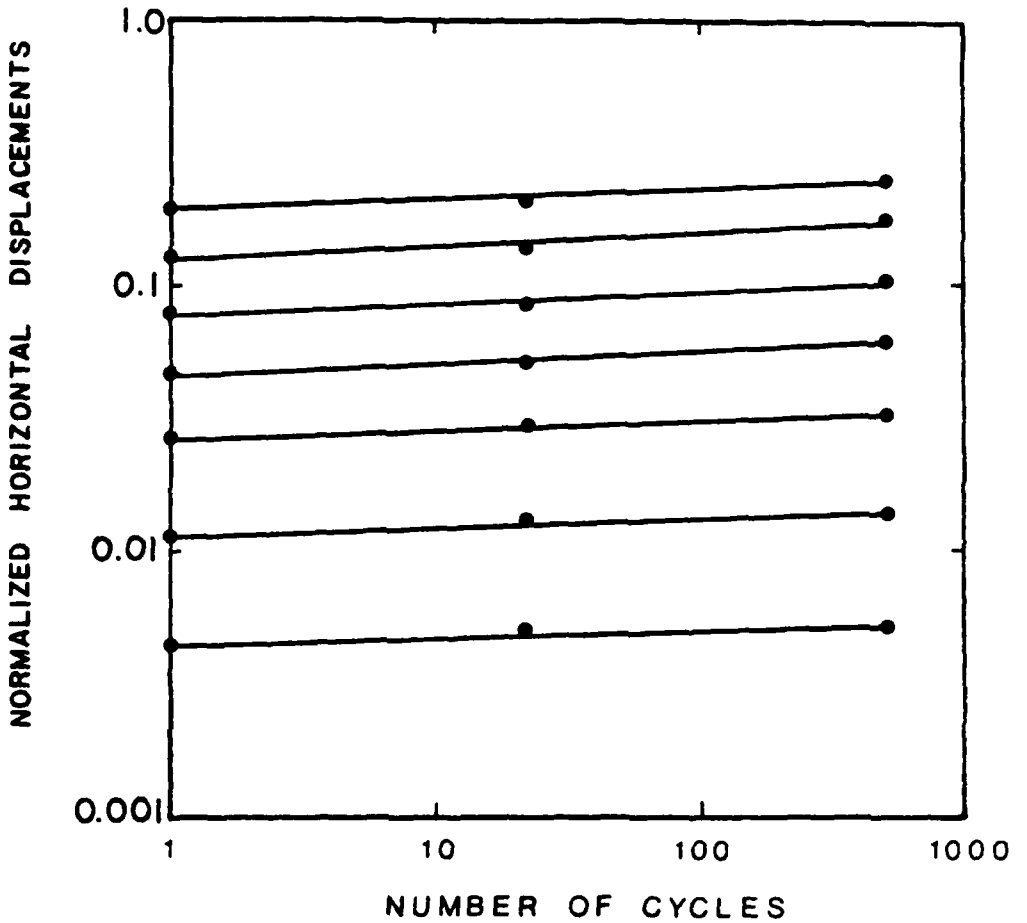

FIG. 3.28. Normalized lateral deflection versus number of cycles at Lake Austin site

mens obtained from several borings in the test area. Shown in Fig. 3.29 is a summary of the results of laboratory and field tests.

As the piles were driven, special care was taken to keep the piles vertical, and to minimize any soil disturbances in the top few pile diameters. Pile-head restraint was varied for the cyclic tests; thus, both free and restrained-head tests were conducted. Here, as in the tests performed at Lake Austin, water was ponded above the ground surface to allow fluid to enter and exit any gaps forming between the pile and soil.

Cyclic loads were applied at a rate of approximately 20 seconds per cycle; however, values of deflection versus number of cycles was not presented.

In order to get an idea of the magnitude of increased deflection caused by cyclic loading, the static load-versus-deflection curve and the cyclic load-versus-deflection curve are shown in Fig. 3.30a and 3.30b for both the free- and fixed-head conditions. The effect of cyclic loading is more pronounced for the free-head pile than for the restrained-head pile. Two factors contributing to this observation are the increased lateral stiffness of the pile-soil system due to restraining the pile-head, and since deflections are smaller, degradation of soil resistance in the surrounding soil should be less.

Shown also in Fig. 3.31 is a log-log plot of normalized deflection versus number of cycles obtained by assuming the static deflection could be taken as the cyclic deflection for the first cycle. For the free-head piles, the slope of the curves is seen to increase with increasing load level. The curves plotted for the restrained head case show much smaller slopes, and for the lower values of load, the slopes are negative. This

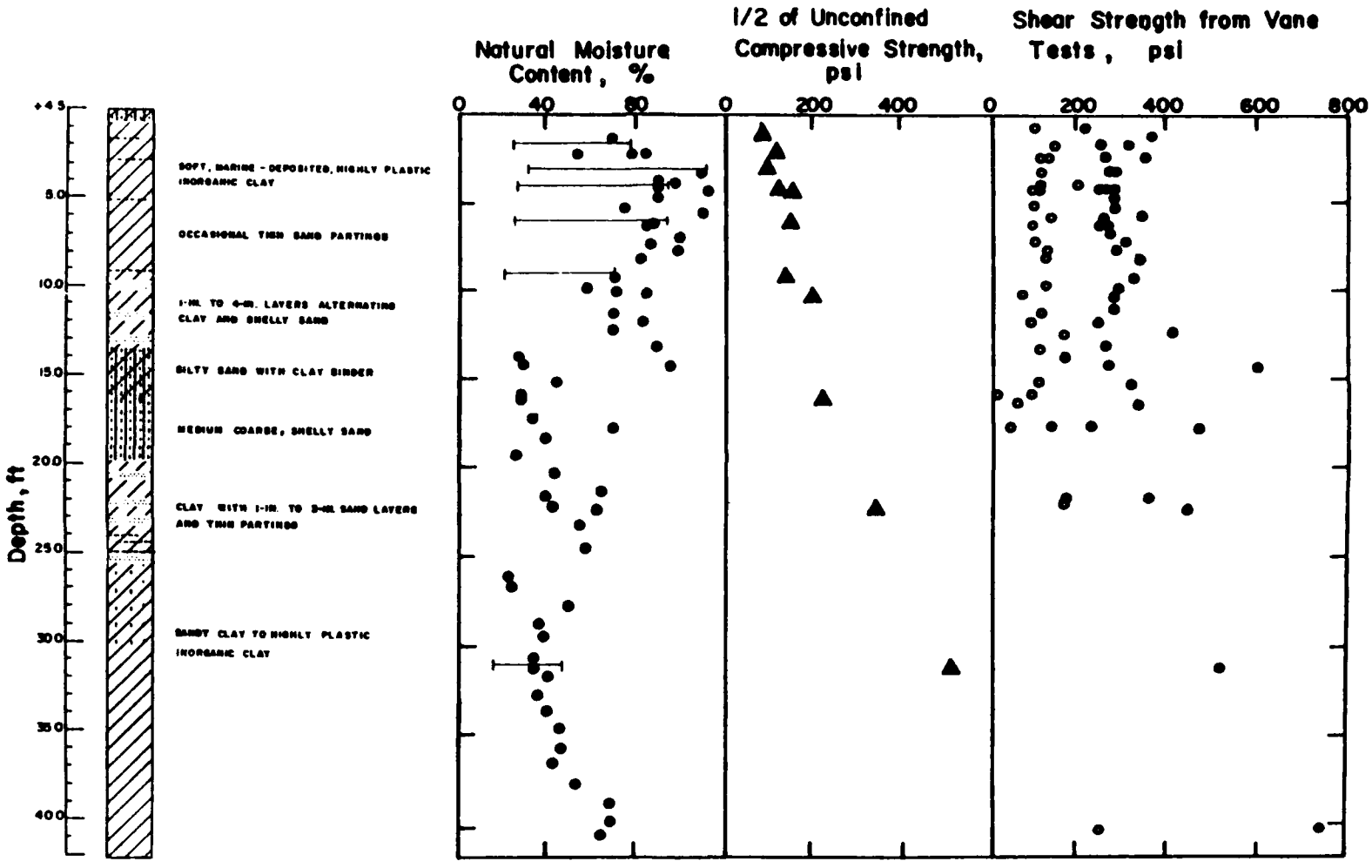

FIG. 3.29. Soil profile for Sabine site (from Matlock, et al, 1961)

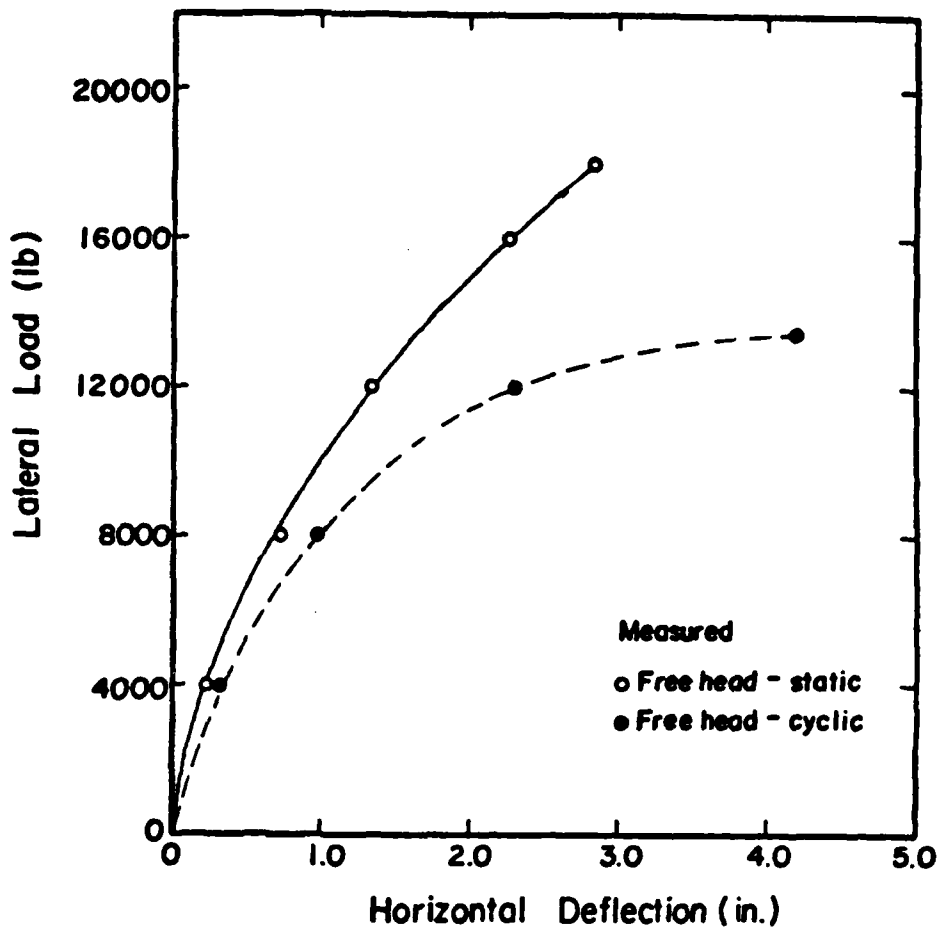

FIG. 3.30a. Load versus deflection relationship at groundline for free-head test at Sabine

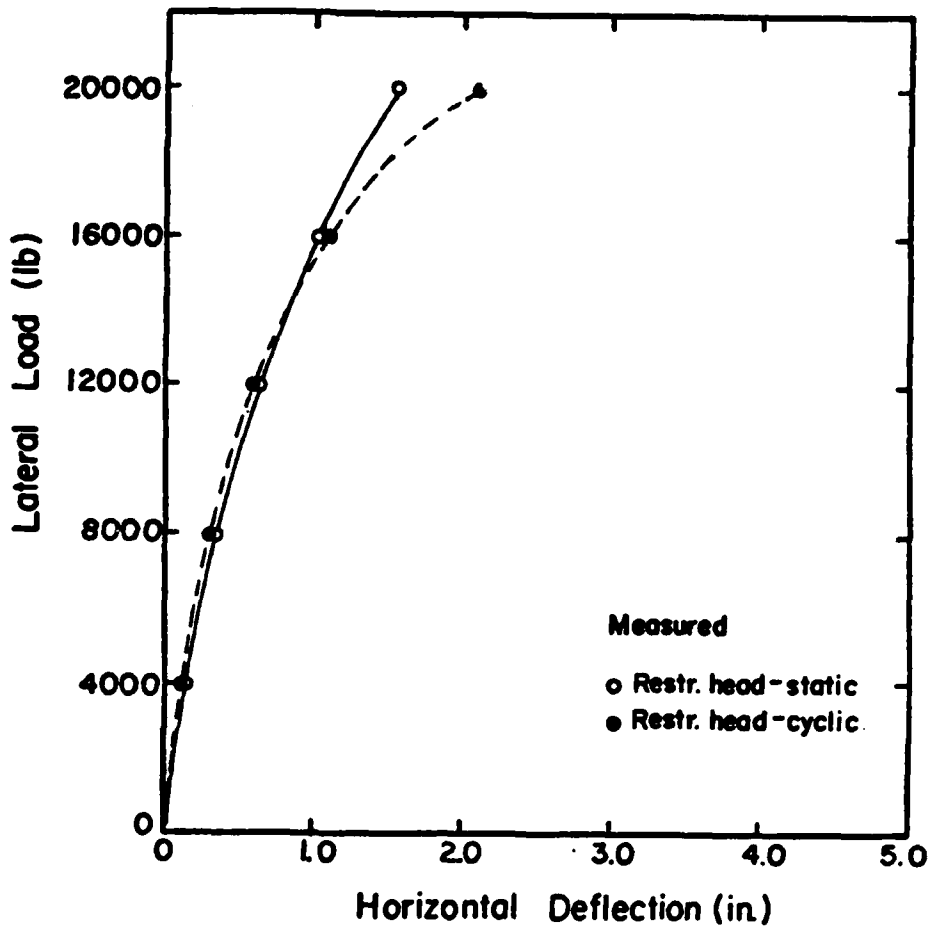

FIG. 3.30b. Load versus deflection relationship at groundline for restrained-head test at Sabine

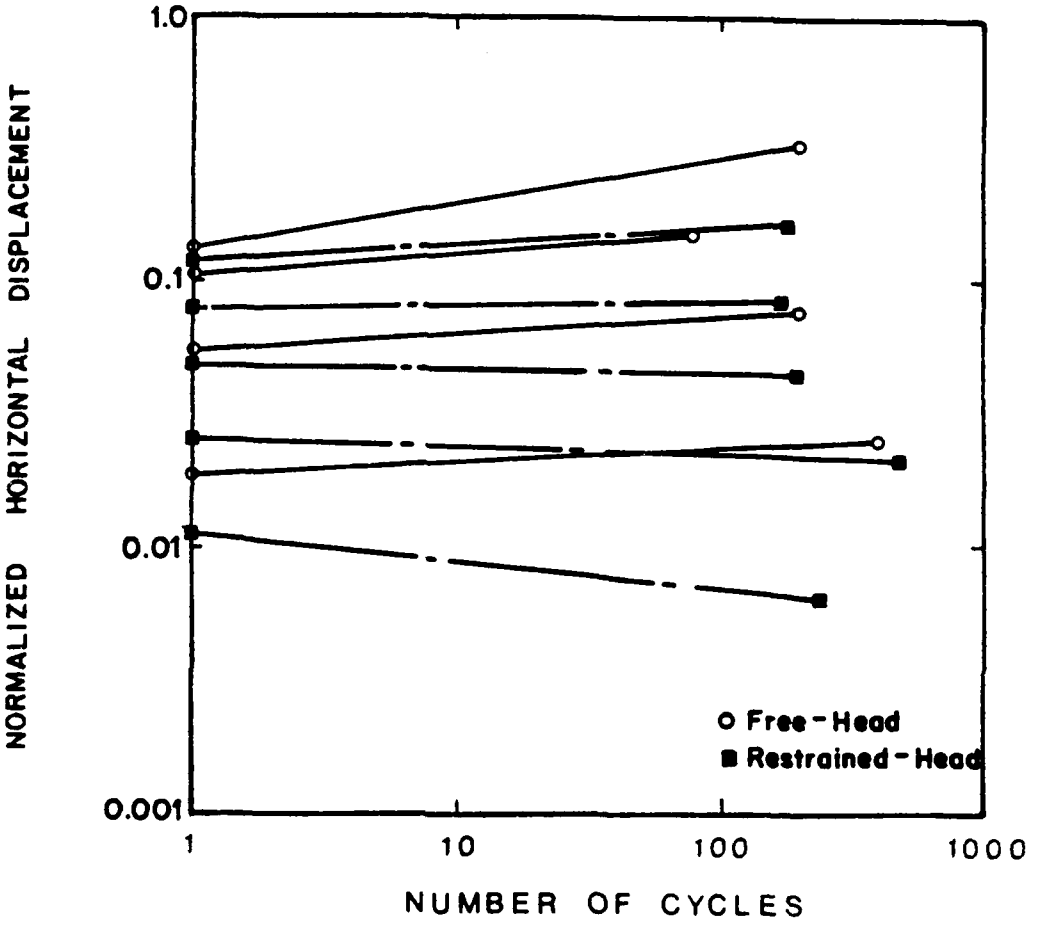

FIG. 3.31. Normalized lateral deflection versus number of cycles at Sabine site

observation can be explained by emphasizing that the value plotted for the first cycle was obtained from the static test results.

Reese and Welch (1972)

A cyclic-loading test was conducted on an instrumented drilled shaft in Houston in a stiff, slightly fissured clay. The soil characteristics at the site were determined by laboratory testing of specimens obtained from 4-in. diameter thin-walled shelby tube specimens. The laboratory tests consisted of visual classification, Atterberg limits, unconsolidated-undrained triaxial compression tests, and repeated-load triaxial tests. The soil profile and strength and water contents versus depth are shown in Fig. 3.32 .

The heavily reinforced concrete shaft had a diameter of 30 in., and the shaft extended to a depth of 42 ft below the ground surface. The shaft was loaded up to a specific value of lateral load, and then cycled. Each cycle of load took approximately two minutes. The number of cycles at each load level varied between 10 and 25 cycles.

The value of EI of the shaft was determined experimentally to be 1.34×10^{11} lb/sq in.

In Fig. 3.33 are curves showing load-versus-displacement cyclic loading, and in Fig. 3.34 is a plot of the normalized displacement versus number of cycles. As can be seen, cycling increased the head deflection at each load level, and furthermore, the slopes of the line are seen to increase with increasing load level.

Reese, Cox and Koop (1975)

A series of lateral load tests were conducted on four piles in a test pit located near Manor, Texas. Two piles were 24 in. in diameter, and two

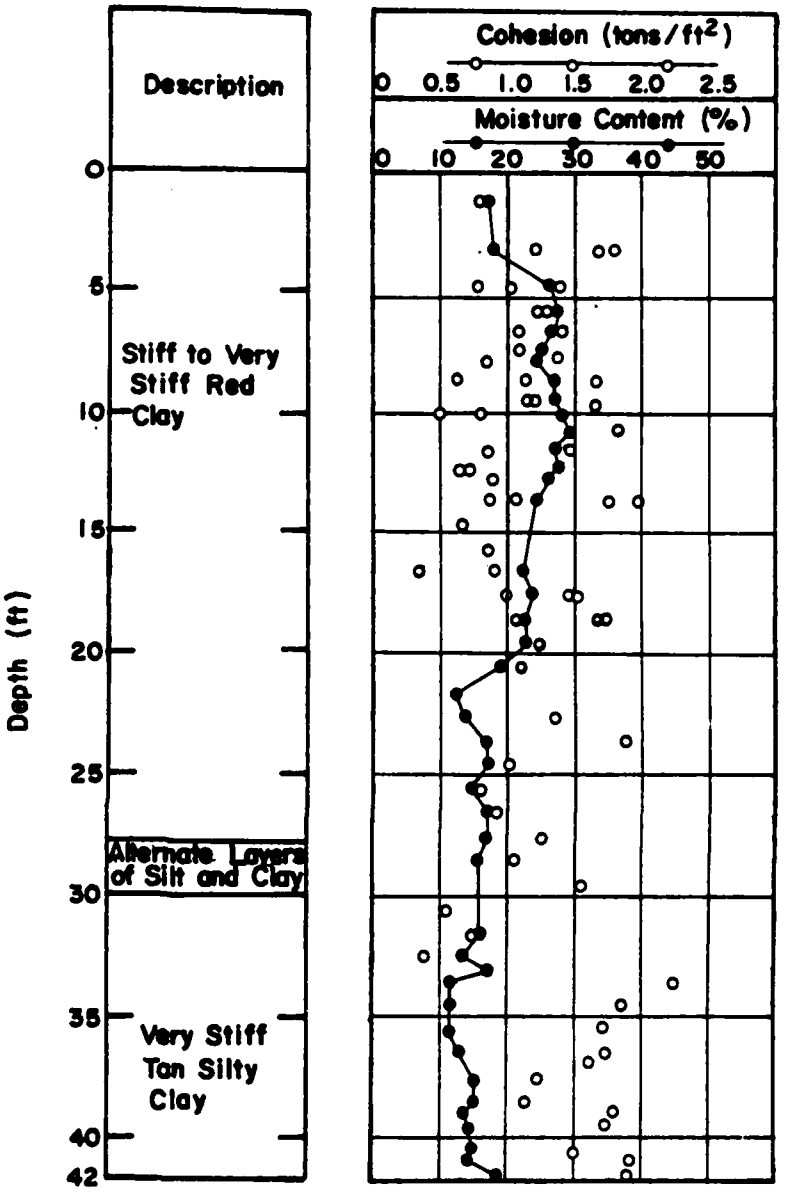

FIG. 3.32. Soil profile at Houston site (from Welch and Reese, 1972)

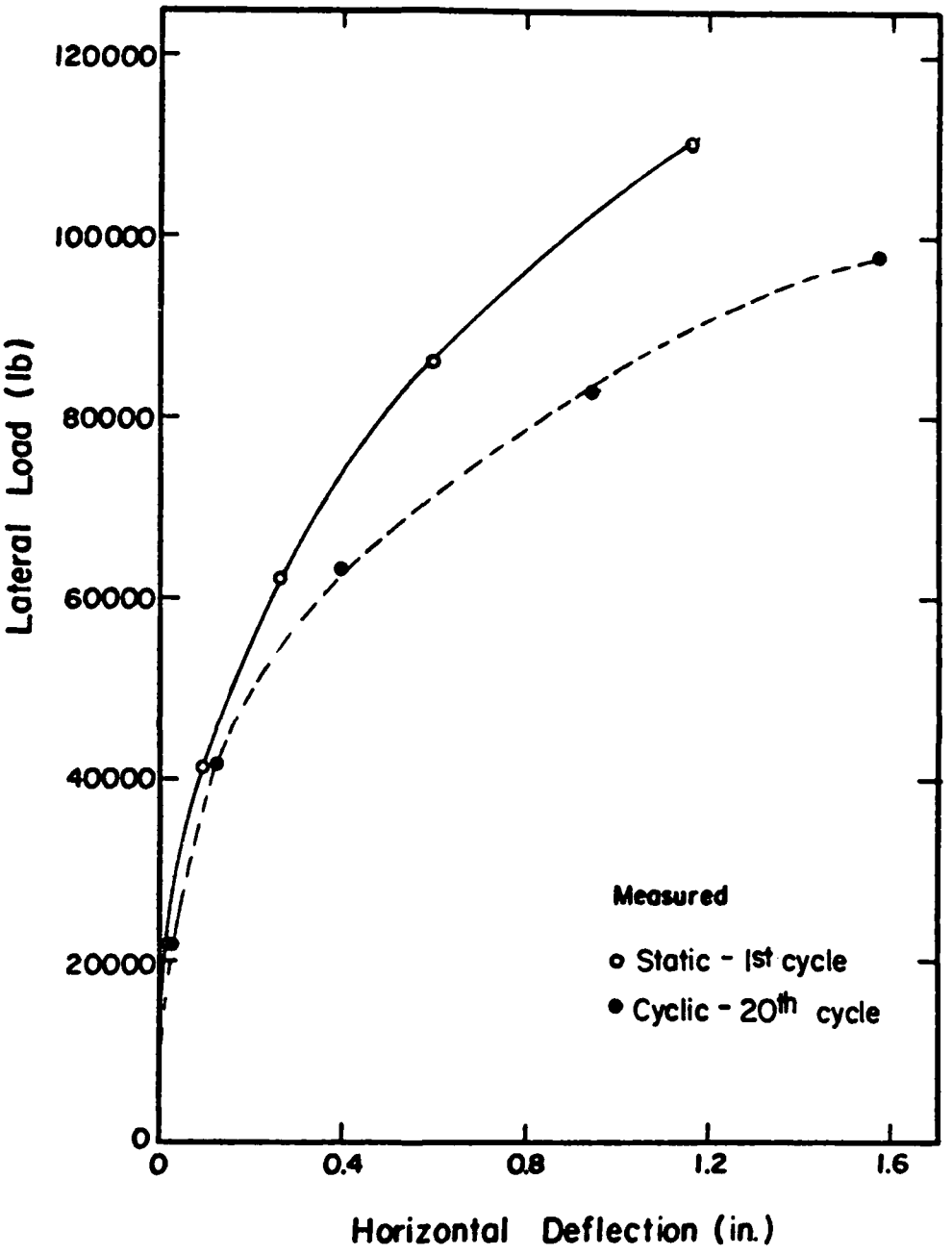

FIG. 3.33. Measured relationship of lateral load versus deflection at pile head for the Houston site

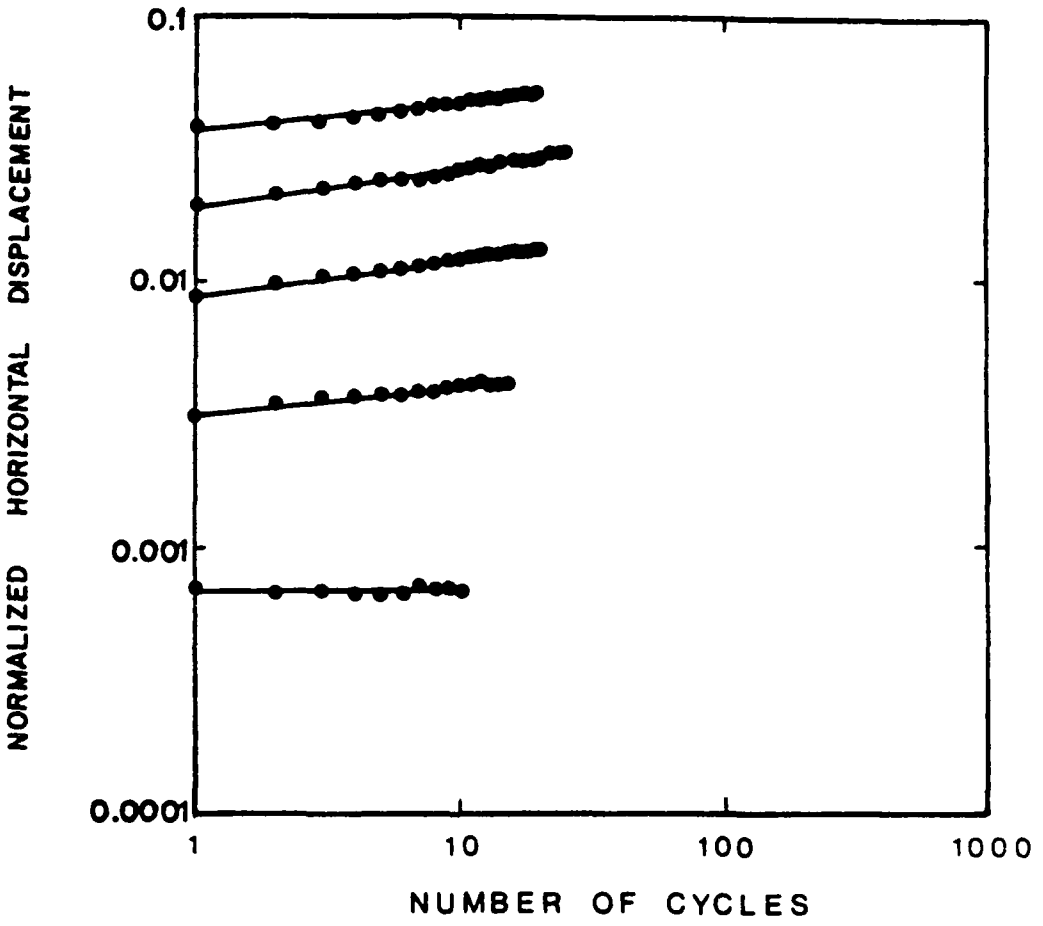

FIG. 3.34. Normalized lateral deflection versus number of cycles for Houston site

were 6 in. in diameter. The geometric and material properties of each pile are shown below:

Pile No.	OD	ID	EI (lb/sq in.) from 0-23 ft	EI (lb/sq in.) from 23-50 ft
1	25.25	23.25	17.204 EI	5.8671 E10
2	25.25	23.25	16.915 E10	6.0853 E10
			from 0-28 ft	from 28-43 ft
3	6.625	0.718	1.8298 E9	8.4426 E8
4	6.625	0.718	1.8298 E9	8.4426 E8

The soil surrounding the piles was classified as a medium stiff clay of high plasticity. The clay was slightly jointed and fissured with many of the fissures having different colored, softer clay within them. The shear strength of the clay varied linearly from about zero at the ground surface to about 3.5 T/sq ft at a depth of 13 ft below the ground surface. The shear strength, Atterberg limits, and natural water content are shown as a function of deph in Fig. 3.35, along with visual classifications for the soil.

The stress-strain curves for the soil are shown in Fig. 3.36 and varied considerably depending on the joints and fissures located within the triaxial specimens.

Piles 1 and 2 were carefully instrumented in the laboratory, and then driven in the field to their required depth. Piles 3 and 4 are in fact the same pile. They were assigned different numbers to distinguish the different testing sequences applied to the pile head.

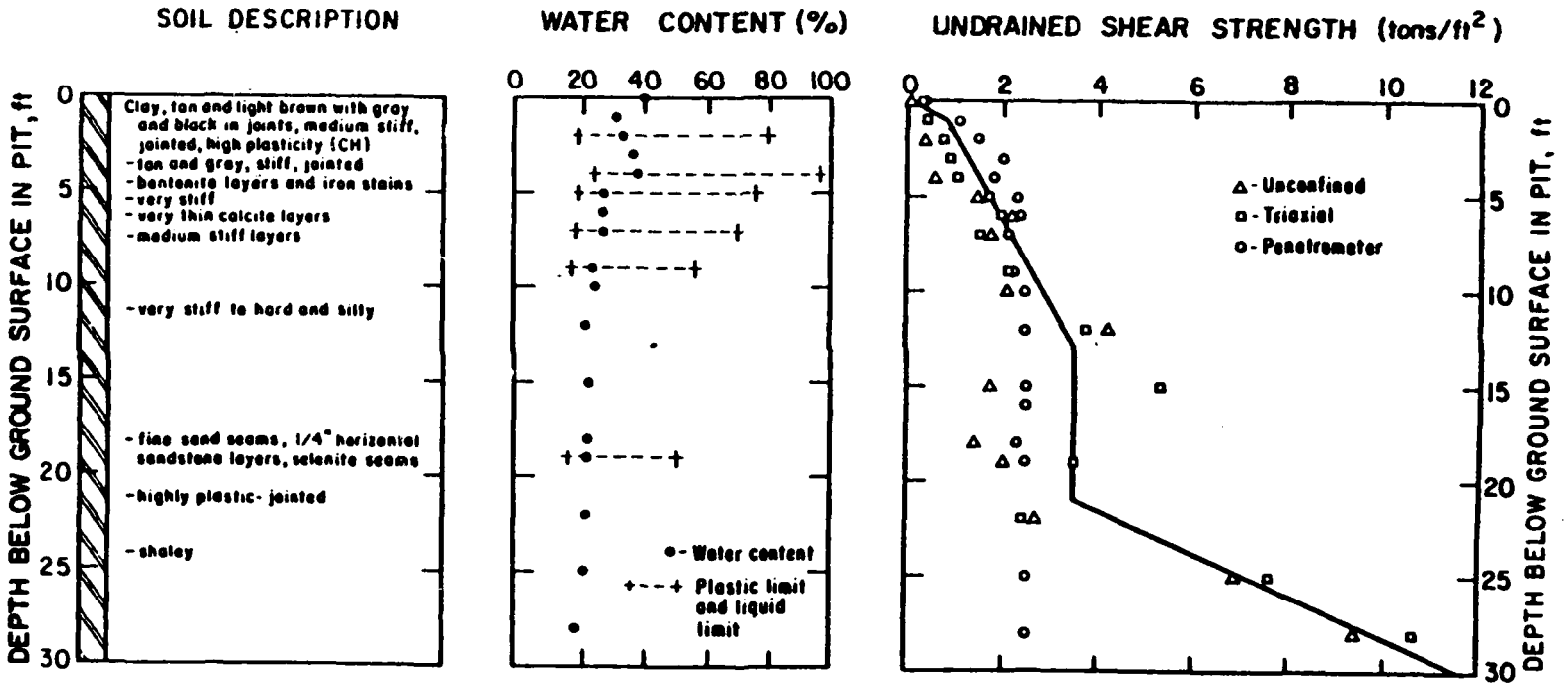

FIG. 3.35. Soil profile at Manor site (from Reese, et al, 1975)

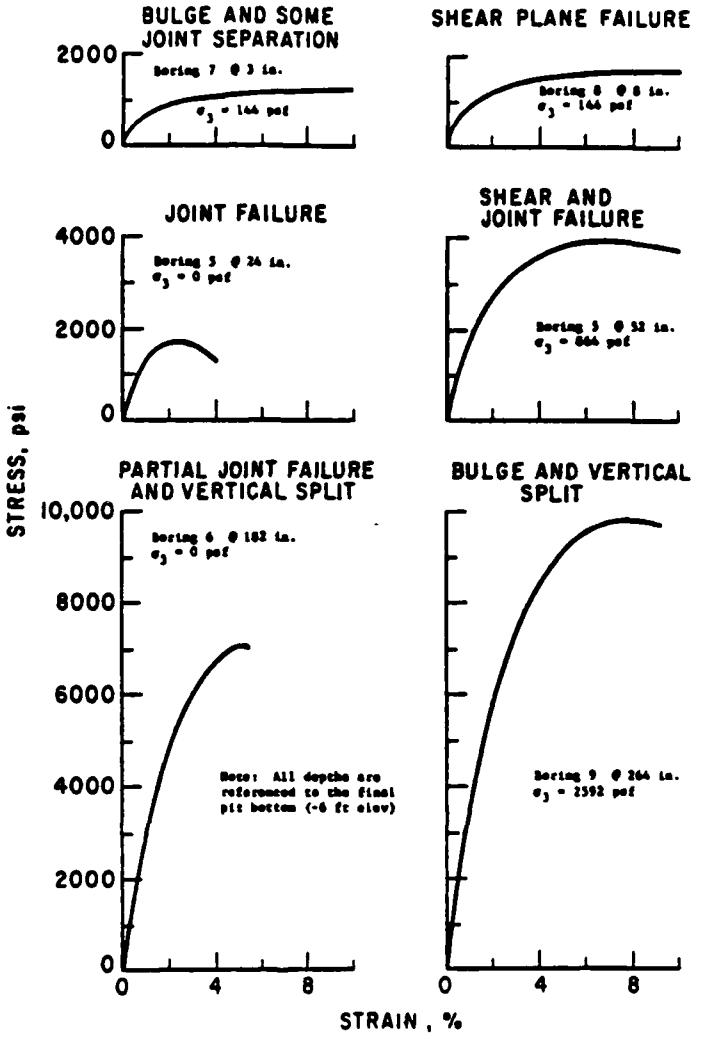

FIG. 3.36. Stress-strain curves for the fissured Manor soil (from Reese, et al, 1975)

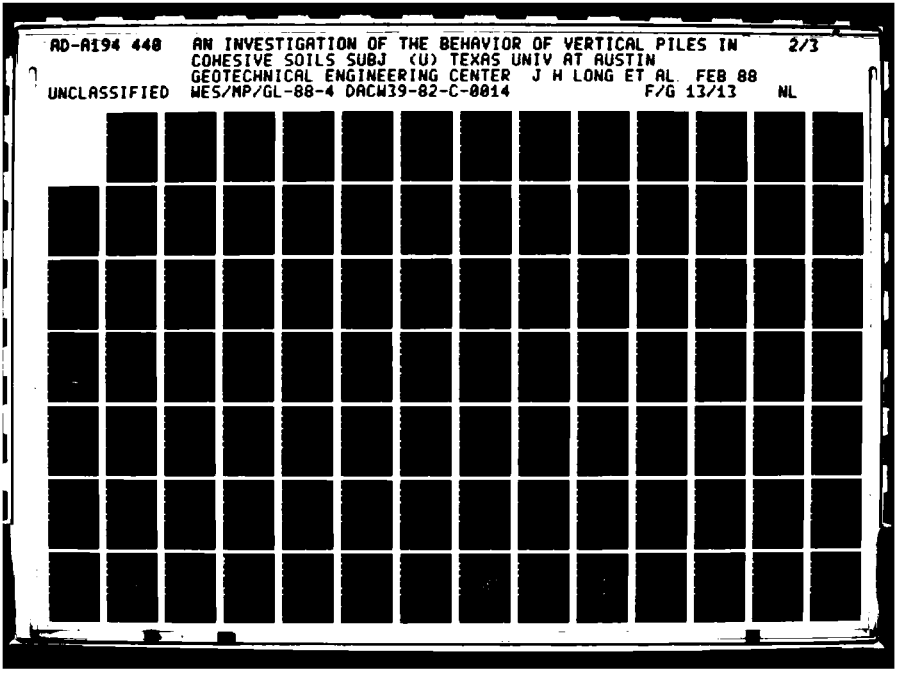
AD-A194 448 AN INVESTIGATION OF THE BEHAVIOR OF VERTICAL PILES IN 2/3
COHESIVE SOILS SUBJ (U) TEXAS UNIV AT AUSTIN
GEOTECHNICAL ENGINEERING CENTER J H LONG ET AL. FEB 88
UNCLASSIFIED WES/MP/GL-88-4 DACW39-82-C-0014 F/G 13/13 NL

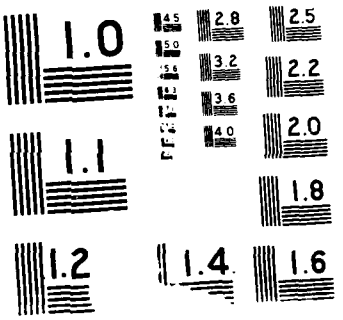
1.0
1.1
1.2
1.4
1.6
1.8
2.0
2.2
2.5
2.8
3.2
3.6
4.0
4.5
5.0
5.6

All the piles were loaded with hydraulic jacks. Piles 1, 2 and 3 were loaded with a free-head condition, with the load applied one foot above the groundline. Pile 4 was loaded with a restrained-head condition. All the piles were tested under both cyclic and static loading. The rate of loading for the cyclic loading tests required approximately 20-40 seconds per cycle depending on the magnitude of load and deflection. The results of static and cyclic tests are presented below.

Pile 1 was loaded statically and the resulting load-versus-deflection-at-groundline curve is shown in Fig. 3.37. At a maximum load of 136,000 lbs, the lateral deflection was approximately 0.87 in. From the start of the test to peak loading took approximately three and one-half hours.

Upon completion of the static loading of Pile 1, cyclic loads were applied. Three separate series of loads were applied with the direction of the maximum load opposite to the direction applied during the static loading. The results are plotted as negative values in Fig. 3.37.

In the first series of loadings, 10 cycles of load were applied at each level of load below 80,000 lbs. At a load level of approximately 80,000 lbs, 20 cycles of load were applied, at 105,000 lbs, 25 cycles and at 115,000 lbs, 30 cycles. At a maximum load of 122,000 lbs, 70 cycles of load were applied. The resulting load-deflection curve is shown in Fig. 3.37.

In the second series of loadings, 10 cycles of load were applied to the pile head from a magnitude of load of 0 to 137,000 lbs. At the end of the tenth cycle of load, the resulting deflection at the groundline was approximately 1.3 in. The pile was then unloaded, and once again loaded to approximately 118,000 lbs and cycled 20 times, resulting in a final deflection of about 1.26 in., as shown in Fig. 3.37.

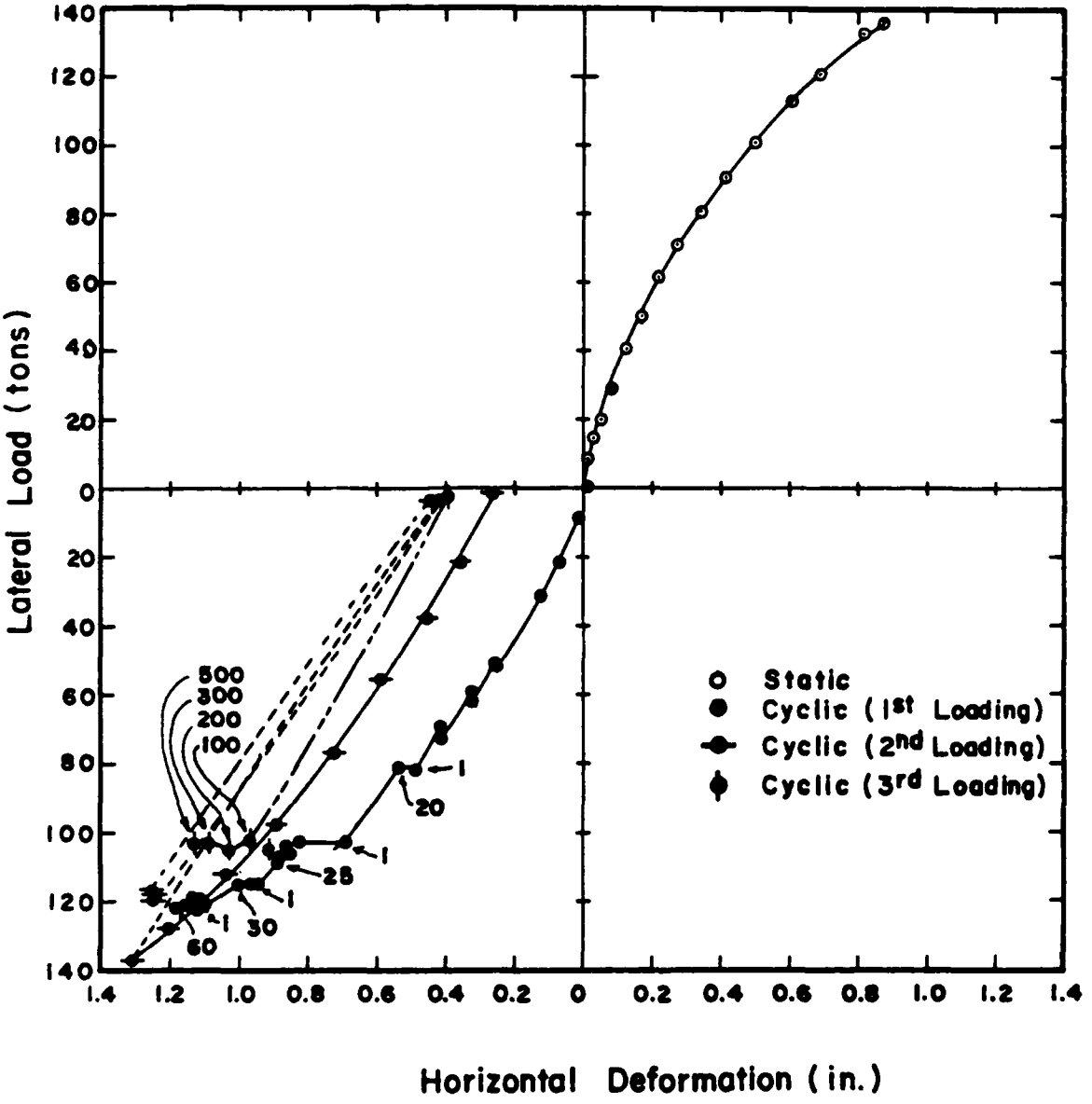

FIG. 3.37. Load-versus-deflection curves for pile no. 1 at Manor site

The final series of loadings on Pile 1 was performed by loading the pile to a load of approximately 104,000 lbs and cycling for 500 cycles. The values of load versus horizontal deflection at the groundline are shown for cycle numbers 100, 200, 300, 400 and 500 in Fig. 3.37.

On the basis of the results from the load tests conducted on Pile 1, several observations can be made. Deflections under cyclic loading were larger than those for static loading for the same magnitude of load, and continued cycling caused increased deflection, especially at the higher levels of loading. At the lower levels of loading, the cycling influenced the deflection to a lesser degree than at the larger loads.

Cyclic loads were applied first to Pile 2 and loading was discontinued when it was determined that further cycling caused no increase in deflection. The resulting load schedule was 20 applications of load for each load level up to 15,000 lbs, 30 cycles for each load level up to 35,000 lbs, 40 cycles for 50,000 lbs, 600 cycles for each load level up to 67,000 lbs, and 100 cycles of load up to 100,000 lbs of load. The curve of load versus deflection is shown in Fig. 3.38.

After the cyclic test of Pile 2, a static test was conducted with the direction of load the same as applied in the cyclic load test. The results of the static test are shown in Fig. 3.38.

The results from the tests of Pile 2 showed that cycling at lower levels of load caused less increase in deflection than cycling at higher levels of load. Also, at higher levels of load continued cycling caused an increase in deflection. The load-deformation curve for the static reloading was very flat.

Pile 3 was first loaded statically, and then cyclically with the major load oriented opposite to the direction of static loading. The

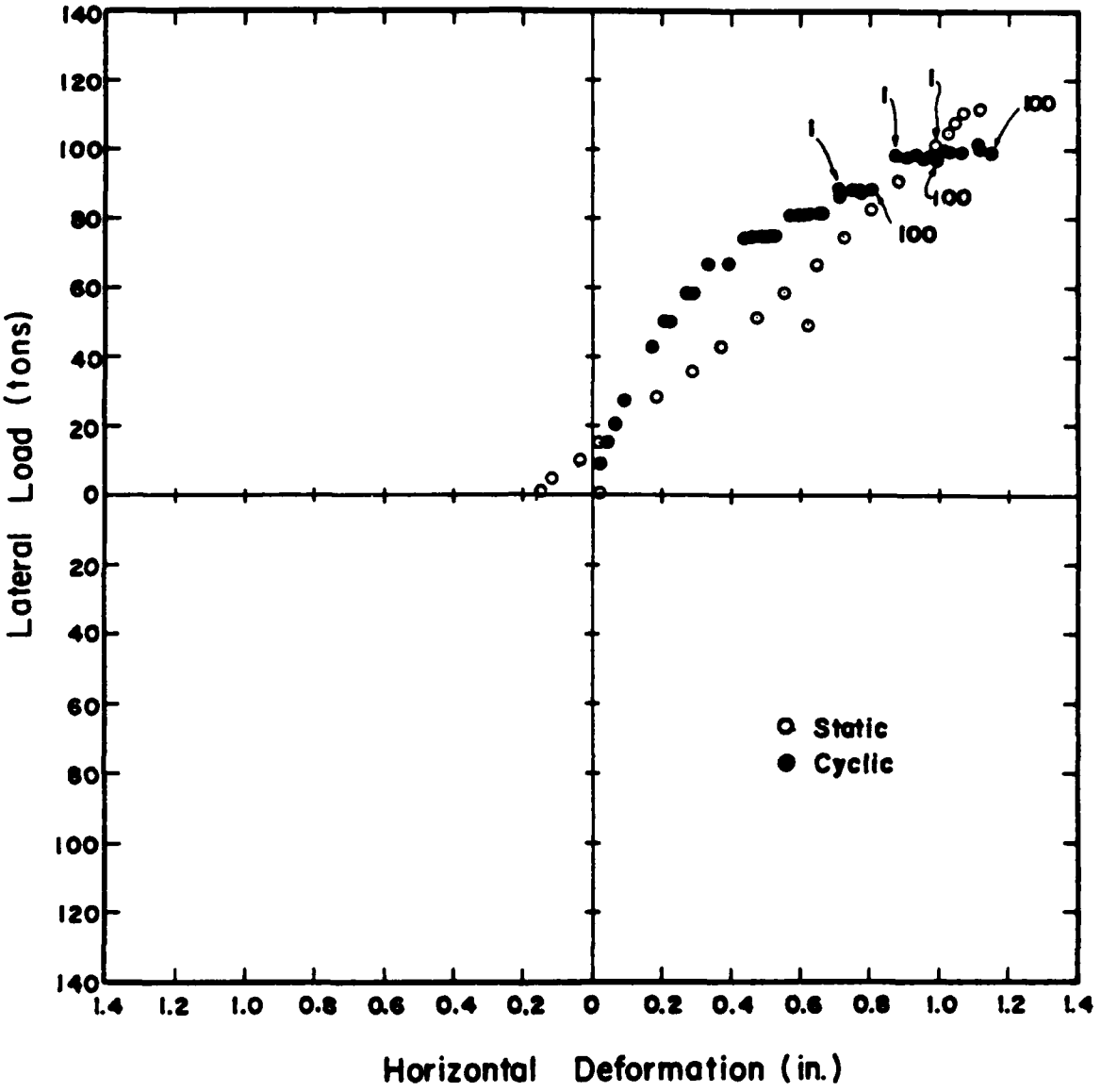

FIG. 3.38. Load-versus-deflection curves for pile no. 2 at Manor site

static loads were increased in increments to a load of 10,500 lbs; maximum groundline deflection was 0.83 in. The time for the test was about three hours. The curve of load versus deflection is shown in Fig. 3.39. After the static loading was completed, a cyclic load test was conducted. During the cyclic load test, several applications of load were applied to the pile head for each level of load. For loads below 4,000 lbs approximately 20 cycles were applied for each load. For loads between 4000 and 6000 lbs, 40 to 50 cycles were applied for each load, and for loads above 6000 lbs, 100 cycles of load were applied. The curve for the the cyclic load test is shown in Fig. 3.39.

The same observations can be made about the pile behavior measured for pile 3 as mentioned before; that is, that continued cycling leads to an increase in deflection, and the load versus deflection curve for the static load yields a smaller deflection for a given load than does the cyclic load.

The top of Pile 4 was partially restrained against rotation during loading by a truss mechanism. Static loading was done first; the resulting curve of load versus deflection is shown in Fig. 3.40. A maximum load of 16,900 lbs resulted in a measured deflection of 0.98 in. The load was applied 1 ft above the groundline in testing Pile 4. As may be seen by comparing Figs. 3.40 and 3.39, the use of the restraint at the head of Pile 4 led to a stiffer curve than for Pile 3. A cyclic loading test was conducted on Pile 4 after the static test was completed. Several cycles of load were applied at each load level with 100 cycles being applied at the higher loads. The resulting curve of load versus deflection is shown in Fig. 3.40.

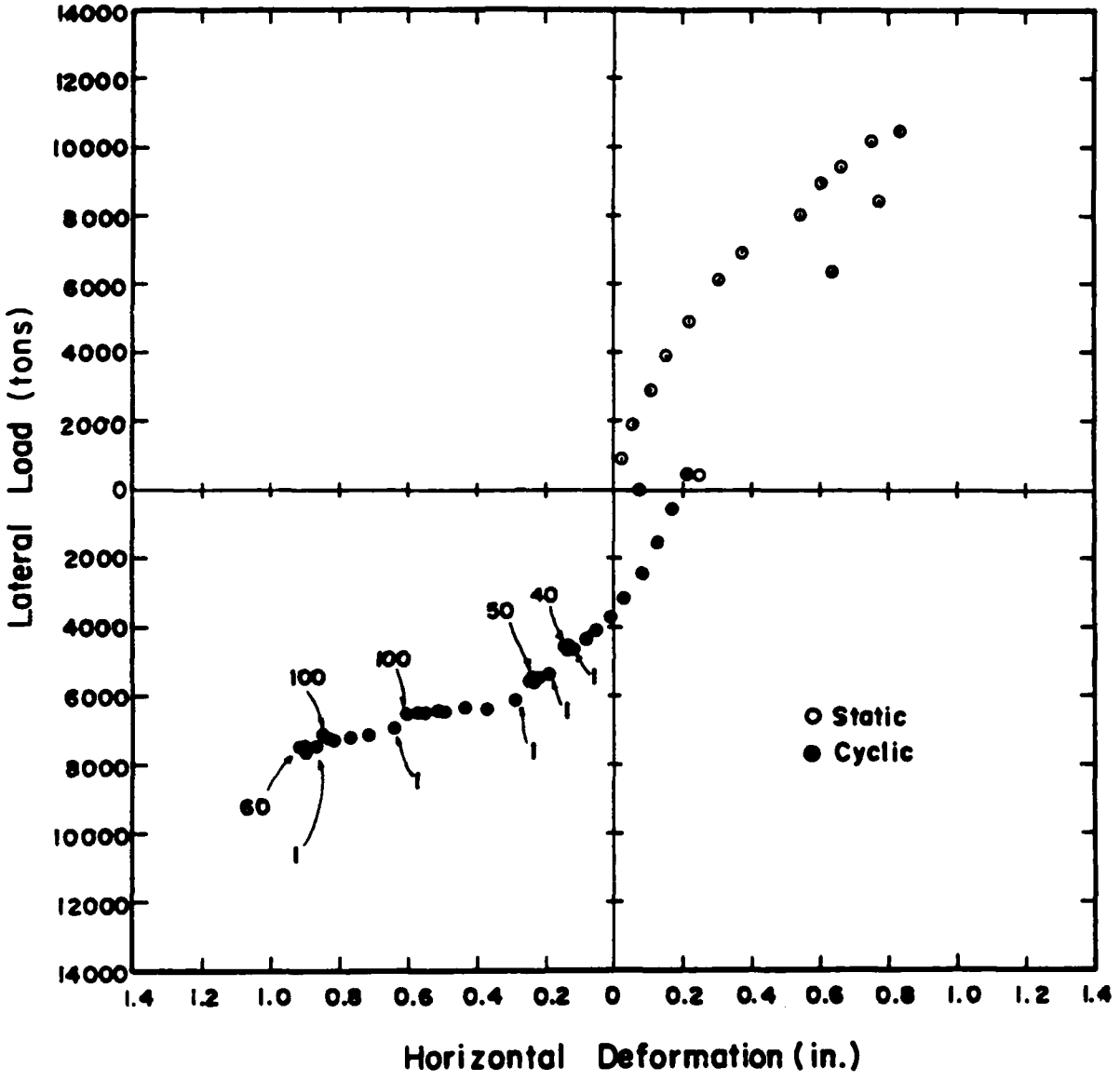

FIG. 3.39. Load-versus-deflection relationship for pile no. 3 at Manor site

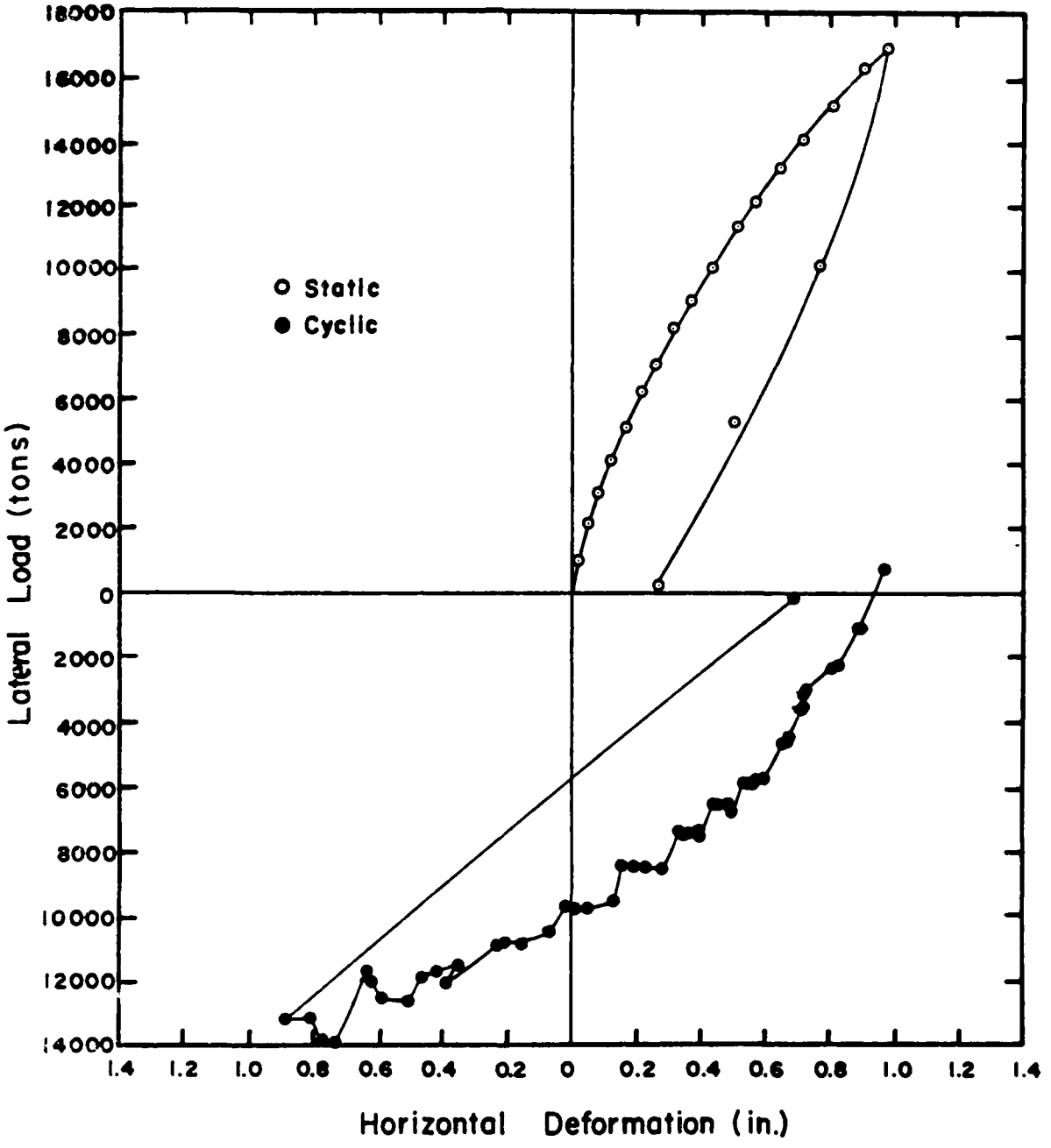

FIG. 3.40. Load-versus-deflection curves for pile no. 4 at Manor site

CONCLUSIONS

Several conclusions may be drawn from the results of these lateral load tests regarding the behavior of piles due to cyclic lateral loading. The main conclusions are listed below:

1) Depending on the load level and soil characteristics, the results of static and cyclic loading can be very similar, as found from the results of tests performed by Gaul (1958), and Price and Wardle (1982), or the results of static and cyclic loading can be very different such as found in the results of tests performed near Manor, Texas.

2) The rate at which the pile is loaded laterally affects the corresponding behavior as seen in the tests of Valenzuela and Lee (1976), and Price and Wardle (1981). In the tests performed by Valenzuela and Lee, deflections increased due to cyclic loading; however, deflections during the first few cycles were measured to be less than measured static deflections. For the tests performed by Price and Wardle, lateral deflections also increased with number of cycles; however, in many cases, the lateral deflection measured on the last cycle was less than that measured for the static test.

3) Several of the lateral load test results could be presented as normalized displacement versus number of cycles (log-log relationship). In most of the lateral load tests, the relationship could be approximated with a straight line. For tests conducted at several values of lateral load, it was observed that the slope of the lines increased with increasing load level.

4) As demonstrated in the test results of Tassios and Levendis, Franki piles installed identically driven into the same soil behaved differently when subjected to cyclic loading. Lateral deflections experienced by one pile were seen to be 10 percent greater than the other pile. In addition, results from a single pile loaded cyclically in opposite directions showed deflections in one direction to be 100 percent greater than measured in the opposite direction.

5) As shown in the Manor test results, where static test results were compared with the first cycle of each load level in the cyclic tests results, cycling at lower levels of load affects the load deformation behavior of the pile at higher levels of load.

6) For lateral load tests in which water was ponded at the surface, soil was reported to have been eroded along the gap that formed between the pile and soil. The amount of erosion varied at each site, but was reported to be very obvious for tests conducted at Manor, and almost insignificant for the tests conducted at Sabine.

CHAPTER 4. CURRENT STATE-OF-THE-ART

INTRODUCTION

The principal method of solution for a pile under lateral loading requires the modelling of the soil by p-y curves and the computation of the pile response by digital computer. The differential equation that governs the pile behaior, even with nonlinear soil response, can be conveniently solved by use of difference equations.

In addition to the computer solution, the use of nondimensional curves has an important role in the analysis of laterally loaded piles. Nondimensional methods can be used to demonstrate with clarity the nature of the computer method and, furthermore, can be used to obtain a check of the computer results.

Two other methods of anaysis are presented, the methods of Broms (1964a, 1964b, 1965) and Poulos and Davis (1980). Broms' method is ingenious and is based primarily on the use of limiting values of soil resistance. The method of Poulos and Davis is based on the theory of elasticity. Both of these methods have had considerable use in practice.

BROMS METHOD

The method was presented in three papers published in 1964 and 1965 (Broms, 1964a, 1964b, 1965). The ultimate lateral load on a pile can be computed by use of some simple equations or can be found by referring to graphs. The method is based on the following concepts: failure occurs for short piles by unlimited rotation of the pile or unlimited movement through the soil, failure occurs for long piles or piles of intermediate length by the development of one or more plastic hinges in the pile sec-

t ..., and for both types of failure the ultimate soil resistance is assumed to develop at all points along the pile except at the point where there is a zero deflection.

In addition to the assumption listed above, assumptions were made about the ultimate soil resistance for both clay and sand, as shown in Fig. 4.1 for short piles. In the case of short piles with a free head, the value of P_{ult} can be found that will cause a pile to rotate without limit.

In addition to presenting equations for P_{ult} for piles that are free to rotate, Broms showed equations for piles that are fixed aginst rotation at their tops and for lengths such that plastic hinges will develop. In the case where a plastic hinge or hinges develop, it is necessary to know the value of the yield moment M_y for the pile section. For all the cases, a value of P_{ult} can be computed for the lateral load that will cause a pile to fail.

In the referenced papers, Broms presented methods for computing the groundline deflection of a pile where the lateral load was no greater than one-half of P_{ult}. The methods make use of the coefficients of subgrade reaction and generally follow procedures suggested by Terzaghi (1955). The methods yield a linear relationship between load and deflection.

Some studies, not reported here (Reese, 1983), show that the Broms method has predicted with reasonable accuracy in a number of instances the ultimate lateral load on the pile. The assumptions of constant shear strength with depth, uniform pile section, either fixed-head or free-head boundary conditions, and the development of ultimate soil resistance along the length of a pile, limit the usefulness of the method somewhat.

With regard to cyclic loading, Broms suggested that repetitive loads cause a gradual descrease in the shear strength of the soil located in the

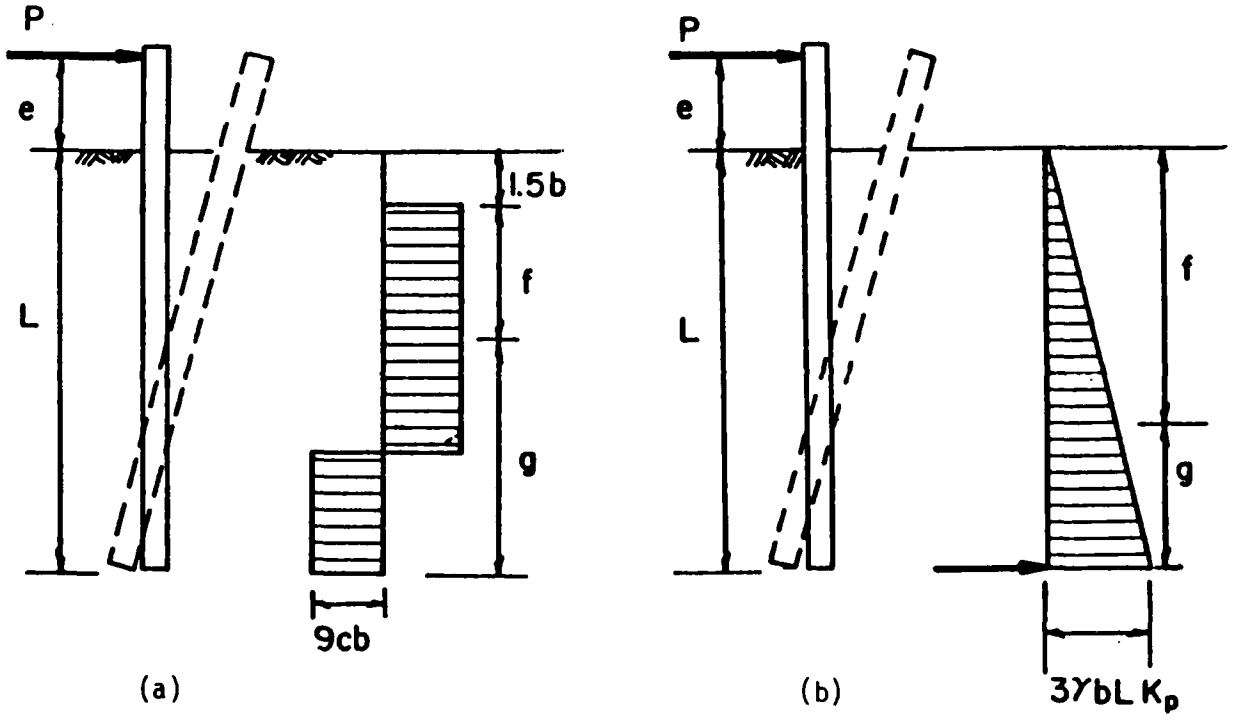

FIG. 4.1. Assumed distribution of soil resistance by Broms for short piles that are unrestrained against rotation: a) cohesive soil, b) cohesionless soil (b = pile diameter, c = undrained shear strength, γ = unit weight of soil, $k_p = \tan^2(45 + \phi/2)$, f and g are found from equations of statics)

immediate vicinity of a pile. He stated that unpublished data indicate that repetitive loading can decrease the ultimate lateral resistance of the soil to about one-half its initial value.

POULOS METHOD

Poulos and his co-workers at the University of Sidney have published several papers concerning the analysis of laterally loaded piles where the equations of elasticity have been used to develop interaction equations (Poulos, 1971a; Poulos, 1971b; Poulos, 1973; Poulos and Davis, 1980; Poulos, 1982). Poulos assumed the pile to be a thin, rectangular, vertical strip of width b, length L, and constant stiffness EI. The pile was divided into elements and each element was acted upon by a uniform, horizontal stress q which was assumed to be constant across the width of the strip.

The soil was assumed to be an ideal, homogeneous, isotropic, linear, elastic material of semi-infinite dimensions.

The Mindlin equation for horizontal displacement due to horizontal load was used to compute soil displacement. Beam theory was used to compute pile displacement. With the given assumptions, Poulos used a computer program, with the pile divided into 21 elements, to develop equations and curves for determining pile-head deflection and maximum bending moment. Solutions were developed for both fixed-head and free-head piles. An example equation is shown below with the relevant family of curves in Fig. 4.2. The solution is for a pile that is free to rotate.

$$y_{tP} = I_{yP} \frac{P_t}{E_{sp} L} \tag{4.1}$$

where

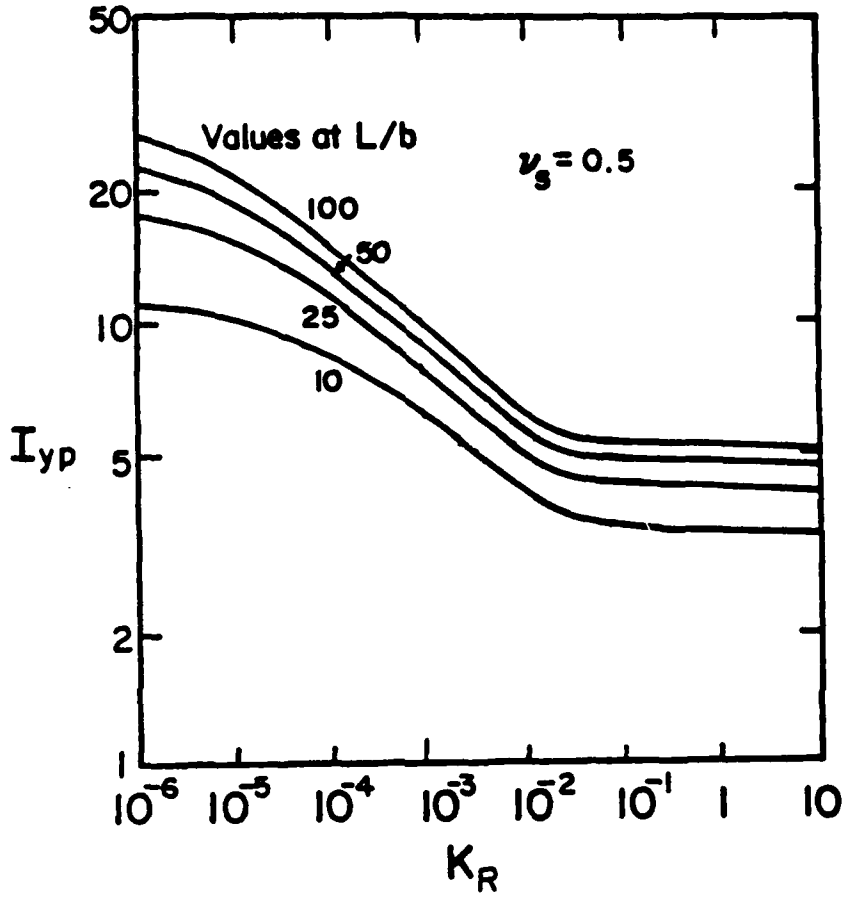

FIG. 4.2. Influence factors I_{yp} for free-head pile (after Poulos, 1971a)

y_{tP} = pile-head deflection

I_{yP} = influence factor (see Fig. 4.2)

P_t = lateral load

E_{sP} = soil modulus

L = pile length

Poulos made suggestions for obtaining numerical values of soil modulus from the undrained shear strength of clay and from the relative density of sand.

The Poulos method is limited in its application, principally because soil does not behave according to the assumptions in the theory of elasticity, except possibly for a small range of strains.

Poulos (1982) gave an extended discussion of the behavior of a single pile due to cycling the lateral load. He identified two effects: the structural "shakedown" of the pile-soil system in which permanent deformations accumulate with increasing load cycles with no changes in the pile-soil properties, and a decrease in strength and stiffness of the soil due to cyclic loading. His paper dealt mainly with the degradation of the soil due to cyclic loading.

Poulos defined degradation parameters for soil modulus D_E and for yield pressure D_p as shown by Eqs. 4.2 and 4.3, respectively.

$$D_E = E_{cP}/E_{sP} \tag{4.2}$$

$$D_p = q_{yc}/q_{ys} \tag{4.3}$$

where

E_{cP} = soil modulus after cyclic loading

E_{sP} = soil modulus for static loading

q_{yc} = limiting pile-soil interaction stress (yield pressure) after cyclic loading

q_{ys} = yield pressure for static loading

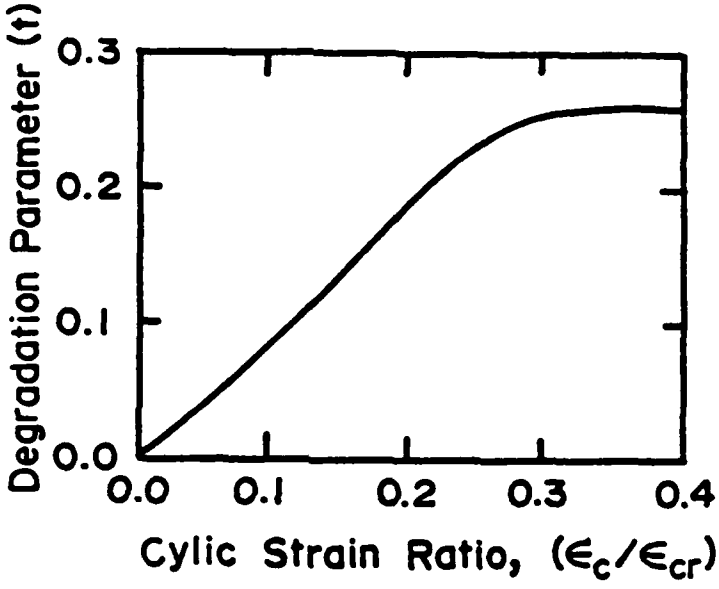

FIG. 4.3. Degradation parameter t (after Poulos, 1982)

Poulos noted that a limited amount of data are available on degradation factors and he suggested the use of data summarized by Idriss, et al (1978). Poulos prepared Fig. 4.3 from the Idriss data, with ε_c redefining the cyclic strain and ε_{cr} redefining a representative value of cyclic strain. The value of ε_{cr} can be varied to influence the degree of cyclic degradation. The parameter t is defined by Eq. 4.4.

$$D_p = D_E = N^{-t} \tag{4.4}$$

where

N = number of cycles

The effect of the rate of loading on the degradation was also considered. The degradation factors D_E and D_p were multiplied by the rate factor D_R that is defined in Eq. 4.5.

$$D_R = 1 - F_p \log \frac{\lambda_r}{\lambda} \tag{4.5}$$

where

F_p = rate coefficient (limited data suggest a range of from 0.05 to 0.3)

λ_r = reference loading rate (perhaps static loading)

λ = loading rate

The computation procedure is initiated by selecting values of soil modulus and yield pressure for each element and a distribution of displacement is computed. The cyclic displacements, number of cycles, and rate of loading are used to establish degradation factors that can be used in the next cycle. The procedure is continued until convergence is achieved. Poulos indicated that a computer program, not presented in his paper, has been written to perform the analysis.

The presentation outlined above is insufficient to allow for the computation of the behavior under cyclic loading of a given pile in a given

soil profile; however, the discussion does serve to illustrate the nature of the problem.

METHOD OF USING DIFFERENCE EQUATIONS AND NONLINEAR p-y CURVES

Recommendations are presented later in this section for obtaining soil resistance p against a pile as a function of pile deflection y. Recommendations have been made for a variety of soils but only those for clay below water are shown here. A family of p-y curves can be developed, taking into account pile geometry, soil properties, and nature of loading on the pile, whether static or cyclic. With such a family of curves, a computer program can be employed that uses difference equations to solve for pile deflection, pile rotation, bending moment, shear, and soil resistance, all as a function of length along the pile.

The computation scheme is shown in Fig. 4.4. Figure 4.4(a) shows a pile subjected to a lateral load. Figure 4.4(b) shows a family of p-y curves where the curves are in the 2nd and 4th quadrants because soil resistance is opposite in direction to pile deflection. Also in Fig. 4.4(b) is a dashed line showing the deflection of the pile, either assumed or computed on the basis of an estimated soil response. Figure 4.4(c) shows the upper p-y curve enlarged with the pile deflection at that depth represented by the vertical, dashed line. A line is drawn to the soil resistance p corresponding to the deflection y with the slope of the line indicated by the symbol E_s. E_s is defined as the soil modulus. Figure 4.4(d) shows the values of soil moduli plotted as a function of depth x. In performing a computation, the computer utilizes the computed values of soil moduli and iterates until the differences in the deflections for the

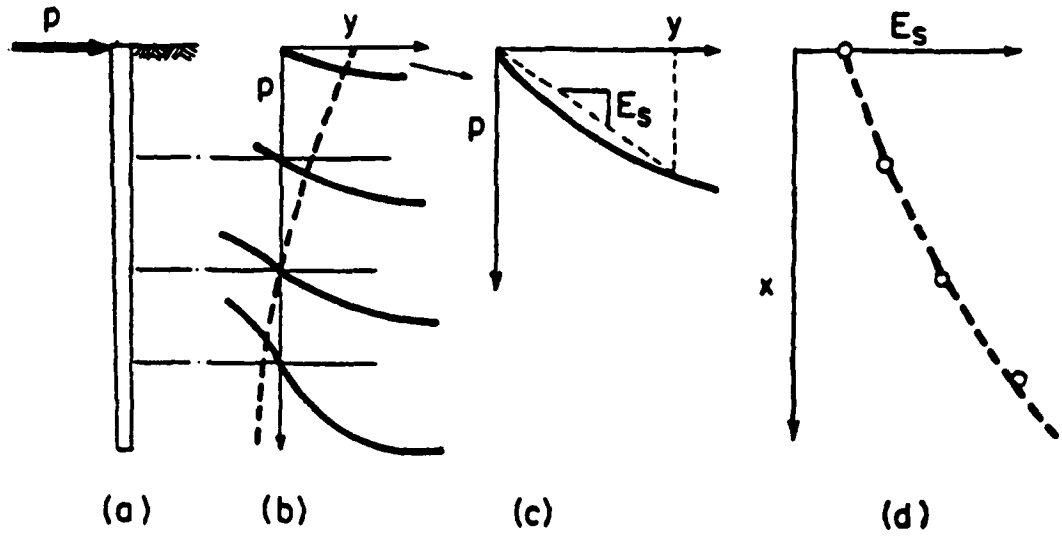

FIG. 4.4. Computation scheme for method using difference equations and nonlinear p-y curves

last two computations are less than a specified tolerance. Difference equations are formulated for a large number of points along the length the pile, perhaps 100, and a p-y curve is developed internally for each of those points. Bending moments and other types of pile response can then be computed.

As may be seen from the above discussion, the accuracy of the computed response of a pile is primarily dependent on how well the p-y curves represent the soil response. The current recommendations for developing p-y curves are based on theory to some extent but more strongly on the results of load tests in the field of full-sized, instrumented piles.

The method can be used to analyze piles subjected to short-term loading and to cyclic loading. An axial load can be applied at the pile head and the pile head may be considered to be free, fixed, or partially restrained. The diameter and stiffness of the pile may vary along its length. The method is considered to be versatile and the best currently available for analyzing single piles under lateral loading.

Soil Response for Soft Clay below Water

Field Experiments. Matlock (1970) performed lateral load tests employing a steel pipe pile that was 12.75 in. in diameter and 42 ft long. It was driven into clays near Lake Austin that had a shear strength of about 800 lb/sq ft. The pile was recovered, taken to Sabine Pass, Texas, and driven into clay with a shear strength that averaged about 300 lb/sq ft in the significant upper zone.

Recommendations for Computing p-y Curves. The following procedure is for short-term static loading and is illustrated in Fig. 4.5.

1 Obtain the best possible estimate of the variation with depth of undrained shear strength c and submerged unit weight γ'. Also

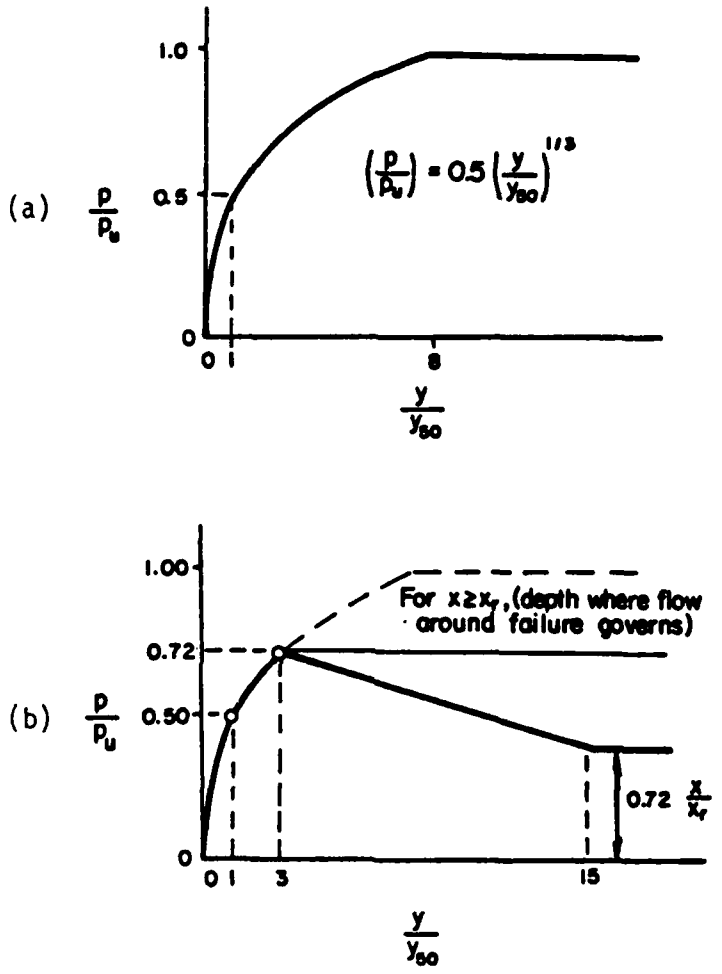

FIG. 4.5. Characteristic shapes of the p-y curves for soft clay below the water table: a) for static loading, b) for cyclic loading (from Matlock, 1970)

obtain the values of ε_{50}, the strain corresponding to one-half the maximum principal-stress difference. If no stress-strain curves are available, typical values of ε_{50} are given in Table 4.1.

TABLE 4.1. REPRESENTATIVE VALUES OF ε_{50}

Consistency of Clay	ε_{50}
Soft	0.020
Medium	0.010
Stiff	0.005

2. Compute the ultimate soil resistance per unit length of pile, using the smaller of the values given by equations below.

$$p_u = \left[3 + \frac{\gamma'}{c} x + \frac{J}{b} x\right] cb \qquad (4.6)$$

$$p_u = 9\ cb \qquad (4.7)$$

where

γ' = average effective unit weight from ground surface to p-y curve

x = depth from ground surface to p-y curve

c = shear strength at depth x

b = width of pile.

Matlock (1970) states that the value of J was determined experimentally to be 0.5 for a soft clay and about 0.25 for a medium

clay. A value of 0.5 is frequently used for J. The value of p_u is computed at each depth where a p-y curve is desired, based on shear strength at that depth.

3. Compute the deflection, y_{50}, at one-half the ultimate soil resistance from the following equation:

$$y_{50} = 2.5\,\varepsilon_{50} b. \tag{4.8}$$

4. Points describing the p-y curve are now computed from the following relationship.

$$\frac{p}{p_u} = 0.5\left(\frac{y}{y_{50}}\right)^{1/3} \tag{4.9}$$

The value of p remains constant beyond $y = 8y_{50}$.

The following procedure is for cyclic loading and is illustrated in Fig. 4.5(b).

1. Construct the p-y curve in the same manner as for short-term static loading for values of p less than $0.72p_u$.

2. Solve Eqs. 4.6 and 4.7 simultaneously to find the depth, x_r, where the transition occurs. If the unit weight and shear strength are constant in the upper zone, then

$$x_r = \frac{6\,cb}{(\gamma' b + Jc)} \quad . \tag{4.10}$$

If the unit weight and shear strength vary with depth, the value of x_r should be computed with the soil properties at the depth where the p-y curve is desired.

4. If the depth to the p-y curve is less than x_r, then the value of p decreases from $0.72p_u$ at $y = 3y_{50}$ to the value given by the following expression at $y = 15y_{50}$.

$$p = 0.72p_u\left(\frac{x}{x_r}\right) \tag{4.11}$$

The value of p remains constant beyond $y = 15y_{50}$.

Recommended Soil Tests. For determining the various shear strengths of the soil required in the p-y construction, Matlock (1970) recommended the following tests in order of preference:

1. in-situ vane-shear tests with parallel sampling for soil identification,
2. unconsolidated-undrained triaxial compression tests having a confining stress equal to the overburden pressure with c being defined as half the total maximum principal stress difference,
3. miniature vane tests of samples in tubes, and
4. unconfined compression tests.

Tests must also be performed to determine the unit weight of the soil.

Example Curves. Figures 4.6(a), 4.6(b), and 4.6(c) show example p-y curves for a 36-in. diameter pile in a soft clay with an undrained shear strength of 500 lb/sq ft. The submerged unit weight of the clay is 50 lb/cu ft and ε_{50} was selected as 0.020. Curves are shown for both static and cyclic loading. The loss of resistance due to cyclic loading is dramatically revealed for the particular case that was selected.

Soil Response for Stiff Clay below Water

Field Experiments. Reese, Cox, and Koop (1975) performed lateral load tests employing steel-pipe piles that were 24 in. in diameter and 50 ft long. The piles were driven into stiff clay at a site near Manor, Texas. The clay had an undrained shear strength ranging from about 1.0 T/sq ft at the ground surface to about 3.0 T/sq ft at a depth of 12 ft.

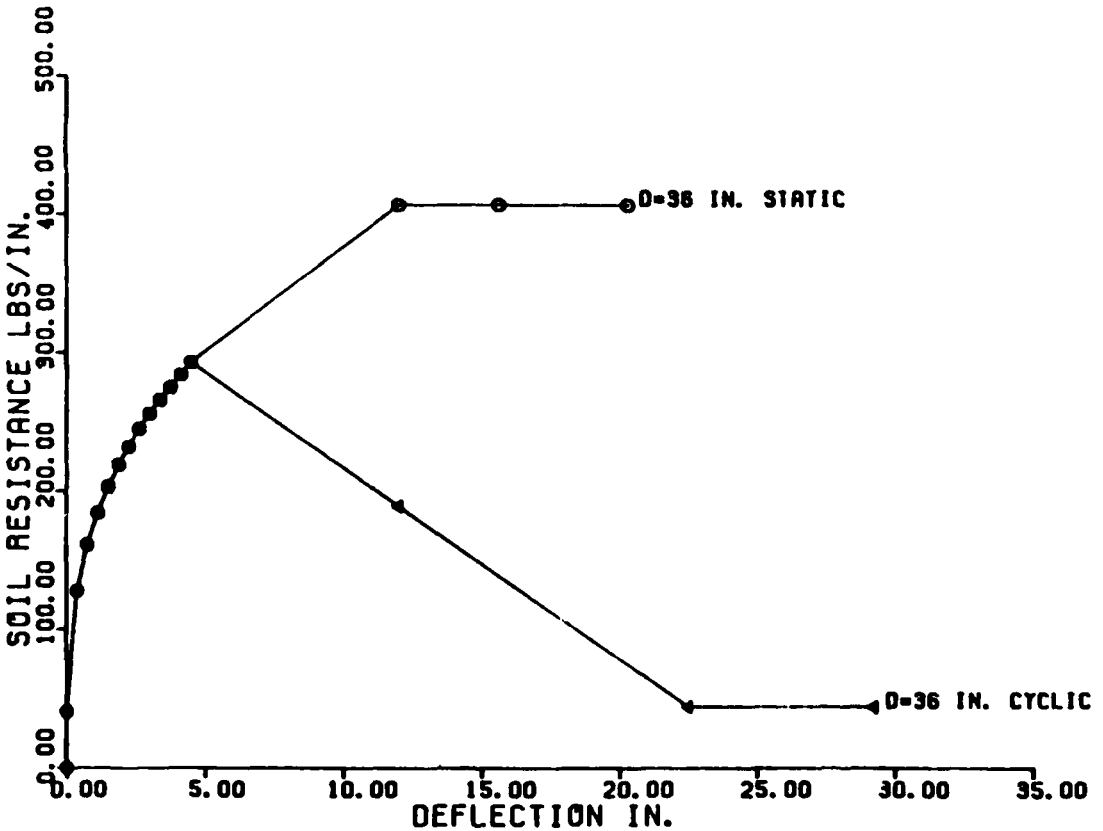

FIG. 4.6a. Example p-y curves for soft clay below the water surface for a depth of 36 in.

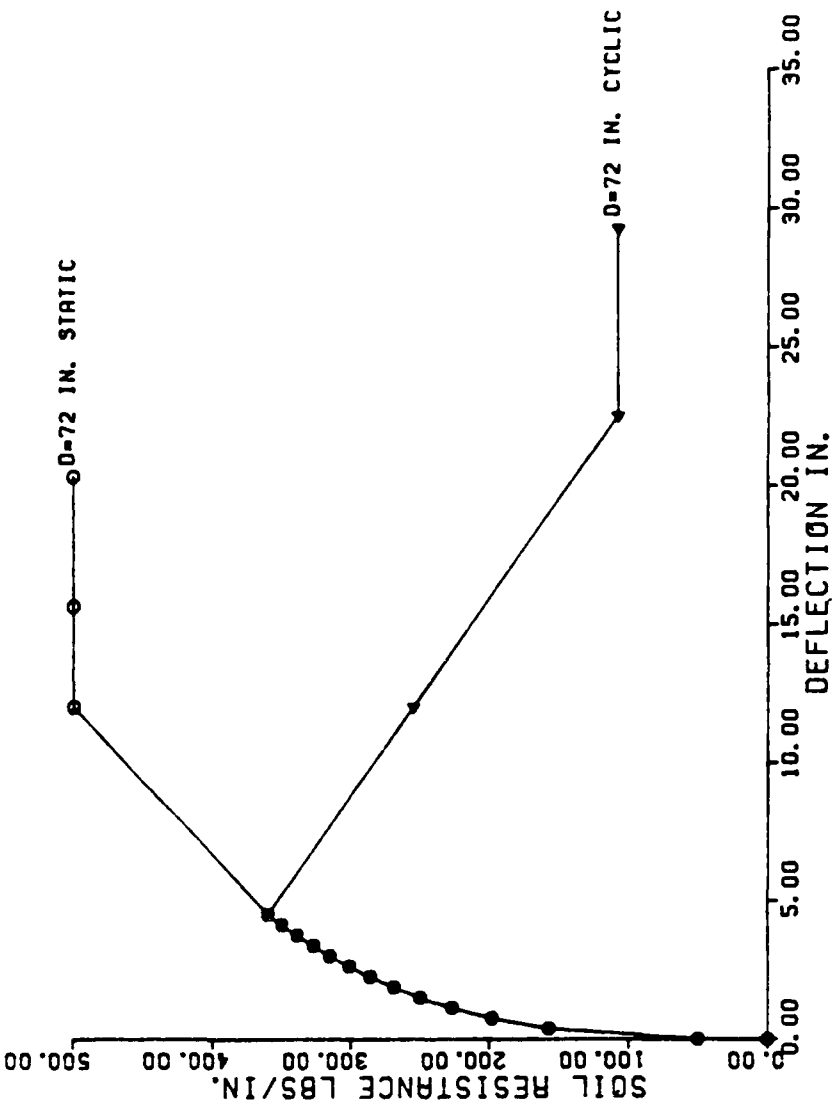

FIG. 4.6b. Example p-y curves for soft clay below the water surface for a depth of 72 in.

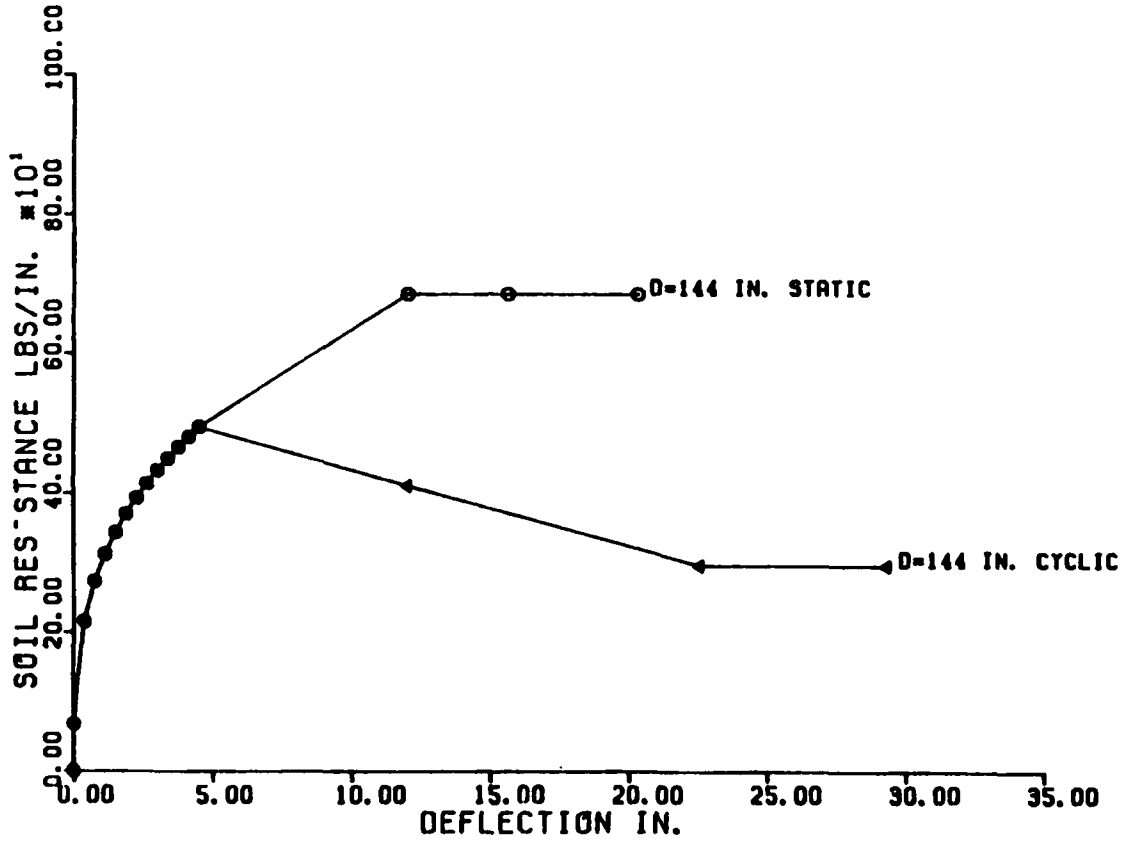

FIG. 4.6c. Example p-y curves for soft clay below the water surface for a depth of 144 in.

Recommendations for Computing p-y Curves. The following procedure is for short-term static loading and is illustrated by Fig. 4.7.

1. Obtain values for undrained soil shear strength c, soil submerged unit weight γ', and pile diameter b.
2. Compute the average undrained soil shear strength c_a over the depth x.
3. Compute the ultimate soil resistance per unit length of pile using the smaller of the values given by the equations below:

$$P_{ct} = 2c_a b + \gamma' bx + 2.83\, c_a x, \tag{4.12}$$

$$P_{cd} = 11\, cb. \tag{4.13}$$

4. Choose the appropriate value of A_s from Fig. 4.8 for the particular nondimensional depth.
5. Establish the initial straight-line portion of the p-y curve:

$$p = (kx)y. \tag{4.14}$$

Use the appropriate value of k_s or k_c from Table 4.2 for k.

6. Compute the following:

$$y_{50} = \varepsilon_{50} b. \tag{4.15}$$

Use an appropriate value of ε_{50} from results of laboratory tests or, in the absence of laboratory tests, from Table 4.3.

7. Establish the first parabolic portion of the p-y curve, using the following equation and obtaining p_c from Eqs. 4.12 or 4.13.

$$p = 0.5\, p_c \left(\frac{y}{y_{50}}\right)^{0.5} \tag{4.16}$$

Equation 4.16 should define the portion of the p-y curve from the point of the intersection with Eq. 4.14 to a point where y is equal to $A_s y_{50}$ (see note in step 10).

8. Establish the second parabolic portion of the p-y curve,

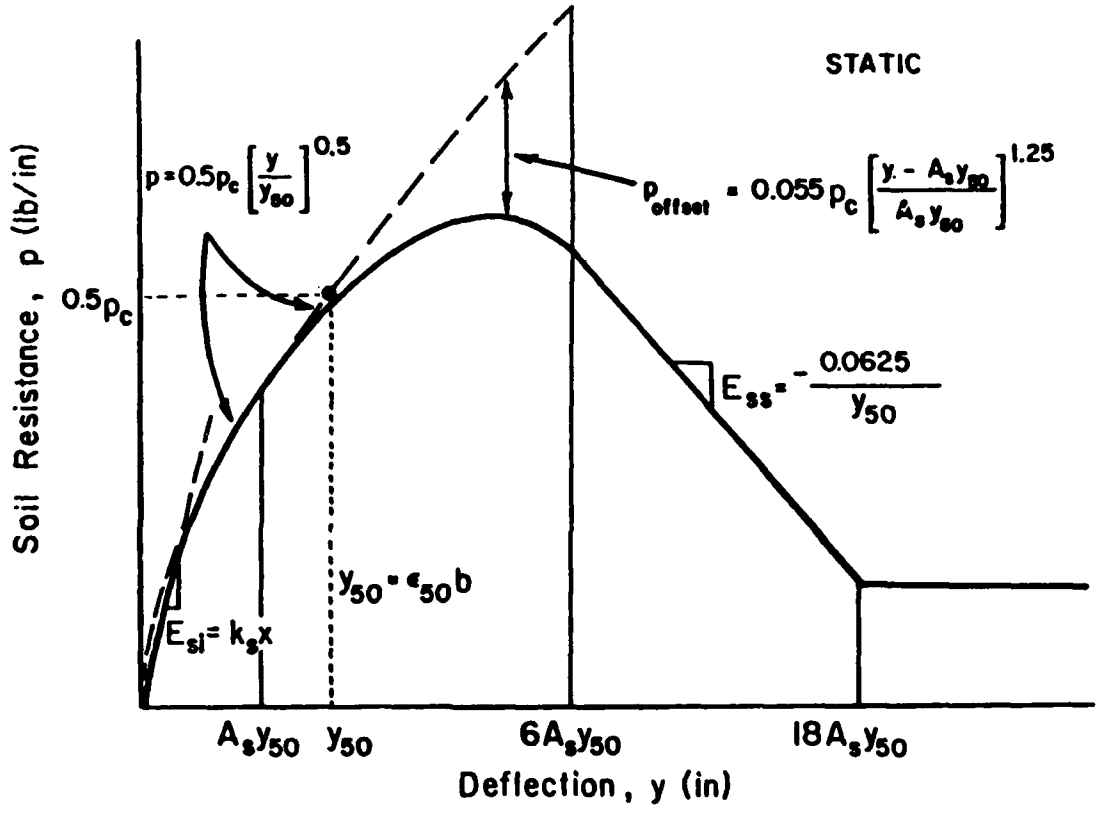

FIG. 4.7. Characteristic shape of p-y curve for static loading in stiff clay below the water table (after Reese, Cox, and Koop, 1975)

TABLE 4.2. REPRESENTATIVE VALUES OF k FOR STIFF CLAYS

	Average Undrained Shear Strength* T/sq ft		
	0.5-1	1-2	2-4
k_s (Static) lb/cu in.	500	1000	2000
k_c (Cyclic) lb/cu in.	200	400	800

*The average shear strength should be computed from the shear strength of the soil to a depth of 5 pile diameters. It should be defined as half the total maximum principal stress difference in an unconsolidated undrained triaxial test.

TABLE 4.3. REPRESENTATIVE VALUES OF ε_{50} FOR STIFF CLAYS

	Average Undrained Shear Strength T/sq ft		
	0.5-1	1-2	2-4
ε_{50} (in./in.)	0.007	0.005	0.004

$$p = 0.5\ p_c \left(\frac{y}{y_{50}}\right)^{0.5} - 0.055\ p_c \left(\frac{y - A_s y_{50}}{A_s y_{50}}\right)^{1.25} . \qquad (4.17)$$

Equation 4.17 should define the portion of the p-y curve from the point where y is equal to $A_s y_{50}$ to a point where y is equal to $6A_s y_{50}$ (see note in step 10).

9. Establish the next straight-line portion of the p-y curve,

$$p = 0.5\ p_c(6A_s)^{0.5} - 0.411\ p_c - \frac{0.0625}{y_{50}}\ p_c(y - 6A_s y_{50}). \qquad (4.18)$$

Equation 4.18 should define the portion of the p-y curve from the point where y is equal to $6A_s y_{50}$ to a point where y is equal to $18A_s y_{50}$ (see note in step 10).

10. Establish the final straight-line portion of the p-y curve,

$$p = 0.5p_c(6A_s)^{0.5} - 0.411p_c - 0.75p_c A_s \qquad (4.19)$$

or

$$p = p_c(1.225\sqrt{A_s} - 0.75A_s - 0.411). \qquad (4.20)$$

Equation 4.20 should define the portion of the p-y curve from the point where y is equal to $18A_s y_{50}$ and for all larger values of y (see following note).

Note: The step-by-step procedure is outlined, and Fig. 4.7 is drawn, as if there is an intersection between Eqs. 4.14 and 4.16. However, there may be no intersection of Eq. 4.14 with any of the other equations or, if no intersection occurs, Eq. 4.14 defines the complete p-y curve.

The following procedure is for cyclic loading and is illustrated in Fig. 4.9.

1. Steps 1, 2, 3, 5, and 6 are the same as for the static case.
4. Choose the appropriate value of A_c from Fig. 4.8 for the particular nondimensional depth.

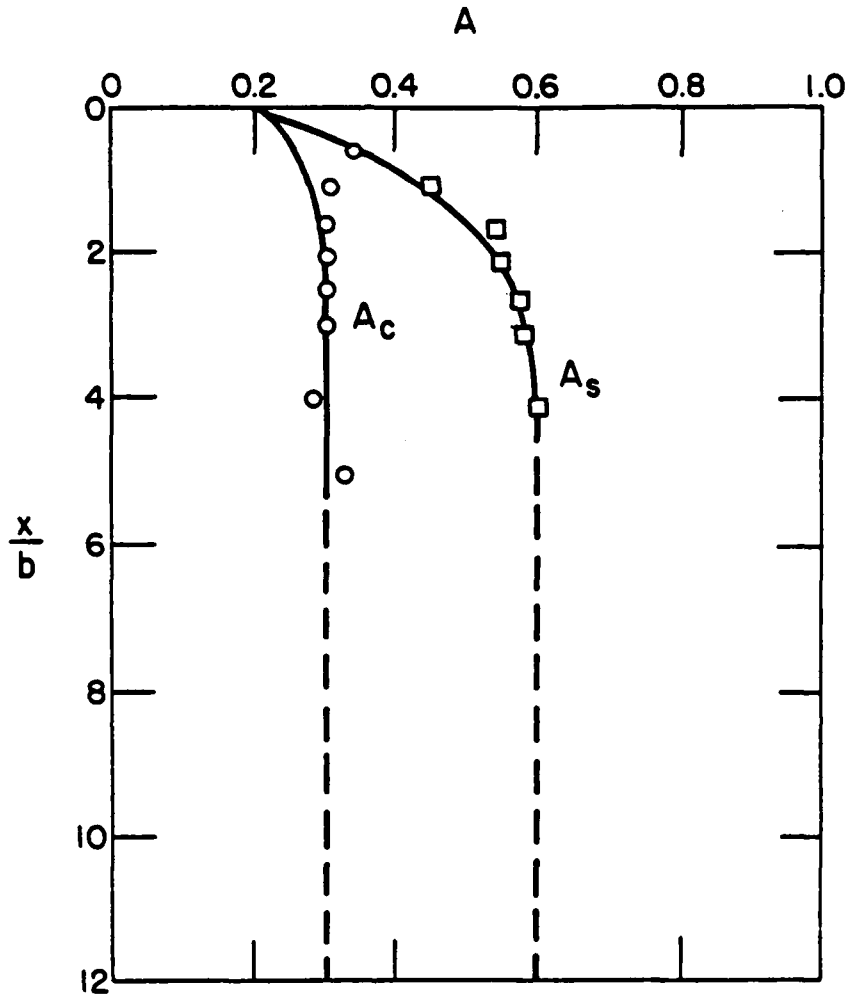

FIG. 4.8. Values of constants A_s and A_c

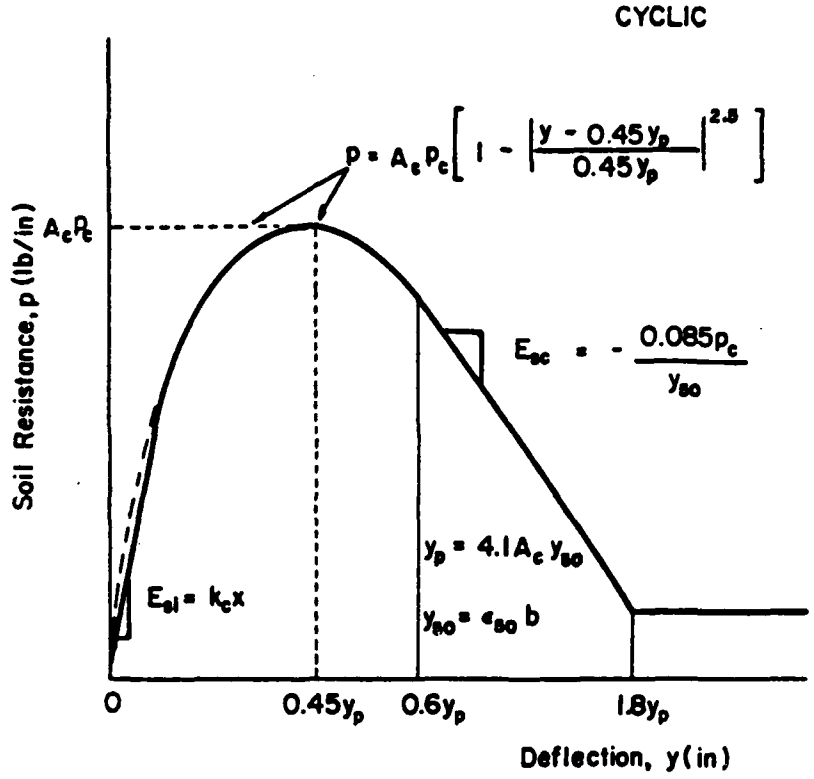

FIG. 4.9. Characteristic shape of p-y curve for cyclic loading in stiff clay below water table (after Reese, Cox, and Koop, 1975)

Compute the following:

$$y_p = 4.1\, A_c y_{50}. \tag{4.21}$$

7. Establish the parabolic portion of the p-y curve,

$$p = A_c p_c \left[1 - \left| \frac{y - 0.45y_p}{0.45y_p} \right|^{2.5} \right] . \tag{4.22}$$

Equation 4.22 should define the portion of the p-y curve from the point of the intersection with Eq. 4.14 to where y is equal to $0.6y_p$ (see note in step 9).

8. Establish the next straight-line portion of the p-y curve

$$p = 0.936A_c p_c - \frac{0.085}{y_{50}} p_c (y - 0.6y_p) . \tag{4.23}$$

Equation 4.23 should define the portion of the p-y curve from the point where y is equal to $0.6y_p$ to the point where y is equal to $1.8y_p$ (see note in step 9).

9. Establish the final straight-line portion of the p-y curve,

$$p = 0.936A_c p_c - \frac{0.102}{y_{50}} p_c y_p . \tag{4.24}$$

Equation 4.24 should define the portion of the p-y curve from the point where y is equal to $1.8y_p$ and for all larger values of y (see following note).

Note: The step-by-step procedure is outlined, and Fig. 4.9 is drawn, as if there is an intersection between Eqs. 4.14 and 4.22. However, there may be no intersection of those two equations and there may be no intersection of Eq. 4.14 with any of the other equations defining the p-y curve. If there is no intersection, the equation should be employed that gives the smallest value of p for any value of y.

Recommended Soil Tests. Triaxial compression tests of the unconsolidated-undrained type with confining pressures conforming to the in situ overburden pressures are recommended for determining the shear strength of the soil. The value of ε_{50} should be taken as the strain during the test corresponding to the stress equal to half the maximum total-principal-stress difference. The shear strength, c, should be interpreted as one-half of the maximum total-stress difference. Values obtained from the triaxial tests might be somewhat conservative but would represent more realistic strength values than other tests. The unit weight of the soil must be determined.

Example Curves. Figures 4.10(a), 4.10(b), and 4.10(c) show example p-y curves for a 36-in. diameter pile in a stiff clay with an undrained shear strength of 2000 lb/sq ft. The submerged unit weight of the clay is 50 lb/cu ft and ε_{50} was selected as 0.005. The value of k to define the initial portion of the p-y curves was selected as 1000 lb/cu in.

As for soft clay, the influence of cyclic loading is shown to be significant.

Soil Response of Stiff Clay above the Water Table

Field Experiments. A lateral load test was performed at a site in Houston where the foundation was a drilled shaft, 36 in. in diameter and an embedded length of 42 ft. A 10-in. diameter pipe, instrumented at intervals along its length with electrical-resistance-strain gauges, was positioned along the axis of the shaft before concrete was placed. The average undrained shear strength of the clay in the upper 20 ft was approximately 2,200 lb/sq ft. The experiments and their interpretation are discussed in detail by Welch and Reese (1972) and Reese and Welch (1975).

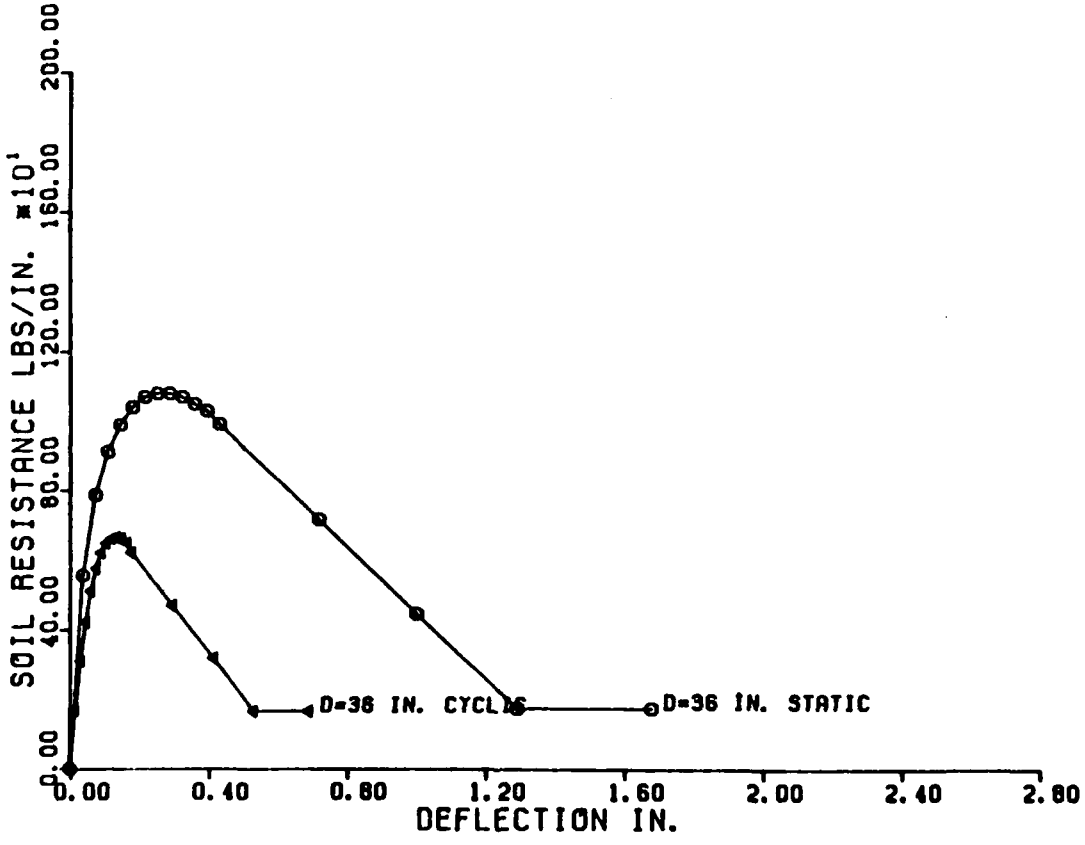

FIG. 4.10a. Example p-y curves for stiff clay below the water surface for a depth of 36 in.

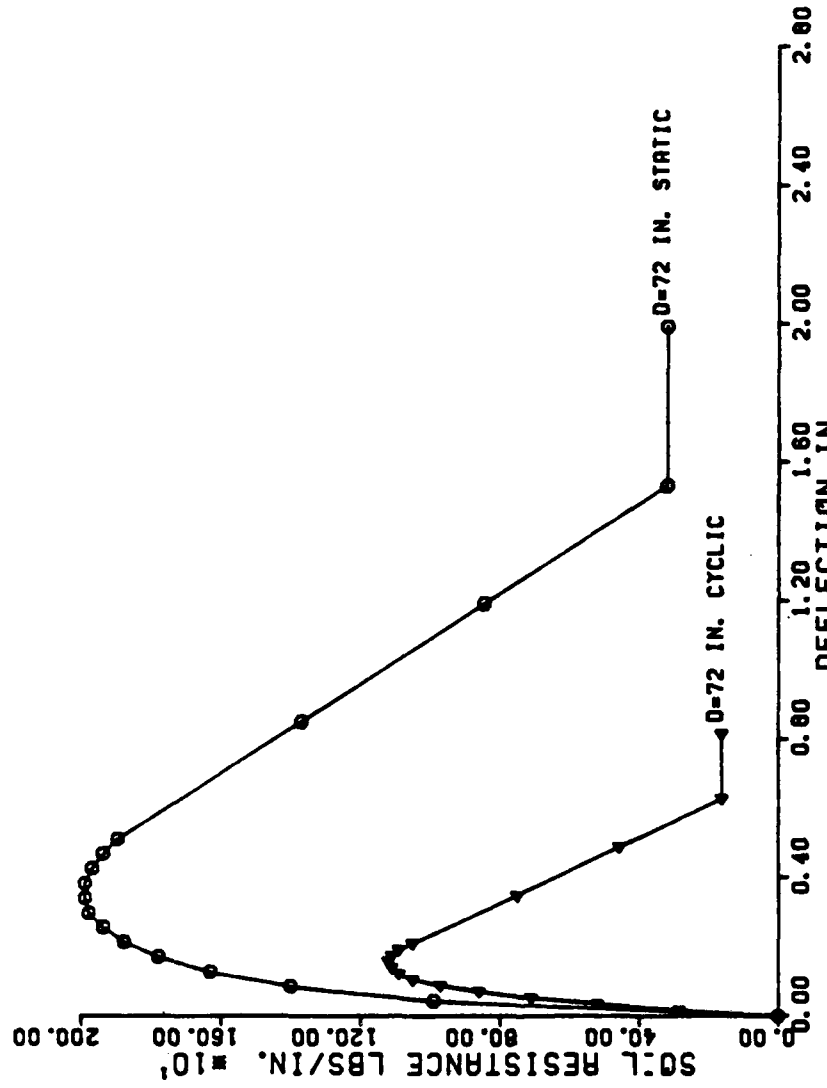

FIG. 4.10b. Example p-y curves for a stiff clay below the water surface for a depth of 72 in.

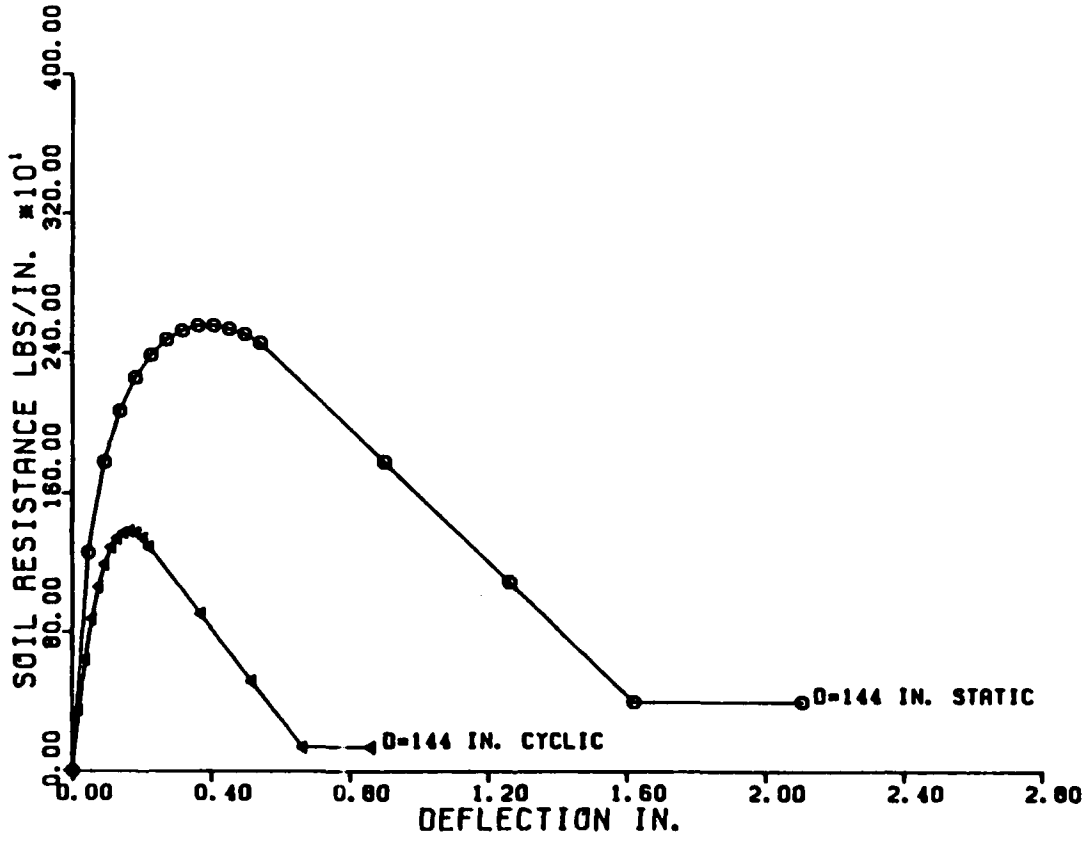

FIG. 4.10c. Example p-y curves for stiff clay below the water surface for a depth of 144 in.

Recommendations for Computing p-y Curves. The following procedure is for short-term static loading and is illustrated in Fig. 4.11a.

1. Obtain values for undrained shear strength c, soil unit weight γ, and pile diameter b. Also obtain the values of ε_{50} from stress-strain curves. If no stress-strain curves are available, use a value of 0.010 or 0.005 for ε_{50} as given in Table 4.1, the larger value being more conservative.
2. Compute the ultimate soil resistance per unit length of shaft, p_u, using the smaller of the values given by Eqs. 4.6 and 4.7. (In the use of Eq. 4.6 the shear strength is taken as the average from the ground surface to the depth being considered and J is taken as 0.5. The unit weight of the soil should reflect the position of the water table.)
3. Compute the deflection, y_{50}, at one-half the ultimate soil resistance from Eq. 4.8.
4. Points describing the p-y curve may be computed from the relationship below.

$$\frac{p}{p_u} = 0.5\left(\frac{y}{y_{50}}\right)^{1/4} \tag{4.25}$$

5. Beyond $y = 16y_{50}$, p is equal to p_u for all values of y.

The following procedure is for cyclic loading and is illustrated in Fig. 4.11b.

1. Determine the p-y curve for short-term static loading by the procedure previously given.
2. Determine the number of times the design lateral load will be applied to the pile.

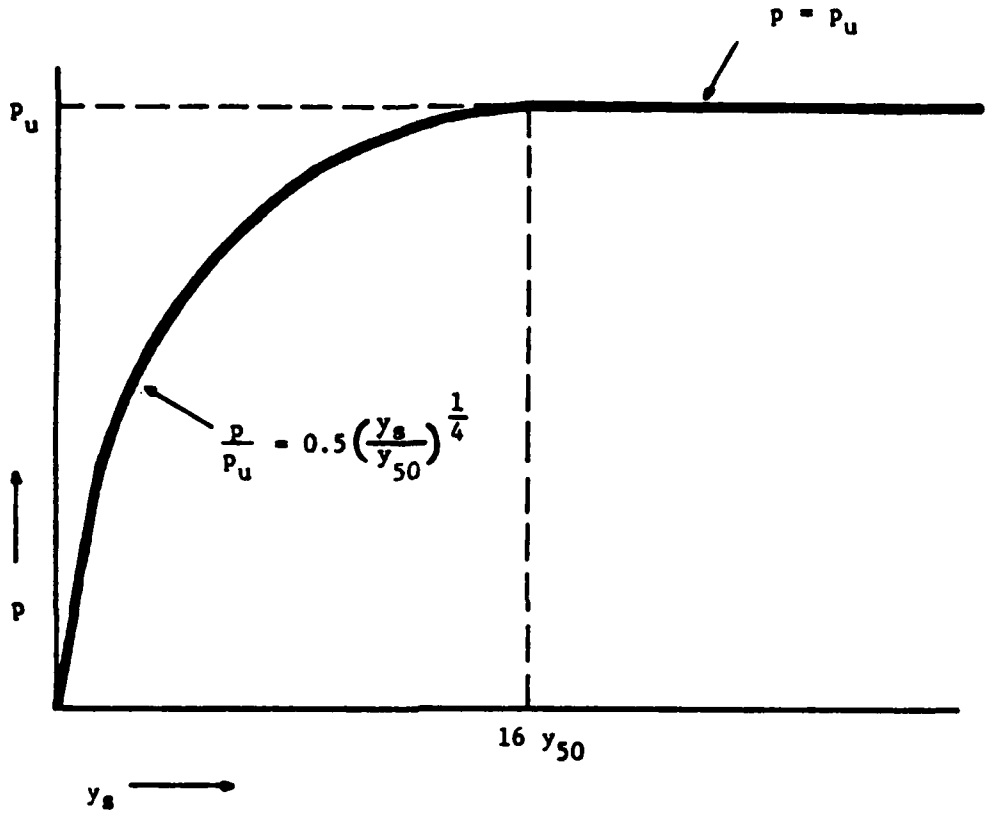

FIG. 4.11a. Characteristic shape of p-y curve for static loading in stiff clay above water surface

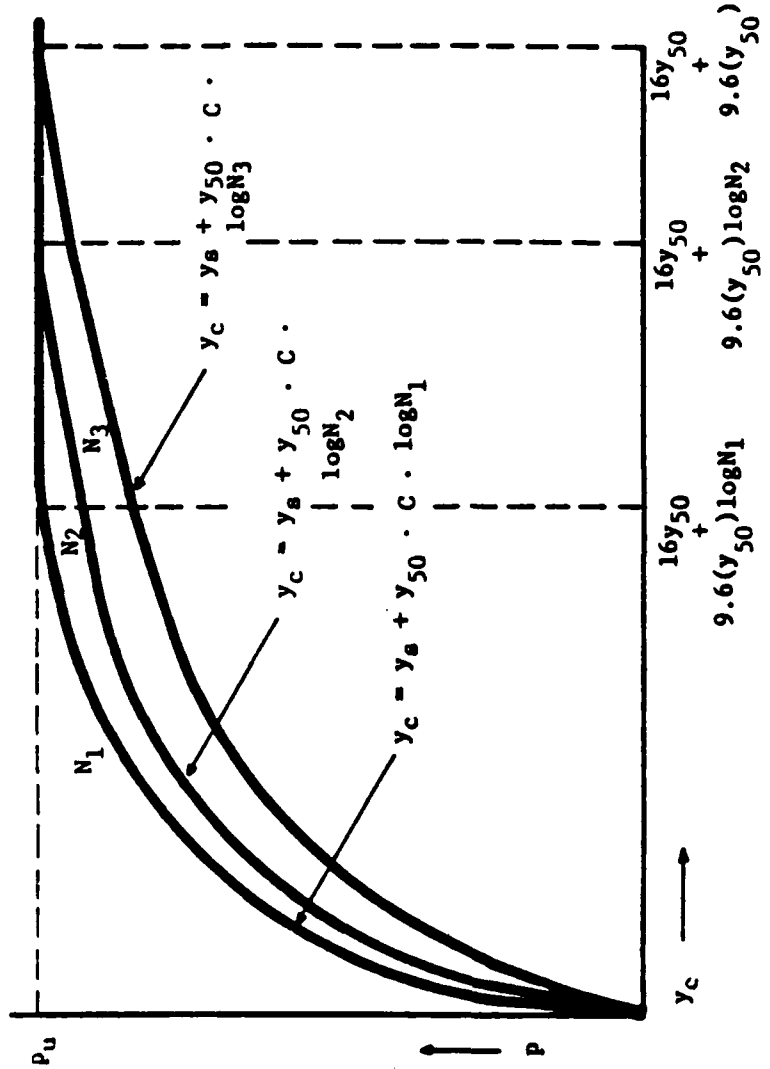

FIG. 4.11b. Characteristic shape of p-y curve for cyclic loading in stiff clay above the water surface

3. For several values of p/p_u obtain the value of C, the parameter describing the effect of repeated loading on deformation, from a relationship developed by laboratory tests, (Welch and Reese, 1972), or in the absence of tests, from the following equation.

$$C = 9.6 \left(\frac{p}{p_u}\right)^4 \tag{4.26}$$

4. At the value of p corresponding to the values of p/p_u selected in step 3, compute new values of y for cyclic loading from the following equation.

$$y_c = y_s + y_{50} \cdot C \cdot \log N \tag{4.27}$$

where

y_c = deflection under N-cycles of load,

y_s = deflection under short-term static load,

y_{50} = deflection under short-term static load at one-half the ultimate resistance, and

N = number of cycles of load application.

5. The p-y curve defines the soil response after N-cycles of load.

Recommended Soil Tests. Triaxial compression tests of the unconsolidated-undrained type with confining stresses equal to the overburden pressures at the elevations from which the samples were taken are recommended to determine the shear strength. The value of ε_{50} should be taken as the strain during the test corresponding to the stress equal to half the maximum total principal stress difference. The undrained shear strength, c, should be defined as one-half the maximum total-principal-stress difference. The unit weight of the soil must also be determined.

Example Curves. Shown in Fig. 4.12a, 4.12b, and 4.12c are example p-y curves for a 30-in. diameter pile in a stiff clay above the water table. The clay has an undrained shear strength of 2000 lb/sq ft, a total unit weight of 115 lb/cu ft and ε_{50} was chosen to be 0.005. The p-y curves are shown for static loading and cyclic loading (100, 200, and 500 cycles).

Using the stiff-clay-above-the-water-table criteria, the influence of cyclic loading is shown to be significant, but less than the effects predicted using the soft clay (below the water table) and stiff clay (below the water table) criteria.

3. For several values of p/p_u obtain the value of C, the parameter describing the effect of repeated loading on deformation, from a relationship developed by laboratory tests, (Welch and Reese, 1972), or in the absence of tests, from the following equation.

$$C = 9.6 \left(\frac{p}{p_u}\right)^4 \tag{4.26}$$

4. At the value of p corresponding to the values of p/p_u selected in step 3, compute new values of y for cyclic loading from the following equation.

$$y_c = y_s + y_{50} \cdot C \cdot \log N \tag{4.27}$$

where

y_c = deflection under N-cycles of load,

y_s = deflection under short-term static load,

y_{50} = deflection under short-term static load at one-half the ultimate resistance, and

N = number of cycles of load application.

5. The p-y curve defines the soil response after N-cycles of load.

Recommended Soil Tests. Triaxial compression tests of the unconsolidated-undrained type with confining stresses equal to the overburden pressures at the elevations from which the samples were taken are recommended to determine the shear strength. The value of ε_{50} should be taken as the strain during the test corresponding to the stress equal to half the maximum total principal stress difference. The undrained shear strength, c, should be defined as one-half the maximum total-principal-stress difference. The unit weight of the soil must also be determined.

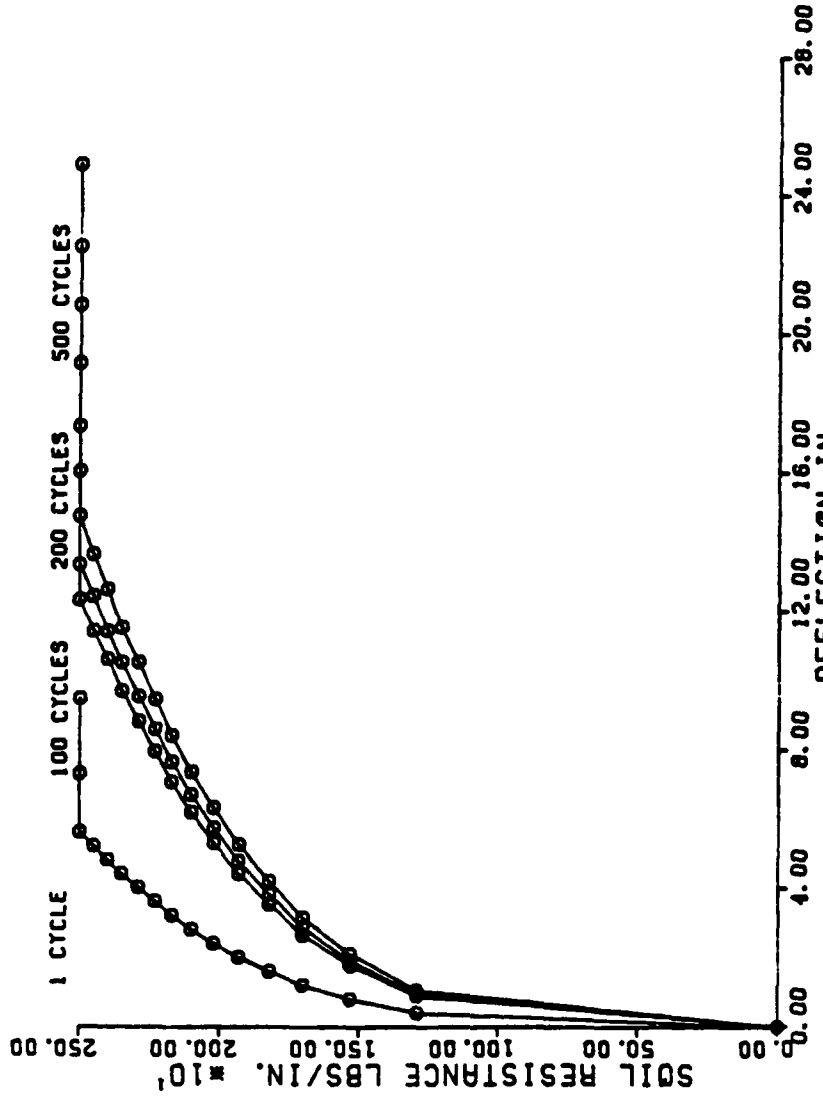

FIG. 4.12c. Example p-y curves for stiff clay above water for a depth of 144 in.

CHAPTER 5. COMPARISON OF MEASURED AND PREDICTED BEHAVIOR OF PILES SUBJECTED TO LATERAL LOAD

INTRODUCTION

Presented in the previous chapter were methods for computing the behavior of piles in cohesive soils subjected to both static and cyclic lateral loading. Of these methods, the p-y approach seems to be best documented and the most employed when cyclic loading is to be considered. As noted earlier, the principal thrust of the research reported herein is to gain additional insight into the exact reasons for the loss of soil resistance of piles in cohesive soil that are subjected to cyclic lateral load. Emphasis is placed on the p-y method. The studies reported in Chapter 3 showed the significant loss of resistance in several of the reported tests due to cyclic loading. Comparison of the behavior of piles computed by the p-y method with measured behavior, as reported in this chapter, is useful. The reader will gain an understanding of the accuracy of the p-y method (assuming the experimental results to be correct) for predicting both static and cyclic behavior and the importance of the studies reported herein will be emphasized.

In order to compare the measured and predicted behavior, p-y analyses were performed for most of the case histories presented in Chapter 3. For each case history, three p-y analyses were made. The three analyses are termed as soft clay, stiff clay below the water table (stiff clay (bwt)), and stiff clay above the water table (stiff clay (awt)).

The comparisons of predicted and measured response of most of the case histories are presented in the form of curves of lateral load versus deflection. Although comparisons of predicted and measured bending

moments as a function of pile length would also be desirable, measured values of moment versus lateral load were, in most cases, not presented. Therefore, to maintain consistency in this presentation, only load versus deflection curves are compared. The only exception is for Gaul's (1958) data in which only the measured moments were presented.

For many of the case histories presented in Chapter 3, enough data were presented to allow the p-y analyses to be conducted; however, in some cases, assumptions regarding soil or pile properties were necessary. The particular assumptions made are presented in the discussion of each case history.

Finally, it should be mentioned that the computed deflections using the p-y method are very sensitive to the soil and pile parameters used in the analyses. Previous studies have shown that the computation of the maximum bending moment is much less sensitive to changes in soil and pile properties.

MODEL TESTS

The results of three model tests were described in Chapter 3; however, only the results of the tests by Gaul (1958), and Valenzuela and Lee (1978) are studied herein. The test described by Scott (1977) is not included because it was described as a silty material and behaved as a cohesionless soil. In both model tests, no free water was present to enter or exit any gaps that might form between the pile and soil.

Gaul (1958)

In the series of model pile tests that Gaul performed, measured values of moment were recorded for both the static and cyclic cases; however,

no data on load versus deflection were presented. Therefore, only comparisons are made of lateral load versus maximum bending moment.

Values of the shear strength of the clay were not given and are estimated by varying the values of shear strength used with the soft clay p-y analyses until a reasonable agreement was reached between computed and measured bending moment. A shear strength of 0.5 lb/sq in. was selected, based on the comparison shown in Fig 5.1a. The value of ε_{50}, axial strain corresponding to half the stress difference at failure in a triaxial compression test, was selected based on recommendations made by Reese and given in Table 4.1. In addition, a parameter, k, describing the initial soil modulus of the clay is necessary to define the p-y curves for stiff clay (bwt), and the recommendations of Reese, outlined in Table 4.2 were used to obtain a value of 1000 lbs/cu in. for the static case and a value of 400 lbs/cu in. for the cyclic case.

Analyses were performed with all three p-y criteria; the soft clay, stiff clay (bwt), and stiff clay (awt), and are shown in Fig. 5.1a, 5.1b, and 5.1c. As can be seen, the measured values of moment show little or no increase after cycling. Predictions made using the soft clay criteria also indicate no increase in moments due to cyclic loading. Analyses performed using the stiff clay (bwt) criteria do predict an increase in maximum moment beginning at a lateral load of approximately 20 lbs and ending at a lateral load of approximately 50 lbs. Predictions of lateral behavior using the stiff clay (awt) criteria show an increase in moment for 10 and 100 cycles along the whole range of loading from 0 to 90 lbs.

Valenzuela and Lee (1978)

Shown in Figs. 5.2a, 5.2b, and 5.2c are curves showing computed and measured values of load versus deflection. The three sets of p-y criteria

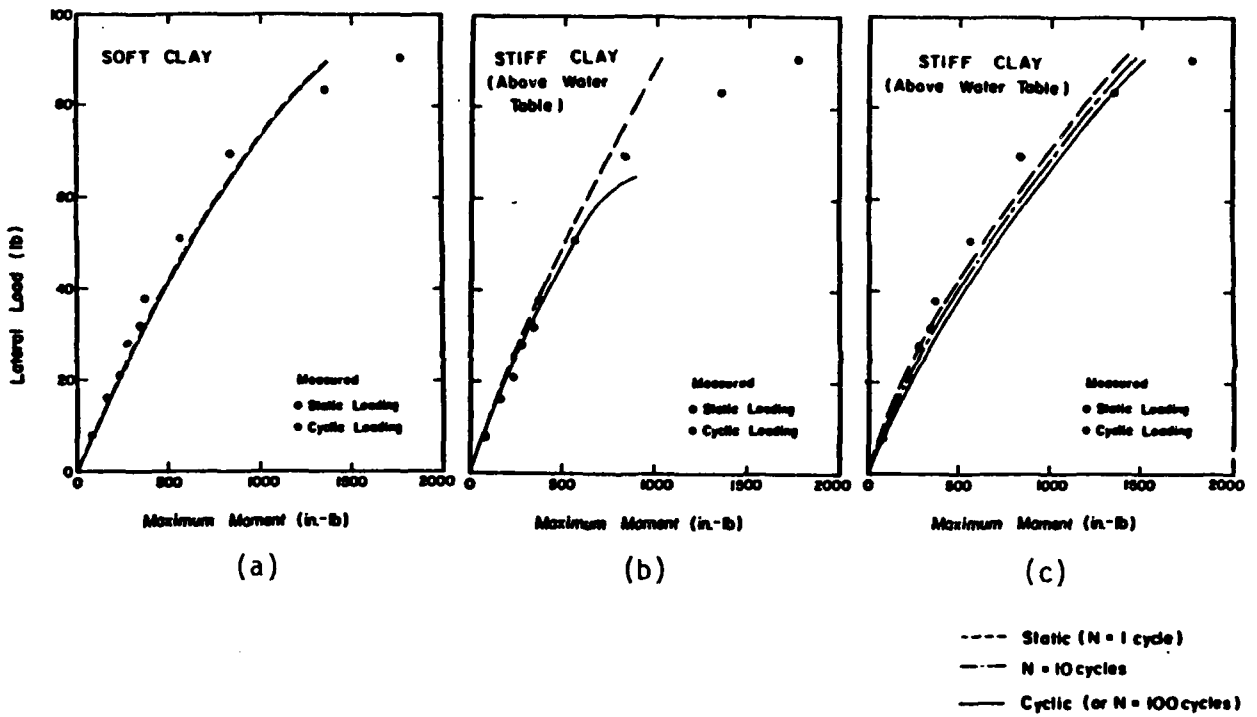

FIG. 5.1. Curves showing comparisons of computed and measured maximum bending moment for model tests of Gaul

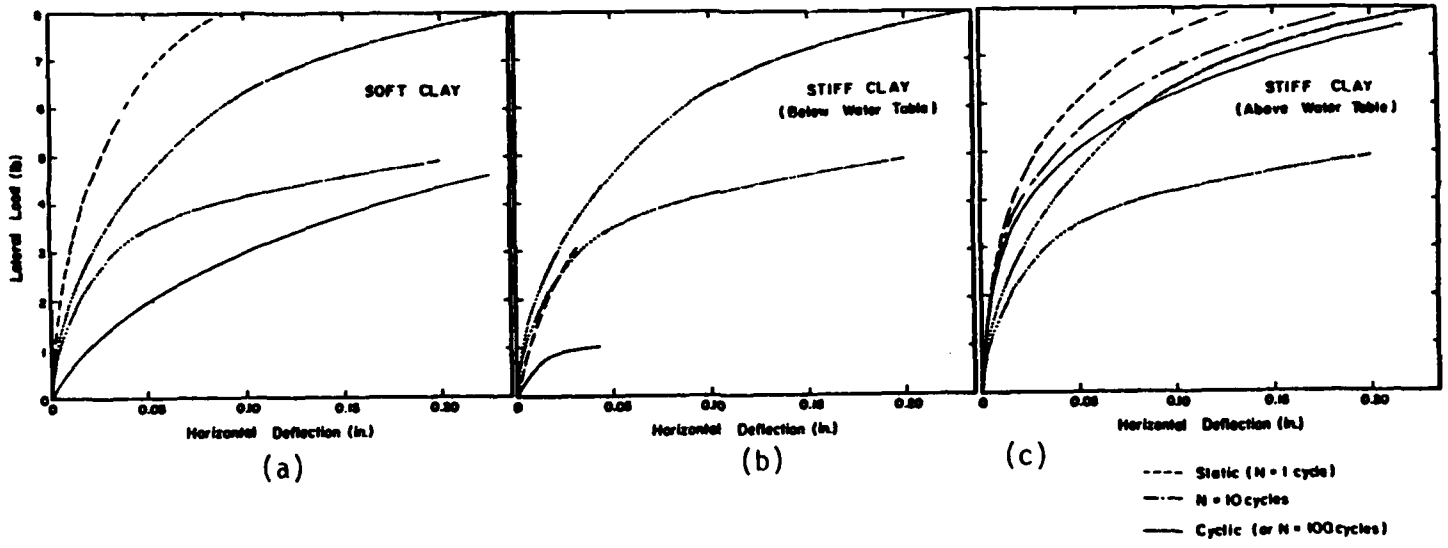

FIG. 5.2. Curves showing comparison of computed and measured deflections for model tests of Valenzuela and Lee

were used in the computations. The curves from the experiments are plotted as dotted lines rather than specific symbols because the curves are averages from many model pile tests.

A factor that must be considered in analyzing the comparisons in Fig. 5.2 is that Valenzuela and Lee reported that the model pile yielded structurally at a deflection of approximately 0.1 in. with a static load of approximately 6 lbs. Although no mention was made of the pile yielding during cyclic loading, it is expected that yielding would occur at a cyclic load less than 6 lbs. Therefore, all comparisons between measured and predicted values are made for lateral deflections less than 0.1 in.

As before, and in the studies that follow, predictions were made using the three sets of p-y criteria for cohesive soils. Curves showing comparisons of computed deflection versus lateral load and the results from the experiments of Valenzuela and Lee are shown in Figs. 5.2a, 5.2b, and 5.2c. In Fig. 5.2a it may be seen that the static behavior is predicted to be much stiffer than the measured behavior, whereas the predicted cyclic behavior is much softer than measured. Thus, the effect of cycling in increasing deflection for a given load is predicted to be much greater than the measurements indicate.

Using the stiff clay (bwt) criteria, values of static and cyclic deflections for a given load are predicted to be much greater than measured. In addition, the difference between static and cyclic deflections for a given load are predicted to be much greater than measured.

Using the stiff clay (awt) criteria, predicted values of deflection for a given load are less than the measured values; however, the effect of cyclic loading, as measured by the increase in deflection for a given load, is similar for measurement and prediction.

FIELD TESTS CONDUCTED WITH NO FREE WATER AT GROUND SURFACE

The results of 7 pile load tests are discussed herein. Comparisons are shown between deflection versus lateral load from predictions and from measurements. Predictions were made using the three sets of p-y criteria previously mentioned. Some of the case histories involve testing at the same site, but with changes in the characteristics of the pile or loading conditions. In each of the cases cited below, free water was not available at the ground surface. Therefore, no water could enter or exit gaps formed between the pile and soil.

Price and Wardle (1982), Tubular Pile

In order to obtain predicted values of lateral load versus deflection, shear strength versus depth was obtained from the triaxial tests and field tests shown in Fig. 3.10. The shear strength was assumed to vary linearly between the depths at which shear strengths were specified.

Values of ε_{50} were obtained from the relationship of shear strength and secant modulus shown in Fig. 3.10. For each data point, a value of ε_{50} was calculated by dividing the shear strength by the corresponding modulus value. These values were plotted versus depth and estimated values of ε_{50} were based on the plot.

The measured and predicted curves of lateral load versus deflection are shown in Figs. 5.3a, 5.3b, and 5.3c. With the use of soft clay criteria, shown in Fig. 5.3a, the predicted and measured relationships seem to be in reasonable agreement. Very little difference between the static and cyclic behavior is seen for both measured and predicted relationships of lateral load versus deflection.

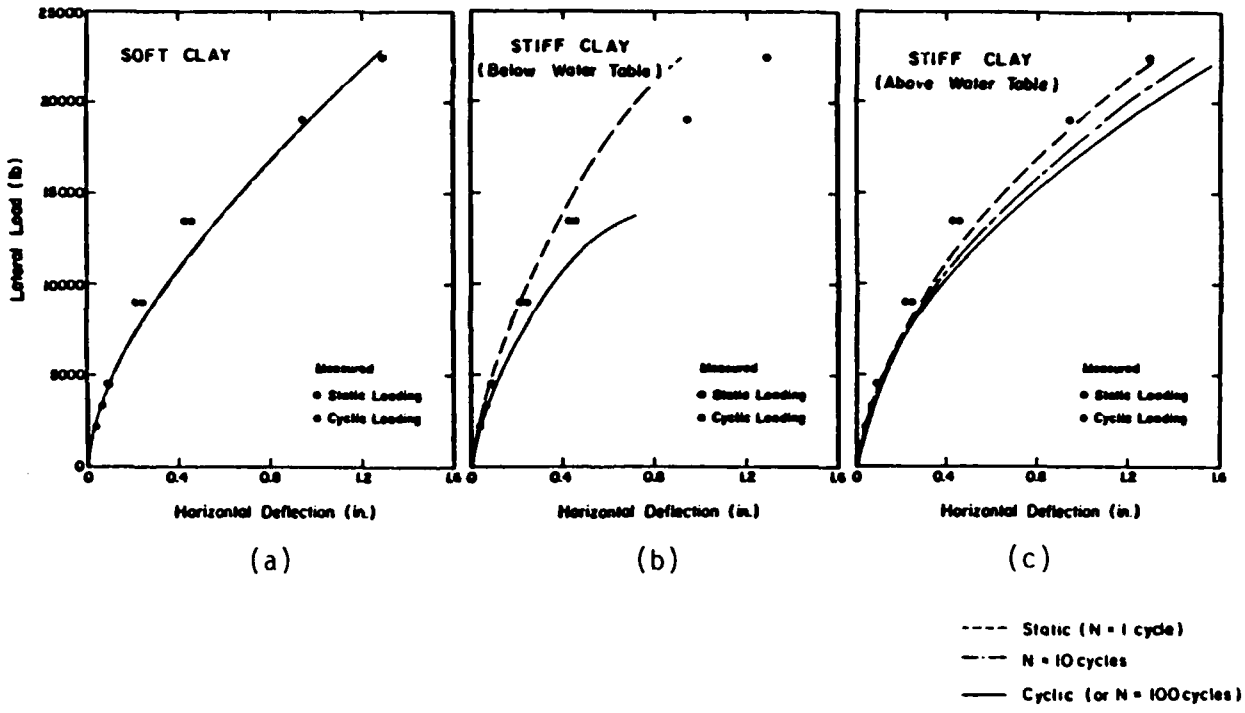

FIG. 5.3. Curves showing comparison of computed and measured deflections for field tests of Price and Wardle (circular pile)

Using the stiff clay (bwt) criteria, the influence of cyclic loading is shown to increase horizontal deflections for a given lateral load much more significantly than was measured.

For the stiff clay (awt) criteria, values of deflection are also shown to increase with cyclic loading, contrary to the measurements.

Price and Wardle (1982), H-Shaped Pile

An H-pile was also tested at the site used by Price and Wardle. Because the site conditions were identical, the same soil profile was used as that presented for the tubular pile.

Shown in Figs. 5.4a, 5.4b, and 5.4c are measured and predicted curves of lateral load versus deflection for both static and cyclic loading. In Fig. 5.4a the experimental points are shown along with curves predicted using the soft clay criteria. Comparisons of measured static and cyclic behavior can only be made up to a lateral load of about 9000 lbs because no measurements of static deflection are presented for larger loads. However, at a lateral load of about 9000 lbs, some effect of cyclic loading is seen as an increase in horizontal deflection of the pile head.

Predicted behavior of the pile based on soft clay criteria shows no influence of cyclic loading up to a lateral load of approximately 23,000 lbs. Shown in Fig. 5.4b are predictions using the stiff clay (bwt) criteria. As can be seen, a much greater influence on cyclic loading is shown than either of the other two prediction methods or by the measurements. The lateral load versus deflection behavior predicted using the stiff clay (awt) criteria appears to give the influence of cyclic loading in close agreement with the measured influence. However, at levels of load between 0 and 1000 lbs, the predicted curves for static and cyclic loading are stiffer than indicated by the measurements.

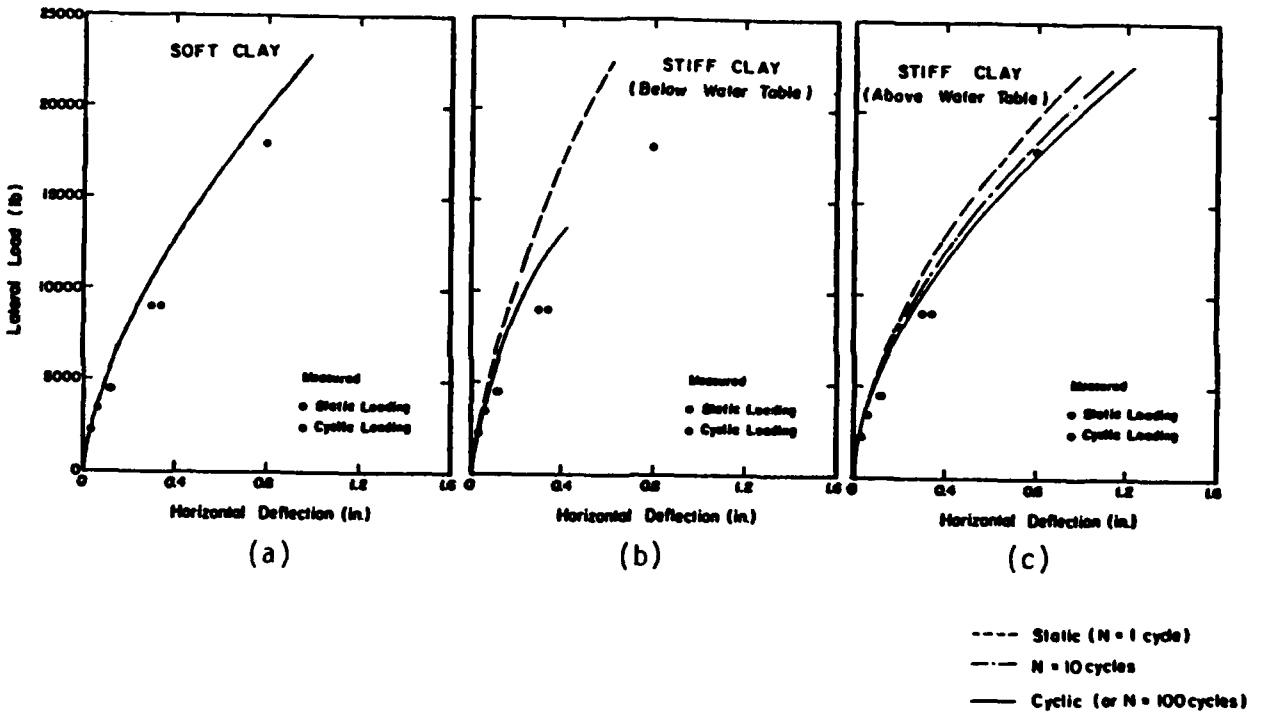

FIG. 5.4. Curves showing comparison of computed and measured deflections for field tests of Price and Wardle (H-pile)

U. S. Naval Civil Engineering Lab, Free-Head Loading

Comparisons between predictions and measurements from the testing of the special pile constructed by USNCEL, described in Chapter 3, are shown in Figs. 5.5a, 5.5b, and 5.5c. In order to make the analyses, estimates of shear strength and ε_{50} were made based on results of triaxial tests of samples obtained from the site. However, during the testing program, which lasted over one year, no provision was made to keep the water content constant in the top several feet of soil. Thus, there was a wide variation of soil strength, as shown in Fig. 3.12. Values of shear strength were estimated by back computation, assuming the clay to behave as stiff clay above the water table. However the computed shear strength was unrealistically high (in fact, higher than any values measured and shown in Fig. 3.12); therefore, a value of 10.0 lbs/sq in. was used because it was the highest reasonable value of shear strength. The shear strength was assumed to vary with depth in the following manner: from the ground surface to a depth of 6 ft, 10 lb/sq in., below 6 ft, 2.0 lbs/sq in. Values of ε_{50} were based on recommendations provided by Reese, and presented in Chapter 4.

Shown in Fig. 5.5, is a definite effect of cyclic loading in the experiment with increased deflection measured at each load level.

For the soft clay criteria, the measured and predicted results are in reasonable agreement, although the predicted values of deflection at any load above 5000 lbs greatly exceeds the measured values. No effect of cyclic loading is predicted using the soft clay criteria which obviously does not agree with the measurements. Using the stiff clay (bwt) p-y criteria, the prediction for static loading agrees well with the measured values; however, for cyclic loading, much greater deflections were pre-

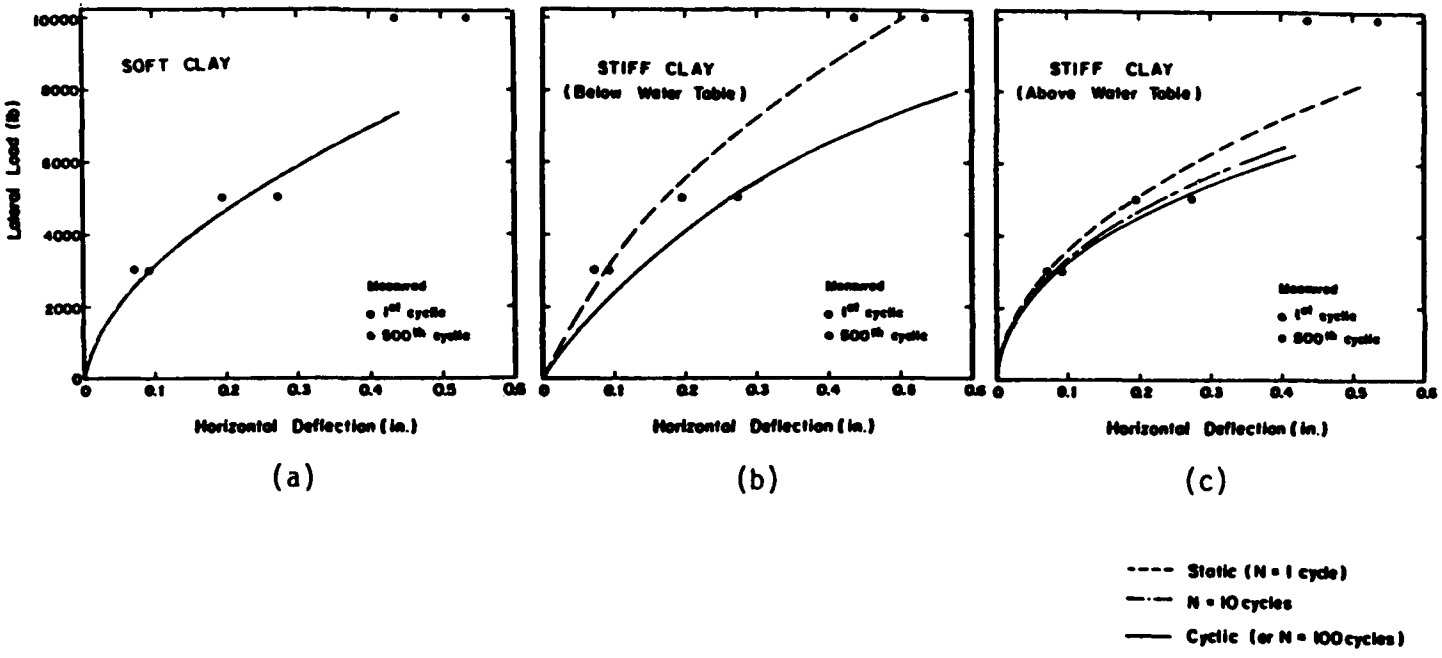

FIG. 5.5. Curves showing comparison of computed and measured deflections for field tests performed by U. S. Navy (free-head conditions)

dicted than measured for lateral loads above 6000 lbs. For the stiff clay (awt), predictions for both static and cyclic behavior agree well with the measured values; however, for loads above 5000 lbs the predicted values of deflection exceed measured values.

U. S. Naval Civil Engineering Laboratory, Restrained-Head Loading

In addition to the free-head tests, restrained-head tests were conducted. The investigators attempted to keep the pile head vertical, and the fixed-head condition is assumed in the analyses. Because these tests were performed at the same site as the free-head tests, the same soil profile is employed.

Results of analyses, along with experimental results, are shown in Figs. 5.6a, 5.6b, and 5.6c. The measurements are inconsistent with observed behavior at other locations and with theory because the curvature of the load-deflection curve is opposite to what was expected. No specific reason can be given for the unexpected data. However, significant increases in deflection due to cyclic loading can be seen. As shown in Fig. 5.6a, predictions using the soft clay criteria show no effect due to cyclic loading. Predictions using the stiff clay (bwt) criteria show both the static and cyclic behavior of the pile to be stiffer than measured; however, the predicted effect of cyclic loading appears to be similar to the measured effect. The stiff clay (awt) criteria also exhibits a stiffer relationship than the measured values, although at a lateral load of 10000 lbs, agreement between predicted and measured values of both static and cyclic deflections is good.

Gilbert (1980), Piles A and B

As described in more detail in Chapter 3, two piles, piles A and B, were tested in a very soft clay. The two piles were driven into essen-

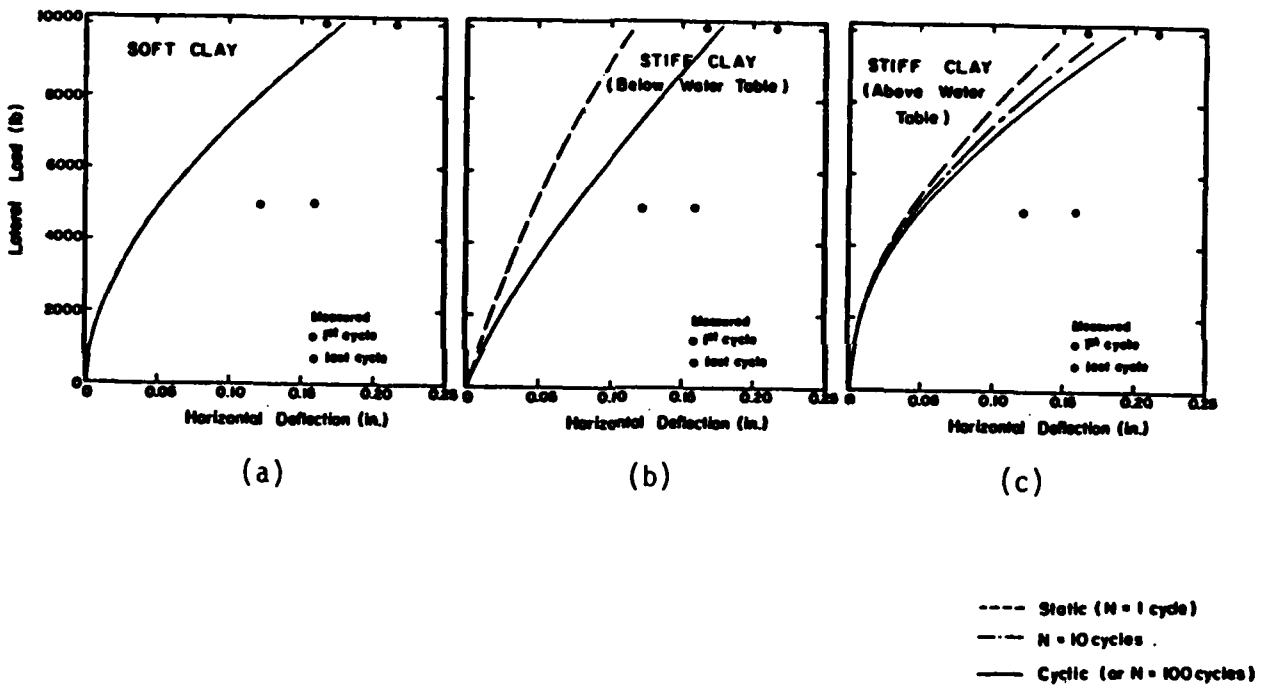

FIG. 5.6. Curves showing comparison of computed and measured deflections for field tests performed by U. S. Navy (restrained-head conditions)

tially the same material; thus, the soil profile was assumed to be identical for both piles. The differences in the load-versus-deflection behavior of the two piles are assumed to be due to the characteristics of the piles only. The behavior under lateral load of the piles, measured and predicted, are shown in Figs. 5.7a, 5.7b, and 5.7c for pile A and Figs. 5.8a, 5.8b, and 5.8c for pile B.

Both piles show an increase in lateral deflection due to cyclic loading at a given lateral load; however, for both piles, all three prediction methods greatly under-predicted the load carrying capabilities of the pile. A comparison of the effects of cyclic loading as measured and as predicted is difficult; however, it is of interest to note that very little effect of cyclic loading was predicted using the soft clay criteria, as shown in Figs. 5.7a and 5.8a. For the other two criteria, the predicted effects of cyclic loading are certainly apparent as shown in Figs. 5.7b, 5.7c, 5.8b, and 5.8c. The agreement between the measured and predicted behavior under static loading for the two piles, however, is so poor that comparisons between measured and predicted effects of cyclic loading are of little importance.

Tassios and Levendis (1974)

The results of cyclic, lateral-load tests for both one-way, and two-way loading are shown in Figs. 5.9a, 5.9b, and 5.9c. In order to perform analyses of this load test, assumptions were required in regard to soil and pile properties. Values of shear strength versus depth were determined from Fig. 3.19. Values of ε_{50} were selected from the recommendations made by Reese and presented in Chapter 3. The geometric properties of the pile were given; however, neither the strength of the concrete nor the rotational stiffness (EI) of the piles were provided. In order to

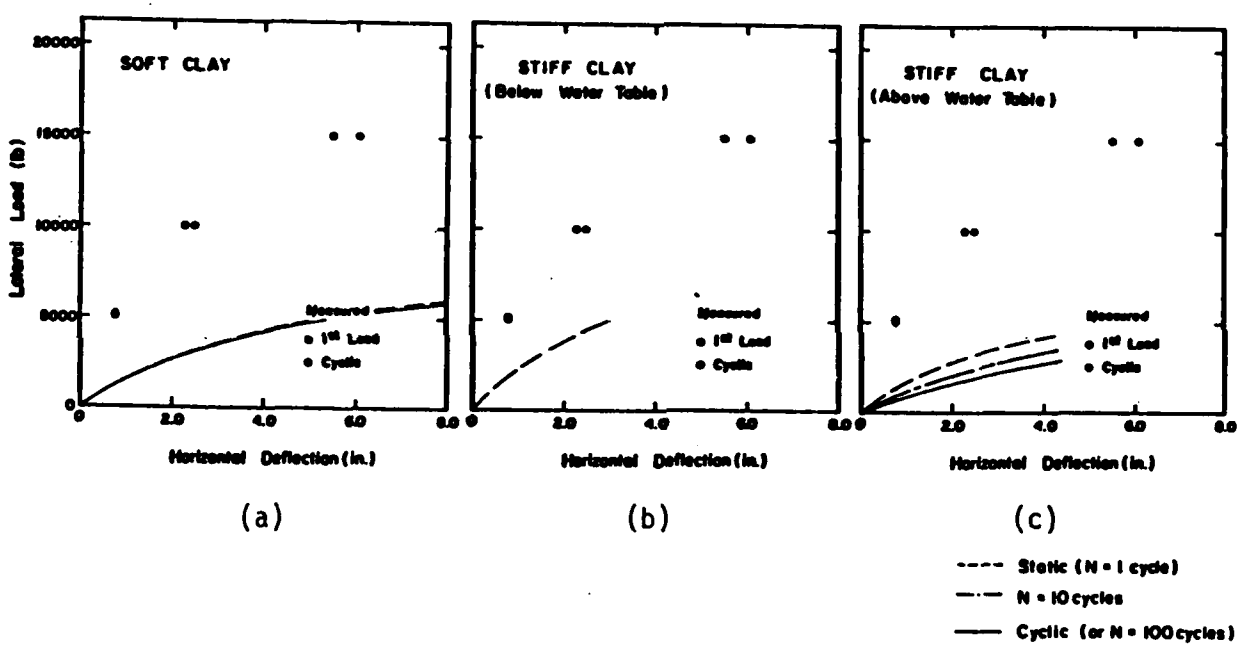

FIG. 5.7. Curves showing comparison of computed and measured deflections for field tests of Gilbert (pile A)

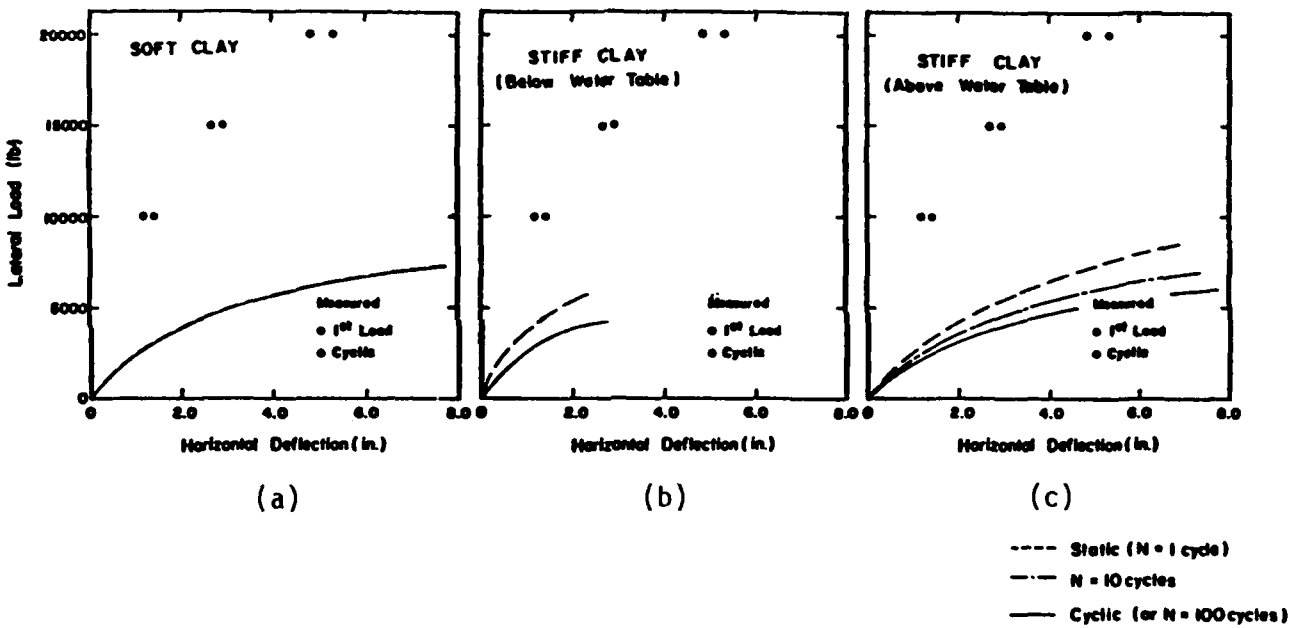

FIG. 5.8. Curves showing comparison of computed and measured deflections for field tests of Gilbert (pile B)

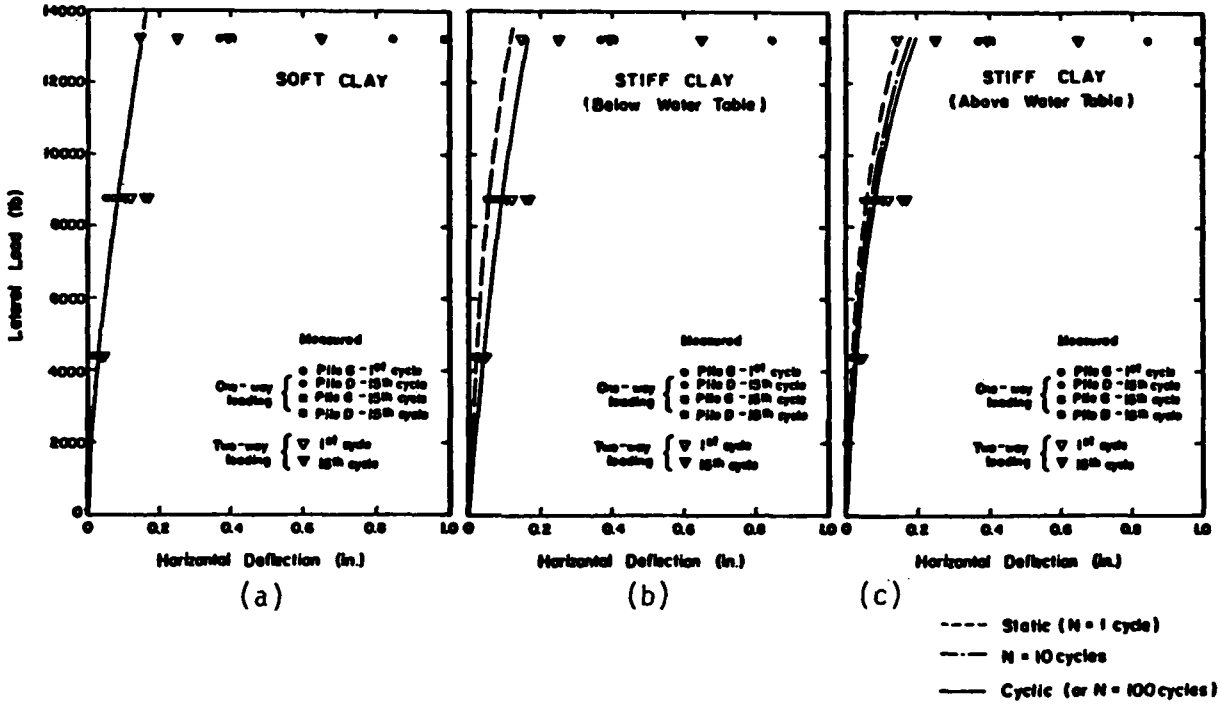

FIG. 5.9. Curves showing comparison of computed and measured deflections for field tests of Tassios and Levendis

calculate values of EI, a value of E was estimated using the following equation:

$$E = 57000 \sqrt{f_c}$$

where

E = modulus (lb/sq in.)

f_c = compressive strength of concrete (assumed to be 4000 lbs/sq in.).

Shown in Fig. 5.9a are the predicted and measured load versus deflection relationships using the soft clay criteria. As can be seen, the predicted and measured behaviors under static load agree reasonably well, but the agreement between the predicted and measured effect of cyclic loading is poor. No effect of cyclic loading was predicted; however, in all cases and at all levels of lateral load, increased deflection with number of cycles was experienced.

Using the stiff clay (bwt) and stiff clay (awt) criteria, some effect of cyclic loading was predicted and is shown in Figs. 5.9b and 5.9c. Although the agreement between measured and predicted effect of cyclic loading is close for load levels below approximately 8800 lbs, the predicted increases in deflection at the higher load levels were much less than measured.

Reese and Welch (1972)

Shown in Figs. 5.10a, 5.10b, and 5.10c are the measured and predicted load versus deflection for a laterally loaded drilled shaft. The prediction using the soft clay criteria follows the measured values for static loading; however, no influence of cyclic loading is predicted. Obviously, the effect of cyclic loading is significant as shown from the measured values plotted in Fig. 5.10a.

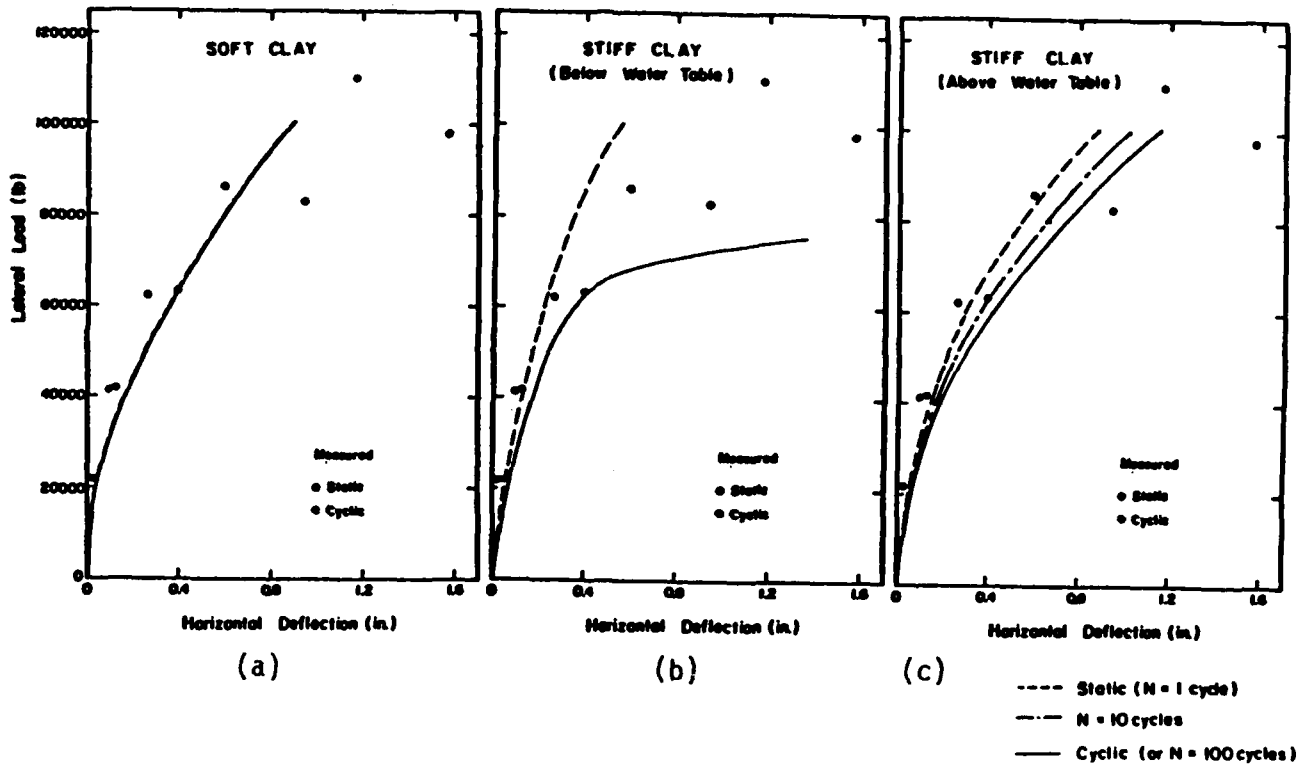

FIG. 5.10. Curves showing comparison of computed and measured deflections for field tests of Reese and Welch

Using the stiff clay (bwt) criteria, the predicted deflections for static loading are slightly less than measured; however, predicted deflections for cyclic loading are greater than measured for loads above 6000 lbs. The best agreement is found with the results of the stiff clay (awt) criteria. This is hardly surprising because the stiff clay (awt) criteria were developed from this test.

FIELD TESTS CONDUCTED WITH FREE WATER ABOVE GROUND SURFACE

The results of four series of lateral load tests are discussed below. As explained previously, predictions of load-versus-deflection behavior were made for each case history and compared with the measured behavior. Predictions were made based on the three sets of p-y criteria presented in Chapter 4. In cases cited below, water was ponded above the ground surface; thus, water was free to enter and exit any gaps that formed between the soil and pile.

Harvey

A structural framework was used at the Harvey site that was designed to cause equal values of displacement at two points along the portion of the pile located above the ground surface. To model the pile-head boundary conditions in the computer program used for the analyses an equivalent rotational stiffness was calculated for the pile head.

The results of the lateral load test and the corresponding p-y analyses are shown in Figs. 5.11a, 5.11b, and 5.11c. The analyses employ a value of shear strength of 3.2 lbs/sq in.

Using the soft clay criteria, the predicted and measured results were found to be in close agreement; however, the effect of cyclic loading was

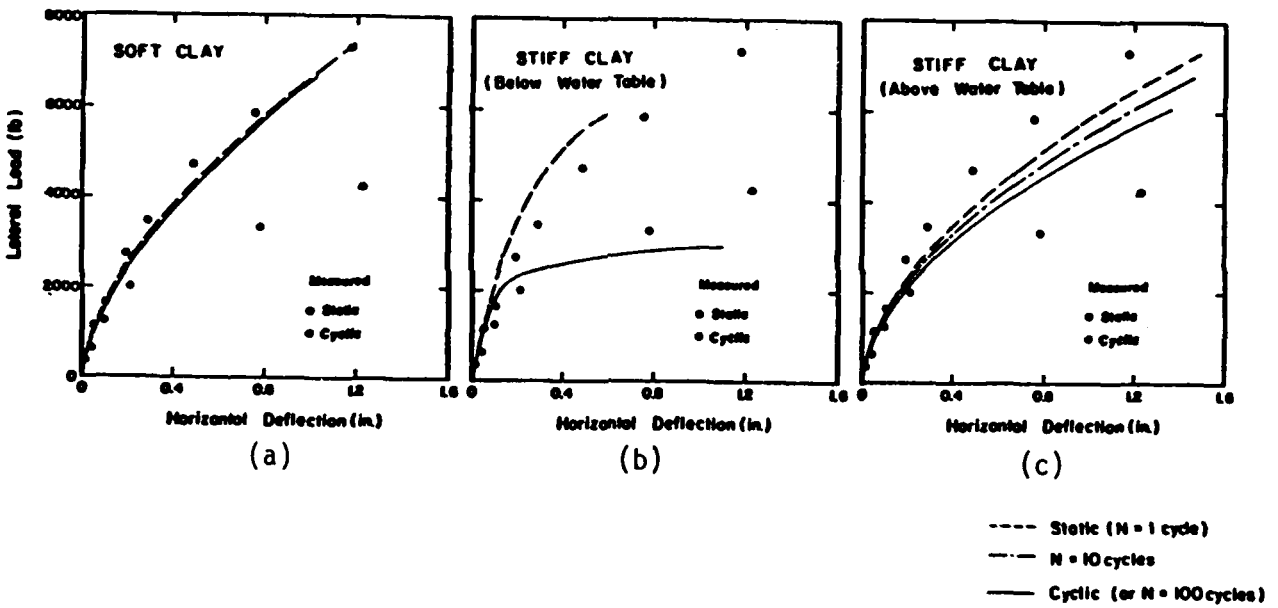

FIG. 5.11. Curves showing comparison of computed and measured deflections for field tests performed at Harvey

predicted to be much less than measured. Using the stiff clay (bwt) criteria, the predicted effect of cyclic loading is too severe beginning at a lateral load above 2500 lbs. The effect of cylic loading using the stiff clay (awt) criteria, Fig. 5.11c, is less than was measured.

Lake Austin

The results of the tests performed at Lake Austin are shown in Fig. 5.12a. Three data points for each load level are plotted to demonstrate the effect previous cycling had on the behavior of the pile at higher load levels. Data points termed static are representative of load-deflection behavior measured during a test in which the load was monotonically increased to the maximum value of lateral load. The points corresponding to 1st cycle and 500th cycle are representative of the load and deflections measured during the cyclic test in which the pile was loaded to a certain magnitude and cycled at that load. Upon completion of the last cycle (or 500th cycle), the load level was increased and cycling was reinitiated. Thus, the effect of the previous load cycles at lower levels of loading can be seen by comparing the load-versus-deflection relationship for the static test with the load-versus-deflection relationship measured during the first cycle of loading in the cyclic test.

The predicted curve of load versus deflection using the soft clay criteria is shown in Fig. 5.12a. The predicted and measured behavior under static load are in good agreement; however, the effect of cyclic loading is predicted to be much less than measured. The predicted behavior using the stiff clay (bwt) criteria is shown in Fig. 5.12b. The predicted behavior under static loading is stiffer than measured; however, the predicted behavior under cyclic loading exhibits a much more severe increase in deflection between 10,000 and 13,000 lbs than was measured.

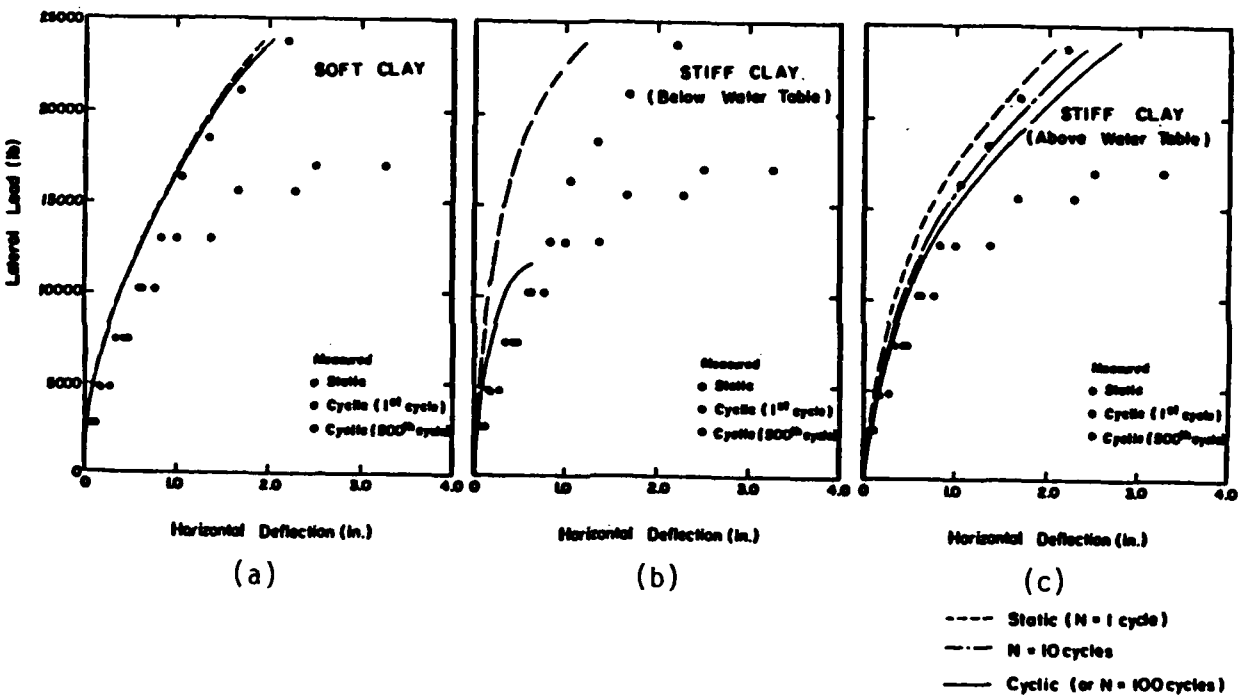

FIG. 5.12. Curves showing comparison of computed and measured deflections for field tests performed at Lake Austin

The stiff clay (awt) criteria was used to predict lateral-load behavior as shown in Fig. 5.12c. Although the predicted relationship for static loading is reasonably close to that measured, the effect of cyclic loading was predicted to be much less than measured.

Sabine, Free- and Restrained-Head Tests

The results of a series of tests are shown in the form of lateral load versus deformation in Figs. 5.13 and 5.14 for free-head and restrained-head conditions. Because the tests were performed at the same site, identical soil properties were used for each of the p-y analyses. A value of shear strength of 2.4 lbs/sq in. was selected based on both the shear-strength profile presented in Fig. 3.29 and the close fit between measured and predicted behavior of the free-head pile subjected to static loading. Values of ε_{50} were selected to be 0.0091 on the basis of results from triaxial tests conducted on soil from the Sabine site.

Under free-head conditions, the measured and predicted values of load versus deflection were close when the soft clay criteria were employed. The measured values of load versus deflection under static loading were followed closely by predicted values up to loads of approximately 18,000 lbs. For cyclic loading, predicted increases in deflection were slightly less than measured.

For the stiff clay (bwt) criteria, predictions of behavior for both static and cyclic loading did not agree well with measured behavior. For both types of loading, excessive deflection was predicted and excessive deformations at loads less than half of the maximum lateral loads measured during the tests. Predictions of lateral-load behavior employing the stiff clay (awt) criteria are shown in Fig. 5.13c. The agreement between

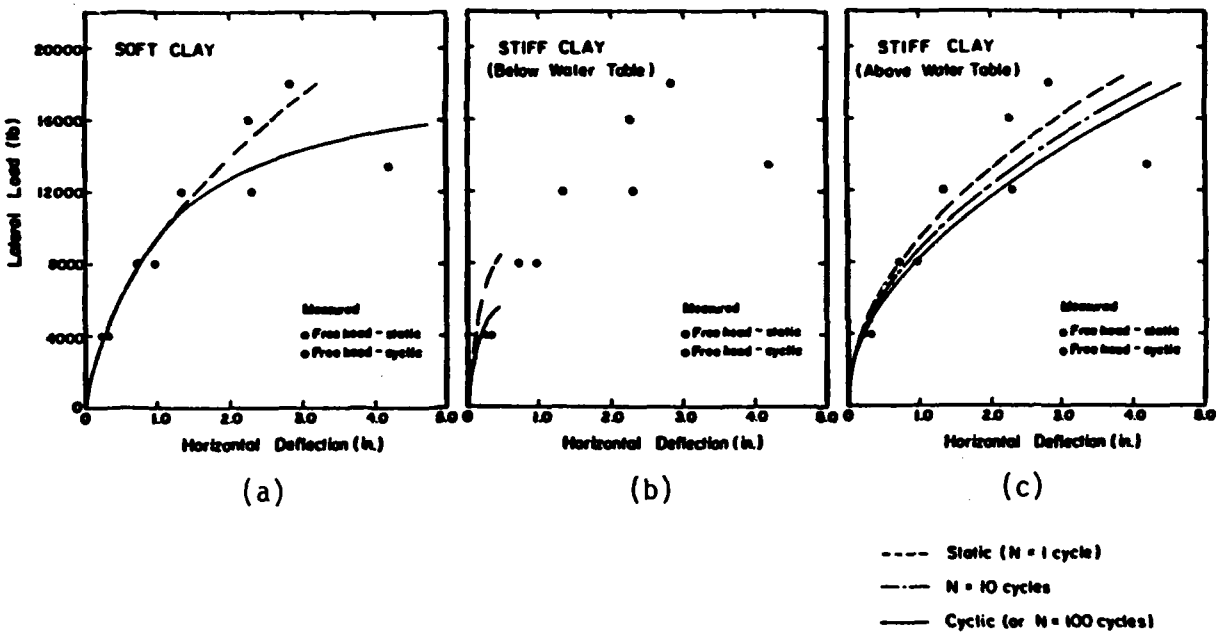

FIG. 5.13. Curves showing comparison of computed and measured deflections for field tests performed at Sabine (free-head conditions)

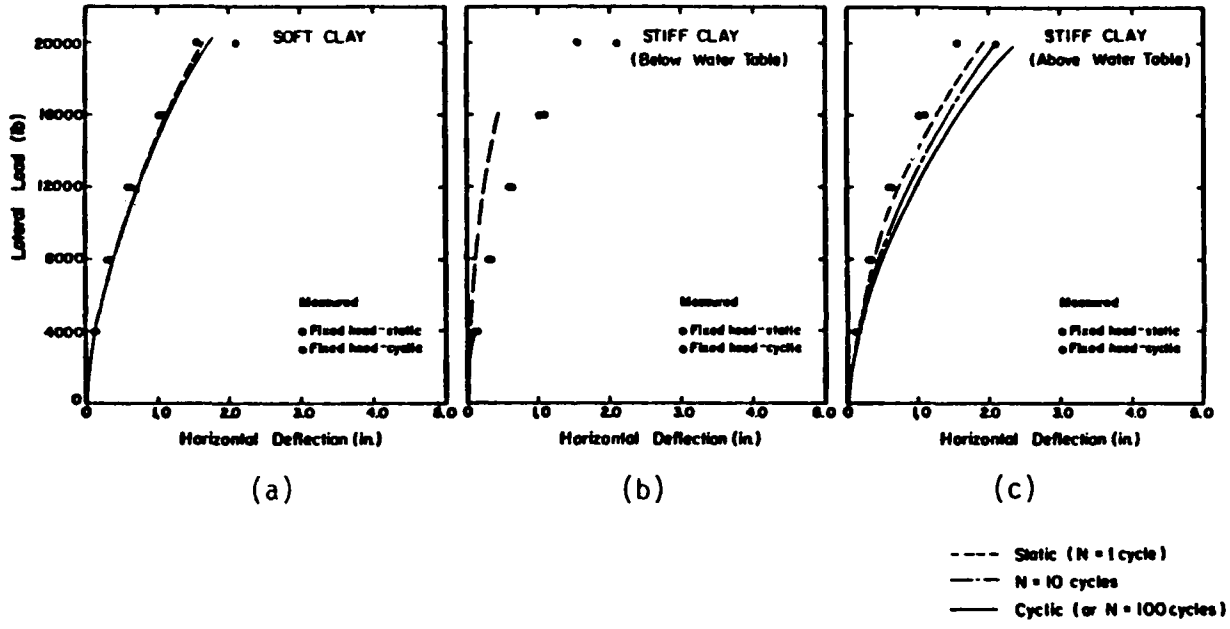

FIG. 5.14. Curves showing comparison of computed and measured deflections for field tests performed at Sabine (restrained-head conditions)

predictions and measurements is closer than that for the stiff clay (bwt) criteria, but not as good as that using the soft clay criteria.

In addition to the free-head tests performed on the piles, restrained-head tests were also conducted. Values of lateral load and bending moment were recorded for each testing sequence. These recorded loads and moments were used to obtain values of lateral load and the corresponding restraining moment at the pile head for use as boundary conditions in the computer program.

Shown in Figs. 5.14a, 5.14b, and 5.14c are the measured and predicted relationships of load versus deflection for the soft clay, stiff clay (bwt), and stiff clay (awt) criteria. The predicted behavior using the soft clay criteria agrees best with measurements; however, cyclic loading is seen to increase deflection more than predicted.

Using the stiff clay (bwt) criteria, computed deflections for both the static and cyclic loading are greater than those measured. Deflections predicted by the stiff clay (awt) criteria are slightly larger than those measured under static loading; however, agreement is good between measured and computed increase in deflection due to cyclic loading.

Manor, Piles 1 and 2

The soil and pile properties for this lateral load test were presented in Chapter 3. Shown in Figs. 5.15a, 5.15b, and 5.15c are measured values of pile behavior and predictions using the three sets of p-y criteria. Three measured values for each load level are shown and correspond to a static load, the 1st cycle, and the 100th cycle. The three points give an indication of the effect of previous cycles at lower load levels in determining the deflection of the 1st cycle at a new load level.

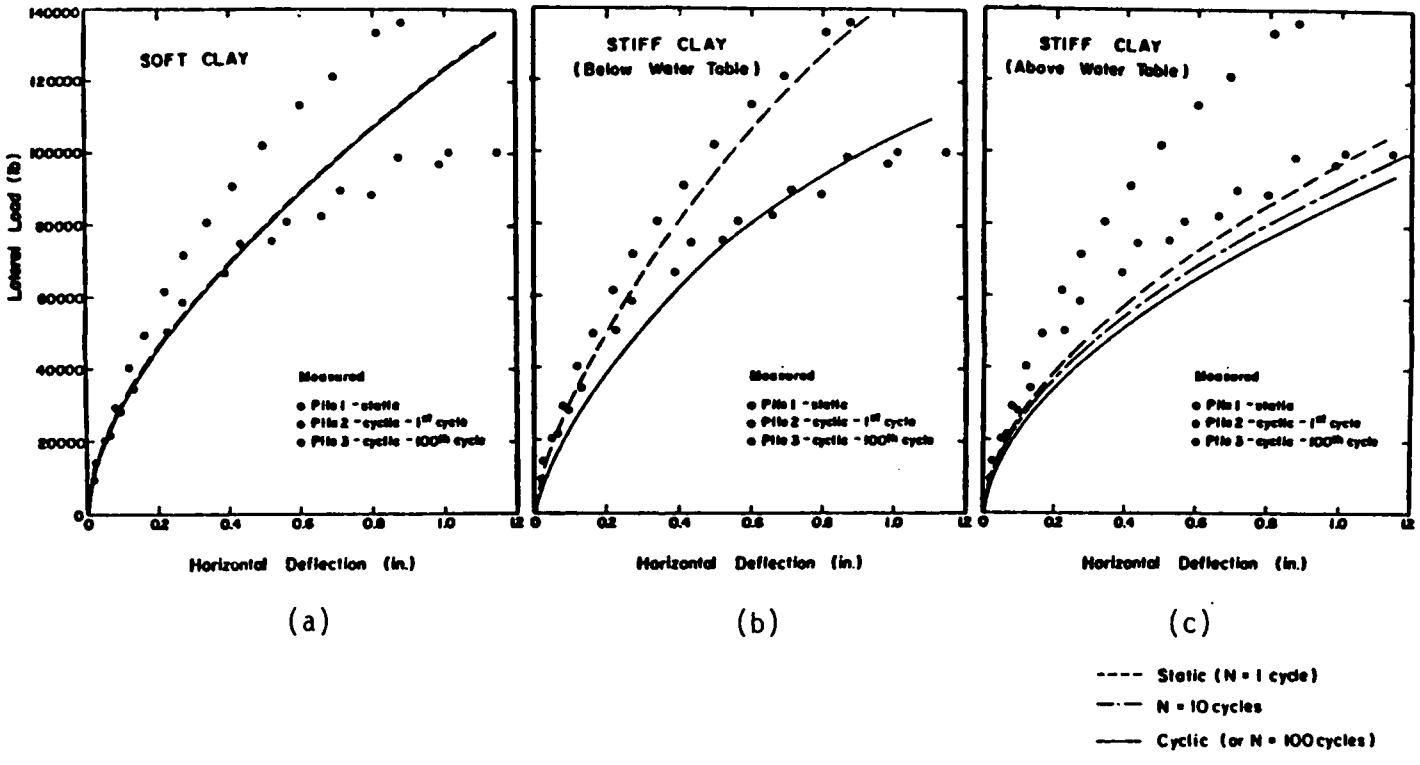

FIG. 5.15. Curves showing comparison of computed and measured deflections for field tests performed at Manor (piles 1 and 2)

Shown in Fig. 5.15a are the measured deflections versus lateral loads and the behavior computed by using the soft clay criteria. The prediction for static load agrees poorly with measured values and the p-y criteria predict no increased deflection with cyclic loading, obviously in disagreement with the measurements. Using the stiff clay (bwt) criteria, excellent agreement is shown in Fig. 5.15b between predictions and measurements for both static and cyclic loading. This was expected because these tests form the basis for the stiff clay (bwt) criteria. Using the stiff clay (awt) criteria, predictions of deflection for both static and cyclic loading are larger than measured.

Manor, Pile 3

In addition to the lateral load tests performed on the 25.25-in. diameter piles, lateral load tests were performed on a pile measuring 6.625 in. in diameter. The results of the lateral load test and the predictions of lateral load behavior are presented in Figs. 5.16a, 5.16b, and 5.16c.

As shown in Fig. 5.16a, the deflections predicted using the soft clay criteria agree well with measured values. However, much less effect due to cyclic loading is predicted than measured. Predictions of behavior for both cyclic and static loading are best by the stiff clay (bwt) criteria; however, a slightly stiffer relationship is predicted for the static case, and excessive deflections are predicted at slightly lower loads than measured in the cyclic case. The stiff clay (awt) criteria shows an effect of cyclic loading; however, neither static nor cyclic predictions are seen to be close to those measured.

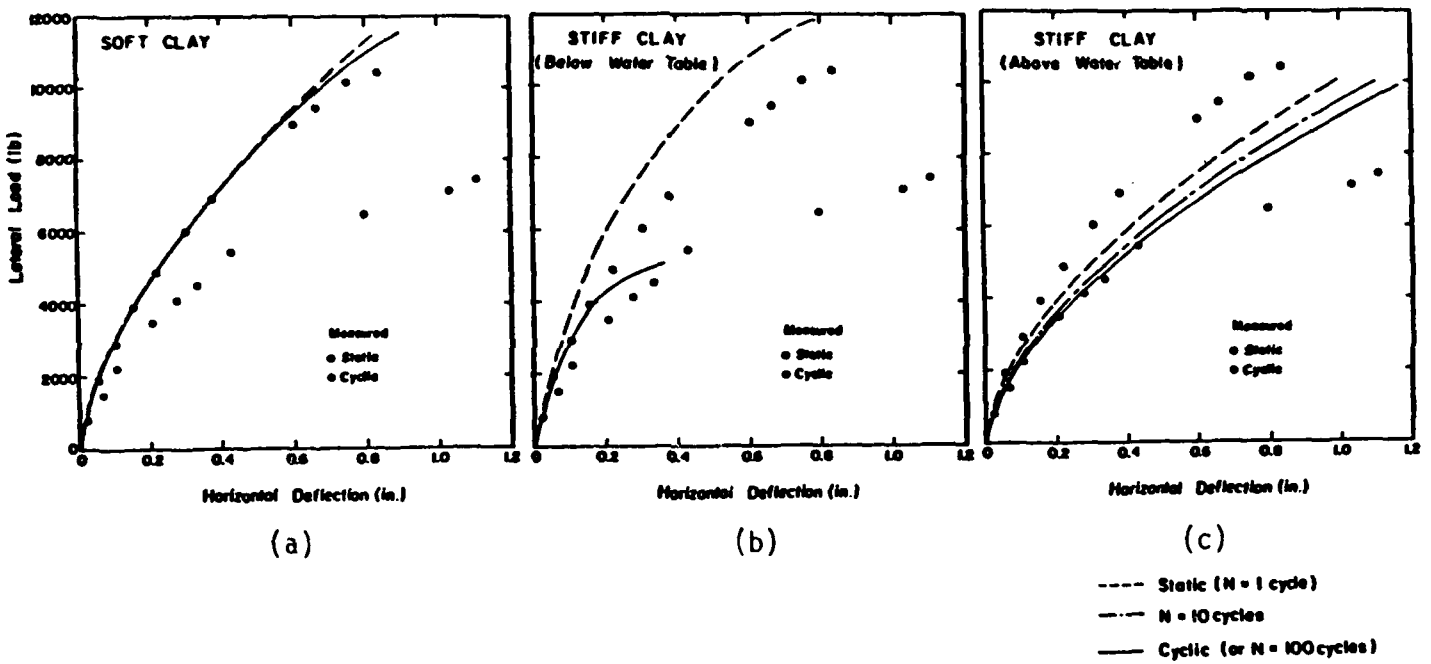

FIG. 5.16. Curves showing comparison of computed and measured deflections for field tests performed at Manor (pile 3)

SUMMARY

Sixteen case histories have been reviewed and their behavior compared with the load verus deflection behavior predicted using the soft clay criteria, the stiff clay (bwt) criteria, and the stiff clay (awt) criteria. As expected, no particular method provided clearly superior agreement between measured and predicted behavior; however, a closer look at the comparisons presented in Figs. 5.1 to 5.16 yields some interesting results. Shown in Table 5.1 is a list defining which p-y criteria best predicted the effects of cyclic loading for each case history. Each criteria was assigned a number (1, 2, or 3) depending on how well the criteria predicted the measured behavior with respect to the other criteria. Thus, the number 1 was assigned to the criteria which best predicted the measured effect of cyclic loading, and the number 3 was assigned to the criteria that least agreed with measured behavior.

For clays above the water table, it appears that the stiff clay (awt) criteria predicted the effects of cyclic loading best. This observation is expected because the stiff clay (awt) criteria seems the most appropriate.

For the lateral load tests conducted in which water was ponded above the ground surface, no single p-y criteria was clearly superior in predicting the effects of cyclic loading. This was expected because two p-y criteria (soft clay and stiff clay (bwt)) are currently available for predicting the lateral load behavior. Only two lateral load tests, Manor (piles 1 and 2), and Manor (pile 3), fall into the category particularly suited for a p-y analysis using the stiff clay (bwt) criteria. The agreement between the predicted and measured effect of cyclic loading was good;

TABLE 5.1. COMPARISON OF PREDICTIONS MADE USING THE THREE p-y CRITERIA

Case History	p-y Criteria			
	Soft Clay (bwt)	Stiff Clay (bwt)	Stiff Clay (awt)	Comments Regarding Assigning Numbers to Analyses
Above water surface				
Gaul	1	2	3	all analyses very similar
Valenzuela & Lee	2	3	1	
Price & Wardle (tubular)	1	3	2	soft and stiff (awt) very close
Price & Wardle (H)	2	3	1	
U. S. Navy (free-head)	3	2	1	
U. S. Navy (restrained-head)	3	1	2	stiff (bwt) and stiff (awt) were close
Gilbert (pile A)	2	3	1	
Gilbert (pile B)	2	3	1	
Tassios & Levendis	3	1	2	stiff (bwt) and stiff (awt) were close
Reese & Welch	3	2	1	stiff (awt) criteria based upon results of this test
Below water surface				
Harvey	3	1	2	
Lake Austin	3	2	1	soft clay criteria based upon the results of these tests
Sabine (free-head)	1	3	2	
Sabine (restrained-head)	2	3	1	
Manor (Piles 1 and 2)	3	1	2	stiff clay (bwt) criteria based upon the results of this test
Manor (Pile 3)	3	1	2	

however, this agreement was expected because the p-y criteria were based on the results of these tests.

For lateral load tests conducted in soils that may be considered medium (Lake Austin), or soft (Harvey, and Sabine), the soft clay p-y criteria seems the most appropriate. However, although the Sabine test results appear to agree with predictions from the soft clay p-y criteria, the results from tests performed at Harvey and Lake Austin exhibit a much greater effect of cyclic loading than predicted. This is an important point because it emphasizes that the cyclic behavior of piles in clay may be very different, and not easily predicted by current techniques. Additional knowledge is required regarding the behavior of the soil subjected to cylic loading and the susceptibility of the soil to the scouring action of the water.

Other, more general conclusions can be drawn from reviewing the predictions plotted in Figs. 5.1 through 5.16. In most of the cases studied herein, the soft clay criteria predicted the smallest effect of cyclic loading and the stiff clay (bwt) predicted the greatest effect of cyclic loading. The stiff clay (awt) usually predicted the effect of cyclic loading to be at some intermediate value between the soft clay and stiff clay (bwt) criteria. These observations are limited to the cases being studied currently and therefore will probably vary for pile or soil properties different than those studied here.

CHAPTER 6. SPECIAL PROCEDURES FOR TESTING SOILS FROM SITES WHERE LATERAL-LOAD TESTS WERE PERFORMED

INTRODUCTION

It is obvious that the behavior of a pile subjected to static and cyclic lateral loads is dependent on the characteristics of the soil surrounding the pile. In order to determine these characteristics, laboratory tests were conducted on soil specimens obtained from soils very near two locations at which lateral load tests were conducted. Of course, soil testing was performed at the time the testing program was conducted; however, tests were not performed originally that now appear to be important. Two aspects of the soil that are deemed particularly important are the behavior of the soil subjected to cyclic loading and the resistance of the soil to erosion when subjected to water flowing over the soil surface. Discussed herein is a description of the testing equipment and testing procedures used to assess the behavior of the soil when subjected to cyclic and static loading, and to assess the resistance to erosion of the soil.

TRIAXIAL TESTING

In order to determine the static stress-strain characteristics of the soil, and its behavior when subjected to cyclic loads, two types of triaxial tests, static and cyclic, were conducted. The set-up procedure, triaxial cells, and all procedures except for the application of axial load, were the same for all triaxial specimens, whether they were to be tested cyclically or statically.

Set-up Procedure

Specimens of soil that were to be tested triaxially were first vertically extruded from three inch-shelby tubes, and then carefully trimmed to the dimensions required; 3.0 in. in length and 1.5 in. in diameter. During trimming, loss of moisture was retarded by covering the exposed parts of the trimmed specimens with a plastic wrapping. Upon completion of trimming, soil specimens were placed on the base pedestal of the triaxial cell, lateral filter-paper drains added, and a thin latex rubber membrane was used to seal the specimen.

After the base of the triaxial cell was flushed of any air bubbles, the cell was filled with de-aired water and a pre-set cell pressure was applied using a self-compensating mercury-pot system (Bishop and Henkel, 1962). Volume changes of the specimen were measured versus time. Upon completion of consolidation, back-pressure and cell pressure were applied at a rate of 10 lb/sq in. per day until acceptably high values of B-coefficient were measured. Final B-values measured during the tests were generally in excess of 0.97. The procedures followed thereafter were dependent on whether the triaxial test was to be conducted statically or cyclically.

Static-Triaxial Tests

After back-pressure saturation, the cell was moved onto a Wykeham-Farrance loading press and a proving ring and dial gauges were installed to measure load and deflection of the triaxial specimen. The loading rod was then lowered until slight contact was made with the top cap. At this time, shearing was started, and readings of load, deformation, and pore pressure were recorded. Shearing rates were preset and were calculated to shear the specimen at a rate slow enough to allow pore

pressures generated in the center of the specimen to be measured at the base of the specimen.

After the specimen failed, the specimen was removed from the triaxial cell and water contents were taken. Failure was defined as either 20 percent strain or as the specimen passed through both maximum principal stress difference and maximum principal stress ratio.

Cyclic-Triaxial Tests

In order to apply cyclic loads to the triaxial specimen, a device to apply constant levels of cyclic deformation was fabricated and is shown in Fig. 6.1. The device consists of a rotating disk upon which a freely rotating rod is connected. The position of the rod on the disk is adjustable; therefore, variable eccentricities are possible. Connected to the rod is an arm which is restricted to linear motion by two linear-motion stainless-steel bearings. The motion at the end of this arm varies approximately in a sinusoidal manner, and its amplitude can be adjusted by varying the eccentricity of the connection at the rotating disk. In addition, the frequency can be controlled by a variable-speed motor that rotates the disk.

Between the linear-motion arm and the loading rod of the triaxial cell are located connections for the load cell and a direct-current-displacement-transducer (DCDT). These two devices measure the load applied to the loading rod and the deformation of the triaxial specimen. The output from these electrical sensors were recorded using an X-Y plotter.

Before any testing was initiated, the loading rod had to be brought into contact with the top cap. This particular connection was more complicated than the static case because tensile loads between the loading

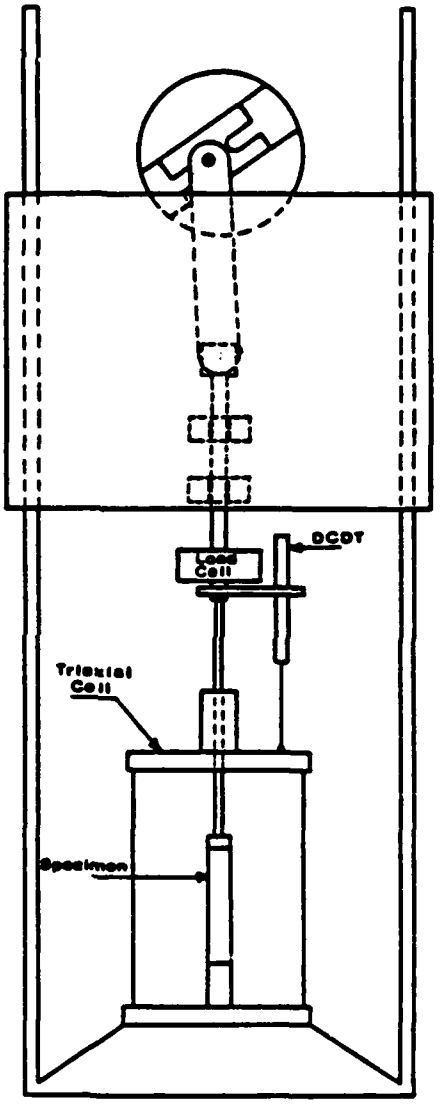

FIG. 6.1. Laboratory device for applying cyclic strains to triaxial specimens

rod and the top cap developed during the extension phase of the applied cyclic deformations. In order to allow necessary tensile loads to develop, a specially designed loading head and top cap was fabricated. The top cap and loading head were designed to come into contact along their perimeter and form an air- and water-tight seal. After the seal was made, a vacuum could be drawn in a chamber inside the loading head. The total tensile force that the connection could resist was then calculated as the cross-sectional area of the chamber times the differential pressure between the outside cell pressure and the inside chamber pressure. A schematic drawing of the loading head and top cap is shown in Fig. 6.2.

After contact was made between the loading head and the top cap, a vacuum was applied to the chamber within the connection. At this point, the cyclic triaxial test was ready to begin; thus, the motor controlling the cyclic device was activated and applied cyclic deformations as the X-Y plotter recorded the load-deformation behavior of the triaxial specimen. Pore pressures at the bottom of the specimen were measured for most of the specimens; however, the values obtained from these measurements are thought to be unrepresentative of the pore pressures at the center of the specimen. The pore pressures generated near the center of the sample have too little time to equalize during the short duration of one cycle.

Several cycles of loading were applied to each specimen, generally greater than 100. After testing was completed, either another cyclic or static triaxial test was performed, or the specimen was removed from the triaxial cell and water contents were determined.

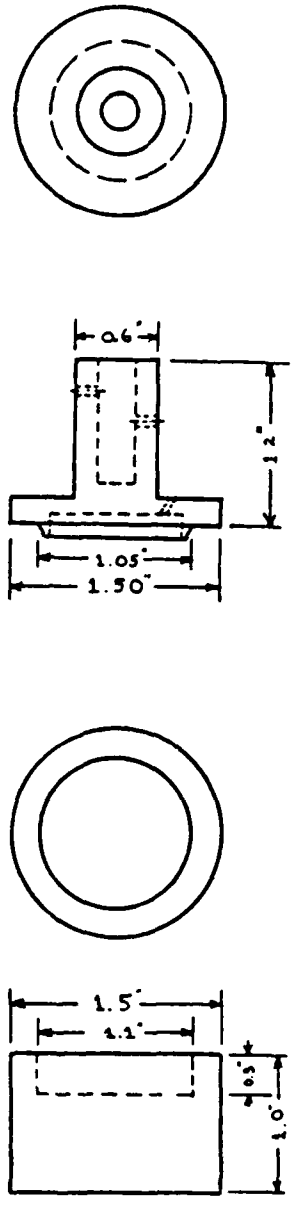

FIG. 6.2. Special top cap and loading head used to apply loads to specimen

EROSIONAL TESTING

An aspect of the behavior of cohesive soil believed to play an important role in the response of piles subjected to cyclic lateral loading is the susceptibility of the soil to erosion along the interface of the pile and soil. As water rushes up and down along the gap, the water has the tendency to erode or scour the soil. In order to investigate this phenomenon, two types of tests were conducted. One test involved a rod inserted into soil and moved cyclically in the horizontal direction (Wang and Reese, 1982). Although it was not intended to model the behavior of a real pile exactly, it was felt that perhaps some of the elements important in a real pile would also be important in the experiment with the rod. After the pile was inserted into the sample of soil and cyclic deformations applied, the amount of soil scoured out between the soil and the model pile wall was measured. The weight of soil measured during the rod test was used as an index parameter for assessing the sucepibility of the soil to scour.

Another test used and performed in parallel with the rod tests was the pinhole-dispersion test. The pinhole-dispersion test is conducted by flowing water through a one-eighth in. diameter hole that has been drilled through the specimen. The dimensions of the specimen as well as the applied gradient are specified and measurements are made of the color and turbidity of the water exiting the specimen. A more detailed description of the test procedure and requirements are presented by Wang and Reese (1982) and by Sherard, et al (1976).

CHAPTER 7. RESULTS OF SOIL EXPLORATION AND PROGRAM OF TRIAXIAL TESTING

INTRODUCTION

In order to obtain information on the behavior of the soils encountered at locations where lateral load tests were conducted, a program was initiated to obtain samples at the site. These samples would then be brought back to the laboratory and tested to evaluate specific aspects of the behavior of the soil and see if the behavior measured in the laboratory could be correlated in some manner to the behavior measured in the field.

Two sites were selected for this study. The first site was located near Manor, Texas where the soils in the area are considered to be stiff, fissured clays. The second site was located near Sabine Pass, Texas. In general, the soil found at this site consisted of soft clays and silts. The field investigation and results of the laboraory testing program for both sites are described herein.

MANOR SITE

Site Location

As shown in Fig. 7.1, the site is located along U.S. Highway 290 between Austin and Manor, Texas, about 3.7 miles northeast of the intersection of Highway 183 and 290. Specifically, the site is located along U.S. Highway 290 at Station 319.5, and just west of a residence with the address 9741 U.S. Highway 290E.

In 1966, a 50 ft by 45 ft test pit was excavated to a depth of 6 ft and all the lateral-load tests were performed within this excavation.

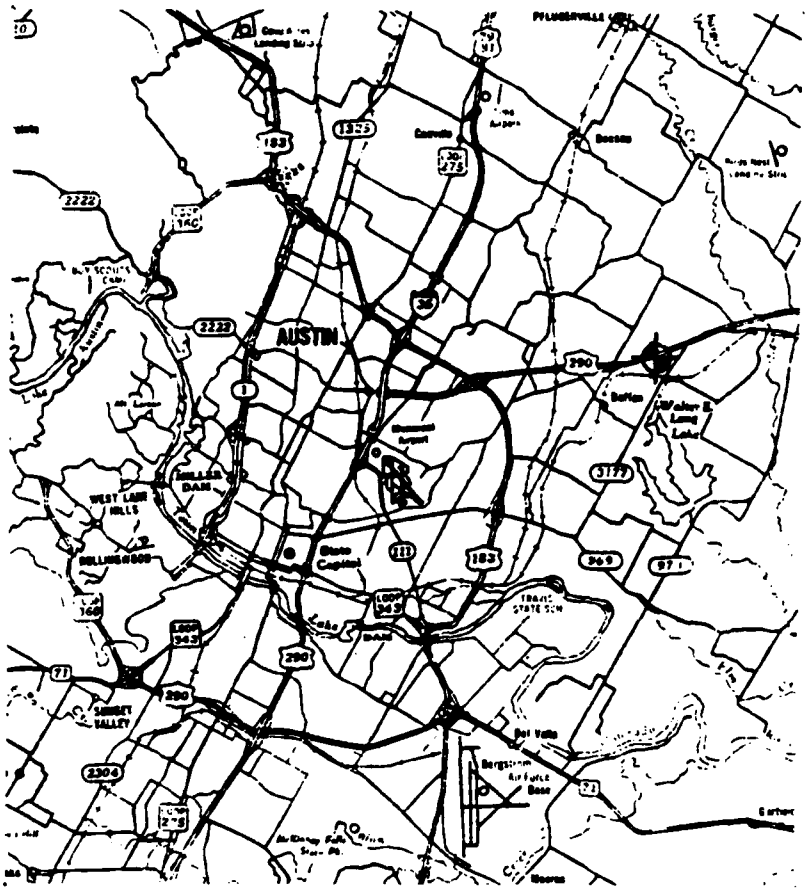

FIG. 7.1. General location of Manor site

This excavated area is located approximately 70 ft south of U.S. Highway 290, and approximately 30 ft west of the nearest residence as shown in Fig. 7.2.

History of Site

In 1966, an investigation was made to assess the behavior of full-scale piles in stiff clay subjected to lateral loads. A suitable site was selected and a pit was excavated. As the excavation proceeded, soil borings were made and soil specimens were tested to determine moisture content, Atterberg limits, and shear strength. A chronological list of the borings with respect to the excavation of the pit and pile installation is shown below:

Borings	Date of Borings	Status of Test Program
B-1, B-2	October 14, 1966	Before excavating test pit.
B-3, B-4	December 15, 1966	After excavating pit to 3 ft depth and just prior to ponding.
B-5, B-6	April 19, 1967	After ponding for 4 months. Prior to installation of test piles in period of May 2-9, 1967.
B-7, B-8	June 30, 1967	Pit excavated another 2½ ft to total depth of 5½ ft on April 21, 1967. Test piles installed and pit excavated a final ½ ft to total depth of 6 ft in period May 2-9, 1967.

The location of these borings, and the locations of the two piles are shown in Fig. 7.2.

After interpretation was completed of the data obtained from the soil-testing program, the original investigators reached conclusions

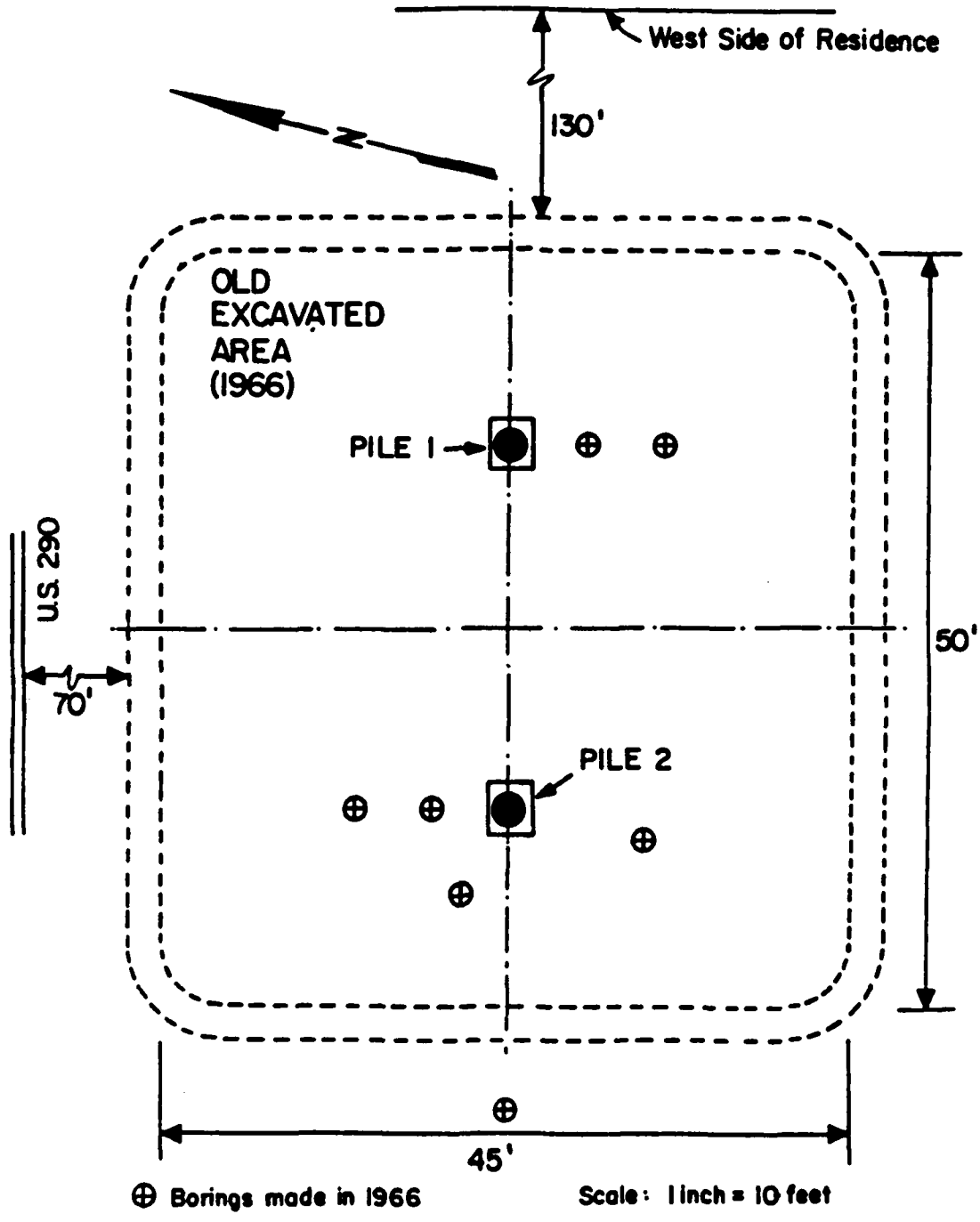

FIG. 7.2. Detailed map of location of Manor test site and location of boreholes (from Reese, et al, 1975)

regarding in situ shear strength. Shown in Fig. 7.3 is the resulting soil profile, along with the original estimate of the shear strength of the soil. The original estimate of the shear strength (shown as the heavy solid line) was based on results of unconfined compression tests, unconsolidated-undrained compression tests, and pocket penetrometer tests. After completion of the testing program, the excavated area was filled, and the site was abandoned. No further work or research was done at this site until 1981.

Boring Campaign in 1981

During the time from September 28 to October 2, a subsurface investigation of the test site was performed. The purpose of the investigation was to define the current subsurface conditions and relate them to the conditions described in 1966. Several boreholes were advanced to define soil stratigraphy and to obtain shelby tube samples.

In order to compare the current soil profile with the profile that existed in 1966, an exploratory borehole was advanced, and shelby tube samples were taken continuously from a depth of 5.0 ft to a depth of 15.0 ft. After each sample was taken, the soil was extruded, and visually classified. The depths of easily distinguishable layering were compared with the depths of similar layers reported in the 1966 investigation. It was concluded that the top of the pit excavated in 1966 was approximately 6 ft below the current ground level.

After establishing the depth to the top of the previously excavated area, shelby tube samples were taken. A total of four holes were advanced with continuous sampling; however, due to large pieces of gravel and very stiff soil, some tubes were either bent or lost in the hole. Shown in Fig. 7.4 is a plot of the depths at which soil samples were taken, and shown in

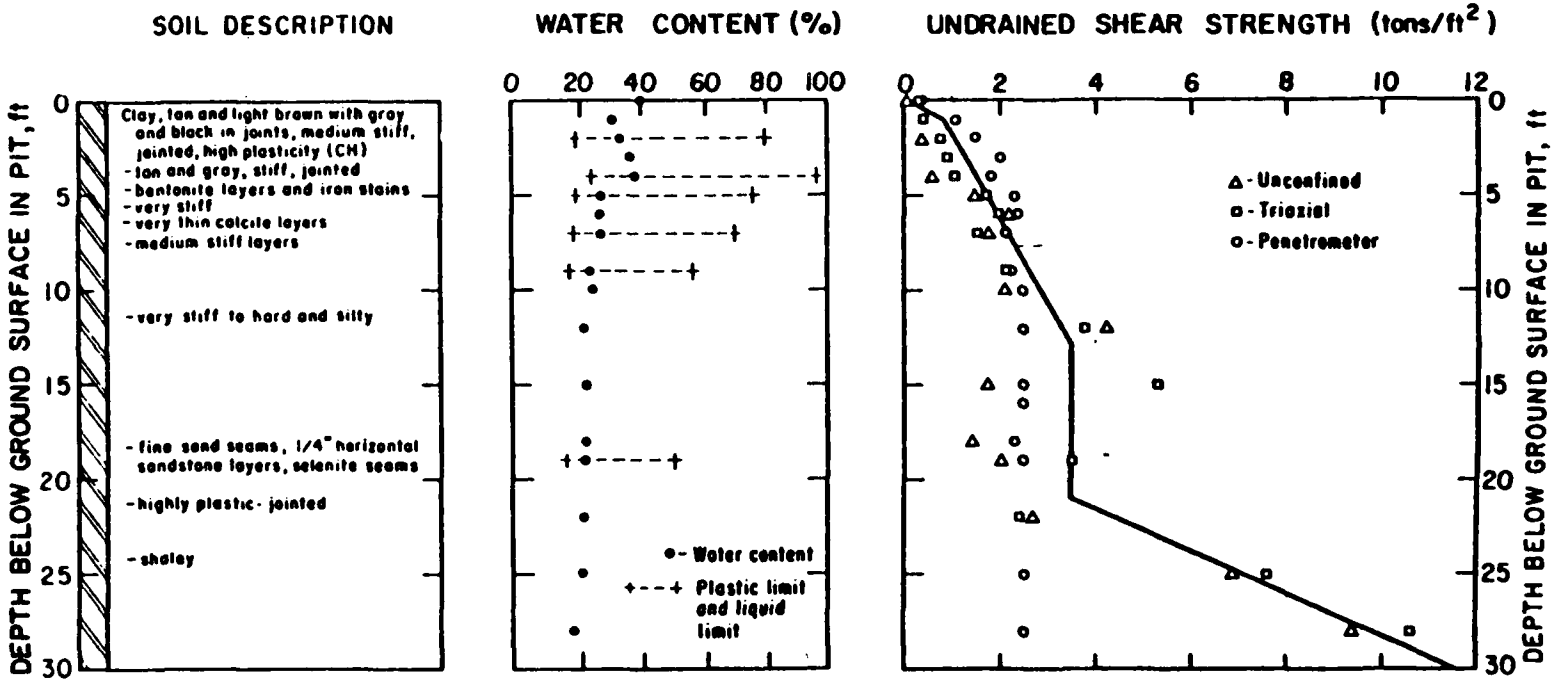

FIG. 7.3. Soil profile and shear strengths at Manor site from original investigation (from Reese, et al, 1975)

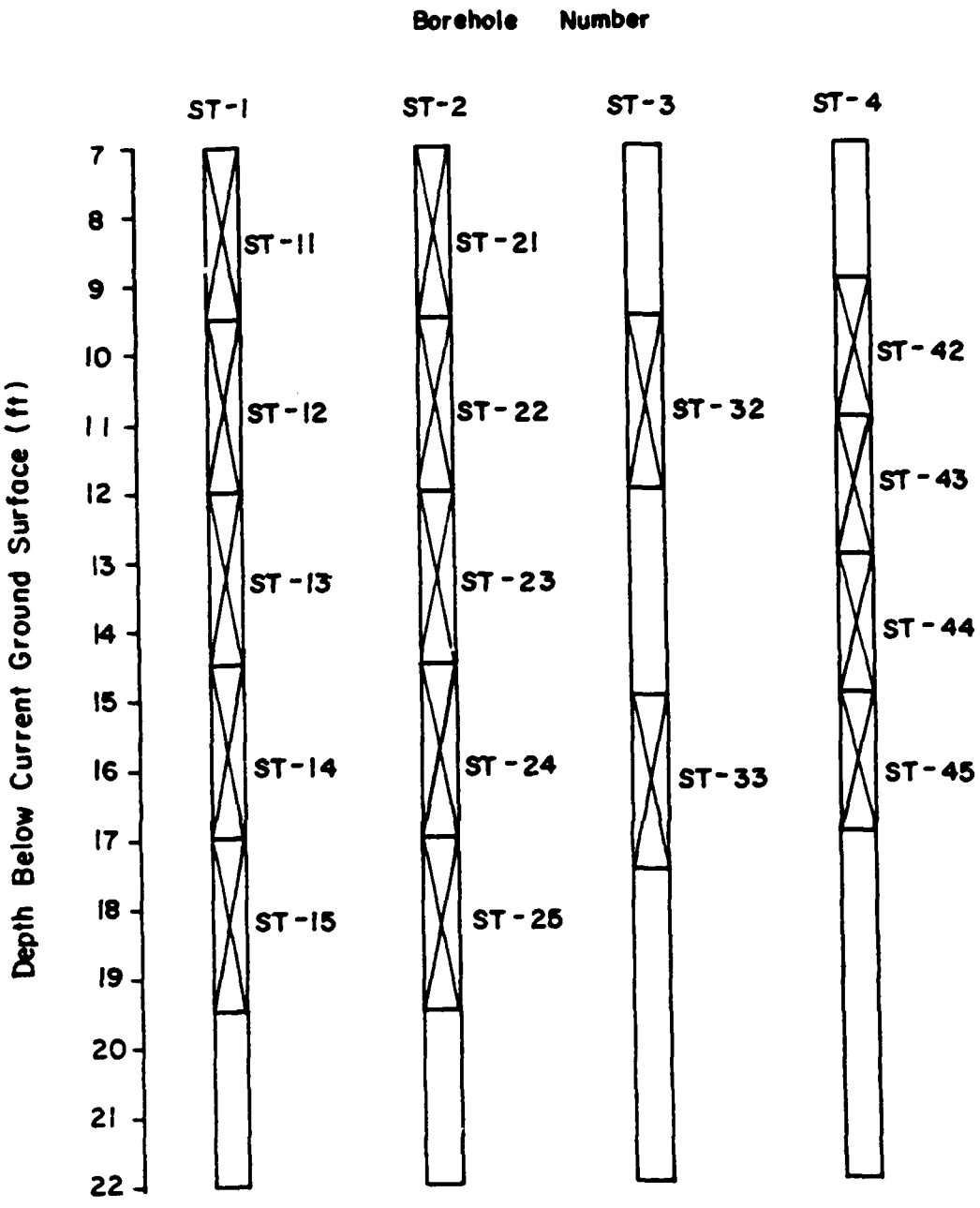

FIG. 7.4. Depths at which soil samples were taken at Manor site

Fig. 7.5 is a best estimate of the locations at which the soil borings were advanced. The exact location of the boreholes could not be ascertained because some landmarks used in he 1966 investigation were not present during the 1981 investigation.

Laboratory and Testing Procedures

In order to define characteristic-material parameters for the soil specimens taken at the Manor site, one-dimensional consolidation tests, static triaxial and cylic triaxial tests were performed. The special procedures that were used for some of these tests are described in Chapter 6.

One-Dimensional Consolidation Tests. One-dimensional consolidation tests were performed on samples 2.5 in. in diameter and 0.5 in. in height. Upon trimming the specimen into the consolidation ring and mounting the ring in the consolidation device, a vertical pressure of 125 lb/sq ft was applied to the specimen. The dial gauge was watched carefully to determine if any swelling occurred. If swelling was detected, additional pressure was applied until no swelling was apparent.

Geometric-loading increments were applied at approximately 24-hour intervals during loading whereas for unloading, a factor of four (64000 lb/sq ft, 16000 lb/sq ft, 4000 lb/sq ft, ... etc.) was used at approximately 48-hour intervals.

A total of five one-dimensional consolidation tests was performed and the resulting consolidation curves are shown in Fig. 7.6 on a plot of vertical strain versus log of the effective vertical pressure.

The shape of the one-dimensional consolidation curves presented in Fig. 7.6 is characteristic of a heavily overconsolidated clay. There is no clear indication of any point which might be selected as a maximum previous overburden pressure.

AD-A194 448 AN INVESTIGATION OF THE BEHAVIOR OF VERTICAL PILES IN COHESIVE SOILS SUBJ (U) TEXAS UNIV AT AUSTIN GEOTECHNICAL ENGINEERING CENTER J H LONG ET AL FEB 88 3/3

UNCLASSIFIED WES/MP/GL-88-4 DACW39-82-C-0014 F/G 13/13 NL

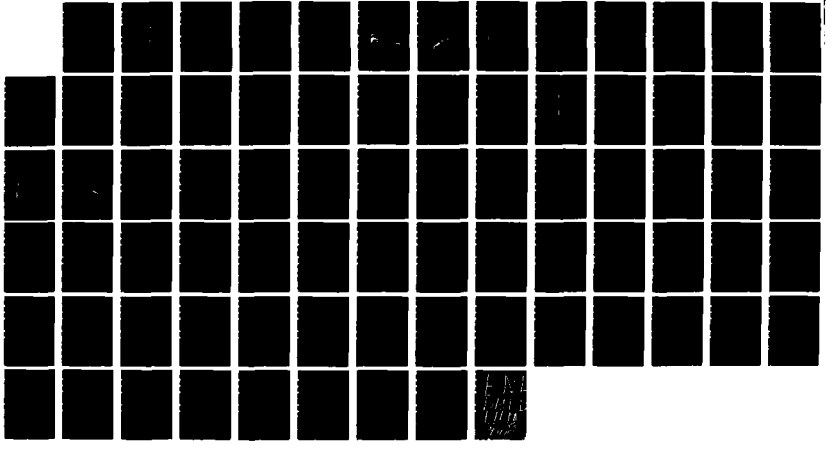

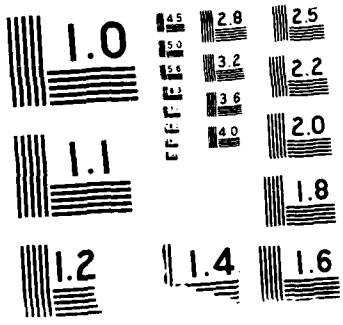
1.0
1.1
1.2
1.4
1.6
1.8
2.0
2.2
2.5
2.8
3.2
3.6
4.0
4.5
5.0

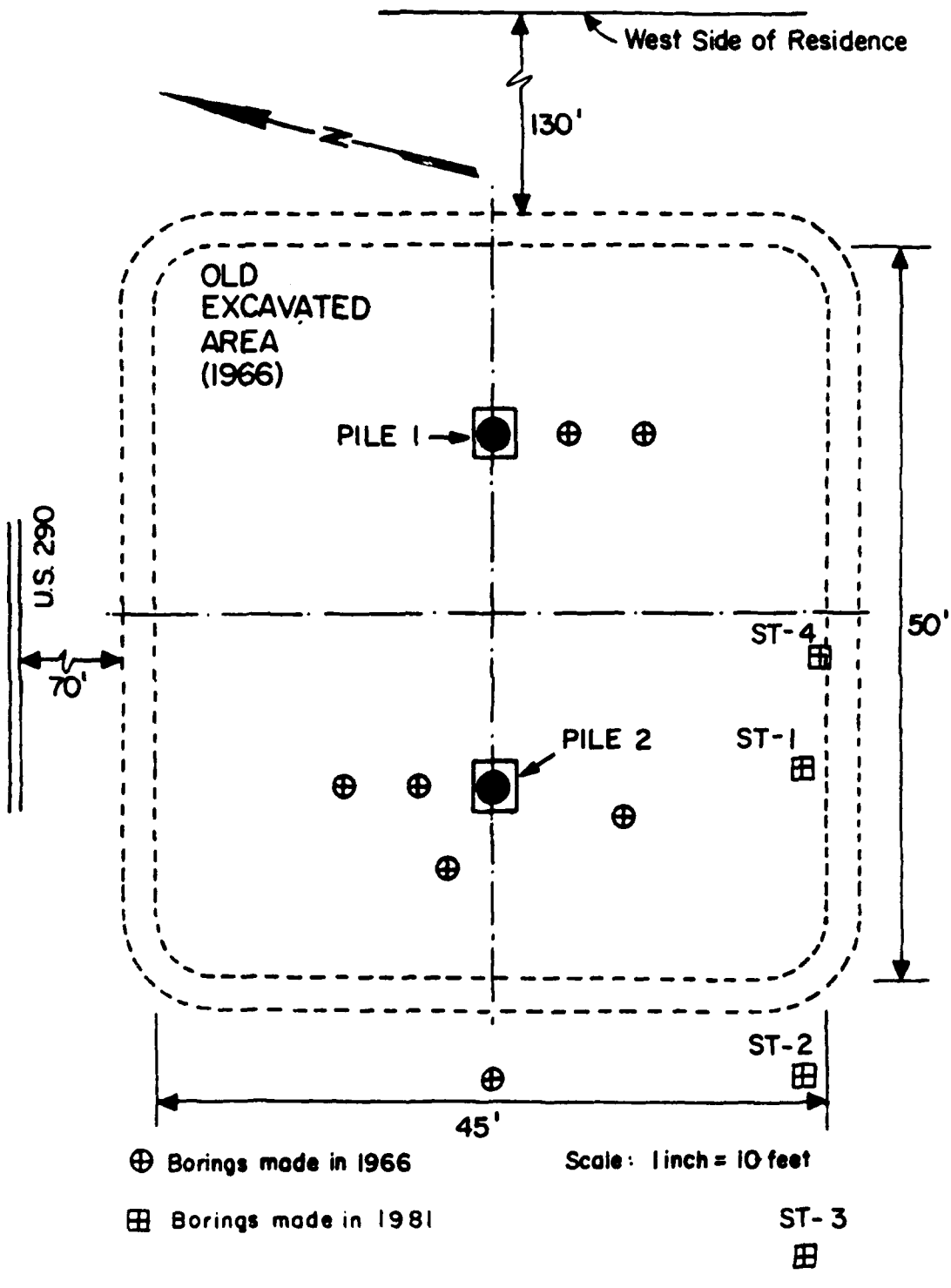

FIG. 7.5. Location of boreholes made in 1981

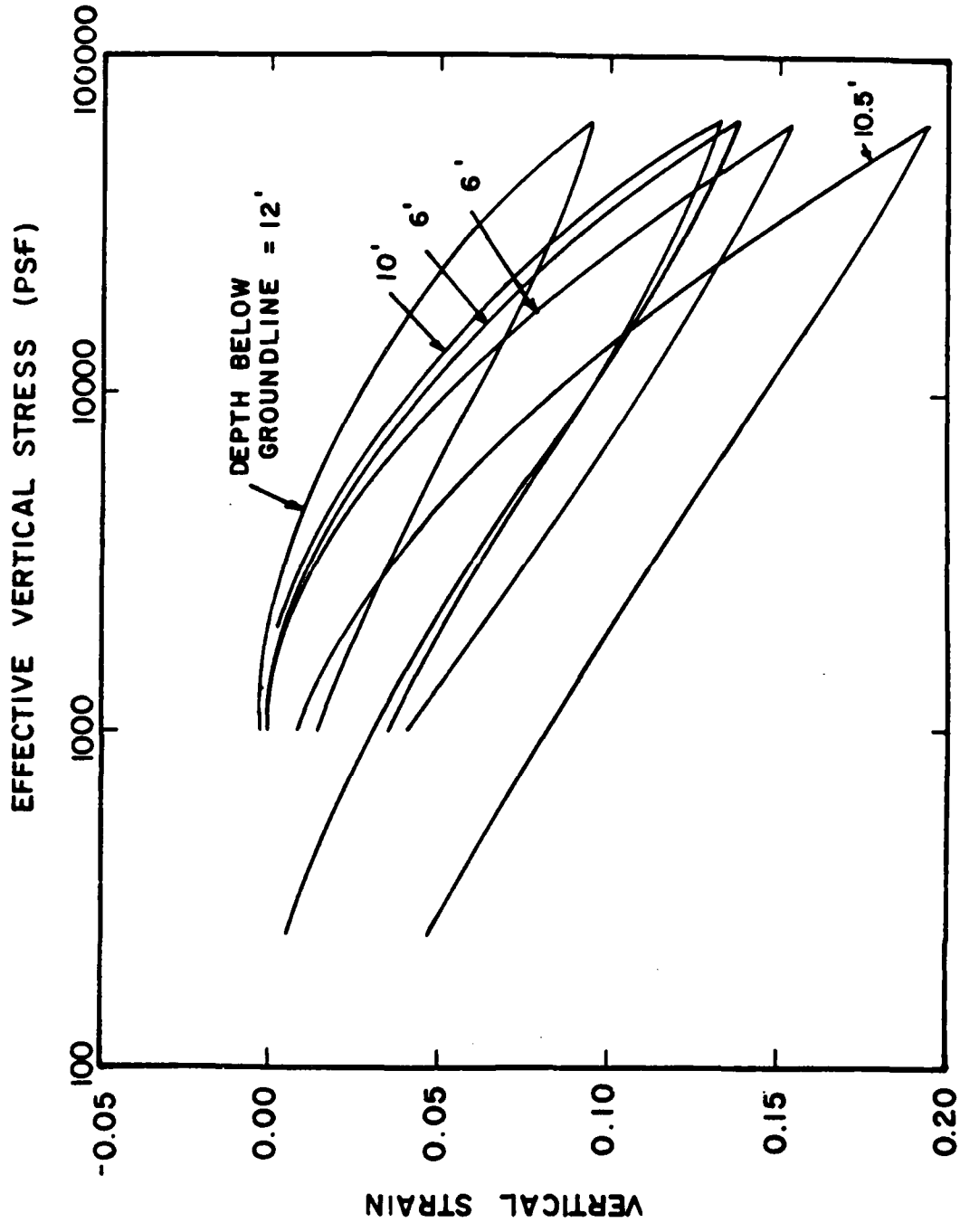

FIG. 7.6. Results of one-dimensional consolidation tests on Manor soil

Static-Triaxial Tests. Two types of static triaxial tests were performed on the soil specimens taken from the Manor site. These two tests are (1) isotropically-consolidated, undrained triaxial compession test with pore pressure measurement ($\overline{CIU}$-TC), and (2) isotropically-consolidated, undrained triaxial extension test with pore pressure measurement ($\overline{CIU}$-TE). Chapter 6 presents details of the procedures employed.

Results of all the triaxial tests of soils from the Manor site are shown in Table 7.1. Stress-strain curves and pore pressure-strain curves for the triaxial compression tests are shown in Fig. 7.7 and the corresponding effective stress paths are shown in Fig. 7.8. Stress-strain curves and pore pressure-strain curves for the triaxial extension tests are shown in Fig. 7.9 and the corresponding effective stress paths are shown in Fig. 7.10.

Cyclic-Triaxial Tests. Several controlled-strain, cyclic triaxial tests were conducted on specimens obtained from the Manor site. The results of these tests are summarized in Table 7.1, and the relationship of stress difference versus number of cycles measured during the tests are shown in Fig. 7.11 through 7.18. The peak stress difference is seen to decrease with increasing number of cycles.

Erosion and Pinhole-Dispersion Tests. In addition to the triaxial tests performed on the Manor soil, rod tests and pinhole dispersion tests were performed as described in Chapter 6. The results of thest tests were used to determine the susceptibility of the soil to the scouring action that takes place in the gap that is formed along the pile wall. For the rod study, a scour index value of 0.27 was determined. The scour-index value is meant to be compared with scour-index values obtained from tests

TABLE 7.1 RESULTS OF LABORATORY TESTS ON SPECIMENS FROM MANOR, TEXAS

Date	Test #	Tube #	Depth (ft)	Type of Test	$\bar{\sigma}_{3c}$ (psi)	wc tube	wc final	Static Triaxial			OCR	Cyclic Triaxial		Comments
								$(\sigma_1-\sigma_3)_f$ (psi)	ε_f (%)	t_f (min)		$\pm\varepsilon_a$	# of cycles	
17 Mar 82	1	ST-11	8.0	CTU-TC	3.0		32.6	12.8	18.9	1494				
17 Mar 82	2	ST-11	9.0	CTU-TC	5.0		31.0	15.2	20.0	1494				
17 Mar 82	3	ST-11	8.5	CTU-TC	7.0		33.0	18.5	14.4	1203				
8 Apr 82	4	ST-12	9.5	CTU-TC	2.0		43.1	9.5	3.8	300				
10 Apr 82	5	ST-12	11.0	CTU-TC	4.0		29.5	17.5	1.5	400				
12 Apr 82	6	ST-12	11.5	CTU-TC	7.0		29.4	15.7	2.1	240				
10 Apr 82	7a	ST-12	10.0	Cyclic	2.0		31.5					±0.5	80	1st time cyclic load test was run
	7b											±1.0	130	
	7c											±2.0	70	
	7d											±4.0	188	
17 Jun 82	8	ST-13	12.0	CTU-TC	7.0		29.5	36.0	18.7	1710				
24 Jun 82	9	ST-13	13.0	CTU-TC	7.0		28.1	46.5	11.0	0.125				
24 Jun 82	10a	ST-13	12.5	Cyclic	7.0		28.0					+2.3	107	Test was performed in compression only
	10b											+9.2	100	
23 Jun 82	11a	ST-14	15.0	Cyclic	7.0		27.6					+0.76	40	Test was performed in compression only
	11b											+3.6	40	
	11c											+8.8	40	
8 Jul 82	12a	ST-21	8.5	Cyclic	7.0	38.0	39.2					±5.0	100	
	12b											±15.0	1	
8 Jul 82	13a	ST-22	11.5	Cyclic	7.0	29.3	32.6					±2.8	100	
	13b											±9.3	1	Sample separated from base during extension
8 Jul 82	14	ST-23	12.0	Cyclic	7.0	27.8	29.1					-	-	Equipment failure
16 Jul 82	15	ST-41	10.0	Cyclic	7.0	36.7	40.5					±6.3	1	Sample failed due to hole formed in membrane during testing
16 Jul 82	16	ST-41	9.5	Cyclic	7.0	39.7	44.8					±2.7	200	
10 Aug 82	17	ST-23	12.75	CTU-TC	10.0	29.0	29.1	31.86	20.2	1545				
10 Aug 82	18	ST-23	13.25	CTU-TC	11.0	27.4	27.5	26.68	18.6	1601				
10 Aug 82	19	ST-23	13.50	CTU-TC	11.0	28.6	29.4	29.75	19.8	2166				
11 Aug 82	20	ST-23	13.75	CTU-TC	11.0	27.9	27.4	80.00	11.0	0.12				
26 Aug 82	21	ST-24	14.75	CIU-TC	6.0	25.1	26.4	17.21	20.0	2205				
26 Aug 82	22	ST-24	15.75	CTU-TC	13.0	23.9	26.9	28.10	6.8	487				
26 Aug 82	23	ST-24	16.25	Cyclic	13.0	25.7	28.1					+0.69 -1.0	200	Unsymmetric loading extension 1.03%, comp = 0.6% - quick test followed - otherwise good test
26 Aug 82	24	ST-24	16.75	CTU-TC	27.5	26.0	28.5	48.34	3.3	309				
27 Aug 82	25	ST-32	10.75	Cyclic	9.0	48.0	53.8							Sample was very fissured and x-y plotter was set too sensitive
27 Aug 82	26	ST-32	11.25	Cyclic	9.0	30.4	30.1					±3.0	200	small amount of slippage occurred in extension
30 Mar 83	27	ST-23	14'0"	Cyclic	10.0	25.2	27.3					±0.44	231	slightly more extension than compression
29 Mar 83	28	ST-23	14'2"	Cyclic	10.0	27.0	27.6					±1.47	261	
												±4.51	50	
28 Mar 83	29	ST-43	12'5"	Cyclic	10.0	28.2	29.6					±4.37	30	

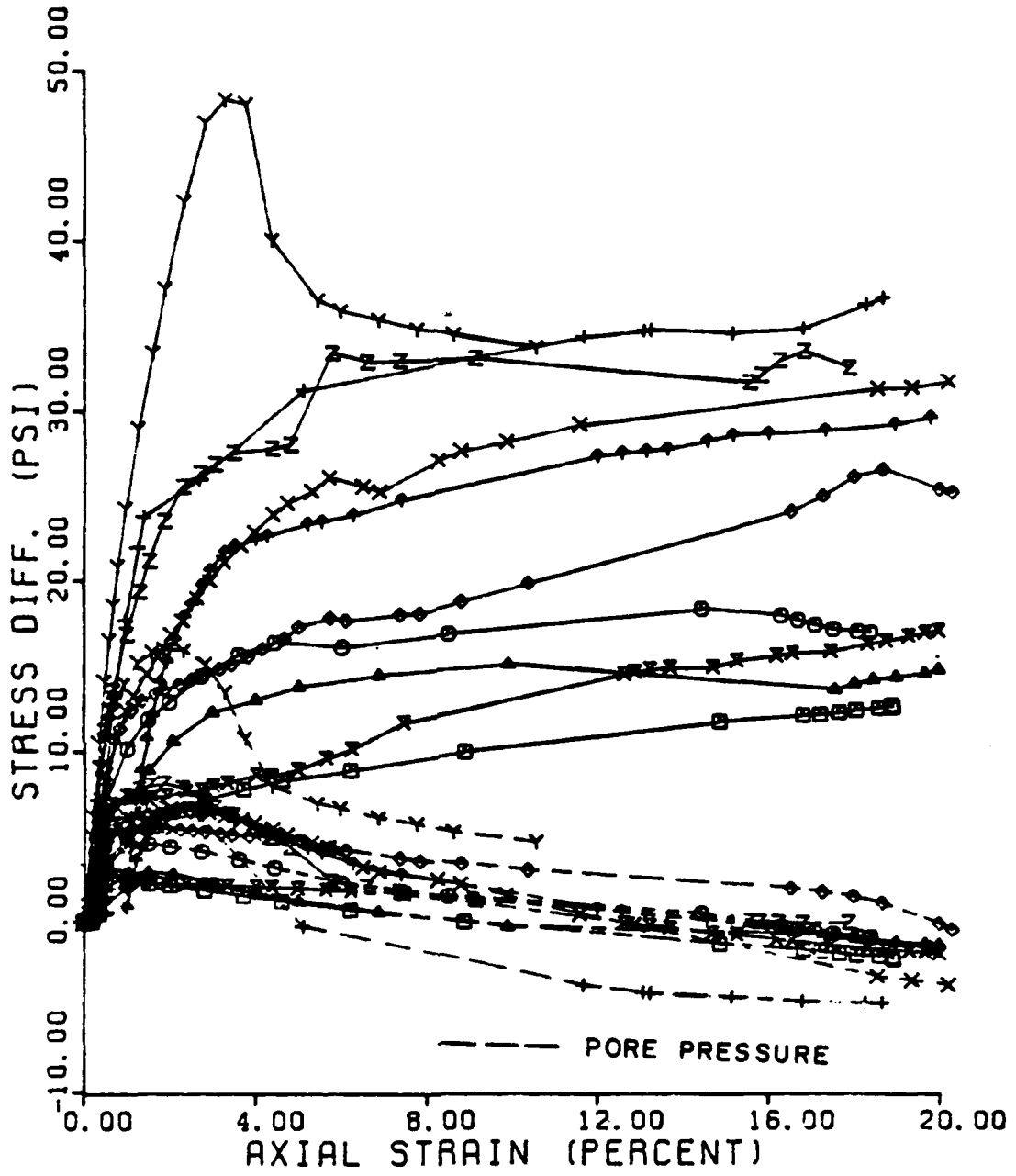

FIG. 7.7. Stress-strain and pore pressure-strain curves for triaxial compression tests on Manor soils

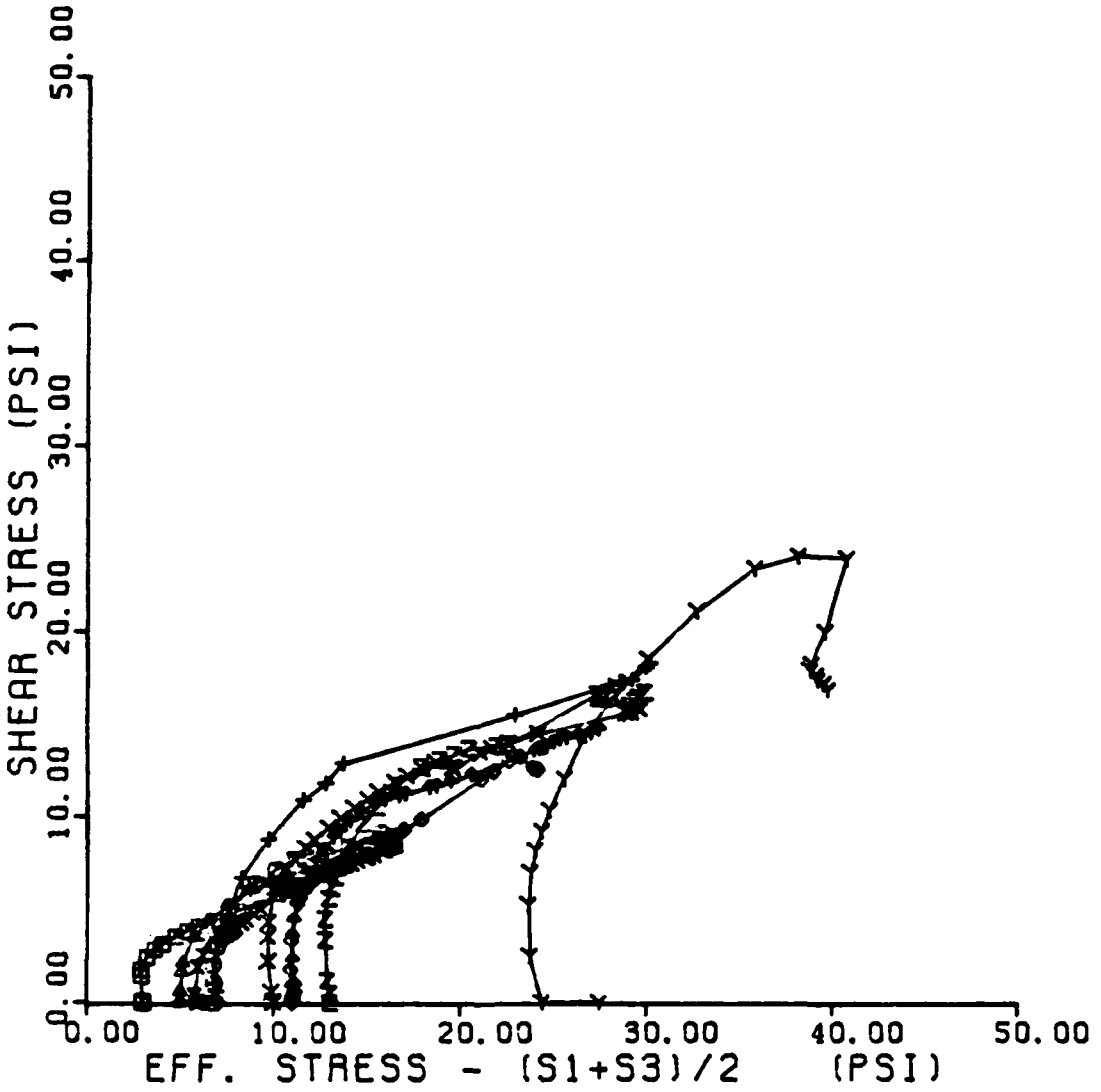

FIG. 7.8. Effective stress paths for triaxial compression tests on Manor soils

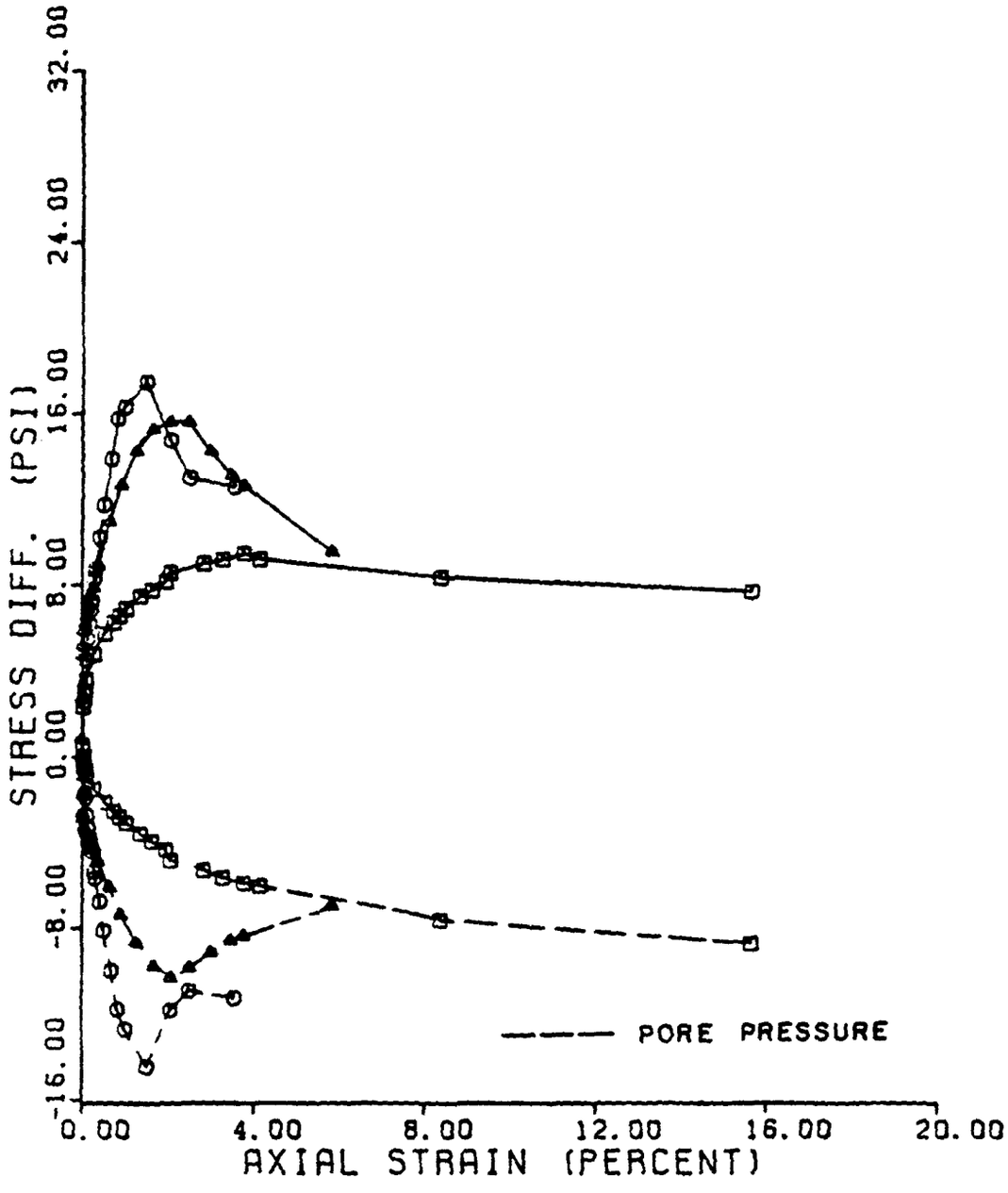

FIG. 7.9. Stress-strain and pore-pressure-strain curves for triaxial extension tests on Manor soils

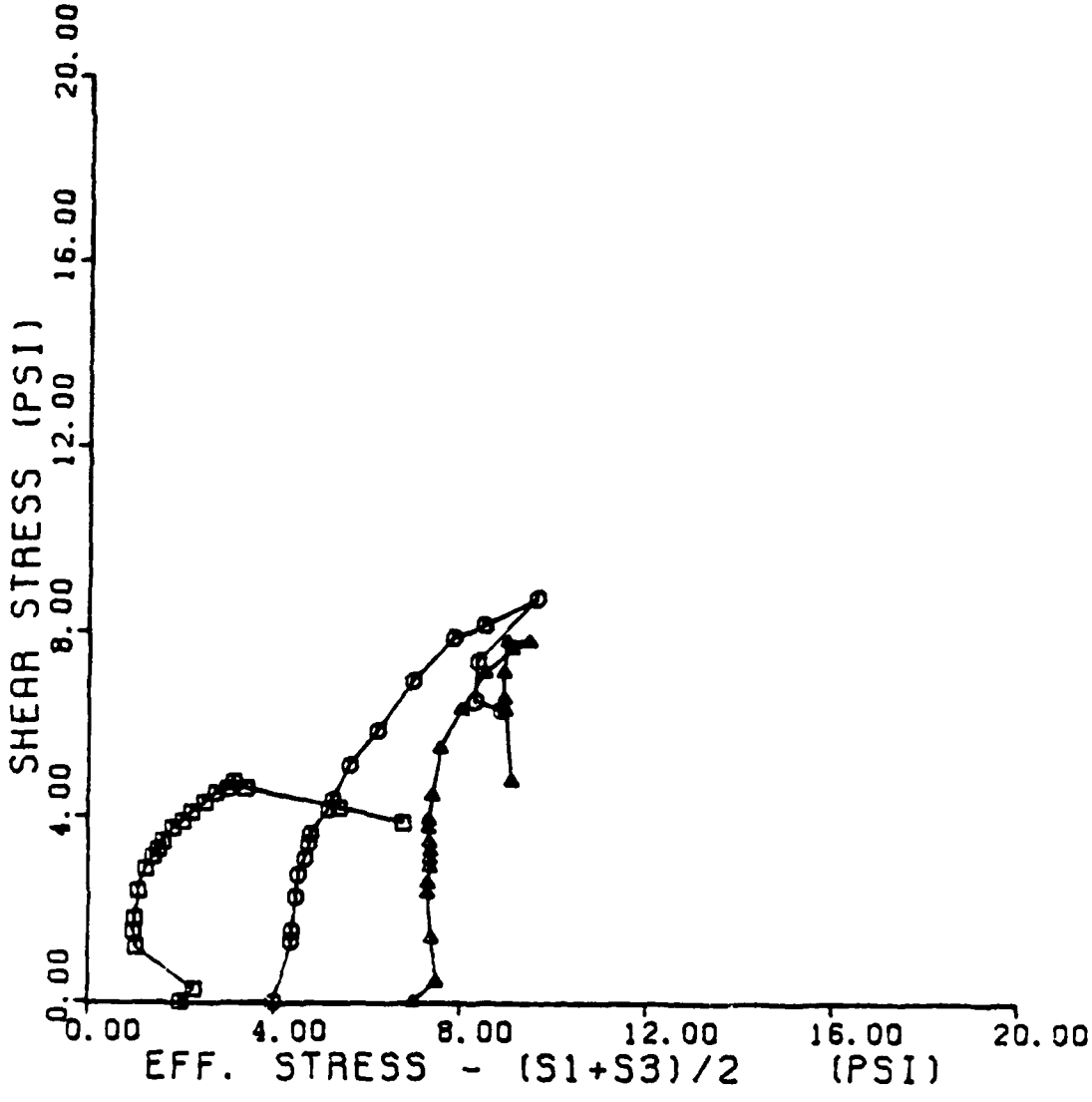

FIG. 7.10. Effective stress paths for triaxial extension tests on Manor soils

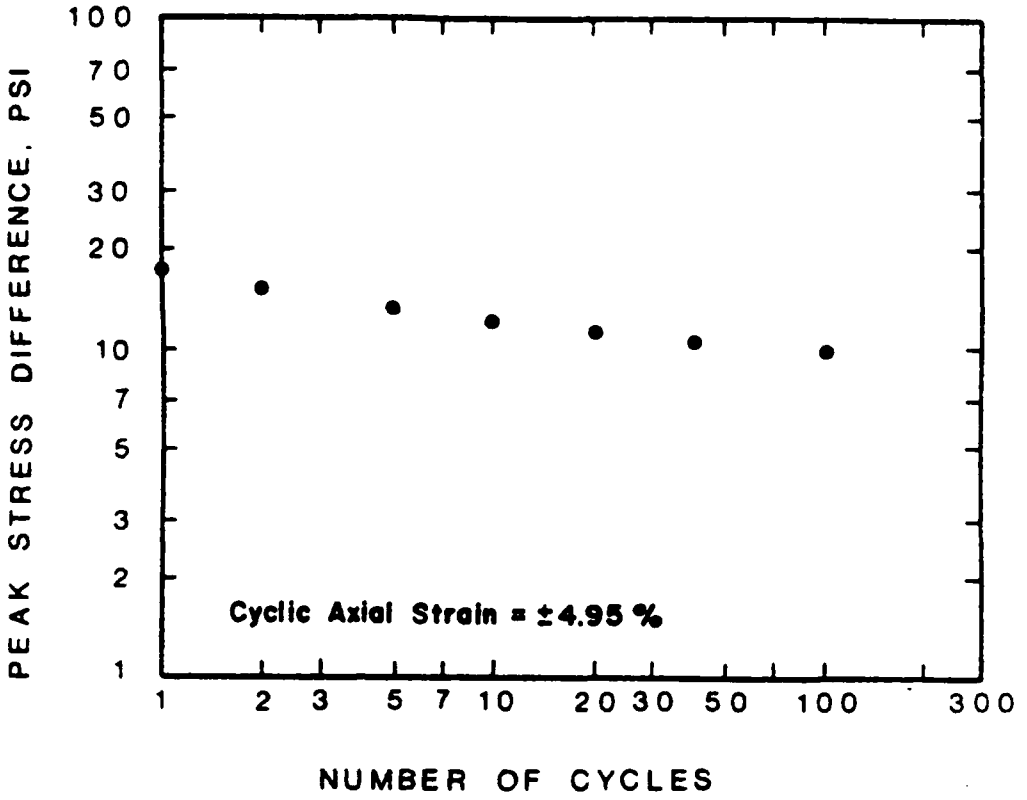

FIG. 7.11. Cyclic stress versus number of cycles for test 12, Manor

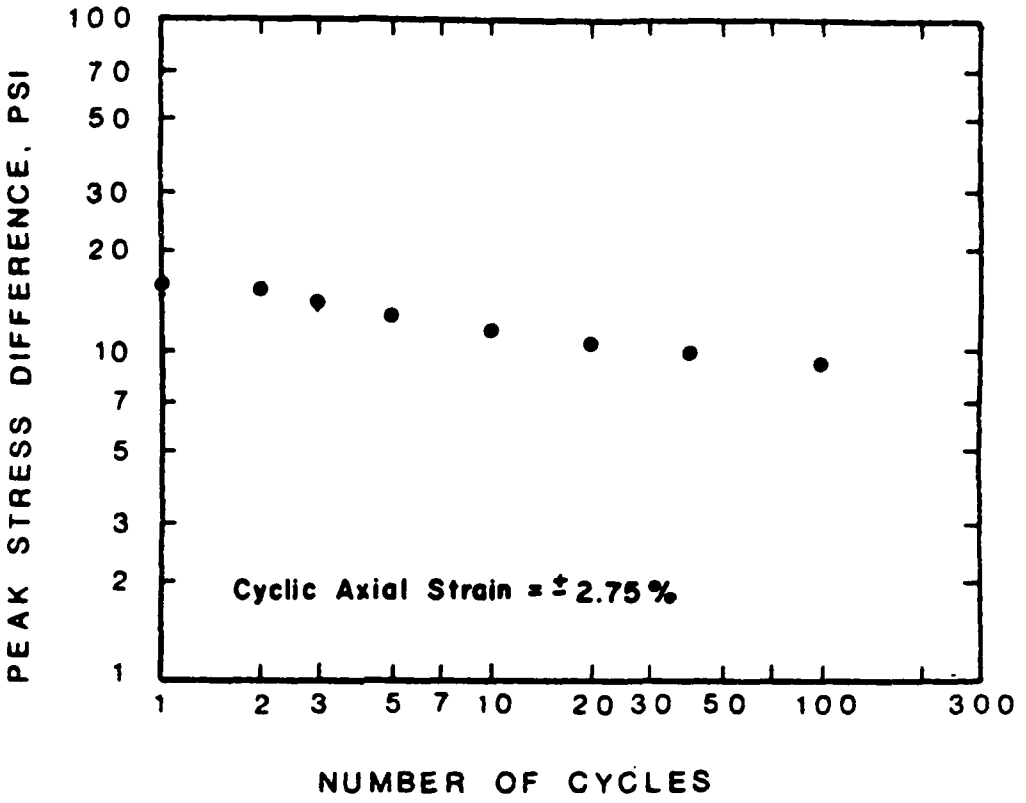

FIG. 7.12. Cyclic stress versus number of cycles for test 13, Manor

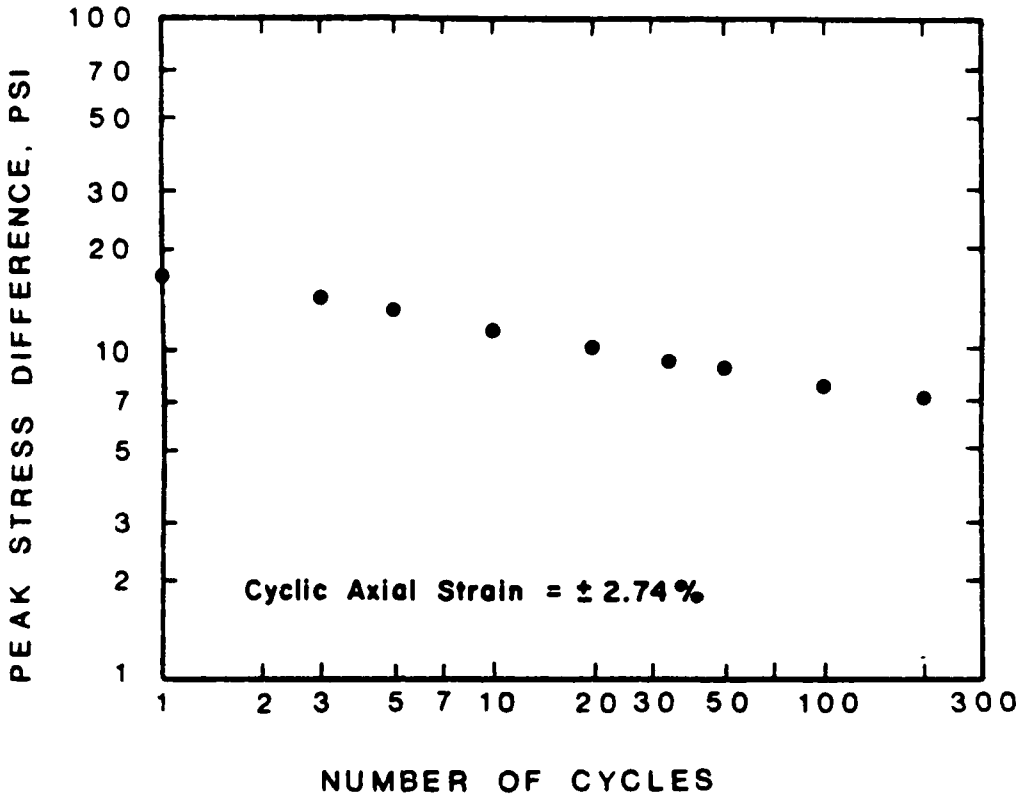

FIG. 7.13. Cyclic stress versus number of cycles for test 16, Manor

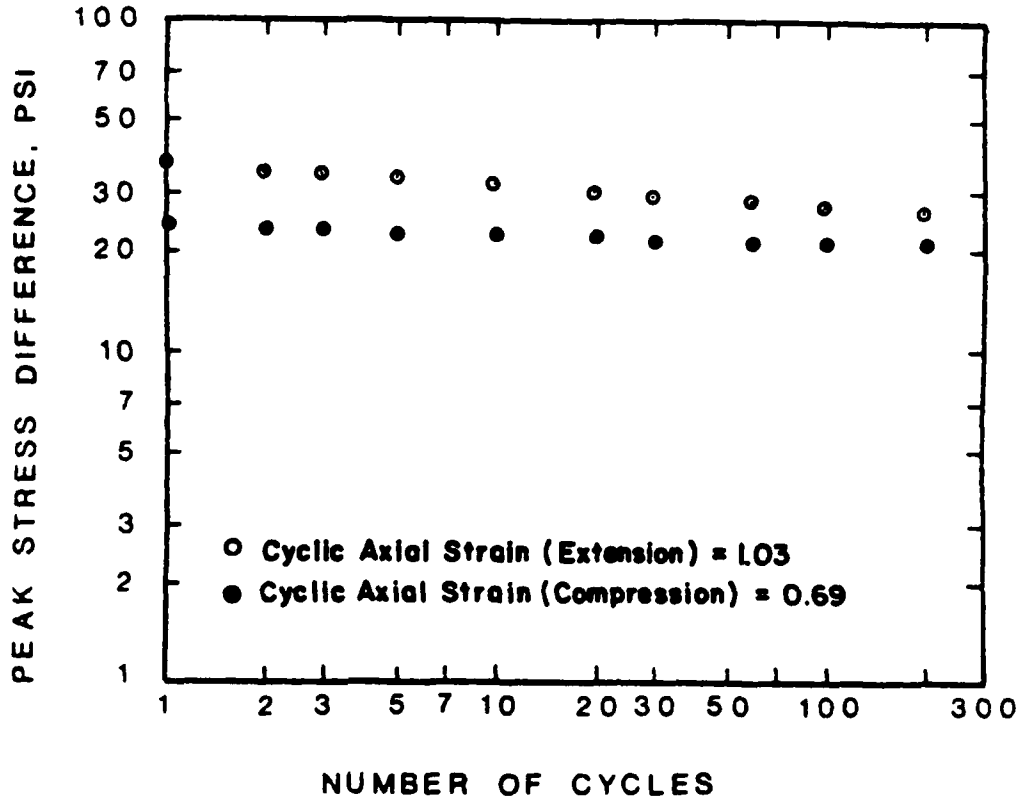

FIG. 7.14. Cyclic stress versus number of cycles for test 23, Manor

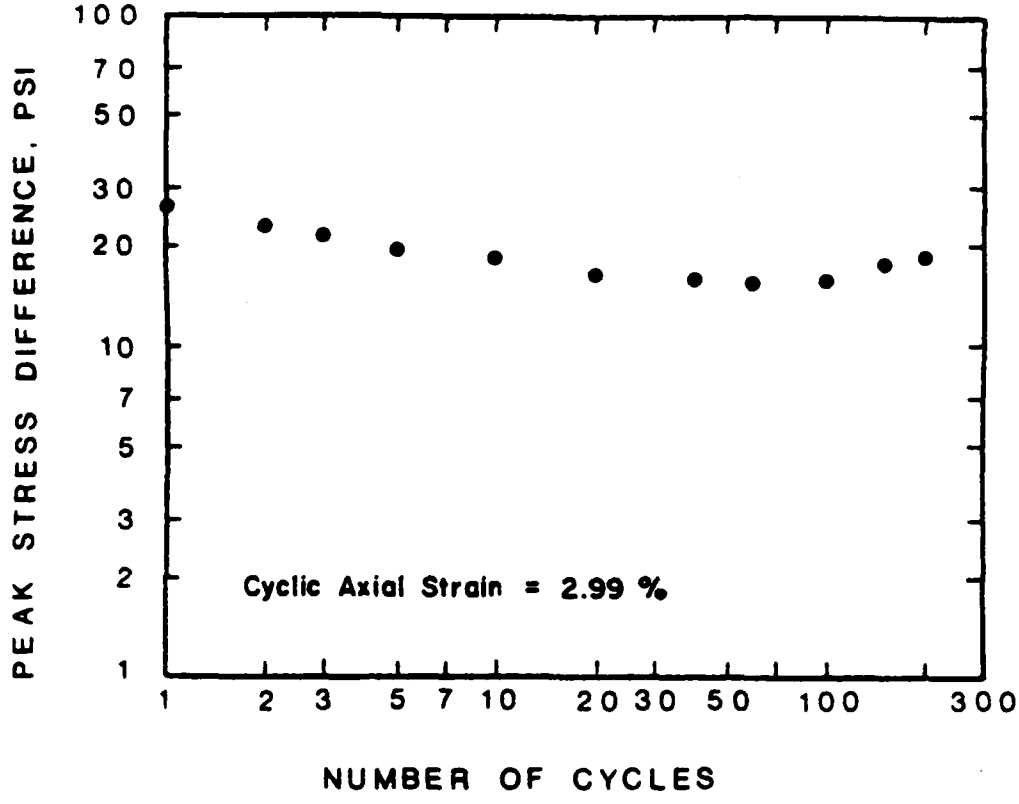

FIG. 7.15. Cyclic axial strains versus number of cycles for test 26, Manor

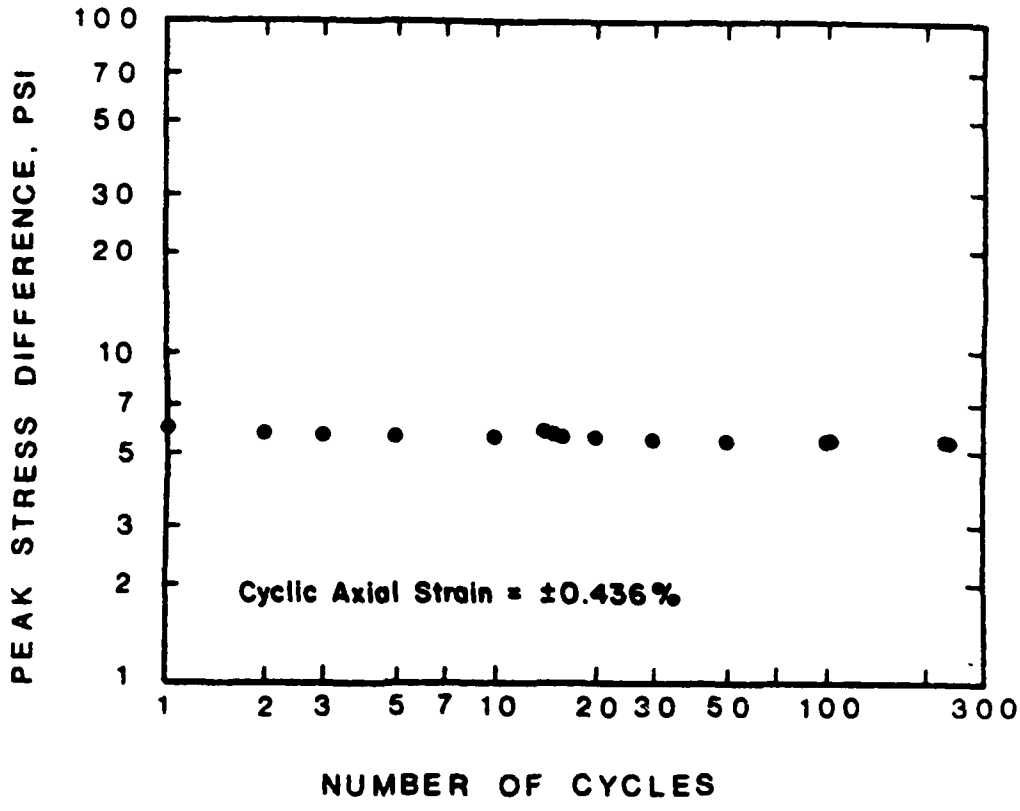

FIG. 7.16. Cyclic axial stress versus number of cycles for test 27, Manor

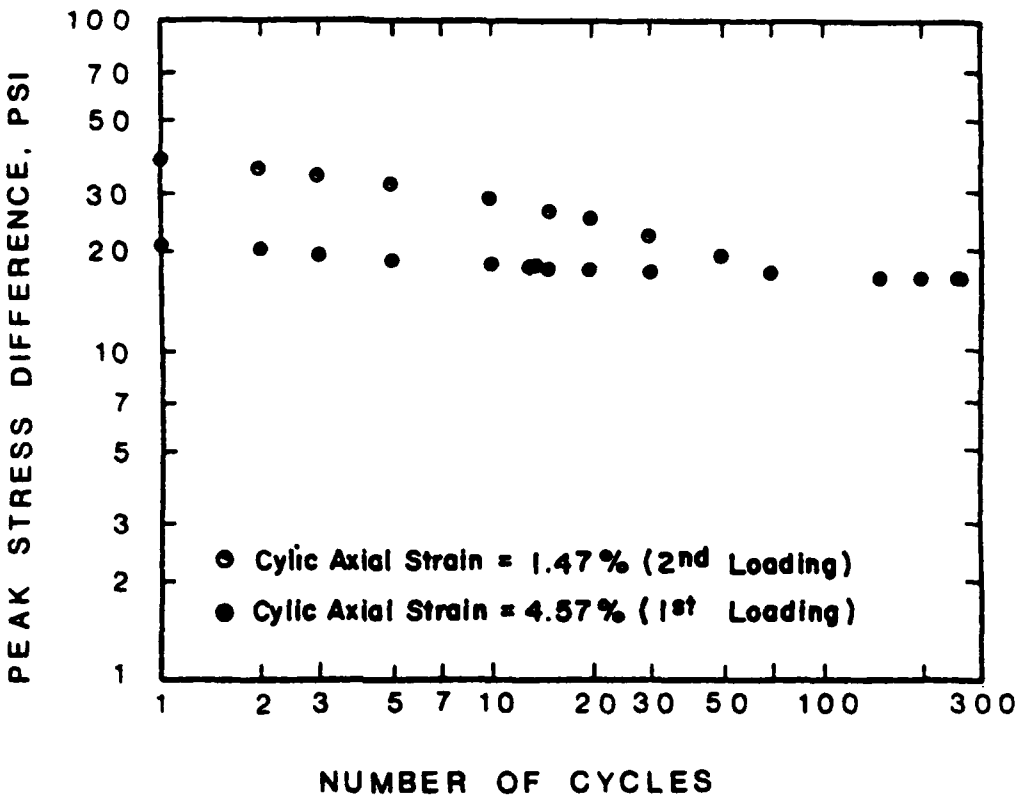

FIG. 7.17. Cyclic axial stress versus number of cycles for test 28, Manor

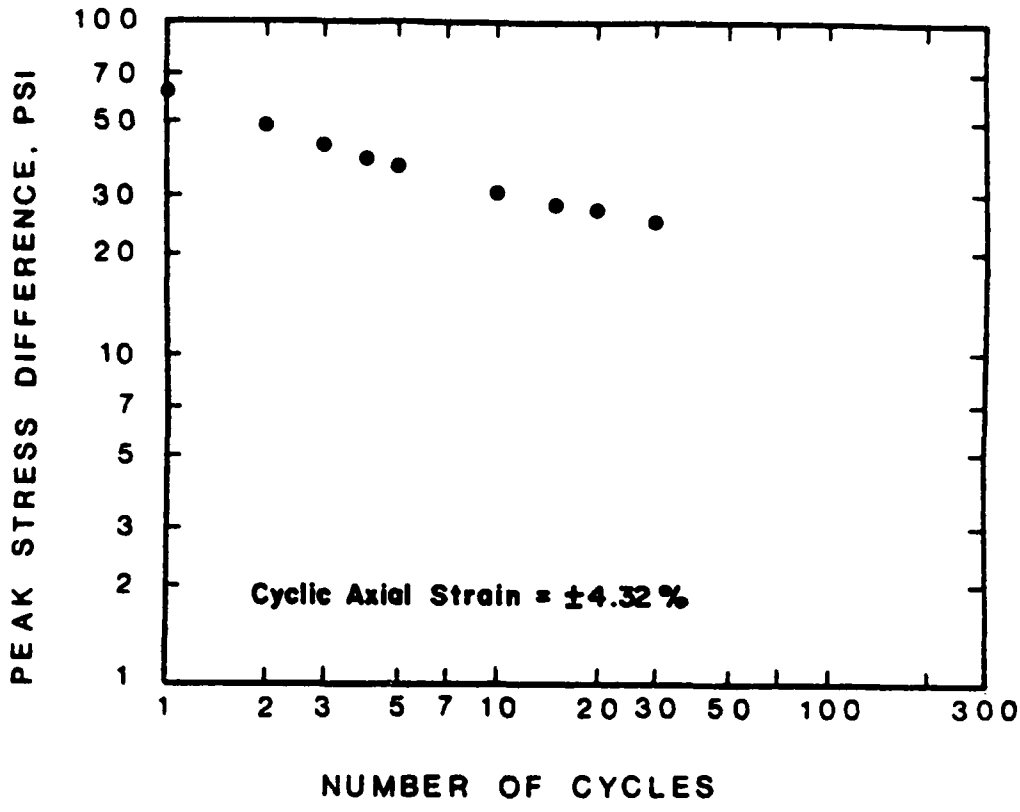

FIG. 7.18. Cyclic axial stress versus number of cycles for test 29, Manor

on other soils. Once experience is gained in correlating scour-index values of soils with observed scouring behavior of the soil around the pile, better methods of predicting pile-soil behavior will become available.

In addition to the scour-index tests, pinhole-dispersion tests were also performed on specimens of Manor soil. The results of pinhole-dispersion tests conducted on both compacted and natural Manor soil indicated the clay to be non-dispersive.

SABINE SITE

Site Location

The Sabine test site is located south of Sabine Pass, Texas, along the west bank of the Sabine River as shown in Fig. 7.19. The original site, and the location of the test pits used in the field study are shown in Fig. 7.20. Unfortunately, it was impossible to return to the original site and obtain samples because the immediate area had been filled, paved, and served as a storage yard for steel casing used in the petroleum industry. Therefore, soil specimens were obtained from the nearest suitable location, which was about 100 to 200 ft from the original site. This location is shown in Fig. 7.20.

History of Site

In 1958, a soil boring and testing program was conducted to determine the subsurface profile and the shear strength of the soil. In addition to visual classification, Atterberg limits, and water content tests, several vane tests and unconfined compression tests were conducted. Shown in Fig. 7.21 are the results of the original testing program.

Upon completion of the soil boring program, the original investigators decided to excavate three rectangularly-shaped test pits measuring

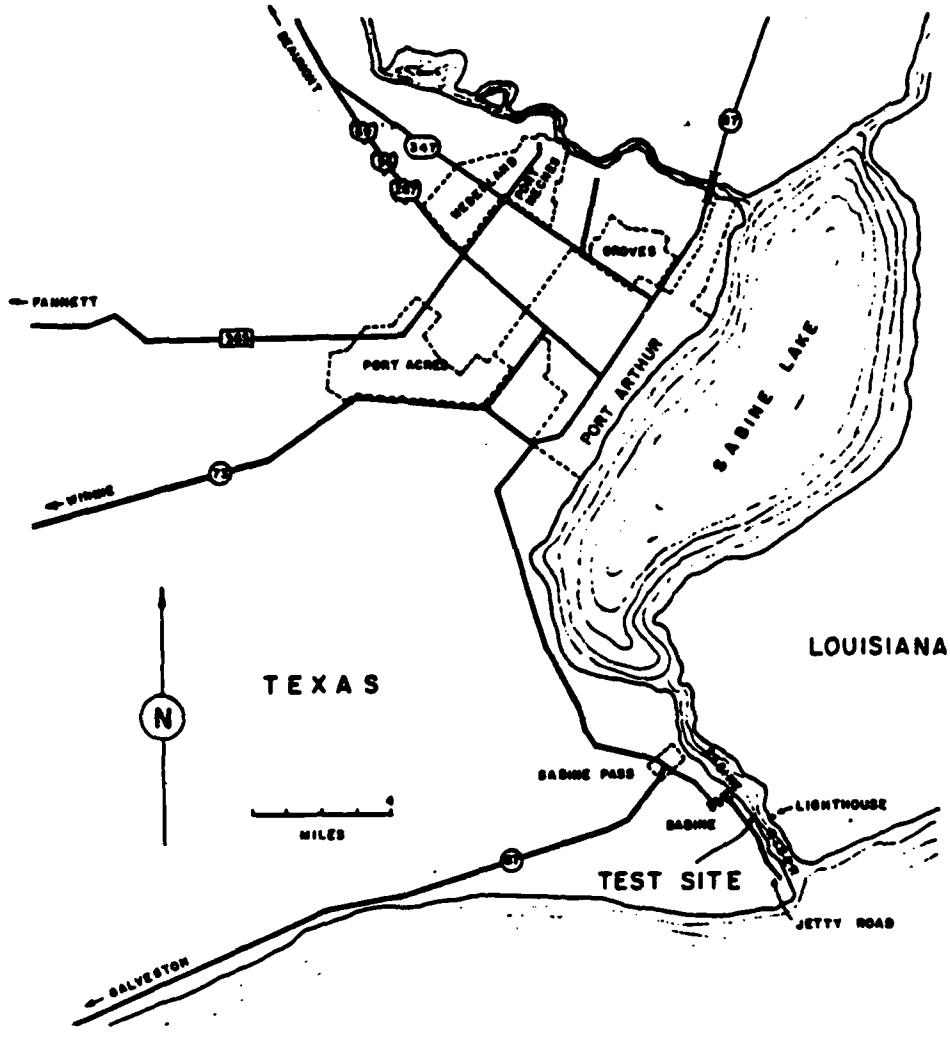

FIG. 7.19. Location of the test site near the mouth of the Sabine River (from Matlock and Tucker, 1961)

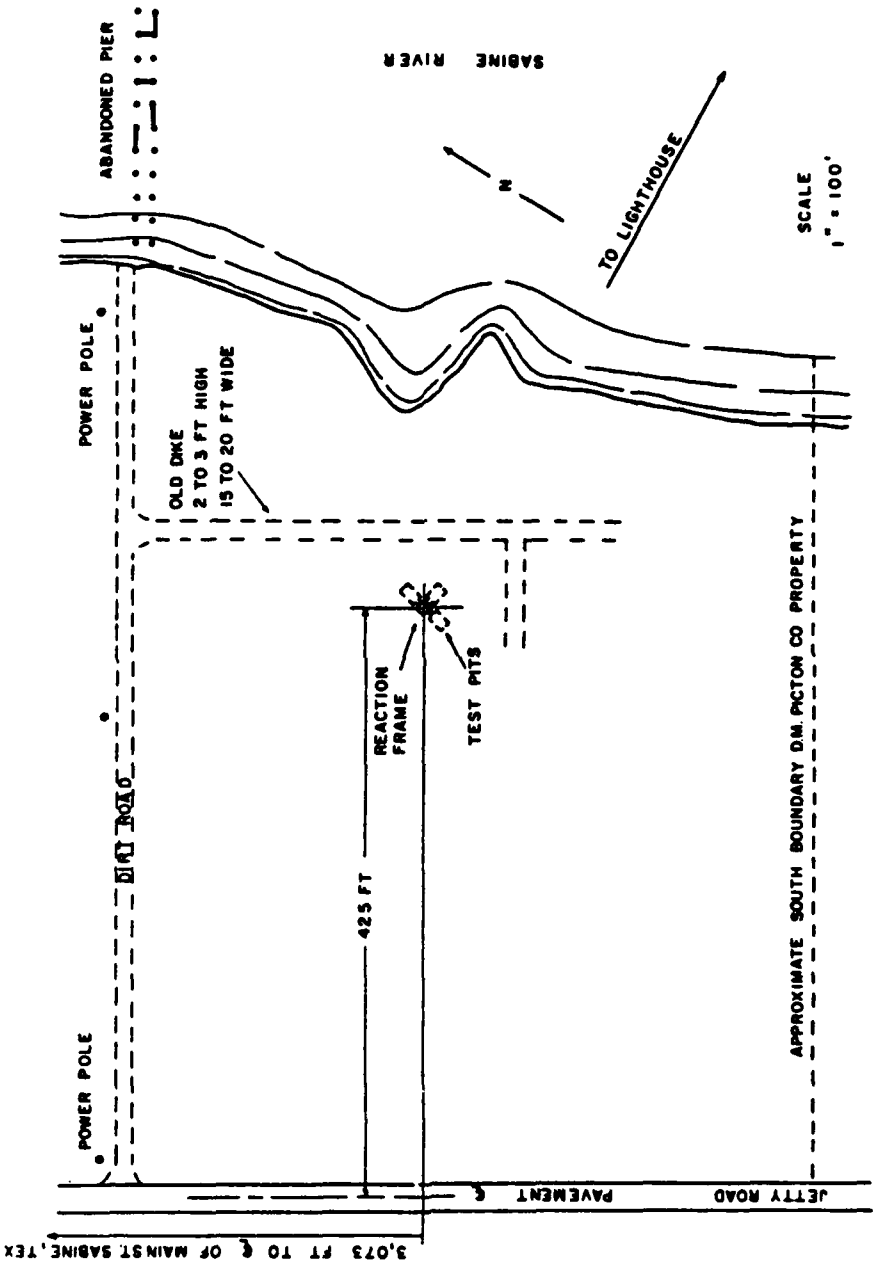

FIG. 7.20. Map of test site at Sabine (from Matlock and Tucker, 1961)

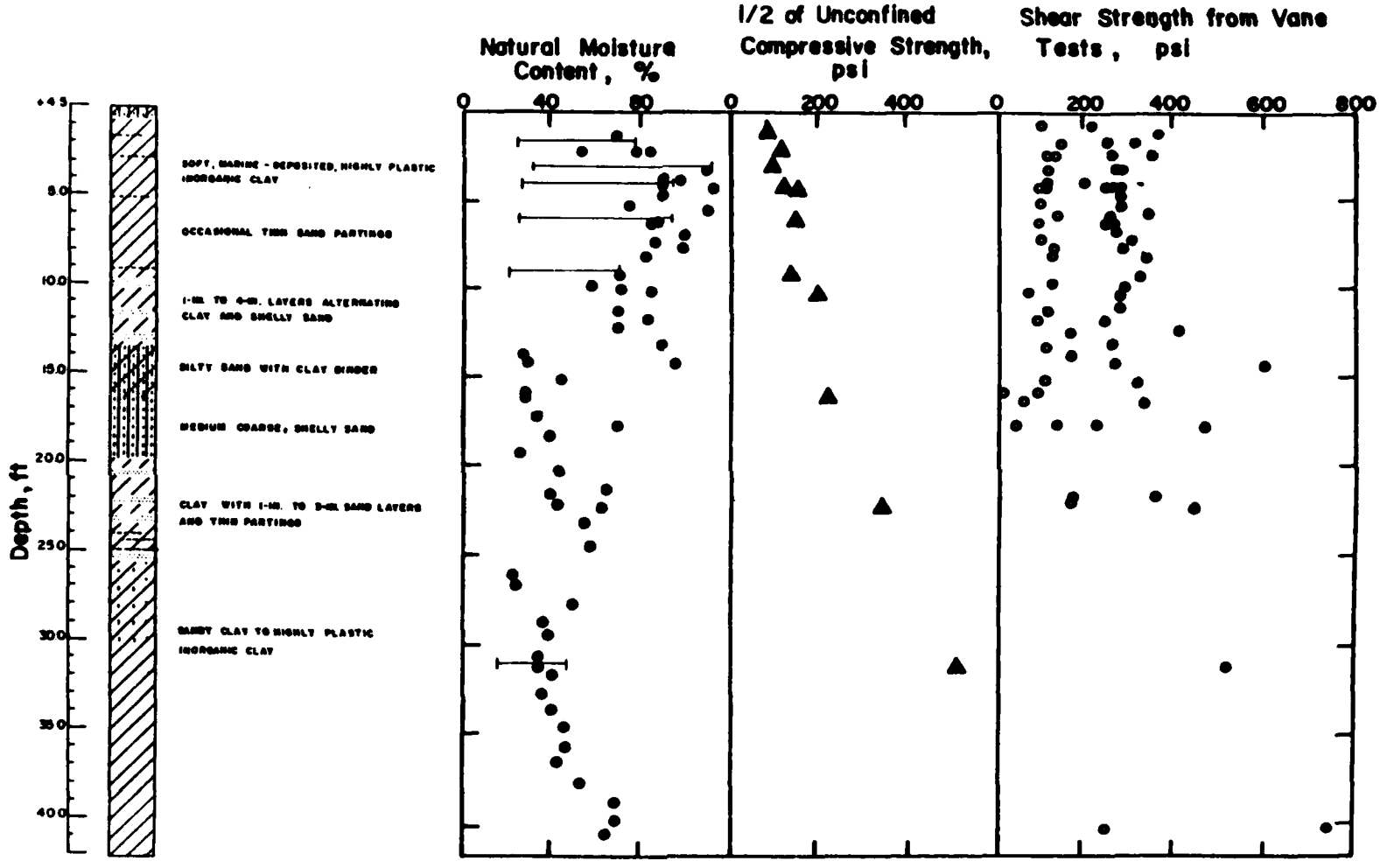

FIG. 7.21. Soil profile for Sabine site (from Matlock and Tucker, 1961)

12 ft wide, 16 ft long and 4.5 ft deep. The excavations were made to eliminate the presence of the stiffer, oil-stained clay near the ground surface, and to expose the softer clay material.

After the lateral-load testing program was completed, the Sabine site was abandoned until 1978. At this time, additional vane tests, triaxial tests, and a series of self-boring pressuremeter tests were conducted. The results of this investigation are shown in Fig. 7.22. Since 1978, no other data concerning shear strength and soil properties of the Sabine site have been made available.

Boring Campaign in 1982

On June 29, 1982, a subsurface investigation of the Sabine test location was conducted. Three boreholes were advanced and 3.0 in. thin-walled shelby tube samples were taken. The holes were drilled approximately on ten ft centers and the depths at which specimens were obtained are shown in Fig. 7.23. The samples were obtained by drilling to a specified depth, then lowering the shelby tubes to the bottom of the borehole while pumping drilling fluid through the tube. When the tube reached the bottom of the hole, the shelby tube was pushed into the ground. The tube was slowly rotated, and then extracted slowly.

After the tube was raised to ground level and disconnected from the drill-string, any cuttings within the tube were removed, and both ends were sealed and waxed. The tubes were then stored vertically in a special wooden box and brought back to the University of Texas for laboratory testing.

Laboratory and Testing Procedures

In order to obtain information on the consolidation characteristics and the static and cyclic stress-strain behavior of the soil obtained from

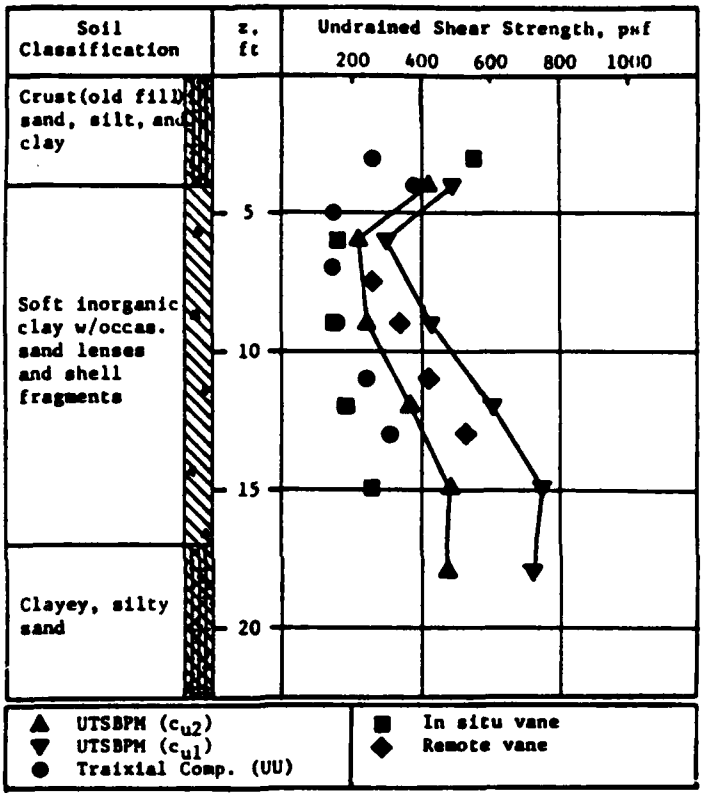

FIG. 7.22. Soil and shear strength profile for site at Sabine Pass(from Steussy)

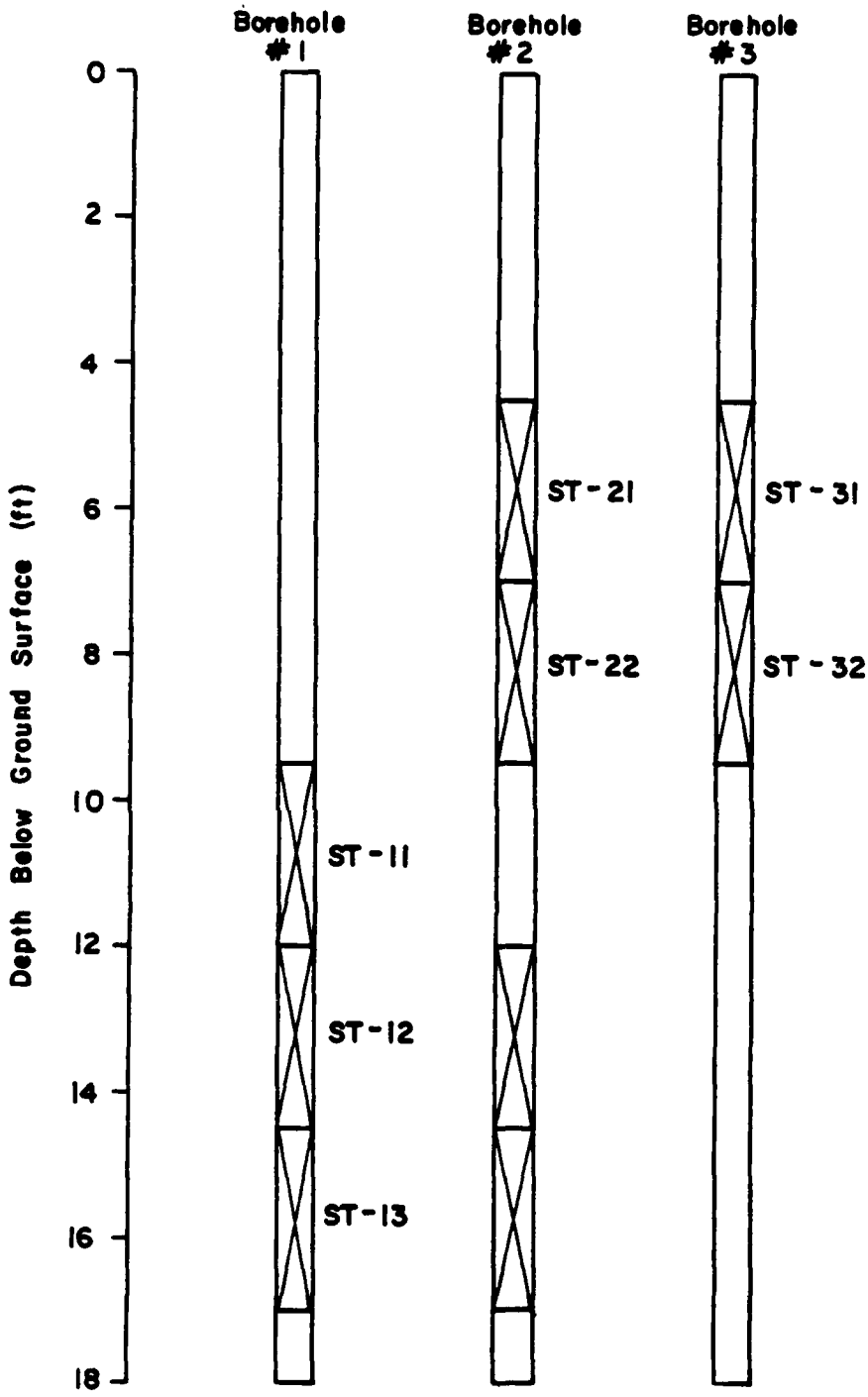

FIG. 7.23. Depths at which shelby tube samples were taken

the Sabine site, several one-dimensional consolidation tests, static triaxial tests, and cyclic triaxial tests were performed. In Table 7.2 are listed the type of tests, corresponding test numbers, and important information for each test.

The results of one-dimensional consolidation tests performed on the Sabine clay are shown in Fig. 7.24. The curves are characteristic of a soft clay.

Four static triaxial compression tests with pore-pressure measurements were also conducted on specimens of soil from the Sabine site. The results of the four $\overline{\text{CIU}}$-TC tests are listed in Table 7.2 and shown in terms of stress-strain and pore pressure-strain curves in Fig. 7.25. Additionally, the effective stress paths measured during the four tests are plotted in Fig. 7.26.

Several controlled-strain, cyclic triaxial tests were performed on the Sabine soils and the results are also listed in Table 7.2. The results of the cyclic triaxial tests are presented in Figs. 7.27 through 7.32 in terms of maximum peak stress difference versus number of cycles of loading. As can be seen in the figures, as the number of cycles increase, the value of peak stress difference decreases.

Erosion and pinhole-dispersion tests were also conducted on specimens of soil from the Sabine site. Results from the rod tests indicated a scour-index value of 0.36. This value is somewhat higher than that measured for the Manor soil.

After the rod test was performed, the equipment was dismantled, the model pile was extracted from the soil, and the soil surrounding the model pile was cut along the pile axis so that a cross-sectional (profile) view of the soil could be observed. It was found that the soil nearest the cav-

TABLE 7.2 RESULTS OF LABORATORY TESTS ON SPECIMENS FROM SABINE, TEXAS

Date	Test #	Tube #	Depth (ft)	Type of Test	$\bar{\sigma}_{3c}$ (psi)	w% tube	w% final	Static Triaxial $(\sigma_1-\sigma_3)_f$ (psi)	Static Triaxial ε_f (%)	Static Triaxial t_f (min)	OCR	Cyclic Triaxial $\pm\varepsilon_a$	Cyclic Triaxial # of cycles	Comments
14 Jul 82	1	1	13'	1-D	-	114.1	-							
14 Jul 82	2	2	5'	1-D	-	38.6	-							
14 Jul 82	3	2	5'10"	1-D	-	34.6	-							
14 Jul 82	4	1	12-14.5'	limits	-	-	-							LL = 104, PL = 32, PI = 72
14 Jul 82	5	2	5.5'	$\overline{CIU}$-TC	20	35.9	25.5	32.81	19.41	1426	4			Overnite, after axial strain reading of 8.25%, the triaxial cell leaked & $\bar{\sigma}_{3TOT}$ went to zero
14 Jul 82	6	2	5.5'	$\overline{CIU}$-TC	80	29.6	20.3	54.96	8.25	454	1			
14 Jul 82	7	1	13'	$\overline{CIU}$-TC	40	96.7	42.6	30.05	10.40	621	2			
14 Jul 82	8	1	13.5'	$\overline{CIU}$-TC	80	101.8	46.3	42.91	17.25	1432	1			
8 Apr 83	9	2	5'6"	Cyclic	40	32.9	25.1				1	±0.64	200	
8 Apr 83	10	2	6'0"	Cyclic	40	33.6	25.9				1	±4.8	201	
8 Apr 83	11	2	6'6"	Cyclic	40	29.2	24.0				1	±2.7	200	
15 Apr 83	12	2	7'6"	Cyclic	40	73.5	52.5				1	±2.0	200	Cam Device was not bolted down, hence, not equal $\pm\varepsilon_a$
15 Apr 83	13	2	8'0"	Cyclic	40	47.9	34.9				1	±2.4	300	
15 Apr 83	14	2	8'6"	Cyclic	40	83.3	53.71				1	±2.3	200	

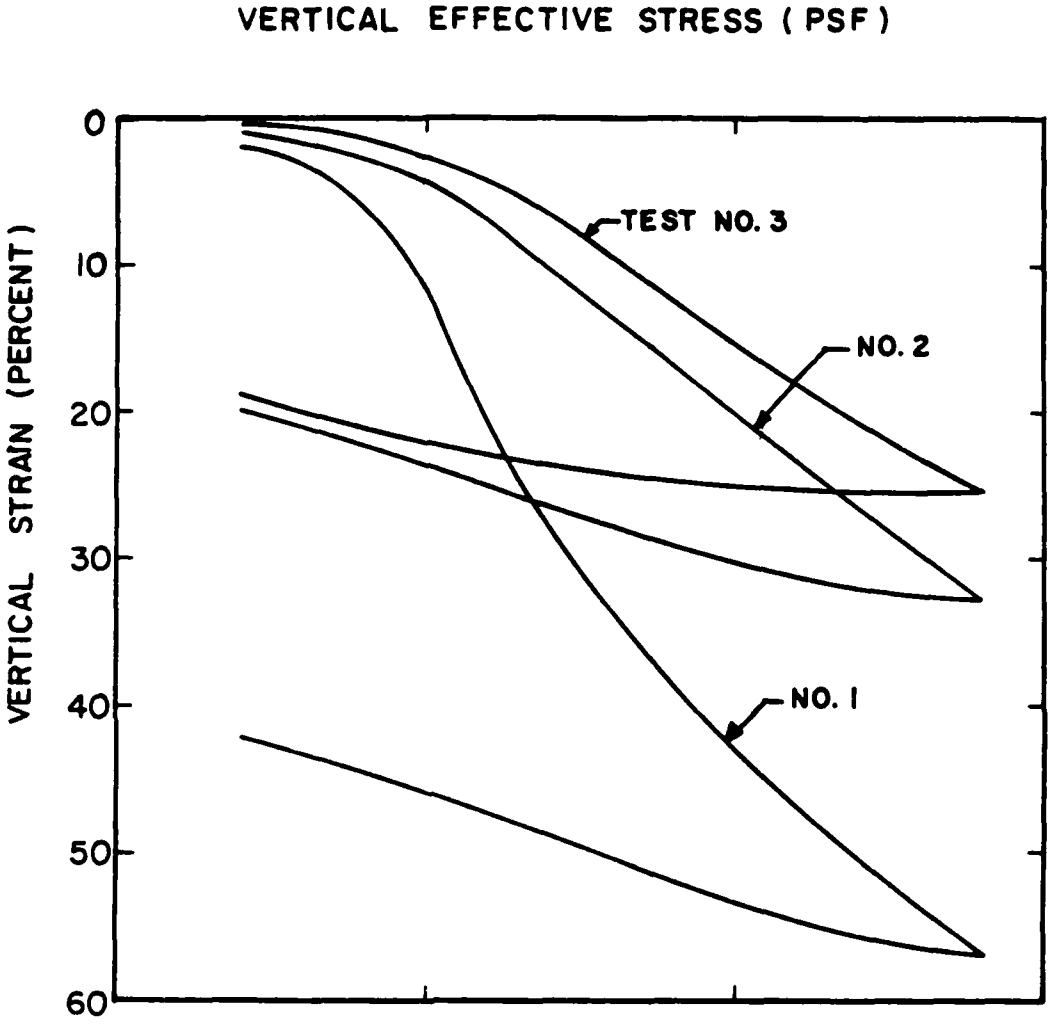

FIG. 7.24. Results of one-dimensional consolidation tests on Sabine soils

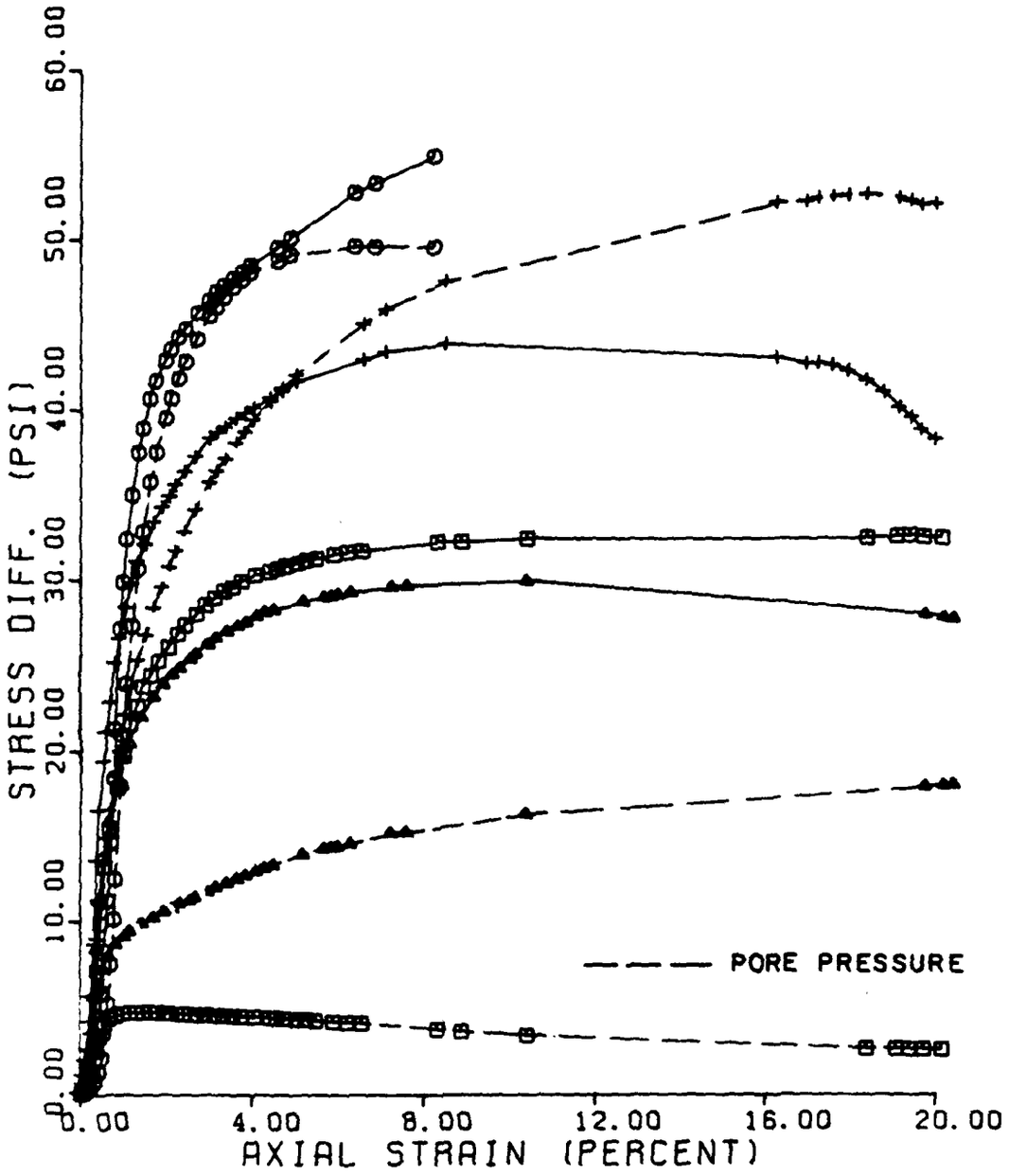

FIG. 7.25. Relationship of stress versus strain and pore pressure versus strain measured during static triaxial tests on Sabine soil

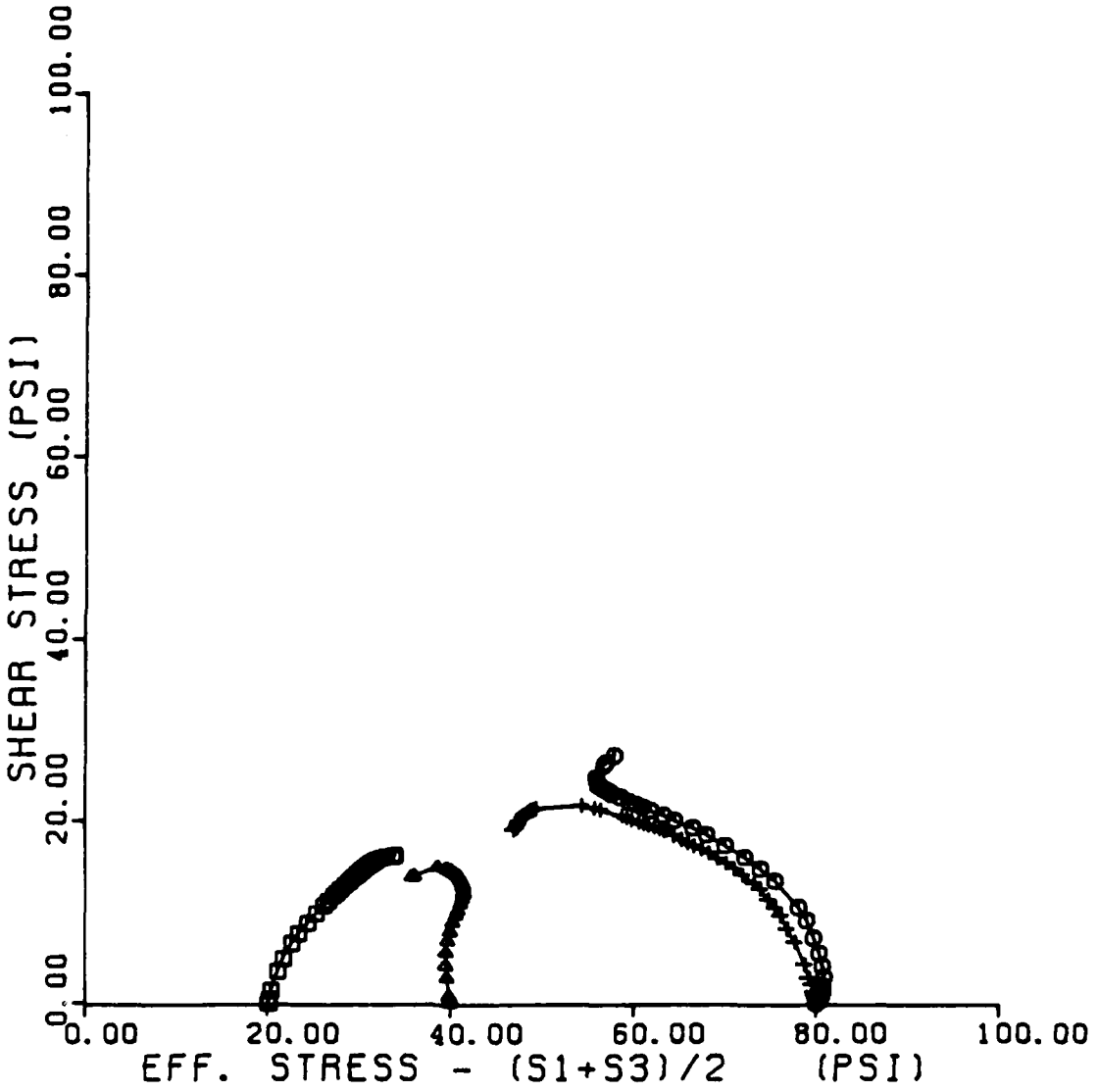

FIG. 7.26. Effective stress paths measured during triaxial tests on Sabine soil

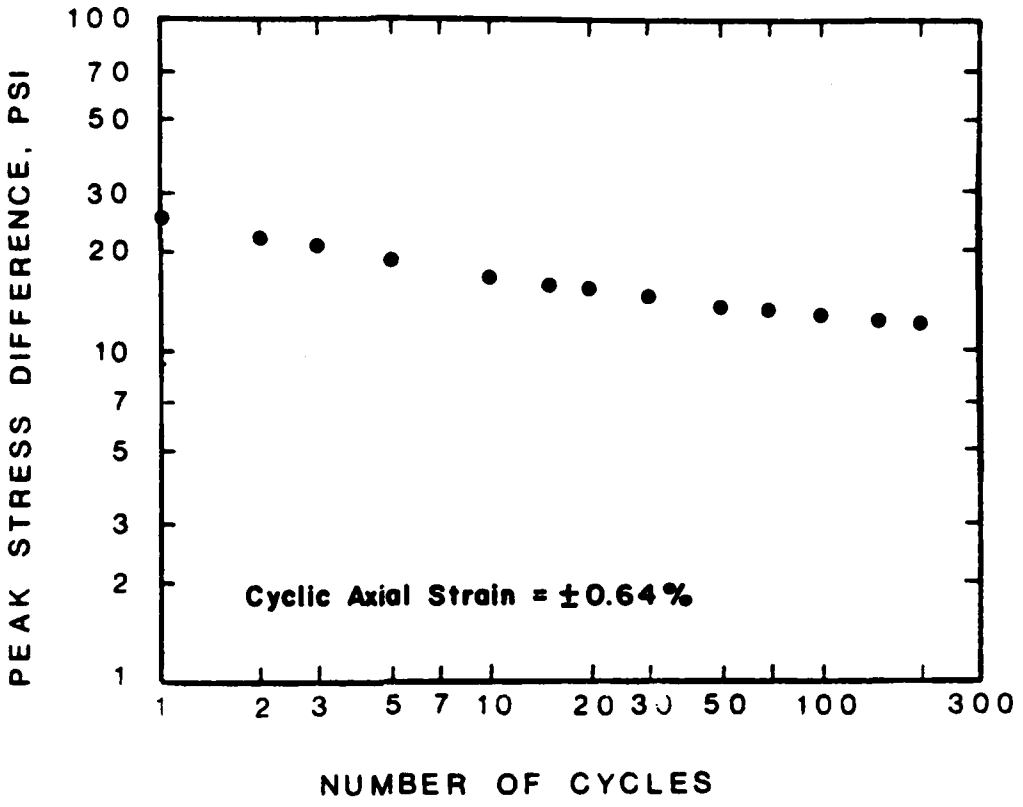

FIG. 7.27. Cyclic stress versus number of cycles for test 9, Sabine

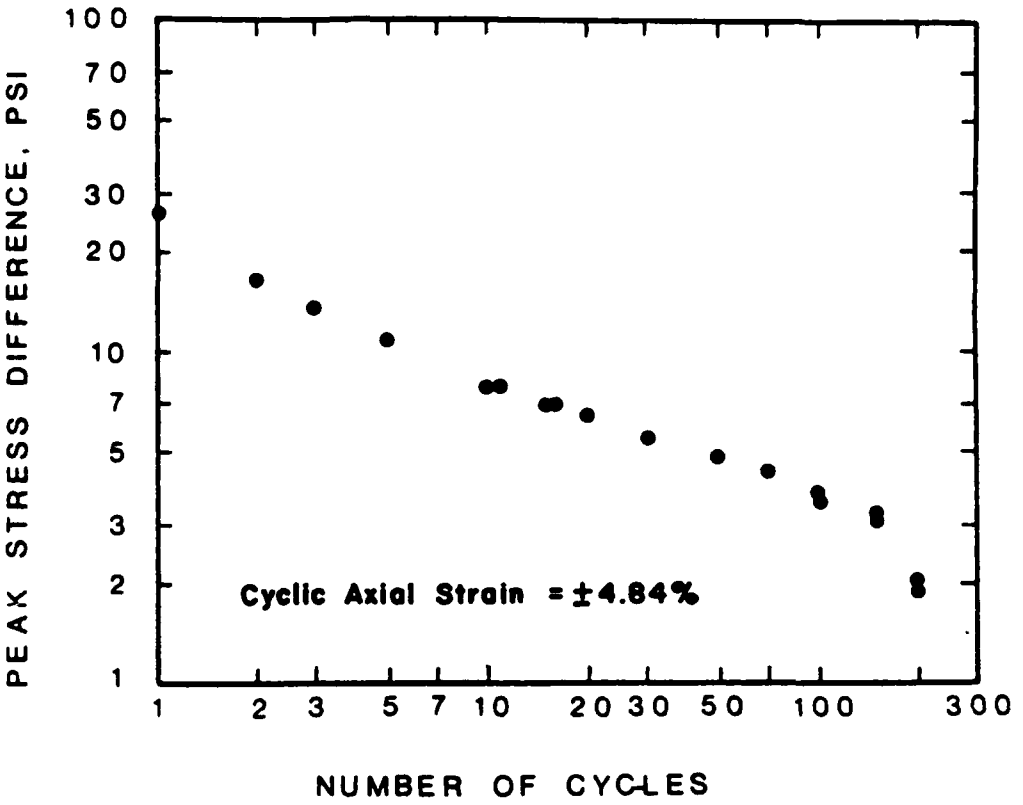

FIG. 7.28. Cyclic stress versus number of cycles for test 10, Sabine

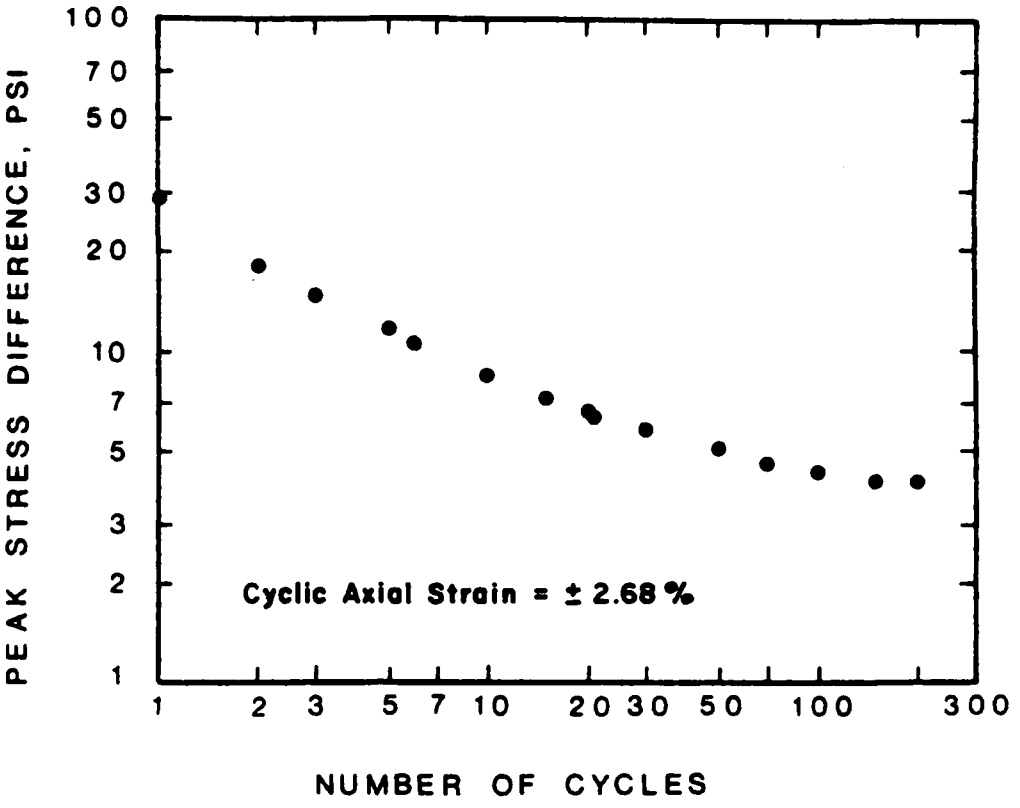

FIG. 7.29. Cyclic stress versus number of cycles for test 11, Sabine

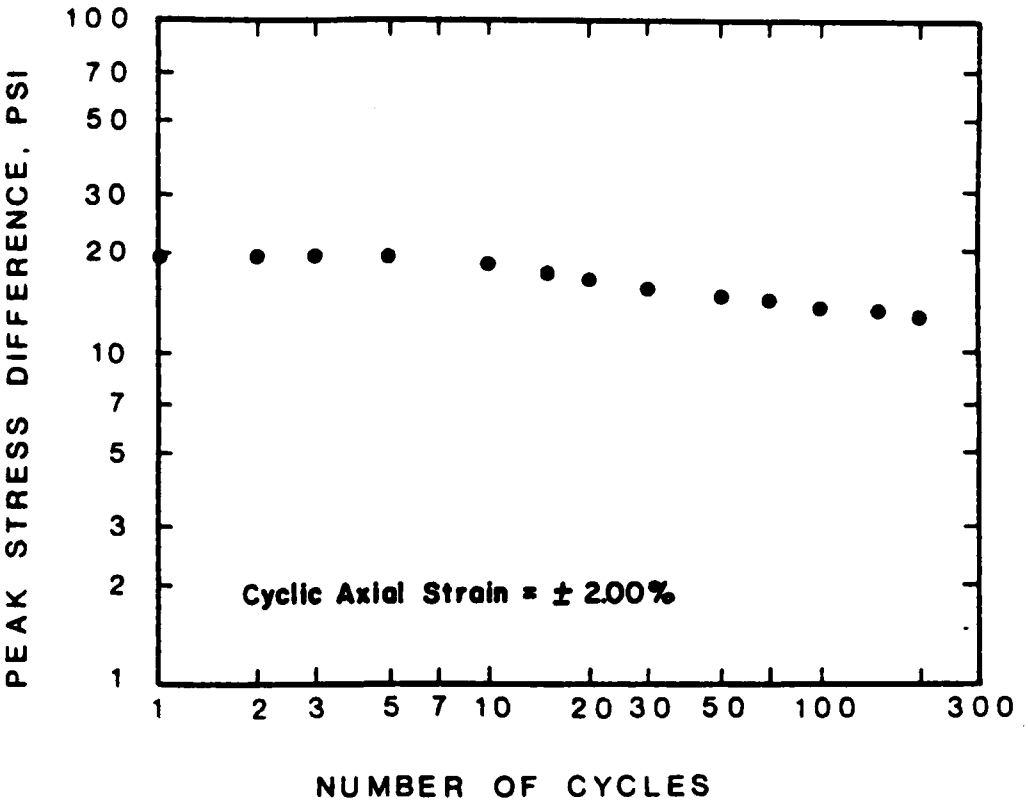

FIG. 7.30. Cyclic stress versus number of cycles for test 12, Sabine

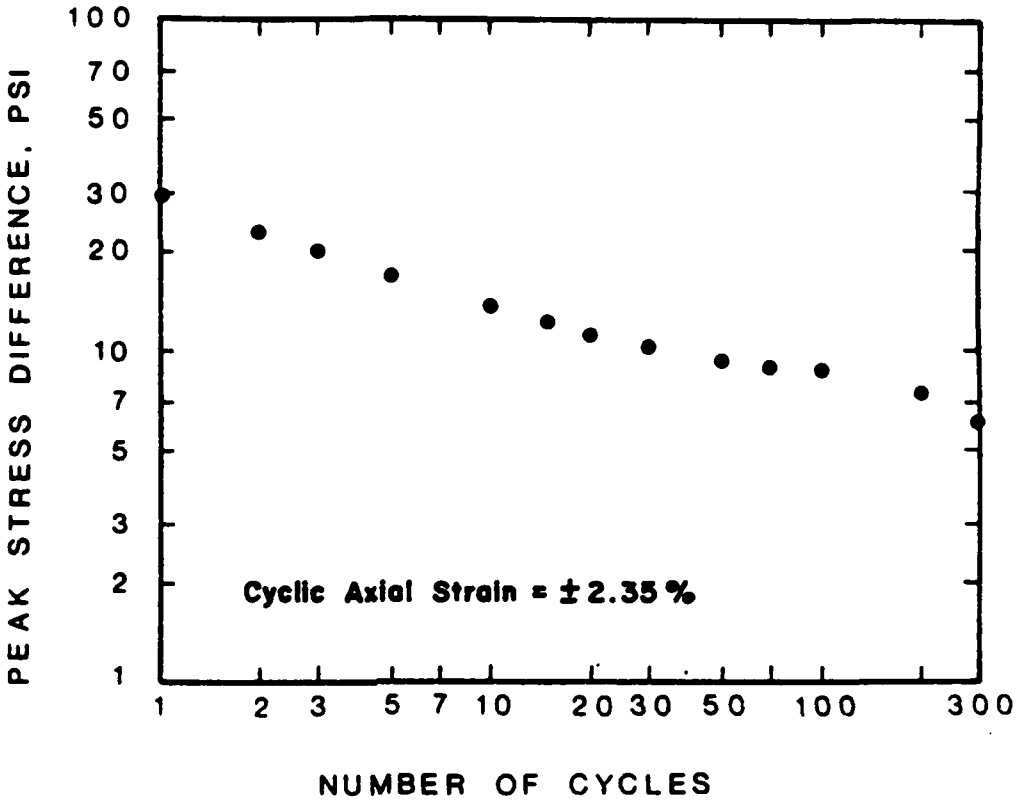

FIG. 7.31. Cyclic stress versus number of cycles for test 13, Sabine

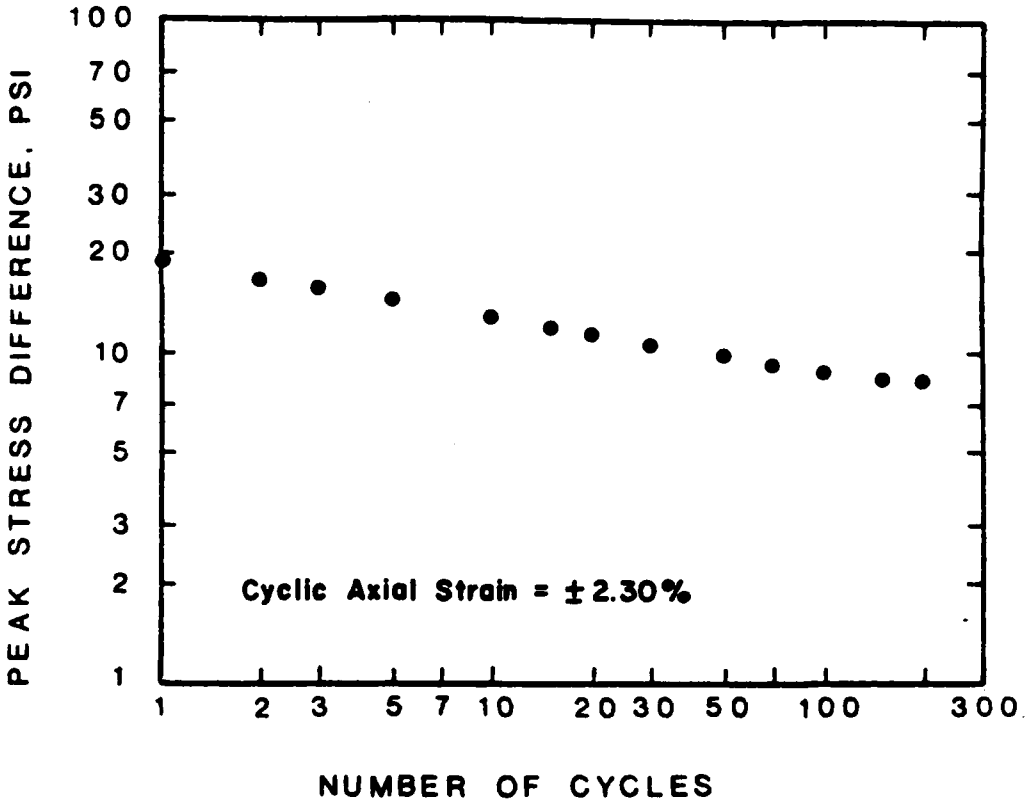

FIG. 7.32. Cyclic stress versus number of cycles for test 14, Sabine

ity formed by the pile consisted primarily of coarse sand. Gradually, the percentage of silt and clay sized particles increases with distance from the pile cavity. The thickness of this transitional layer was observed to be about one-half inch. It is expected that this veneer of coarse materials eventually forms a protective cover that prevents further significant scour of the soil and may therefore aid in reducing the amount of soil resistance lost due to the scouring action that may be present during cyclic loading.

Results of the pinhole-dispersion tests conducted on the soil from Sabine indicated the clay to be non-dispersive.

CHAPTER 8. EFFECT OF CYCLIC LOADING ON PILE BEHAVIOR

INTRODUCTION

Two methods to evaluate the effect of cyclic loading are presented herein. The first method utilizes the results of laboratory tests conducted on soil specimens obtained from two different sites. Results of cyclic triaxial tests and scour tests are compared and conclusions are made regarding their application to pile behavior measured during the field tests.

The other study of pile behavior uses the results of field tests more directly. This approach used the stiff clay (above the water table - awt) procedure as a basis for determining what steps were necessary to allow predicted and measured values of displacement to agree with each other.

ANALYSIS OF LABORATORY RESULTS

As mentioned in Chapter 6, cyclic triaxial tests and scour tests were performed on soils obtained from two sites in which field tests were conducted, namely, Manor and Sabine Pass, Texas. The results of these laboratory tests were presented in Chapter 7 and are summarized and compared with each other herein.

Cyclic-Triaxial Test Results

The behavior of soil subjected to cyclic loading is complex and difficult to model. Of major concern is the stress-strain behavior of the soil and how this relation is affected by the number of applications of load. One method of demonstrating the effect of cyclic loading is to plot the logarithm of the value of the secant modulus at N cycles versus the logarithm of the number of cycles. A straight line is often used to

approximate the relationship; therefore, a simple mathematical equation can be used and is as follows:

$$E_N = E_0 \cdot N^{-t}$$

where

E_N = Secant modulus at N cycles,

E_0 = secant modulus at first cycle,

N = number of cycles, and

t = degredation parameter (defined as the slope of the straight line relationship on the log-log plot described above.

The degredation parameter, t, can be used as a measure of the sensitivity of different soils to cyclic loading. As the value of t increases, the secant modulus decreases more rapidly with number of cycles. Thus, it is expected that results of laboratory tests yielding high values of t are representative of a soil more affected by cyclic loading than those test results on soils that yield low values of the degredation parameter. Idriss, et al (1978) first used this procedure to compare the results of controlled-strain, cyclic triaxial tests on different soft clay soils.

The above procedure was employed to compare the results of laboratory tests on the soils from Manor and Sabine, Texas. Shown in Figs. 8.1 and 8.2 are the values of the degredation parameter, t, versus the axial strain for cyclic loading for Manor and Sabine soils, respectively. For the soils obtained from Manor, the value of t is seen to increase with strain as shown in Fig. 8.1. Scatter of the data is certainly apparent; however, considering the fissured nature of the soil, scatter in the data should be anticipated.

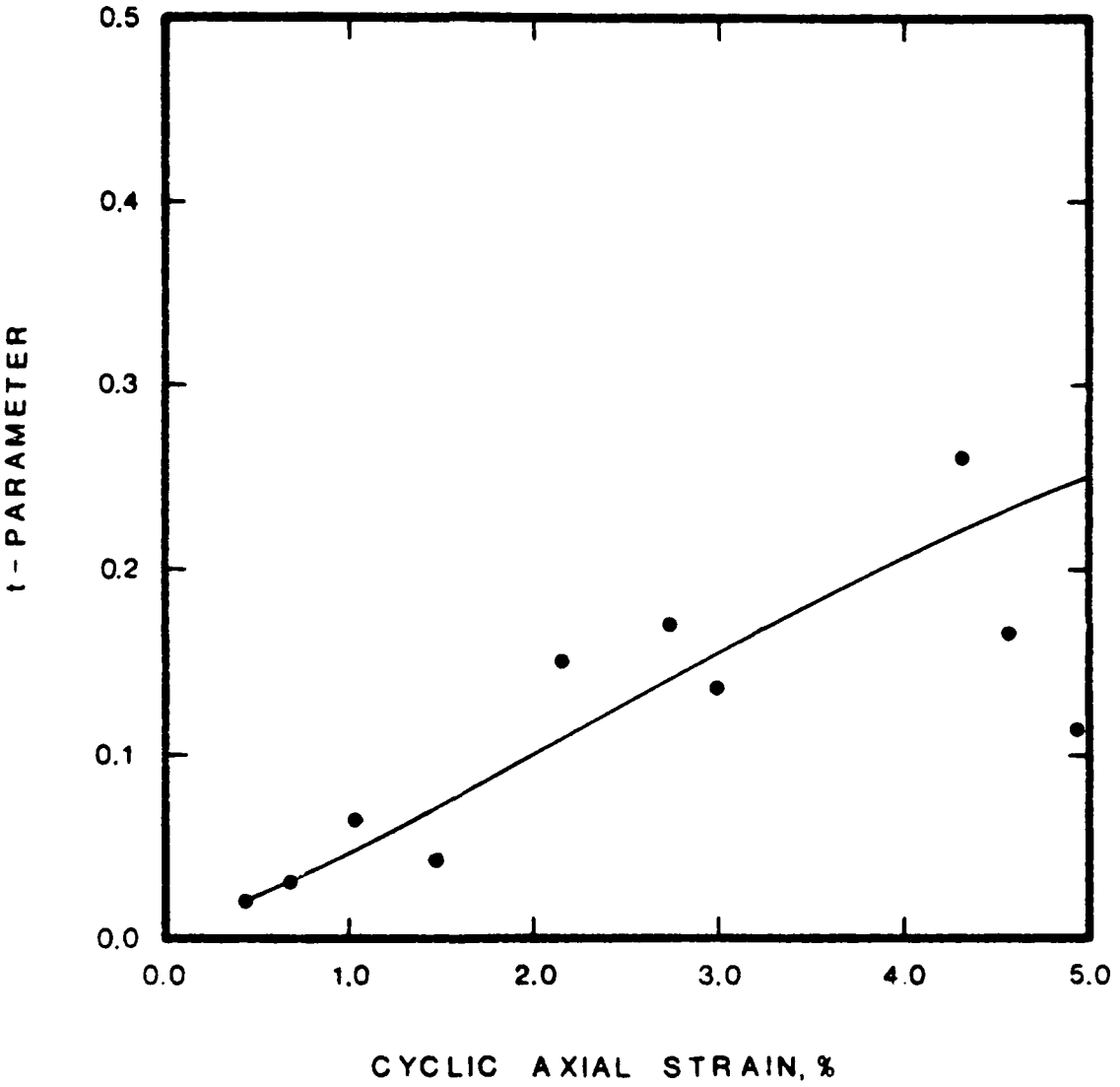

FIG. 8.1. t-parameter versus axial strain for cyclic loading for Manor soil

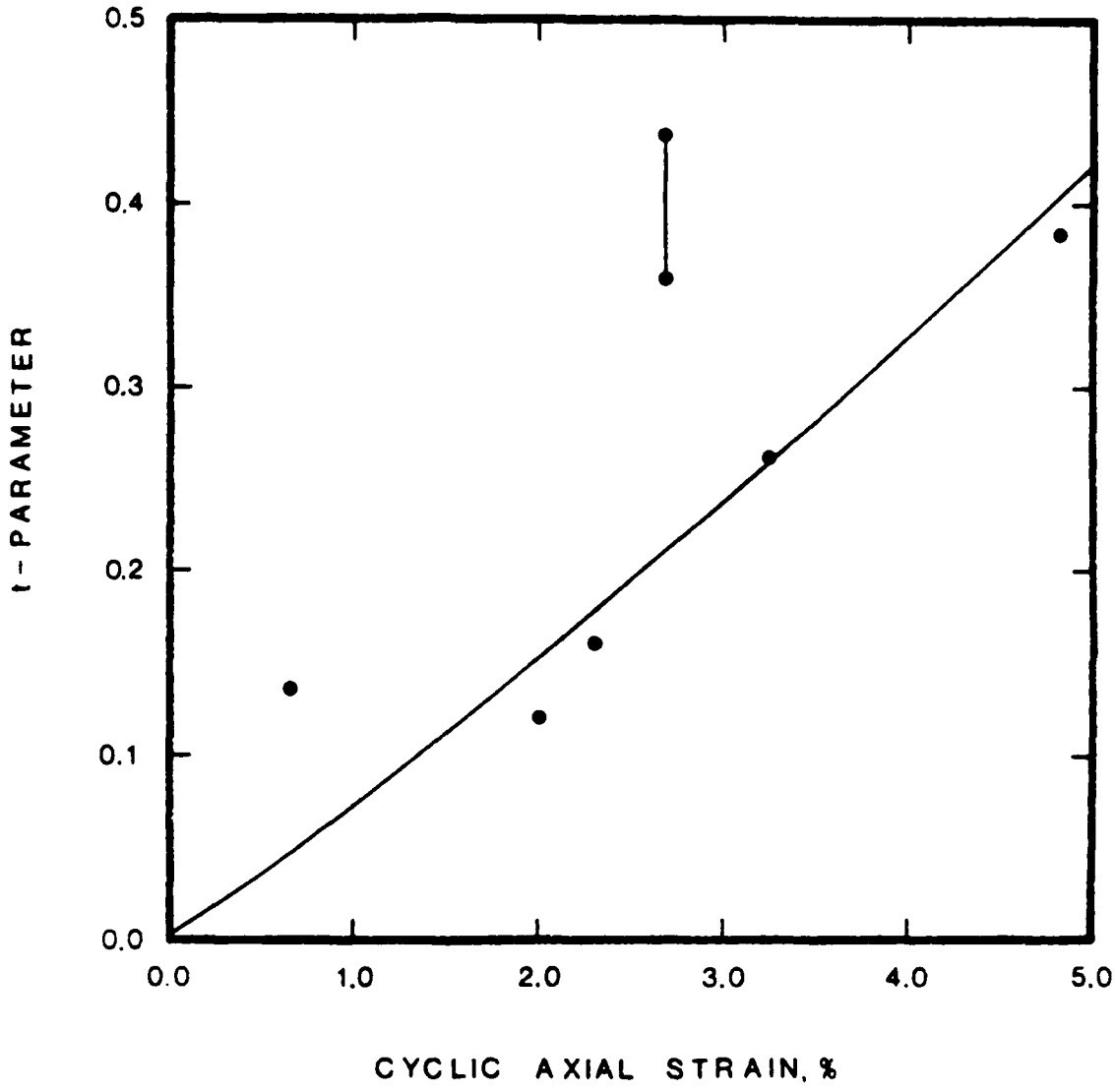

FIG. 8.2. t-parameter versus axial strain for cyclic loading for Sabine soil

Results of tests of soils from the Sabine area are shown in Fig. 8.2 and show the same trend of increasing value of t with increasing strain. By comparing the t versus strain for both Manor and Sabine soils, it can be seen that for a given value of strain, the value of t for the Sabine soil is slightly higher than the value of t for the Manor soil. Thus, based on results from the cyclic triaxial tests, it appears the Sabine soils show slightly higher rates of degredation due to cyclic loading than soils from the Manor site.

Scour Test Results

The soils from Manor and Sabine were subjected to laboratory tests designed to evaluate their susceptibility to scour or erosion. The procedure for the test is described in Chapter 6 and the results are presented in Chapter 7. The laboratory scour-test results yielded values of the scour index of 0.27 and 0.36 for the Manor and Sabine soils, respectively.

The scour index is a parameter that can be associated with degree of scour susceptibility. An increasing scour index indicates an increasing susceptibility of soil to scour. Thus, based strictly on the results of the laboratory tests to evaluate scour, the Sabine soils appear more susceptible to scour than do the soils from Manor.

However, as noted previously in Chapter 7, the soil from Sabine was found to form a layer of sand in the soil along the perimeter of the test rod. The sand could contribute significantly to reducing the effect of cyclic loading by forming a scour-resistant veneer, thus preventing any further erosion. It is unlikely that the rod test was fully effective in measuring quantitatively the influence of the sand particles in the Sabine clay. There were thin strata of sand at the Sabine site, in addition to sand particles in the clay. Thus, although the scour index of the Sabine

soil was measured to be greater than that of the Manor soil, factors such as the precise stratigraphy of the soil are important to consider.

Measured Degredation During Pile Load Tests

Strictly from the quantitative results of the cyclic triaxial tests and the scour tests, it appears that a larger effect of cyclic loading should be seen for the pile at Sabine than for the pile at Manor. However, the results of the field tests show that the opposite was true.

The two field tests were compared by using the stiff-clay (bwt) p-y criteria to analyze the Sabine test and the soft clay p-y criteria to analyze the Manor test. As shown in Fig. 5.12b, the predicted load-deflection curve for Sabine for cyclic loading above 4000 lbs shows much greater deflection than measured. As shown in Fig. 5.15a, the predicted load-deflection curve for Manor shows little effect of cyclic loading compared to the measured results. Thus, based on these results, it can be concluded that the pile-soil system near Manor, Texas was affected by cyclic loading to a greater extent than the pile-soil system located near Sabine.

The reasons why laboratory results indicate that the piles at the Sabine site should have exhibited more effect of cyclic loading than the piles located near Manor, and field tests indicate the opposite to be true, points to the need for consideration of other important factors. Several additional considerations can be proposed and include the following: 1) the scale of the laboratory triaxial tests were much smaller than experienced in the field, 2) the soils from Manor were observed to be fissured, and thus, scale should certainly be expected to have some effect on the soil behavior, and 3) the scale of the rod tests to measure scour potential was also small compared to the field tests. If the fissured

soil at the Manor site did break into small pieces during cyclic loading and then was scoured out by the water rushing in and out of the gap, and through the open fissures as was observed in the field tests, the process could not be accurately modelled by the small rod and small soil speciman used in the laboratory. These considerations are discussed in more detail later in this chapter.

Because the results of the laboratory tests indicated behavior opposite to the measured behavior, additional studies of all the case histories were undertaken to compare the behavior of piles tested in which water was above the ground surface with piles tested in which no water was above the ground surface.

STUDY OF CASE HISTORIES

In order to study and compare all of the case histories presented in Chapters 3 and 5, a consistent p-y criteria had to be selected. In each of the cases, the pile was subjected to cyclic loading; however, the number of cycles of load varied considerably. In some of the tests, only 15 cycles of load were applied, while others were subjected to 500 cycles or more. Both the soft clay and the stiff clay (bwt) p-y criteria have no provision for accounting for the number of load applications; however, the stiff clay (awt) criteria does allow for a different number of cycles. In addition, the "stress level" at which the cycling occurs can have an important effect as indicated by the parameter C_1 as described in Chapter 4. Using the stiff clay (awt) criteria, all the case histories could be analyzed on the same basis, and the effect of cyclic loading could be accounted for in a consistent manner.

In performing the analysis for each case history, a specific procedure was followed. First, the measured static relationship of load versus deflection was modelled using the stiff clay (awt) criteria, and values of shear strength were adjusted until a favorable comparison was obtained between prediction and measurement. Then, the value of C_1 was varied until the predicted cyclic deflection of the pile equalled the measured cyclic deflection of the pile at the proper number of cycles of loading.

The results from the above procedure showed considerable variation in the value of C_1 required to explain the effect of cyclic loading measured in each case history. Shown in Figs. 8.3 and 8.4 for each history are the values of C_1 versus the shear strength of the soil, and the value of C_1 versus the liquidity index of the soil. In Fig. 8.3, there seems to be no consistent trend of C_1 as a function of undrained shear strength. Plots of C_1 versus pile diameter, C_1 versus ε_{50} of the soil, and C_1 versus deflection were also made; however, scatter was observed to be about the same as presented in Fig. 8.3.

However, one consistent trend is apparent. For case histories in which pile tests were conducted under conditions of a free water surface above the ground surface, much greater values of C_1 were required to fit the measured cyclic behavior.

Presented in Fig. 8.4 are the values of C_1 versus the liquidity index of the soil. Although there appears to be some trend of decreasing values of C_1 with increasing values of liquidity index, conclusions regarding this trend should be considered guarded due to the small amount of data, and the apparent scatter of the data points.

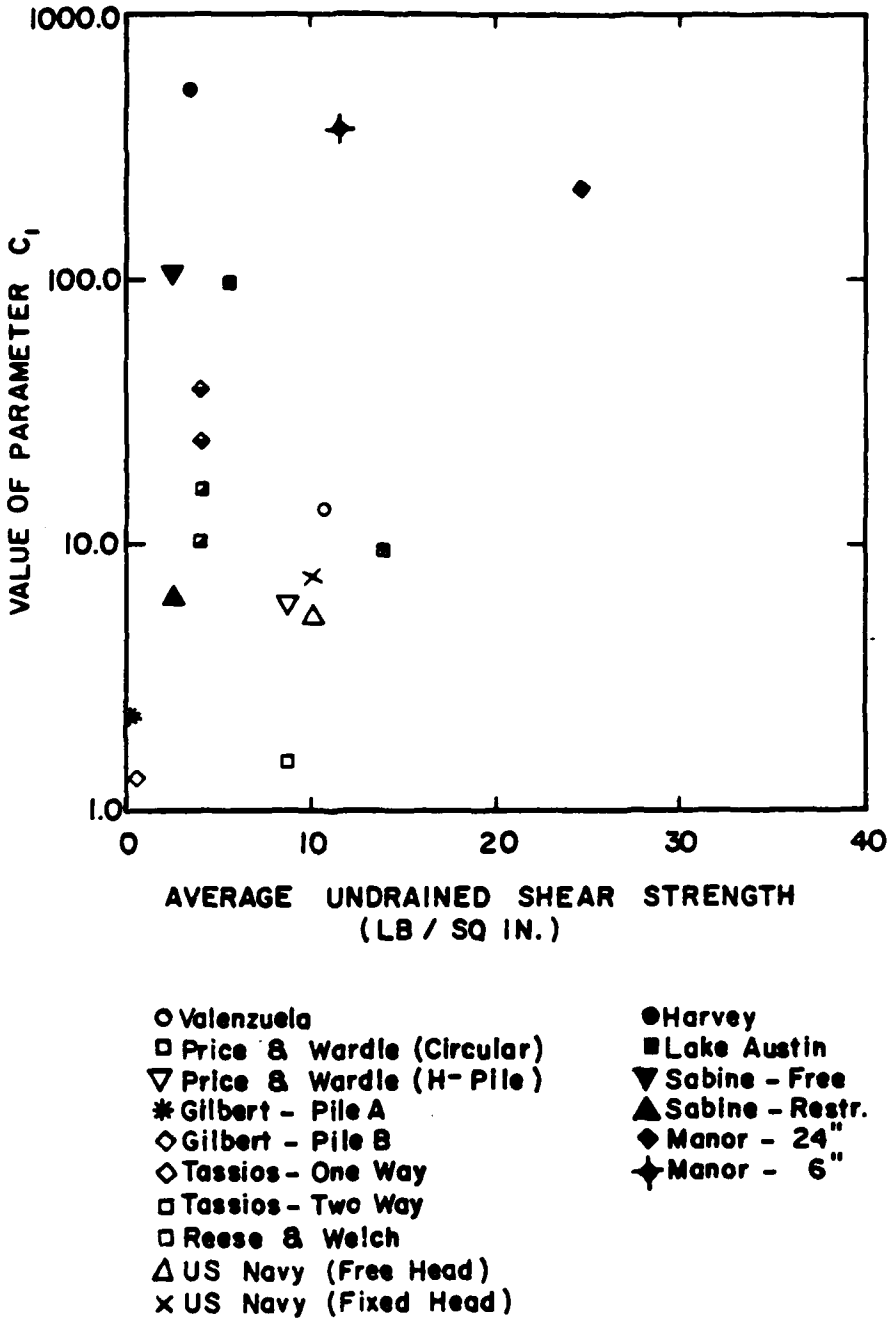

FIG. 8.3. Value of C_1 versus undrained shear strength

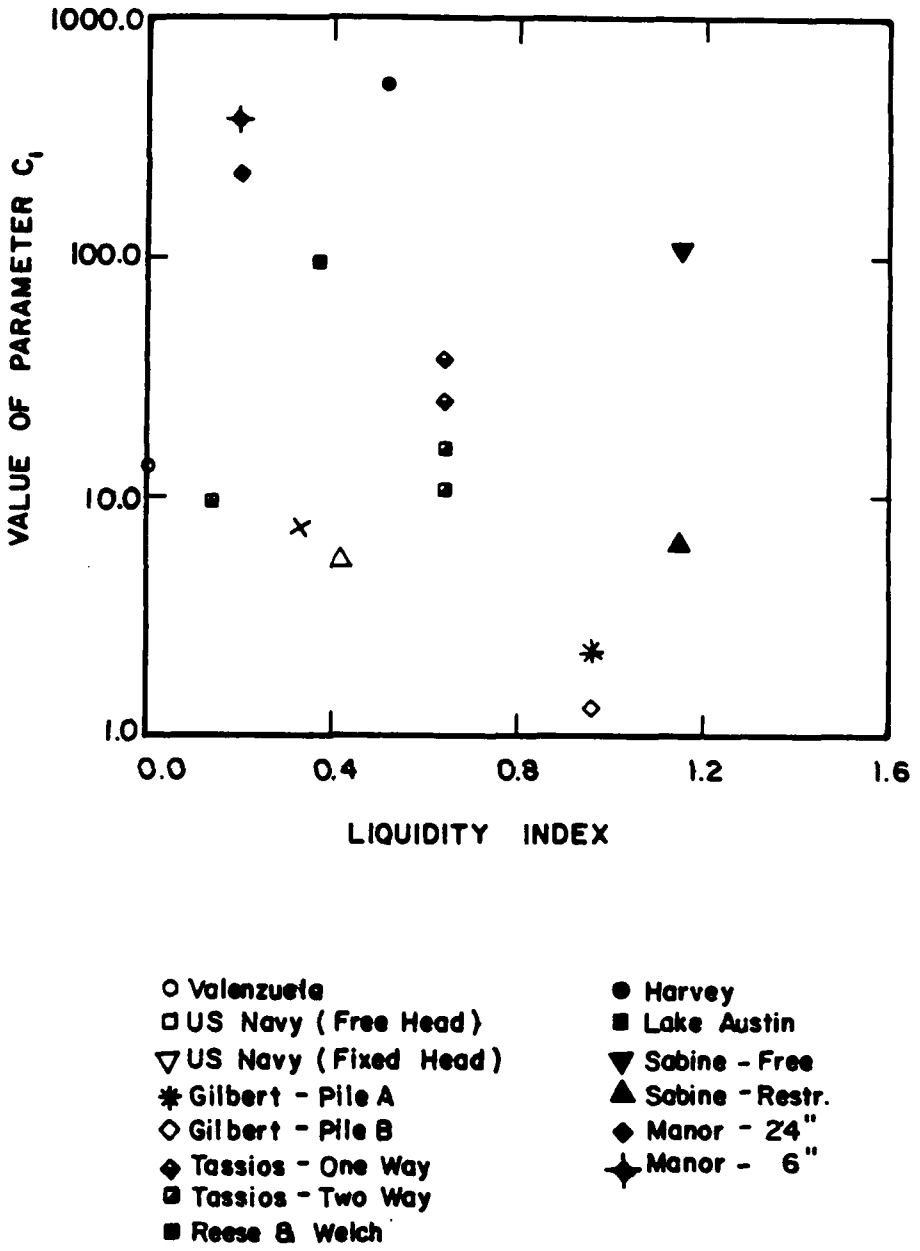

FIG. 8.4. Value of C_1 versus liquidity index of soil

SUMMARY DISCUSSION OF RESULTS

The studies described herein were designed to shed light on the processes involved in the significant, and sometimes severe, loss of soil resistance coincident with the cyclic loading of piles in clay at offshore sites. At the outset of the studies there was some reason to think that the proposed studies could be employed to explain quantitatively the field results where full-scale piles in clay were loaded cyclically. While the detailed analyses that are presented in this Chapter were unable to achieve a complete explanation of the observed field behavior of the test piles, the data that have been obtained in the laboratory do help in identifying the importance of certain parameters and in providing guidance for further research. The following discussion serves to illustrate the significance of the findings from the present studies.

Example Computations

Figure 8.5 shows an offshore pile that has been installed in either soil like the site at Manor or at Sabine. A 24-in. OD pile has been selected for purposes of illustration. Figure 8.6 a shows computed p-y curves for the two cases employing the criteria developed from the Manor tests for both static and cyclic loading and Fig. 8.7 shows the same computations for the Sabine site. The depths selected for the curves were 0, 1, 2, 4, and 8 diameters or 0, 2, 4, 8, and 16 ft. For the Manor site, p-y curves at the ground surface were not plotted because soil resistance is predicted to be zero at all values of deflection. Studies of the behavior of piles under lateral loading show that the response of a pile is dependent strongly on the soils near the ground surface, a factor that determined the depths that were selected.

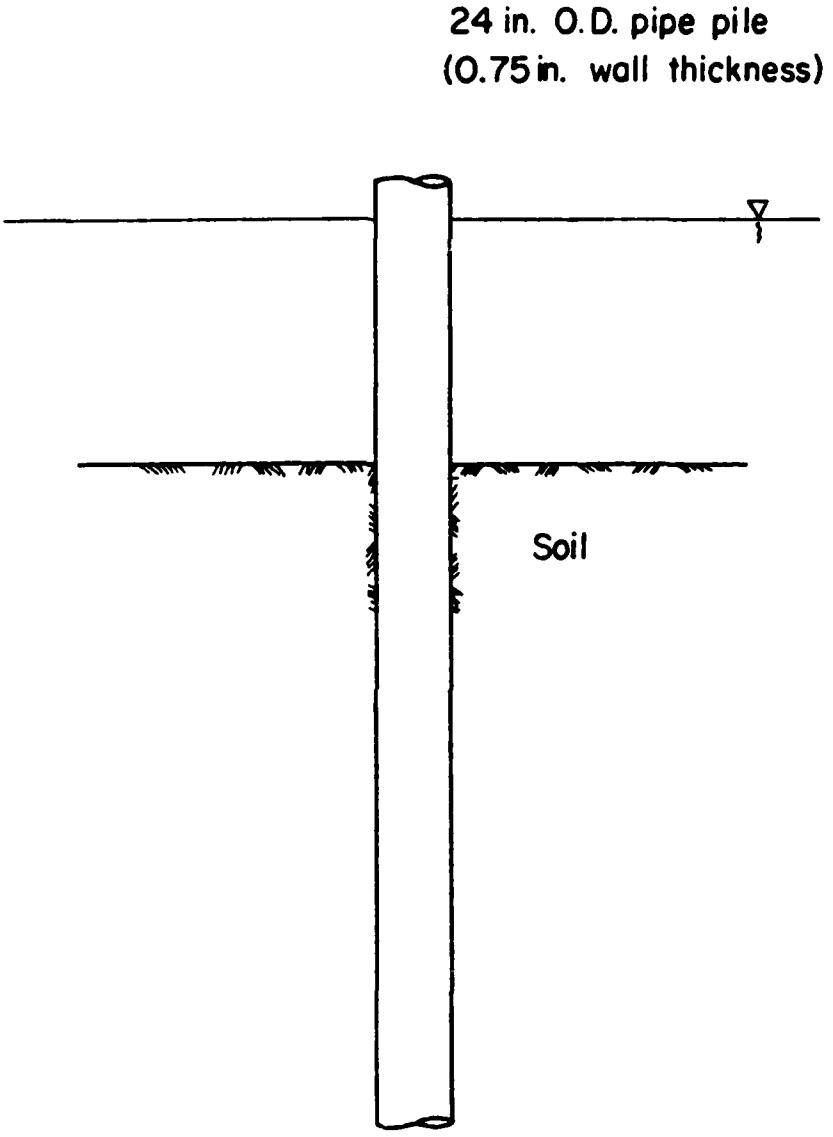

FIG. 8.5. Example submerged pile in cohesive soil

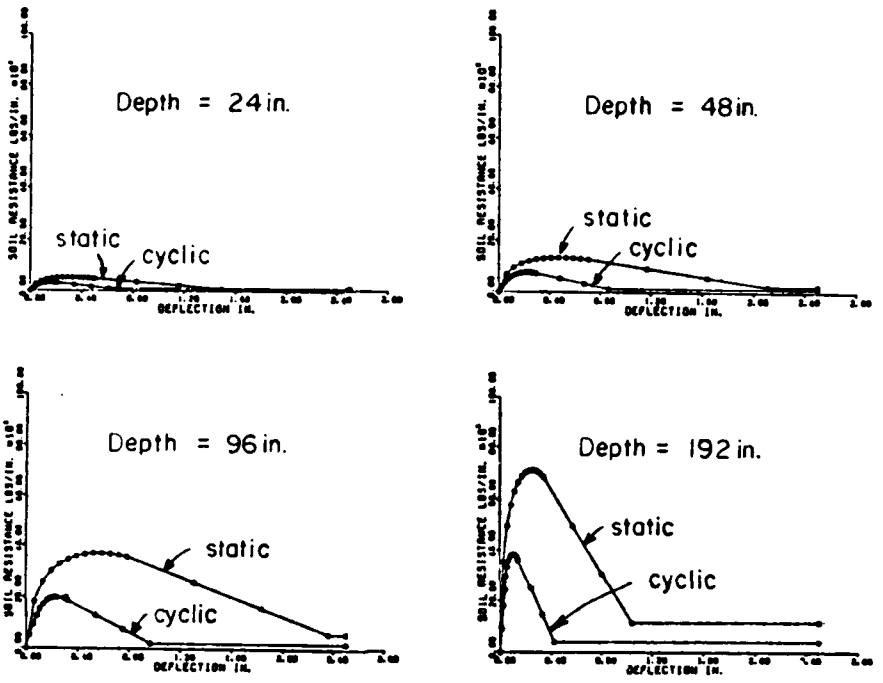

FIG. 8.6. Calculated p-y curves for example pile in Manor soil

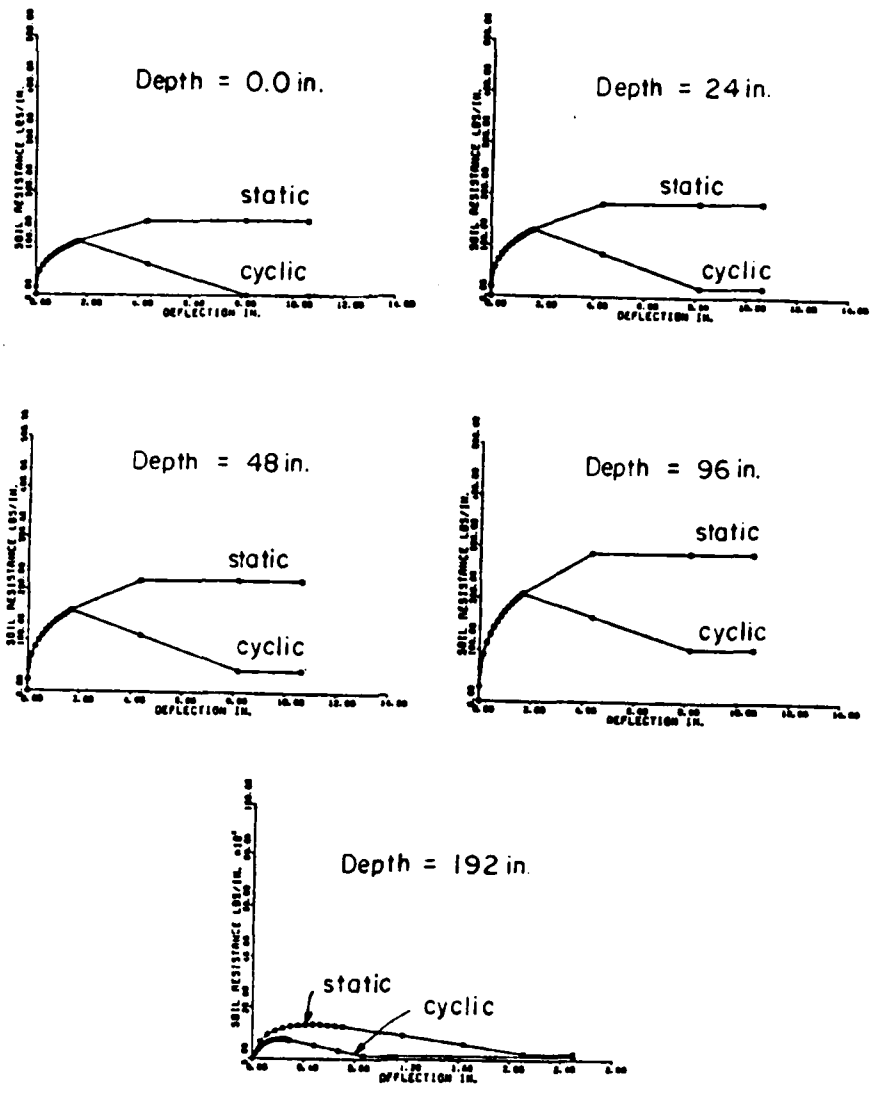

FIG. 8.7. Calculated p-y curves for example pile in Sabine soil

To indicate the importance of the surface soils, the deflected shape of the pile was computed on the assumption that the piles were subjected to cyclic loading, that the pile head was fixed againt rotation, and that a bending stress of 20 kips/sq in. was the maximum that could be sustained.

Influence of Cyclic Strain

In order to determine the influence of cyclic deflections of the pile upon the resistance provided by the soil mass, a study was conducted to compare the amount of reduction predicted using the current soft clay and stiff clay (bwt) p-y procedures with the amount of reduction predicted using the results of the cyclic triaxial tests conducted on the soils located near Sabine and Manor.

Shown by solid lines drawn in Figs. 8.8a through 8.8e and Figs. 8.9a through 8.9d are the relationships between deflection and loss of resistance determined for the soils located near Sabine and Manor, respectively. This relationship was computed by selecting a specific deflection, and then comparing the static and cyclic values of soil resistance predicted using the appropriate p-y analysis. The amount of reduction in soil resistance is defined as follows:

$$R = 1 - P_c/P_s$$

where

R = reduction in soil resistance,

P_c = value of p (lb/in.) predicted for cyclic loading, and

P_s = value of p (lb/in.) predicted for static loading.

As can be seen, at smaller deflections, no loss of resistance is observed (where the static and cyclic p-y curves coincide); however, the

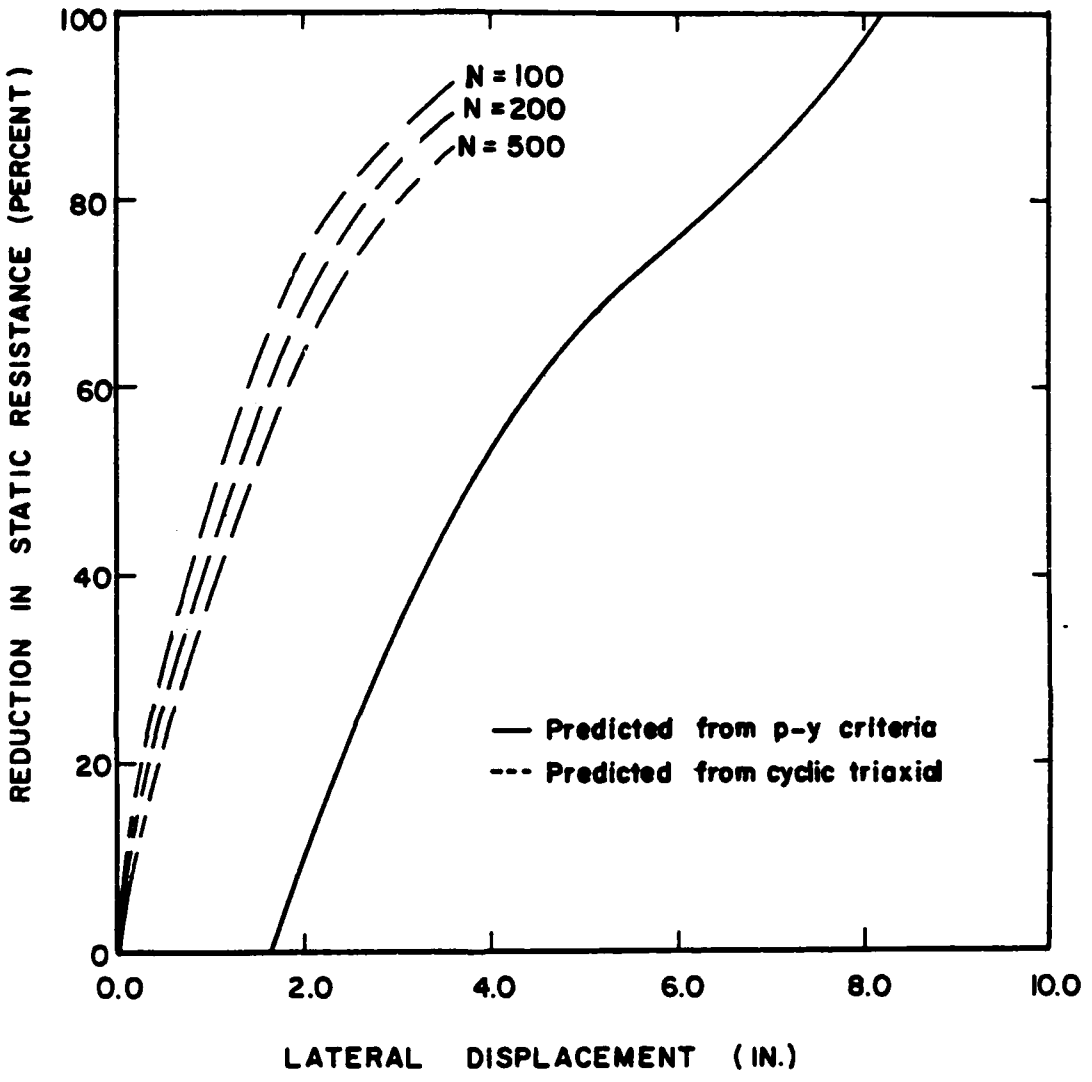

FIG. 8.8a. Reduction of static resistance versus lateral displacement for Sabine soil at ground surface

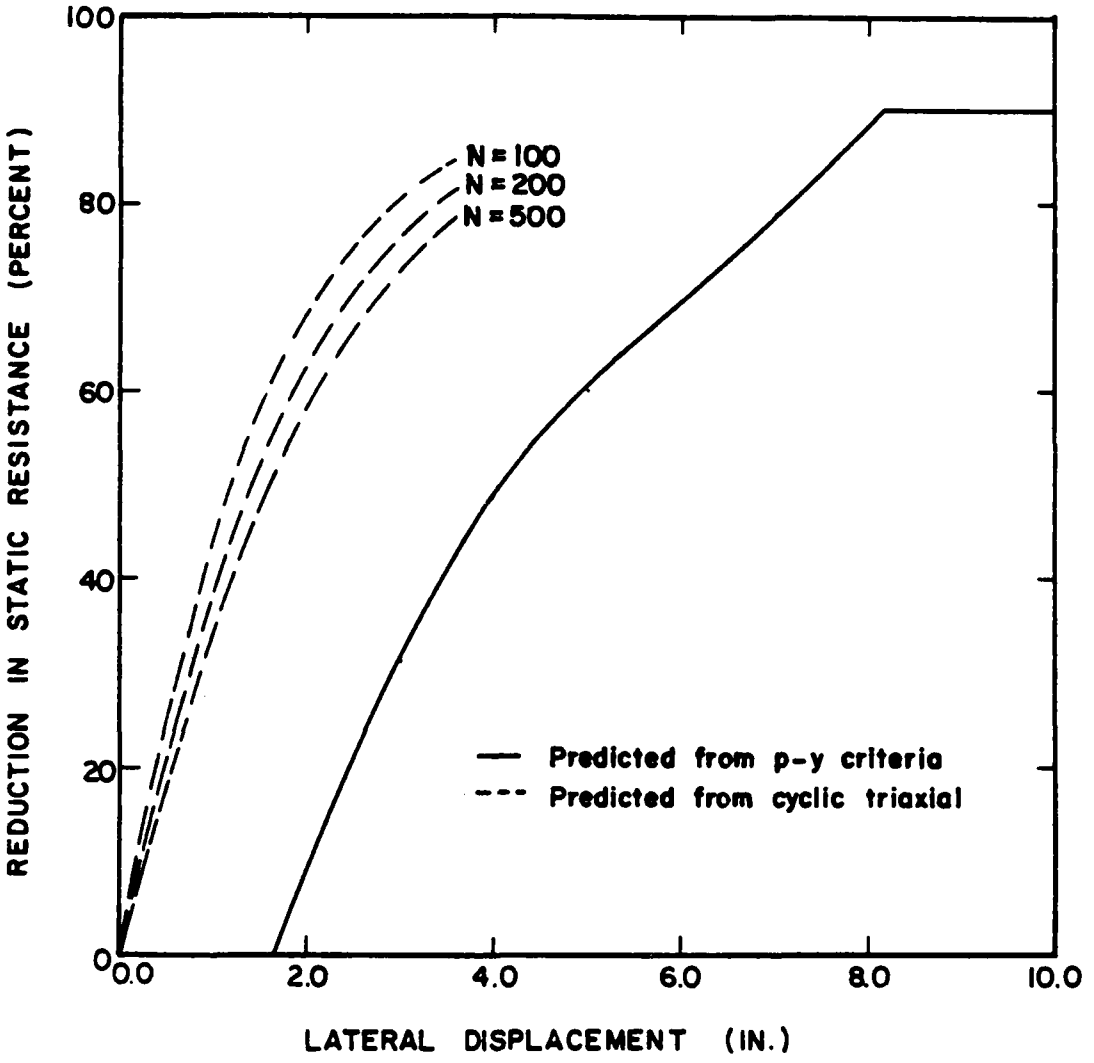

FIG. 8.8b. Reduction of static resistance versus lateral displacement for Sabine soil at a depth of 24 in.

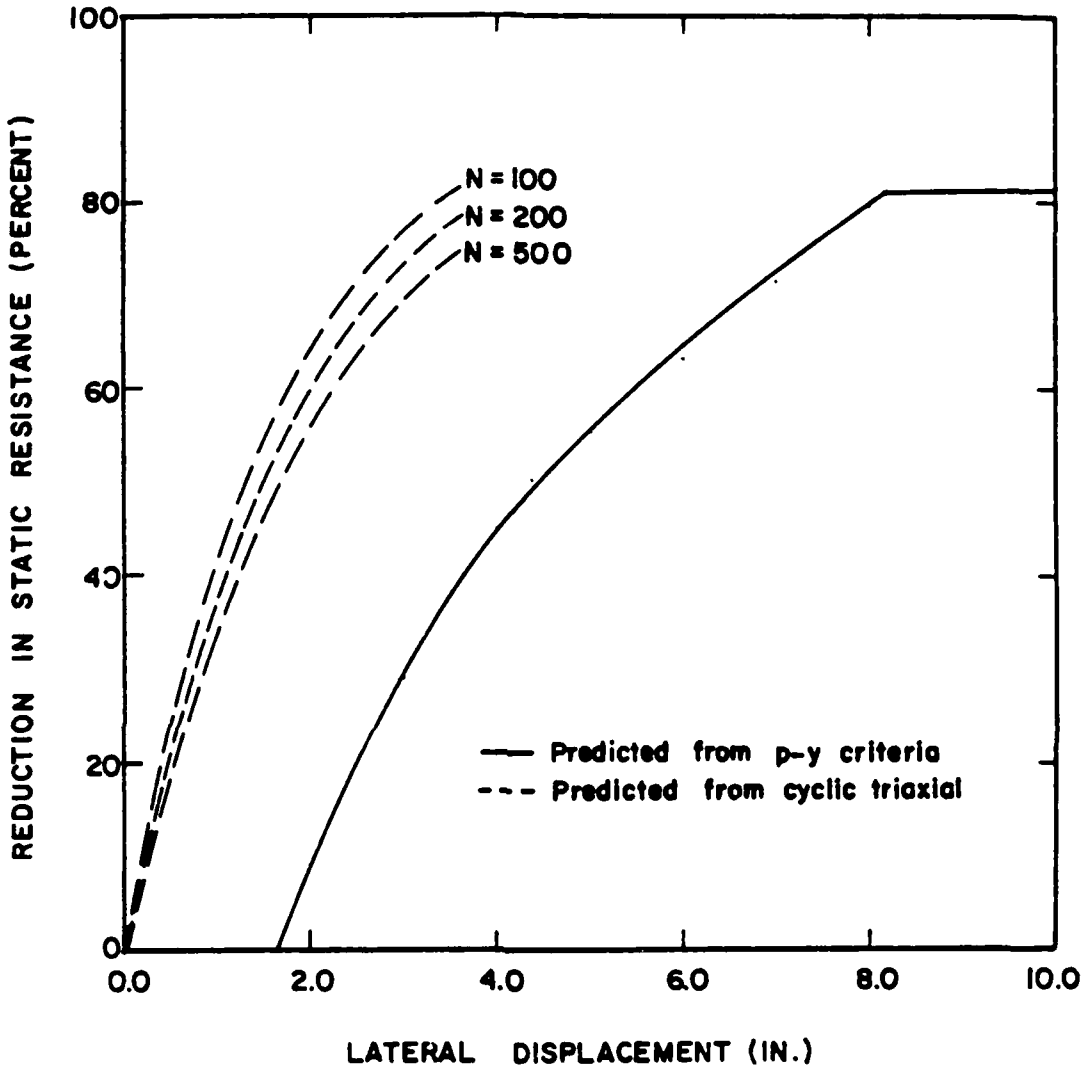

FIG. 8.8c. Reduction of static resistance versus lateral displacement for Sabine soil at a depth of 48 in.

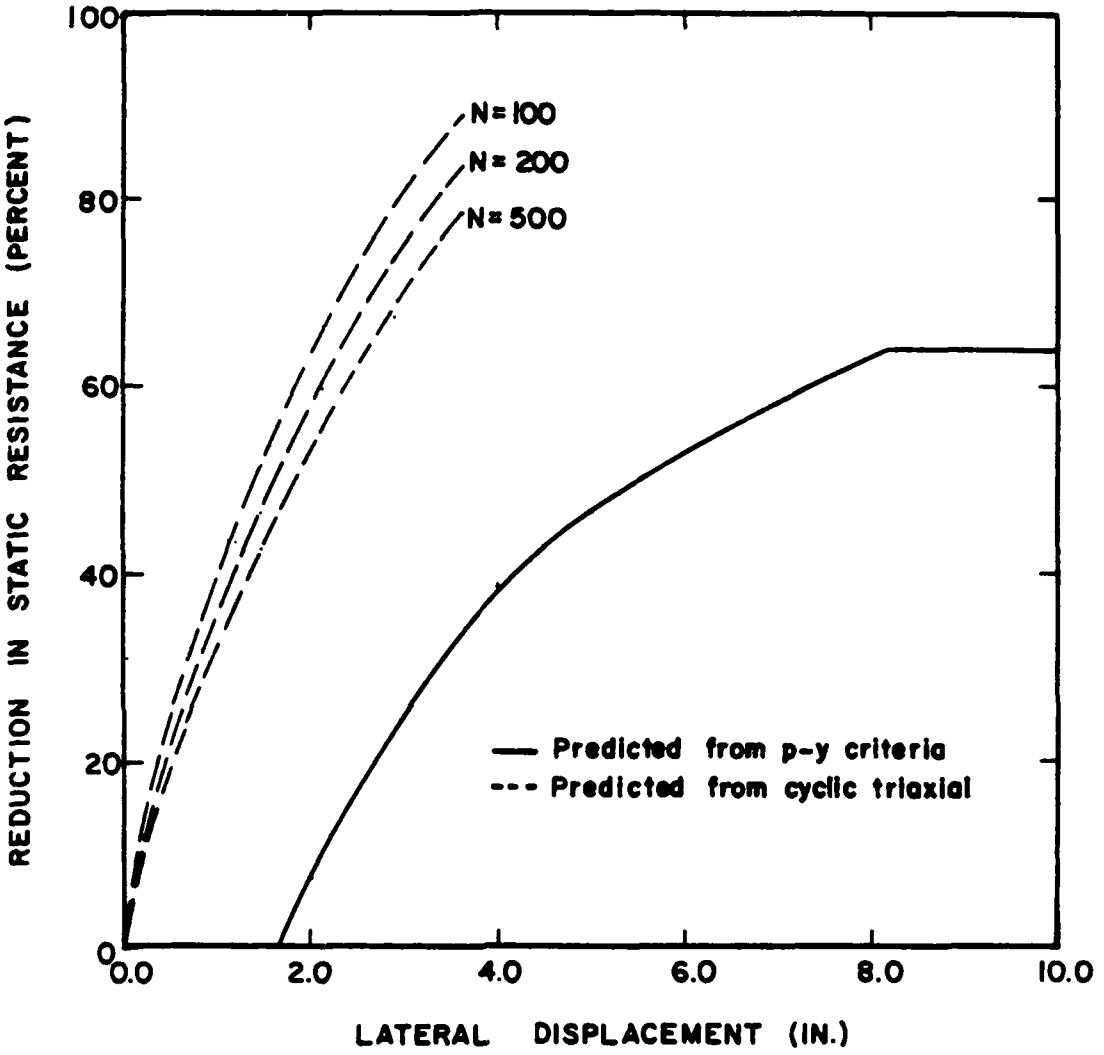

FIG. 8.8d. Reduction of static resistance versus lateral displacement for Sabine soil at a depth of 96 in.

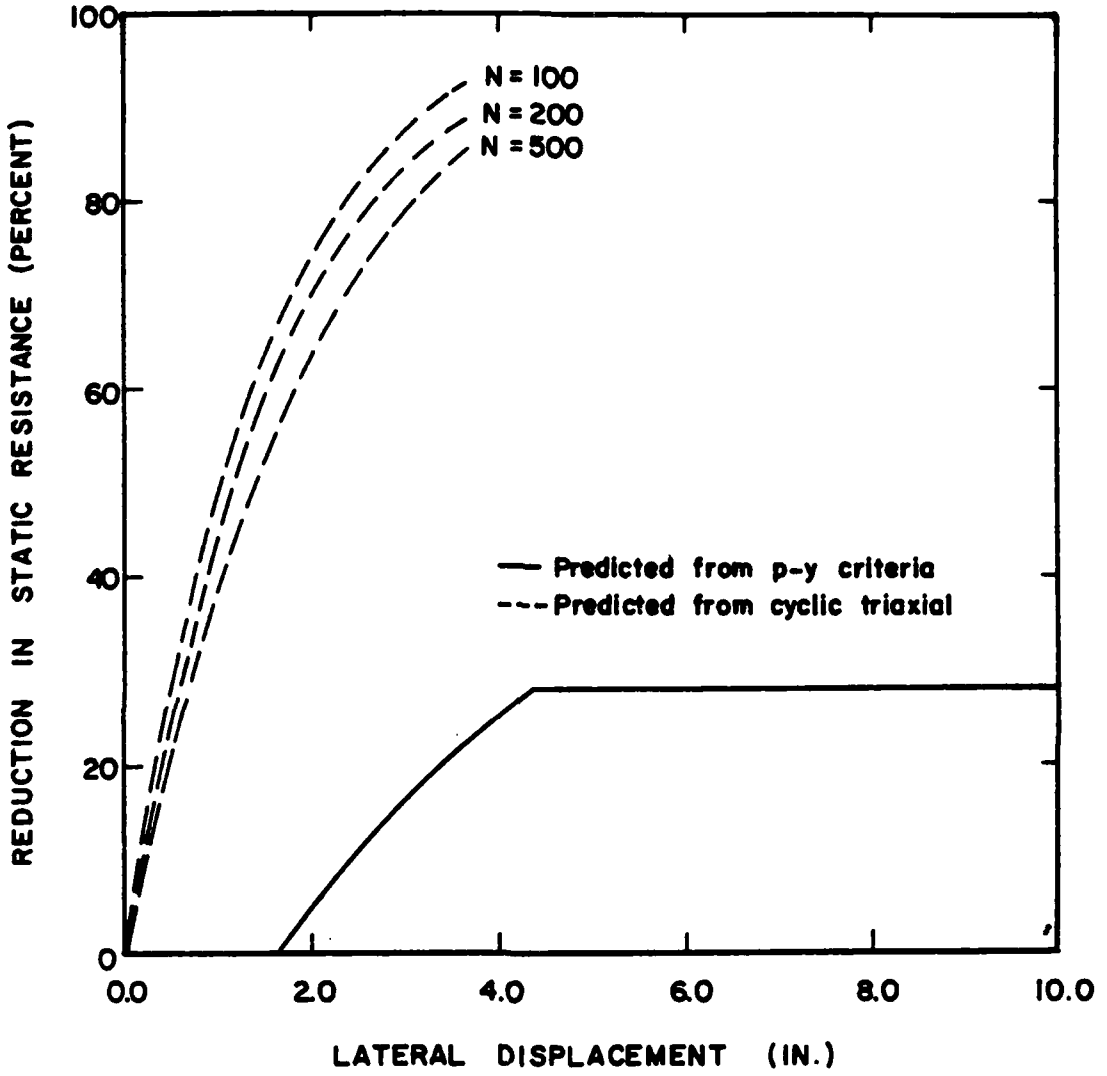

FIG. 8.8e. Reduction of static resistance versus lateral displacement for Sabine soil at a depth of 192 in.

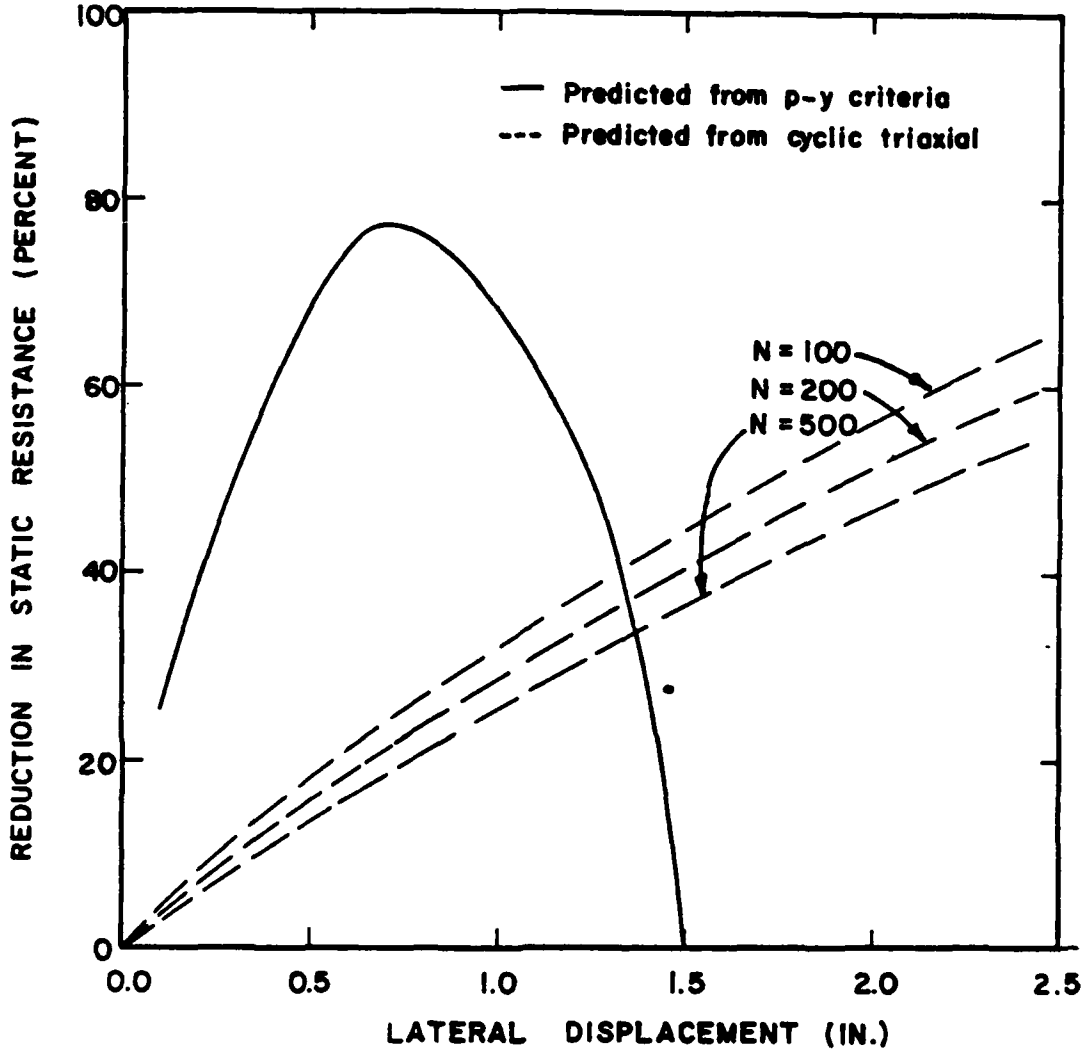

FIG. 8.9a. Reduction of static resistance versus lateral displacement for Manor soil at a depth of 24 in.

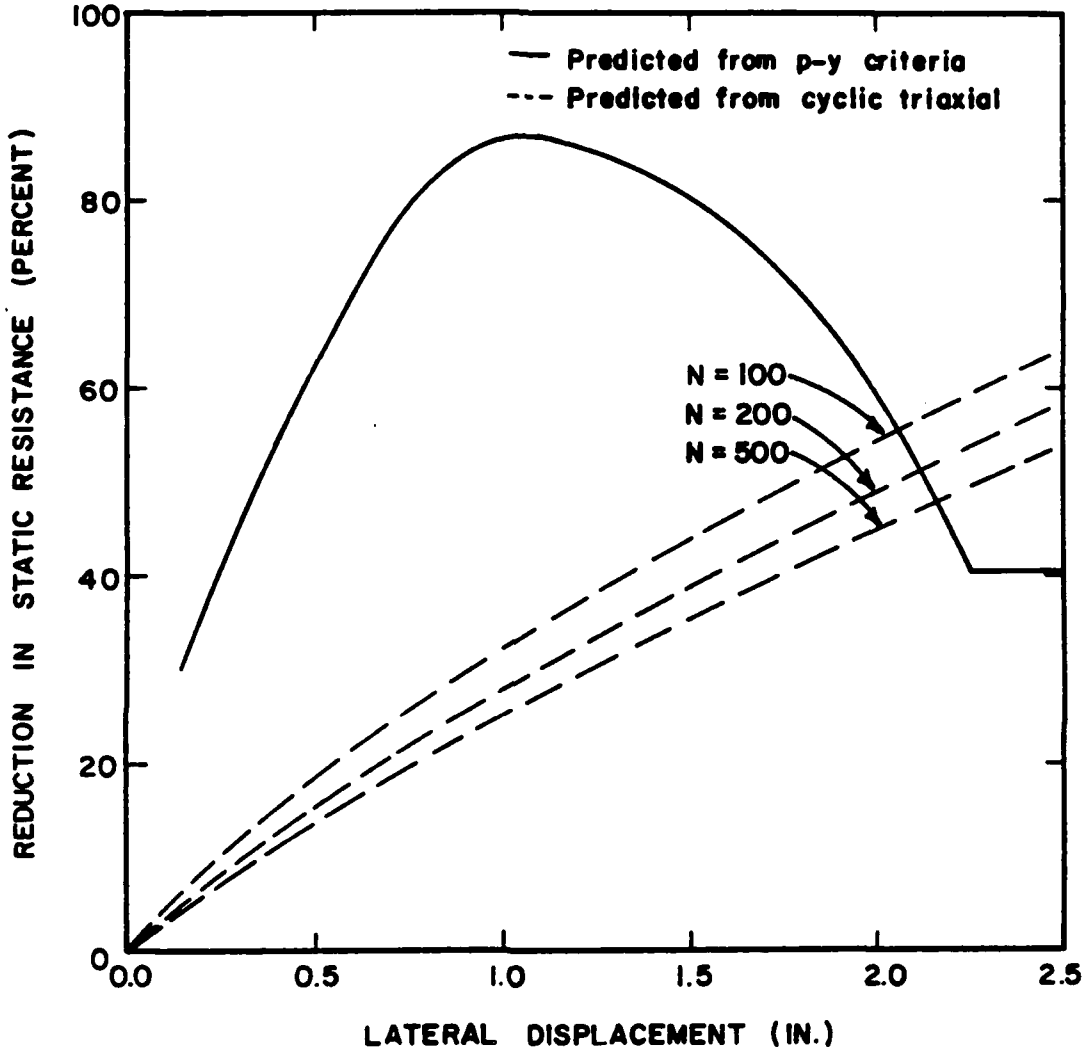

FIG. 8.9b. Reduction of static soil resistance versus lateral displacement for Manor soil at a depth of 48 in.

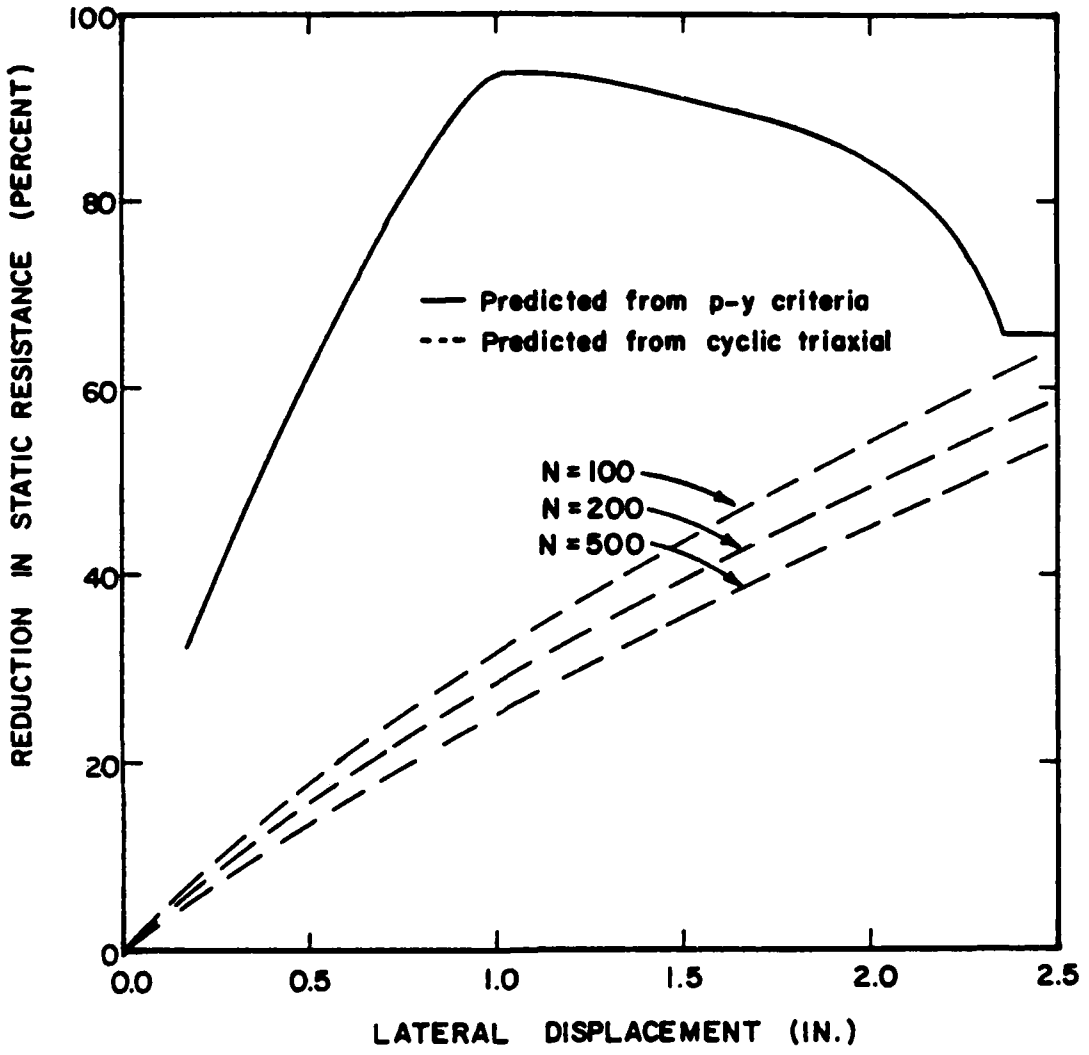

FIG. 8.9c. Reduction of static soil resistance versus lateral displacement for Manor soil at a depth of 96 in.

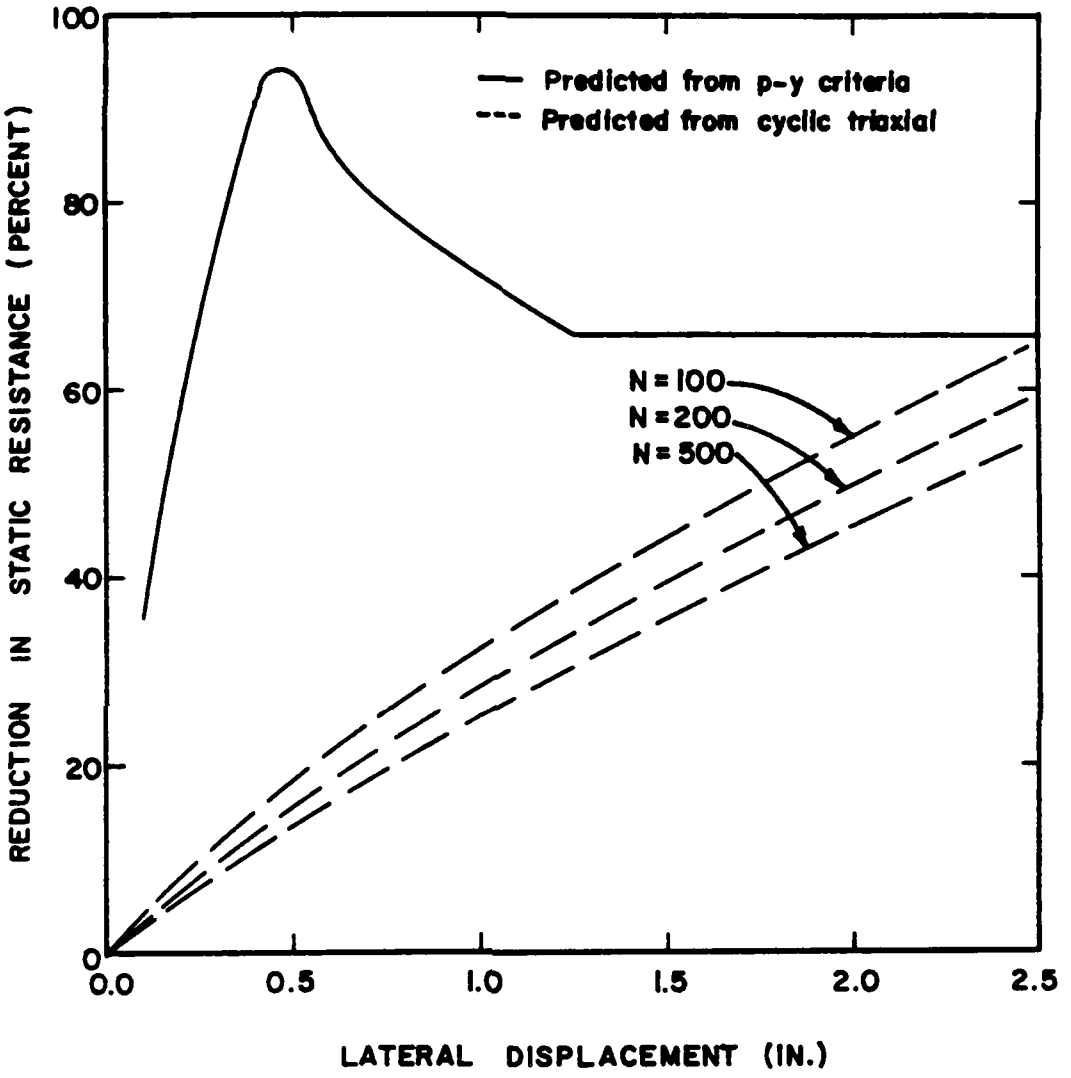

FIG. 8.9d. Reduction of static resistance versus lateral displacement for Manor soil at a depth of 192 in.

loss of resistance increases with deflection and may reach a value of 100 percent depending on the deflection and depth.

In order to compare the amount of reduction predicted using the results of the cyclic triaxial tests, the following procedure was adopted. Firstly, cyclic strains were calculated by taking 1/3 of the pile deflection divided by the diameter. This factor is an approximation based on preliminary finite element calculations and was reported by Poulos (1983). Secondly, the amount of reduction in soil resistance was predicted using the results of the cyclic triaxial tests. For various strains, associated values of the degredation parameter (t) were selected based upon the results of cyclic triaxial tests. The results of these tests are presented in Figs. 8.1 and 8.2 for the Sabine and Manor soils, respectively. Thirdly, t parameters were used to predict a reduction factor by the following equation:

$$F = N^{-t}$$

where

F = reduction factor,

N = number of cycles, and

t = degradation parameter.

In the equations used for predicting soil resistance, terms other than shear strength, such as unit weight, also contribute to soil resistance. Thus, to predict the reduction in soil resistance for one particular level of cyclic deflection, the shear strength of the soil was multiplied by the factor, F, and the value of soil resistance was calculated using the p-y procedures described in Chapter 4. Shown by dashed lines in Figs. 8.8a through 8.8e and 8.9a through 8.9d are the predicted values of reduction

in soil resistance versus cyclic pile deflection at 100, 200,and 500 cycles for the Sabine and Manor soils, respectively.

For the Sabine soil, predictions of reduction in soil resistance using the results of cyclic triaxial tests exceed those using the p-y approach, whereas for the Manor soils, the p-y approach predicts values of reduction in soil resistance greater than those predicted using the results of cyclic triaxial testing. That the procedure using cyclic triaxial results predicts too much loss of resistance for the Sabine soil and not enough for the Manor soil emphasizes that other factors such as scour must play an important role in determining the loss in soil resistance. Reinforcing the above comment is that the original investigators observed much more evidence of scouring action during cyclic loading at Manor than at Sabine. The following sections in this discussion address the factors that can account for loss of resistance in addition to that due to cyclic strain.

Influence of Scour

The earlier report on this project described the development of a laboratory test that could be used to assign an index to the scour resistance of a soil. Early in this study it was considered that the values of the scour index could possibly be used with an empirical adjustment factor to account for the loss of resistance due to cyclic loading that was observed at Sabine and at Manor. Such is not the case, however, because the scour index for the Manor soil is less than that at Sabine and the resistance loss was greater at Manor than at Sabine. Some of the other factors that must be considered, in addition to the scour index, are addressed in the following paragraphs.

One of the factors has to do with the depth to which a space, formed by the forward and subsequent backward motion of a pile, will remain open. If the assumptions are made that the soil around the pile behaves according to plane strain and if failure is assumed to be initiated at the base of the opening, the critical height H_c at which the opening would collapse is given by $2s_u/\gamma$, where s_u is the undrained shear strength of the clay and γ is the unit weight of the soil. Therefore, the greater the shear strength the deeper the gap that could develop.

Perhaps one of the most important elements in determining the degree of scour along the pile-soil interface is the velocity at which the water enters and exits the gap. A tentative procedure for estimating this velocity was proposed by Wang and Reese (1983) and is as follows:

$$V = L/(2\Delta t)$$

where:

V = velocity of fluid exiting the gap,

L = depth of gap, and

Δt = time required for gap to close.

The depth to which the gap may form is considered to be controlled by two factors. The first factor controlling the depth of the gap is the bending characteristics of the pile. In this study, it was assumed that a gap formed between the pile and soil to a depth were the displaced position of the pile intersected its original position.

However, an additional constraint was imposed upon the calculated depth of the gap. Assuming plane strain, failure at the base of the gap would occur at a critical height (H_c) dependent on the undrained shear strength (s_u) of the soil and its effective unit weight (γ'). The critical height is computed as $2s_u/\gamma'$. Therefore, in each case history, the

depth of the gap was determined from the deflection versus depth characteristics measured from the pile load test data, and a maximum depth was calculated using the relationship $2s_u/\gamma'$. The smaller of the two values was selected as the representative value of gap depth.

The time required to close the gap was estimated from the values of frequency reported in the original studies. The value of Δt was selected to be one-fourth of the cyclic period. This approximation is subject to some error because the load versus time relationship was not exactly sinusoidal. A load versus time relationship for cyclic lateral-load tests performed at the Lake Austin site is shown in Fig. 8.10. As can be seen readily, the rate of loading varies considerably during the cyclic loading and unloading of the pile; thus, it is expected that pile displacement rates and the velocity of the fluid entering and exiting the gap would also vary greatly during the cyclic load test.

Shown in Table 8.1 are the factors associated with the calculation of the velocity of the fluid, and the computed value of the gap velocity. The case histories are arranged in increasing order of observed reduction in soil resistance; that is, Sabine was reported to have experienced the smallest amount of reduction of soil resistance whereas the soil at Manor exhibited the most. Soil at the Lake Austin site exhibited more reduction in soil resistance than the Sabine soils, but less than that experienced in the Manor soil.

As can be seen from investigating the results in Table 8.1, the velocity of the fluid for the Lake Austin site is greater than that calculated for the Sabine site; however, the computed velocity of the Manor site is the lowest of all three sites studied. Thus, it appears that other factors are involved as well.

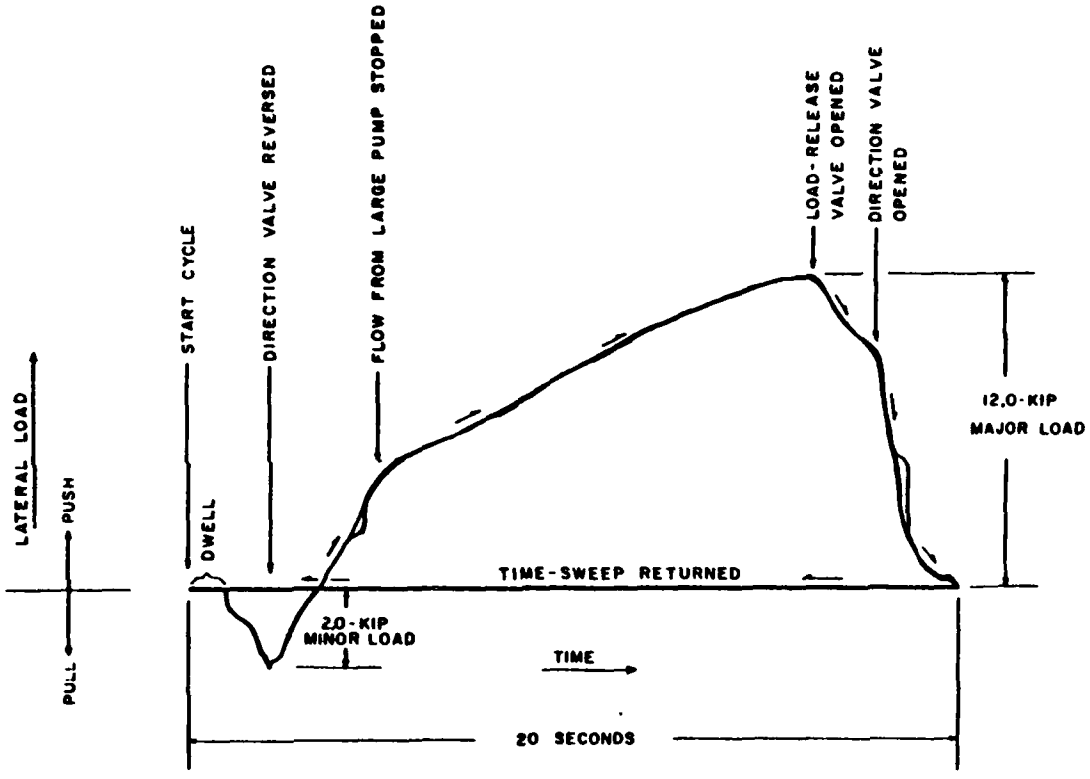

FIG. 8.10. Load versus time relationship for lateral load test conducted at Sabine (from Matlock and Tucker, 1961)

TABLE 8.1. ESTIMATED VELOCITIES OF WATER EXITING GAP FOR SABINE, LAKE AUSTIN AND MANOR TEST SITES

Case History	Depth to Zero Pile Deflection (in.)	$\frac{2S_u}{\gamma}$ (in.)	Δt (sec)	Velocity ft/sec
Sabine	264 to 289	154	5	1.28
Lake Austin	219 to 225	384	3.75	2.50
Manor	192	> 2000	7.5	1.07

There are two other factors that can be considered qualitatively, both of which involve the character of the soil at Manor and at Sabine. The Manor soil has a highly developed secondary structure, probably from desiccation, consisting of cracks and joints. The secondary structure was evident in the vicinity of the ground surface as it existed at the time of the Manor tests. The cyclic loading of the 24-in. pile at Manor not only caused soil to be scoured away at the interface of the pile and soil but after testing was completed an opening was discovered in the clay in front of the pile. The opening was several centimeters across, it began at the face of the pile about a half meter below the ground surface, and exited about one to two ft from the pile. This opening undoubtedly resulted in loss of soil resistance and was certainly due to the joints and cracks that allowed the flow of water from the face of the pile as the water was put under pressure due to the pile deflection.

The second point with regard to the character of the clay concerns the Sabine soil. The site is close to the Sabine River that forms the border between Louisiana and Texas and the soil at the test site is undoubtedly an alluvial deposit. Thin seams of sand were evident at some depths

and, while grain-size-distribution curves are unavailable, it is likely that some sand-sized particles are mixed in with the silt sizes and clay sizes that predominate. The coarser grains could logically have separated from the clay and collected at the interface of the pile and the soil and served as a barrier to more serious degradation than was observed. A similar phenomenon was observed during the cyclic scour tests performed in the laboratory. It was found that the finer particles were washed from the specimen and that the coarser particles collected at the pile-soil interface. It was further noted in the scour tests in the laboratory that sand did not scour appreciably. Thus, the sand-sized particles at Sabine could have served to mitigate the effects of the scour.

It appears the most significant point recognized in this study is the effect of the free water surface upon the value of C_1 required to predict cyclic deformations.

CONCLUSIONS

The results of laboratory tests conducted on soils from two different lateral load test sites demonstrate the need to consider several other characteristics of the soil such as grain size, shear strength, and secondary structure (fissures) of the soil.

The effect of free water above the ground surface was shown to be significant in several ways. The relationship of the degredation parameter, t, versus cyclic strain was similar for both Manor and Sabine soils; however, a much greater loss in soil resistance was experienced at the Manor site than at the Sabine site. In addition, analyses conducted on all the pile load tests showed much higher rates of degradation of soil resistance for piles in which water was above the ground surface.

The loss of soil resistance is therefore sensitive to the effects caused by water above the ground surface. Cohesive soils that have a large percentage of sand-size particles may form a protective layer of coarser sand along the perimeter of the pile due to the water carrying away the fine-grained material. Water velocities, and therefore scour potential, may be higher for piles in soils possessing high shear strengths because the gap between the pile and soil will remain open deeper than for a softer soil. The character of the soil also plays an important role in its susceptibility to the scouring action that occurs. Highly fissured soils may easily be carried away as small particles, whereas intact or slightly fissured soils would demonstrate a much greater resistance to scour.

CHAPTER 9. CONCLUSIONS

Based upon the results of this investigation, several conclusions may be drawn regarding the behavior of vertical piles in cohesive soil due to repetitive lateral loading. Laboratory studies were designed and carried out to investigate (1) the effect of cyclic loading upon the stress-strain characteristics of the supporting soil, and (2) the effect of the scouring action of water as it enters and exits the gap formed along the pile-soil interface. Strain-controlled cyclic triaxial tests, pinhole dispersion tests, and scour tests were conducted on soil specimens obtained from two sites (Sabine and Manor, Texas) which had been used as locations for cyclic lateral load tests.

The results of several cyclic lateral load tests were presented and the following conclusions drawn:

1) horizontal deflection of piles due to cyclic lateral loading at small levels of load (with respect to ultimate lateral load) increase with the number of applications, but may stabilize at a large number of cycles,
2) in many instances, the relationship between deflection and the logarithm of the number of cycles may be approximated with a straight line, furthermore,
3) the slope of this line increases with increasing load levels,
4) cycling at low levels of load affects the behavior at higher levels of load,
5) when both static and cyclic tests are performed on a single pile, the lateral deflection on the first cycle may measure

less than the deflection for static loading due to the differences in the rate of loading of the pile head, and

6) the effect of a free water surface above the groundline may be significant due to the potential for scour along the gap formed between the pile and soil.

Some other methods exist to predict the behavior of piles due to cyclic lateral loading; however,the p-y analyses seem to be well suited for making these predictions because p-y curves are based upon the results of field tests, the analyses require input commonly obtained during field investigations, and specific procedures for generating p-y curves are well documented. Broms' method of predicting pile behavior due to cyclic loading suggests reducing the ultimate soil resistance by a factor of two, and the procedure used by Poulos requires data not commonly obtained in a typical site investigation.

All of the load versus deflection relationships measured during the cyclic lateral tests which were presented in Chapter 3 were analyzed and are compared with predicted relationships in Chapter 5. Using the p-y method and applying each of the three different p-y curve generation relationships, soft clay, stiff clay (below the water table), and stiff clay (above the water table), the following conclusions were drawn:

1) the soft clay criteria, in general, predicts less influence of cyclic loading than the other two methods, and
2) the stiff clay (bwt) criteria, in general, predicts the most influence of cyclic loading,
3) for all of the cyclic lateral load tests conducted with no free water at the ground surface, the stiff clay (awt) performed best in predicting the effect of cyclic loading, and

4) for the cyclic lateral load tests conducted with free water at the ground surface in soft clay, the soft clay p-y criteria predicted the effect of cyclic loading for the tests at the Sabine site well; however, the p-y criteria predicted the effects of cyclic loading to be less than those measured for the Harvey, and Lake Austin test sites.

Soil specimens were obtained from two sites (Sabine and Manor, Texas) in which cyclic lateral load tests were conducted. These specimens were tested in a cyclic controlled-strain triaxial device, and the specimens were also tested to evaluate their susceptibility to scour. The results of these tests are as follows:

1) the soil specimens obtained from Sabine exhibited a greater reduction in shear resistance versus number of cycles than the Manor soils, and
2) the soil specimens from Sabine exhibited a greater susceptibility to scour than did the Manor soils.

The results from the triaxial testing program and scour tests indicated that a greater loss in soil resistance for the Sabine soil should have been experienced; however, from the results of field lateral load tests, the opposite behavior was observed. Therefore, it is important that several additional factors must be considered which include the following:

1) velocity at which the water enters and exits the gap is dependent on both the rate at which the gap closes, and the geometric characteristics of the gap (i.e. depth of crack),

2) the secondary structure of the soil, such as fissures, may allow the water to erode small blocks of soil, or provide a path to flow through during cycling, and

3) if the soil grains are composed of a well graded material (i.e. both sand size and clay size), it is possible for some of the smaller soil particles to be eroded and leave the larger particles to form a type of scour resistant cover.

All of these considerations are necessary to consider and important to recognize when attempting to evaluate the effect of cyclic loading on piles.

REFERENCES

Anderson, K.H., "Behavior of Clay Subjected to Undrained Cyclic Loading," Behavior of Offshore Structures, BOSS, 1976.

Bishop, A.W. and D.J. Henkel, The Measurement of Soil Properties in the Triaxial Test, Edward Arnold Ltd., London, second edition, 1962.

Broms, B.B., "Lateral Resistance of Piles in Cohesive Soils," Journal of the Soil Mechanics and Foundation Division, ASCE, Vol. 90, No. SM3, 1964a, pp. 27-63.

Broms, B.B., "Lateral Resistance of Piles in Cohesionless Soils," Journal of the Soil Mechanics and Foundation Division, ASCE, Vol. 90, No. SM3, 1964b, pp. 123-156.

Broms, B.B., Discussion to paper by Y. Yoshimi, Journal of the Soil Mechanics and Foundation Division, ASCE, Vol. 91, No. SM4, 1965, pp. 199-205.

Egan, J.A., "A Critical State Model for the Cyclic Loading Pore Pressure Response of Soils," Thesis presented to Cornell University in partial fulfillment of the requirements for the degree of Master of Science in Civil Engineering, 1977, 240 pp.

Focht, J.A. III, "A Comparison between Measured and Calculated Pile Group Behavior under Lateral Loading," Report submitted to the University of Texas at Austin in partial fulfillment of the requirements for the degree of Master of Science in Engineering, 1982.

Gaul, Roy D., "Model Study of a Dynamically Laterally Loaded Pile," Journal of the Soil Mechanics and Foundation Division, ASCE, Vol. 84, No. SM1, Proc. paper #1535, 1958.

Gilbert, L.W., "Lateral Load Analysis of Piles in Very Soft Clay," Tulane University, in partial fulfillment of the requirements for the degree of Doctor of Engineering, 1980.

Idriss, Izzat M., R. Dobry, and R.D. Singh, "Nonlinear Behavior of Soft Clays During Cyclic Loading," Journal of the Geotechnical Engineering Division, ASCE, Vol. 104, No. GT12, 1978, pp. 1427-1447.

Lee, K.L. and J.A. Focht, "Cyclic Testing of Soil for Ocean Wave Loading Problems," Marine Geotechnology, Vol. 1, 1976, pp. 305-326.

Martin, G.R., I. Lam, and C-F Tsai, "Pore-Pressure Dissipation During Offshore Cyclic Loading," Journal of the Geotechnical Engineering Division, ASCE, Vol. 106, No. GT9, 1980, pp. 981-996.

Matlock, H., "Correlations for Design of Laterally Loaded Piles in Soft Clay," Offshore Technology Conference, Proc. paper #1204, Vol. I, 1970, pp. 577-593.

Matlock, H., W.B. Ingram, A.E. Kelly, and D. Bogard, "Field Tests of the Lateral-Load Behavior of Pile Groups in Soft Clay," OTC, Houston, Texas, May 5-8, 1980, Vol. IV, pp. 163-174.

Matlock, H., A.E. Kelly, W.R. Hudson, W.P. Dawkins, and J.J. Panak, "Field Tests of the Lateral-Load Behavior of Pile Groups in Soft Clay," Report to Shell Development Company, Exploration and Production Research Division on research conducted by Research Engineers, Inc., Austin, Texas, 1967.

Matlock, H., E.A. Ripperger, and D.P. Fitzgibbon, "Static and Cyclic Lateral Loading of an Instrumented Pile," Report to Shell Oil Company on research conducted by Thompson Associates & Engineering-Science Consultants, Austin, Texas, 1956.

Matlock, H., and R.L. Tucker, "Lateral-Load Tests of an Instrumented Pile at Sabine, Texas," Report to Shell Development Company on research conducted by Engineering-Science Consultants, Austin, Texas, 1961.

Motherwell, J.T., "Cyclic Stress-Strain Properties of a Clay under Wave Loads," Thesis presented to the University of Texas at Austin in partial fulfillment of the requirements for the degree of Master of Science in Engineering, 1976.

Patterson, M.M., "Oceaneographic Data from Hurricane Comille," Sixth Annual Offshore Technology Conference, Houston, Texas, May 6-8, 1974, Vol. 2, Proc. paper #2109, pp. 781-790.

Poulos, H.G., "Behavior of Laterally Loaded Piles: I - Single Piles," Journal of the Soil Mechanics and Foundation Division, ASCE, Vol. 97, No. SM5, 1971a, pp. 711-731.

Poulos, H.G., "Behavior of Laterally-Loaded Piles: II - Pile Groups," Journal of the Soil Mechanics and Foundation Division, ASCE, Vol. 97, No. SM5, 1971b, pp. 733-751.

Poulos, H.G., "Load-Deflection Prediction for Laterally Loaded Piles," Australian Geomechanics Journal, Vol. G3, No. 1, 1973, pp. 1-8.

Poulos, H.G., "Single Pile Response to Cyclic Lateral Load," Journal of the Geotechnical Engineering Division, ASCE, Vol. 108, No. GT3, 1982, pp. 355-375.

Poulos, H.G. and E.H. Davis, Pile Foundation Analysis and Design, John Wiley and Sons, Inc., New York, N.Y., 1980.

Price, G., "Field Tests on Vertical Piles Under Static and Cyclic Horizontal Loading in Overconsolidated Clay," ASTM, Special Technical Publication 670, Raymond Lundgren, Ed., 1979, pp. 464-483.

Price, G., and I.F. Wardle, "The Deformations of Vertical Piles in London Clay under Static and Cyclic Horizontal Working Loads," Proceedings of Recent Developments in the Design and Construction of Piles, Institution of Civil Engineers, London, England, 1980.

Price, G. and I.F. Wardle, "Horizontal Load Tests on Steel Piles in London Clay," Proceedings of the Tenth International Conference on Soil Mechanics and Foundation Engineering, Vol. 2, 1981, pp. 803-808.

Reese, L.C., "Behavior of Piles and Pile Groups under Lateral Load," Manual prepared for U.S. Department of Transportation, Federal Highway Administration, Office of Research, Washington, D.C., 1983.

Reese, L.C., W.R. Cox, and F.D. Koop, "Field Testing and Analysis of Laterally Loaded Piles in Stiff Clay," Offshore Technology Conference, Proc. paper #2312, 1975, pp. 671-690.

Reese, L.C. and R.C. Welch, "Lateral Loading of Deep Foundations in Stiff Clay," Journal of the Geotechnical Engineering Division, ASCE, Vol. 101, No. GT7, 1975, pp. 633-649.

Sangrey, D.A., G. Castro, S.J. Poulos, and J.W. France, "Cyclic Loading of Sand, Silts and Clays," Proceedings, Earthquake Engineering and Soil Dynamics Conference, ASCE, 1978.

Scott, R.F., "Cyclic Static Model Pile Tests in a Centrifuge," OCT, Proc. paper #3492, Vol. 2, 1979, pp. 1159-1168.

Sherard, J.L., L.P. Dunnigan, and R.S. Decker, "Identifying Dispersive Soils," Journal of the Geotechnical Engineering Division, ASCE, Vol. 102, No. GT1, 1976.

Steussy, D. K., "Development of a Self-Boring Pressuremeter for Efficient Use in Stiff Clays," Geotechnical Engineering Thesis, GT80-3, University of Texas at Austin, 1980.

Tassios, T., and E. Levendis, "Efforts Reppetitifs Horizontaux sur Pieux Verticaux," Annales, de L'Institut Technique du Batiment et des Travaux Publics, No. 315, March, 1974.

Terzaghi, K., "Evaluation of Coefficients of Sub-grade Reaction," Geotechnique, Vol. 5, 1955, pp. 297-326.

Thiers, G.R., and H.B. Seed, "Cyclic Stress-Strain Characteristics of Clay," Journal of the Soil Mechanics and Foundation Division, ASCE, Vol. 94, No. SM2, March, 1968, pp. 555-569.

Thiers, G.R., and H.B. Seed, "Strength and Stress-Strain Characteristics of Clays Subjected to Seismic Loading Conditions," Proceedings of the Symposium on Vibration Effects of Earthquakes on Soils and Foundations, ASTM, Special Technical Publication 450, 1969, pp. 3-56.

U.S. Naval Civil Engineering Lab, "Lateral Thrust on Piles," Technical Report R 283, June 15, 1964.

Valenzuela, L.F. and K.L. Lee, "Horizontal Cyclic Load Behavior of Small Scale Piles and Footings on Clay Foundations," Report to the American Petroleum Institute, University of California Engineering Report No. 7836, 1978, p. 235.

Wang, S-T, and L.C. Reese, "Development of a Laboratory Test to Identify the Scour Potential of Soils at Piles Supporting Offshore Structures," Geotechnical Engineering Report, GR 83-2, University of Texas at Austin, 1983.

END

DATED

FILM

8-88

DTIC